

https://dspace.org/

Catalytic oxidation of Carbon Monoxide and Methane with goldbased catalysts

Raphulu, Mpfunzeni Christer

2006-03-23
http://hdl.handle.net/10539/282

Downloaded from a DSpace repository. https://dspace.org/

CATALYTIC OXIDATION OF CARBON MONOXIDE AND METHANE WITH GOLD-BASED CATALYSTS

Mpfunzeni Christer Raphulu

A thesis submitted to the faculty of Science, University of the Witwatersrand, Johannesburg, in fulfilment of the requirements for the degree of Doctor of Philosophy.

Johannesburg, 2004

DECLARATION

I declare that this is my own, unaided work. It is being submitted for the Degree of Doctor of Philosophy in the University of the Witwatersrand, Johannesburg. It has not been submitted before for any degree or examination in any other University.

_____

Signature of candidate

_____ day of December 2004

Abstract

Gold has been regarded as being inert and catalytically inactive for many years compared with for example the platinum group metals. However, for the past decade gold has attracted a growing attention as both a heterogeneous and homogeneous catalyst and it has been shown that it can catalyze a wide range of reactions such as oxidation, hydrogenation, reduction, etc.

This project entails the synthesis, characterization and testing of a suitable gold catalyst for the oxidation of carbon monoxide (CO), and some hydrocarbons (methane). In this project 2 wt% Au/TiO_2; Au/TiO_2-ZrO_2; Au/TiO_2-CeO_2 catalysts were prepared by both deposition-precipitation and co-precipitation methods. Different synthesis conditions such as pH, catalyst ageing, and catalyst pretreatment were investigated in order to find suitable conditions for the preparation of catalyst that would be more active at lower temperature range (25 ^{o}C – 100 ^{o}C). The techniques used for catalyst characterization include, TGA, XRD, BET, XPS, TPR, XANES, HRTEM etc. in order to elucidate the catalyst surface structure and its suitability in affecting adsorption and subsequently catalytic activity.

Carbon monoxide and methane oxidation reactions were undertaken in a tubular glass flow reactor. It was observed that when gold is well dispersed on a suitable support, it can catalyze total oxidation of CO at room temperature, provided that certain preparation and pretreatment conditions are followed. An uncalcined catalyst was found to be more active than the catalyst calcined at higher temperatures. This is due to the agglomeration of gold particles on the surface of the support according to our High Resolution Transmission Electron Microscopy results. With Mössbauer spectroscopy, it was observed that the addition of the second support metal oxide such as zirconia resulted in the decrease in agglomeration of gold particles. In such

catalysts, a considerable amount of ionic species were preserved even after calcination at 400 ^{o}C resulting in the higher activity. With $Au/TiO_{2,}$ a batch of uncalcined catalyst dried at 120 ^{o}C overnight was leached with cyanide to remove the bulk metallic gold particles, supposedly leaving mostly ionic, small, and well dispersed gold particles and the activity of such leached catalyst was higher than that of the unleached sample. Methane oxidation was found to be very difficult compared with carbon monoxide, and only 8% conversion was achieved at 450 ^{o}C whereas a total CO oxidation was achieved at lower temperatures with the same catalyst. It is conclusive that small, ionic well dispersed gold species are necessary for CO oxidation and the adsorption and the active sites for this reaction may be different from those involved in methane oxidation.

Dedicated to: Thompho Raphulu

Publications and Presentations related to this work

Publications:

1. Boyd D, Golunski S, Hearne G.R, Magadzu T, Mallick K, Raphulu M C, Scurrell M S, *"Reductive Routes to Stabilized Nanogold and Relation to Catalysis by Supported Gold"* **Accepted by Applied catalysis A.**
2. Jeffrey H. Yang, Juan D. Henao, Mpfunzeni C. Raphulu, Yingmin Wang, Mayfair C. Kung, Michael S. Stephen, Jeffrey Miller, and Harold H. Kung "*Activation of Au/TiO_2* catalyst *for CO oxidation"* **Accepted by Journal of Physical Chemistry B.**
3. Mahlaba A. Debeila, Mpfunzeni C. Raphulu, Emma Mokoena, Miguel Avalos, Vitalii Petranovskii, Neil J. Coville and Mike S. Scurrell "*The influence of gold on the optical properties of sol-gel derived titania*" Journal Material Science and Engineering: A, 396 (2005) 70
4. Mahlaba A. Debeila, Mpfunzeni C. Raphulu, Emma Mokoena, Miguel Avalos, Vitalii Petranovskii, Neil J. Coville and Mike S. Scurrell "*The effect of gold on phase transformations of titatia*" Journal Material Science and Engineering: A, 396 (2005) 61

Oral Presentations:

1. JH Yang, MC Raphulu, J. Miller, J Henao, Y Wang, MS Scurrell, MC. Kung, and H.H Kung "*Effect of Reduction on CO Oxidation with Au/TiO_2 Catalysts"* in CATSA conference at Potchefstroom University: 14 -17 November 2004.
2. MC Raphulu, T. Letswiti, and MS Scurrell "*Leached Gold Catalysts for CO oxidation*" USA-RSA Gold Catalysis meeting; Paris, Porte de clichy hotel: 17-18 July 2004.

3. Mpfunzeni C. Raphulu and Mike S. Scurrell; "*Characterization of Gold-based catalysts for CO oxidation*" USA-RSA Gold Catalysis meeting; Magaliesburg, Mount Grace hotel: 13-15 July 2003
4. Mpfunzeni C. Raphulu and Mike S. Scurrell; "*Catalytic Oxidation of Carbon Monoxide with Gold Based Catalysts*" SACI Conference, University of Port Elizaberth; 1-5 July 2002
5. Mpfunzeni C. Raphulu and Mike S. Scurrell; "*Catalytic Oxidation of Carbon Monoxide with Gold Based Catalysts*" CATSA conference; Cape Town; 10-13 November 2002

Acknowledgements

I am greatfull to the following persons and institutions:

- Mwali Musikavhathu; *Psalm 23*
- My supervisor, Professor Michael Stephen Scurrell for his constant guidance and helpful discussions concerning this project
- Basil Chassoulas for his technical help on instrumentation
- Professors Harold and Mayfair Kung, and Mr Jeff Yang of Northwestern University, Chicago, Illinois for introducing me to X-ray absorption spectroscopy technique and allowing me to spend some time in their lab.
- Professor Robert Davis and Mr Jasson Calla of University of Virginia for introducing me to laser deposition technique and allowing me to spend some time in their lab.
- The Honours students who worked on this project: Tebogo Letswiti and Mvuyisi Ngqola.
- Allan Bently of Pretoria University for HRTEM analysis.
- Dr G. Hearne of School of Physics, Wits, for Mössbauer analysis.
- University of the Witwatersrand catalysis research group for creating a wonderful working environment and for the helpful general discussions in catalysis.
- My family, Mom, dad, grandma, and my daughter: "*Ndi a livhuwa vhangona*".
- All of my friends; "*a ni ntshileli vha hashu*"
- The main sponsor of this project, Johnson Matthey technology centre, London
- Other financial institutions: NRF/DoL, DAAD, Mellon Foundation Mentoring Scheme, Wits University merit bursary, National Science Foundation (USA).
- University of the Witwatersrand for allowing me to undertake this project.

Table of Contents

Contents Page

Declaration……..…ii
Abstract……..iii
Dedication……...v
Publications and Presentations……...vi
Acknowledgements……..viii
List of Tables…….……xiv
List of Figures……xvi

Chapter 1: General Introduction……...1

1.1.Background 1
1.2 Development of Three-Way Catalysts 2
1.3 Properties of gold 4
1.4 Relativistic effect 9
1.5 Application of Highly dispersed gold catalysts 12
1.6 References 14

Chapter 2: Literature Review

2.1 Introduction 16
2.2 Preparation Method of Au nanoparticles 17
2.2.1 Impregnation 17
2.2.2 Suspension spray reaction method 19
2.2.3 Co-precipitation..... 20
2.2.4 Deposition-precipitation..... 22
2.2.5 Grafting 26

2.2.6 Ion exchange 27
2.2.7 Chemical vapour deposition (CVD) 28
2.2.8 Iwasawa method 29
2.2.9 Other recently developed methods for the synthesis of Au nanoparticles 32
2.3 Catalyst synthesis and pretreatment conditions 34
2.4 Effect of Support 40
2.5 Effect of Particle Size 43
2.6 Oxidation State of Gold 46
2.7 CO Oxidation Reaction Proposed Mechanisms 48
2.8 CO oxidation reaction kinetics 52
2.9 Deactivation and stability of Au catalysts 56
2.10 The effect of moisture on CO oxidation 58
2.11 Other reactions catalyzed by gold nano-particles 60
2.11.1 Selective CO Oxidation in the presence of hydrogen (H_2-SCO) 60
2.11.2 Hydrochlorination of ethyne 63
2.11.3 Epoxidation of propelyene 64
2.11.4 Water Gas Shift reaction (WGS) 65
2.11.5 Methane Oxidation 68
2.12 Characterization of Au nanoparticles 75
2.12.1 Surface area determination (Brunauer, Emett, and Teller) 75
2.12.2 Transmission Electron Microscopy (TEM) 76
2.12.3 X-ray Defractometer (XRD) 77
2.12.4 X-ray Photoelectron Spectroscopy 78
2.12.5 Mössbauer Effect Spectroscopy 79
2.12.6 Infrared Spectroscopy (IR) 80
2.12.7 X-ray absorption fluorescent spectroscopy (XAFS) 81
2.12.8 X-ray Absorption Near Edge Structure (XANES) 82
2.13 References 83

Chapter 3: Experimental Procedures

3.1. Catalyst preparation 90

3.1.1. Preparation of Au/TiO_2-ZrO_2 catalysts 90

3.1.1.1. Zirconia introduction by deposition-precipitation 90

3.1.1.2. Zirconia introduction by impregnation 91

3.1.2 Preparation of Au/TiO_2 Catalysts 92

3.1.2.1 Deposition-precipitation: Method 1 92

3.1.2.2 Deposition-precipitation: Method 2 93

3.1.2.3 Sol-gel catalyst preparation method 94

3.1.2.4 An attempt to control the size of the gold particles by means of pH .. 95

3.1.2.5 Synthesis of the support by sol-gel method and deposition of gold ... 95

3.1.3 Catalyst synthesis of ceria-containing catalysts 96

3.1.3.1 Preparation of CeO_2 from $Ce(NO_3)_3 \cdot 6H_2O$ 96

3.1.3.2 Au/CeO_2 by deposition-precipitation 96

3.1.3.3. Au/CeO_2 by co-precipitation 97

3.1.3.4. $Au/TiO_2 - CeO_2$ by deposition-precipitation 97

3.2 Catalyst Characterization 98

3.2.1 Surface area determination – BET 98

3.2.2 Mössbauer Effect Spectroscopy 99

3.2.3 X-ray Photon Spectroscopy (XPS) 100

3.2.4 High Resolution Transmission Electron Microscope (HRTEM) 100

3.2.5 X-ray Absorption Near Edge Structure (XANES) 1001

3.2.6 Temperature Programmed Reduction (TPR) 103

3.2.7 Thermogravimetric Analysis (TGA) 104

3.2.8 Inductively Coupled Plasma-Optical Emission Spectrometer (ICP-OES) 104

3.3 The leaching process of Au/TiO_2 catalysts 105

3.4 Activity measurement 106

3.4.1 Catalysts prepared by deposition-precipitation (method 1) and by sol-gel method 106
3.4.2 Catalysts prepared by deposition-precipitation by method 2 108
3.5 Calculations 108
3.6. Reference 109

Chapter 4: The effect of zirconia on Au/TiO_2-ZrO_2 catalyst for CO oxidation

4.1. Introduction 110
4.2 Results and Discussion 113
4.2.1 Catalyst Characterization 113
4.2.1.1 Surface Area (BET) 114
4.2.1.2 Mössbauer Spectroscopy 118
4.2.1.3 X-ray Photoelectron Spectroscopy (XPS) 124
4.2.1.4 High Resolution Transmission Electronic Microscopy 130
4.2.1.5 X-ray Powder Diffraction (XRD) 132
4.3 Catalytic Activity 135
4.3.1 Au/TiO_2-ZrO_2 catalysts prepared by deposition-precipitation 136
4.3.2 Sol-gel method prepared catalysts 152
4.3.2.1 Characterization of Sol-gel Synthesized Catalysts 153
4.3.2.1.1 Thermogravimetric Analysis (TGA) 153
4.3.2.2 Results and discussion 159
4.4 Conclusions 164
4.5 References 165

Chapter 5: Au/TiO_2 catalysts

5.1 Introduction 169
5.2 Results and discussions 172
5.2.1 Method 1 catalysts (as described in Chapter 3) 172

5.2.2 Leaching of Catalysts prepared by deposition-precipitation (method 1) . 178
5.2.3 Deposition-precipitation (Method 2) preparation 186
5.2.3.1 CO Oxidation 186
5.2.4 H_2 Pulse experiment on Catalysts prepared by method 2 195
5.2.5 Pulses with CO oxidation interruption 200
5.3 Sample Characterization 204
5.3.1 TPR 204
5.3.2 XANES 205
5.4 Conclusions 210
5.5 References 211

Chapter 6: CO and Methane Oxidation with various Gold Catalysts

6.1 Introduction 214
6.2. CO oxidation 216
6.2.1 Catalyst Characterization 216
6.2.1.1 BET Surface Area 216
6.2.1.2 XRD 218
6.2.2 Catalyst Activity 222
6.3 Methane oxidation 226
6.4 Conclusion 230
6.5 References 231
Chapter 7: General Conclusions 232

List of Tables

Chapter 1

Table 1.1: Properties of Au compared to those of Pt and Hg……5
Table 1.2: Properties of Au compared to those of Cu and Ag……...6

Chapter 2

Table 2.1: Gold particle sizes in catalysts prepared by impregnation…….18
Table 2.2: Catalytic oxidation with various Au/$M(OH)_x$……31
Table 2.3: Mean particle diameters determined by TEM observation of samples prepared by deposition-precipitation and calcined under various conditions……36
Table 2.4: Temperature of 50% conversion obtained for the best catalysts……42
Table 2.5: Rate of CO conversion by Au catalysts with different particle diameter and supports……..54
Table 2.6: Product yield for bimetallic catalysts compared to Au only at 373 K……65
Table 2.7: Summary of activities of different catalysts on WGS reaction……..67
Table 2.8: Catalytic performances for methane combustion with noble metal catalysts ……70
Table 2.9: Summary of reactions catalyzed by gold catalysts…….72

Chapter 3

Table 3.1 Varying the amount of ZrO_2 on Au/TiO_2-ZrO_2 catalyst...……91

Chapter 4

Table 4.1: BET surface areas of Au/TiO_2-ZrO_2 catalysts prepared at different conditions……..117

Table 4.2: Activity of different catalysts containing various amounts of Au^I species ……...123

Table 4.3 Hyperfine interaction parameters of each of the sub-components in the overall fit to each of the spectra measured in this study……123

Table 4.4: Binding energies of gold and percentage composition of different species on the surface of the catalysts……..125

Table 4.5: The binding energies of gold on different catalysts and surface abundances of elements……...127

Chapter 6

Table 6.1: BET surface area of ceria related catalysts……...217

List of figures

Chapter 1

Figure 1.1: Some physical properties of platinum, mercury and metals of group II....4
Figure 1.2: Relativistic contraction for the 6s orbitals of the heavy elements as a function the atomic number, Z……9

Chapter 2

Figure 2.1: Comparison of the activity of Au/CeO_2 catalyst prepared by co-precipitation with that prepared by impregnation method for CO oxidation and NO_x reduction……..21
Figure 2.2: Interaction of gold particles with TiO_2 prepared with different methods ……23
Figure 2.3: Relative equilibrium concentration of gold complexes in $2.5x10^{-3}$ M $HAuCl_4$ solution, calculated with adsorption constants……..25
Figure 2.4: Dependence of the catalytic activity of (a) CO oxidation (b) acetylene Hydrogenation on particle size……45
Figure 2.5: Pictorial representation of supported gold catalysts indicating possible changes under conditions giving oxidation or reduction of the active gold particles……47
Figure 2.6: Proposed mechanism for CO oxidation by Au catalysts……..50
Figure 2.7: Dependence of CO oxidation rate at 273 K over Au/TiO_2 on the moisture Concentration of the reactant as……..59

Chapter 3

Figure 3.1: Flow diagram of gases and X-ray beam during the XANES Experiment…….101

Figure 3.2: Schematic representation of XANES cell……102
Figure 3.3: Schematic representation of the reactor used for both CO and methane oxidation……107

Chapter 4

Figure 4.1: The effect of calcination temperature on BET surface area of Au/TiO_2-ZrO_2 catalyst……...……..114
Figure 4.2: The effect of the amount of ZrO_2 on BET surface area of Au/TiO_2-ZrO_2 catalyst……..……..115
Figure 4.3: Correlation plot of quadrupole splitting (QS) versus isomer shift (IS)…… ……...…119
Figure 4.4: Isomer shift quoted with respect to Au metal at 6 K……..120
Figure 4.5: Deconvoluted Au XPS spectrum of Au/TiO_2-ZrO_2 calcined at 400 ^oC..128
Figure 4.6: Deconvoluted Au XPS spectrum of Au/TiO_2-ZrO_2 calcined at 600 ^oC..129
Figure 4.7: HRTEM picture of uncalcined catalyst……...130
Figure 4.8: HRTEM picture of the catalyst calcined at 600 ^oC…….131
Figure 4.9: XRD spectra of Au/TiO_2-ZrO_2 catalyst precipitated at different pH…..132
Figure 4.10: XRD spectra of Au/TiO_2-ZrO_2 catalyst aged for different periods…...133
Figure 4.11: XRD spectra of Au/TiO_2-ZrO_2 catalyst calcined at different temperatures ….....134
Figure 4.12: The effect of GHSV on the uncalcined catalyst at 25 ^oC reaction temperature and CO/O_2 ration of 1…….136
Figure 4.13: The effect of the amount of Au^I on the rate of CO conversion…….137
Figure 4.14: The effect of temperature on (a) Au/TiO_2-ZrO_2 and (b) Au/TiO_2 catalysts precipitated at pH 9…….138
Figure 4.15: CO oxidation activity at room temperature: (a) initial activity (b) after oxidation at 100 ^oC for 3 minutes……..139
Figure 4.16: The effect of the amount of ZrO_2 in Au/TiO_2-ZrO_2……..140

Figure 4.17: The effect of the amount of impregnated ZrO_2 in Au/TiO_2-ZrO_2…….142
Figure 4.18: Effect of calcination temperature on Au/TiO_2-ZrO_2…….143
Figure 4.19: The effect of catalyst pretreatment at different temperatures……...145
Figure 4.20: The effect of catalyst pretreatment gas…….147
Figure 4.21: The effect of ageing period on Au/TiO_2-ZrO_2 catalysts and different ratios of CO and oxygen at room temperature…….148
Figure 4.22: The effect of precipitation pH on CO oxidation at room temperature..149
Figure 4.23: The effect of reaction temperature on the uncalcined catalyst……..151
Figure 4.24: TGA profile of TiO_2 (P25) (uncalcined)……...154
Figure 4.25: TGA profile of Au/TiO_2 (P25) catalyst (uncalcined)……155
Figure 4.26: TGA profile of Au/ZrO_2 (uncalcined)……...156
Figure 4.27: TGA profile of Au/TiO_2-ZrO_2 (uncalcined) catalyst……157
Figure 4.28: TGA profile of Au/TiO_2-ZrO_2 catalyst (with the support pre-calcined at 400 ^oC)…….……158
Figure 4.29: The effect of reaction temperature on uncalcined catalysts.……..…...159
Figure 4.30: The effect of reaction temperature on calcined catalyst……160
Figure 4.31: The effect of reaction temperature on the catalyst with $HAuCl_4$ solution adjusted to pH 8 before being added to the support solution……...161
Figure 4.32: The effect of temperature on the calcined and the uncalcined catalyst with its support prepared by sol-gel method…….162

Chapter 5

Figure 5.1: The effect of ageing period on Au/TiO_2 catalyst at 25 ^oC reaction temperature……172
Figure 5.2: The effect of pH on Au/TiO_2 catalyst at 25 ^oC reaction temperature……173
Figure 5.3: The effect of time-on-stream on Au/TiO_2 catalysts precipitated at different pH……175

Figure 5.4: The effect of time-on-stream on Au/TiO_2 catalysts aged for different periods……..……...…….176
Figure 5.5: CO oxidation with uncalcined Au/TiO_2 catalyst as a function of time-on-stream at room temperature……...177
Figure 5.6: The effect of different leaching conditions on Au/TiO_2 catalyst……180
Figure 5.7: The effect of leaching conditions on Au loading obtained after leaching ……...……181
Figure 5.8: The effect of the amount of CN^- in the leaching solution on the Au loading obtained after leaching……...182
Figure 5.9: The effect of residual Au loading on the rate of reaction……183
Figure 5.10: The effect of leaching pH on the activity of the catalyst……..184
Figure 5.11: The effect of leaching pH on the rate of reaction……..185
Figure 5.12: The effect of room temperature CO treatment on CO oxidation activity of the Au/P25 (pH 7) catalyst at dry ice temperature …..……186
Figure 5.13: CO oxidation of Au/P25 (pH 7) at -59 ^oC and at -13 ^oC (no CO/He treatment) at 50 ml/min total flow rate…….187
Figure 5.14: Activity of Au/P25 at -13 ^oC and 200 ml/min flow rate……...188
Figure 5.15: The effect of room temperature CO treatment in the activity of the Au/rutile catalyst (pH 7) at dry ice temperature...……189
Figure 5.16: The effect of time on the activity of Au/rutile (pH 7) catalyst at -58 ^oC ……...190
Figure 5.17: The effect of time on the activity of Au/rutile (pH 6) catalyst at -58 ^oC ……...191
Figure 5.18: The effect of drying in helium on Au/rutile (pH 7) catalyst on CO oxidation at -77 oC……..192
Figure 5.19: The effect of drying in helium and various treatments of Au/rutile (pH 7) catalyst on CO oxidation at -77 oC ……..193
Figure 5.20: The effect of drying on Au/P25 (pH 7) catalyst on CO oxidation at -77 ^oC …….195

Figure 5.21: Au/rutile catalyst's (pH 7) reducibility as a function of the number of hydrogen pulses……197
Figure 5.22: Au/rutile catalyst`s (pH 6) reducibility as a function of the number of hydrogen pulses……198
Figure 5.23: Au/P25 catalyst`s (pH 7) reducibility as a function of the number of hydrogen pulses……199
Figure 5.24: Au/rutile catalyst`s (pH 7) reducibility (a) and activity (b) as a function of the number of hydrogen pulses .....……..201
Figure 5.25: Au/P25 catalyst`s (pH 7) reducibility (a) and activity (b) as a function of the number of hydrogen pulses…….……202-203
Figure 5.26: Comparison of the TPR spectra of Au/TiO_2 (P25) before (MC-AuTi-50) and after treatment with CO (AuTi-CO)…….204
Figure 5.27: XANES spectra of different Au standards compared to the as-prepared and the treated gold catalysts…….……205
Figure 5.28: XANES spectra of Au/rutile (pH 7) after different periods of exposure to CO oxidation at -68 ^{o}C……..……206
Figure 5.29: XANES spectra of Au/rutile (pH 7) after different periods of exposure to CO oxidation with increasing temperature……..…….207
Figure 5.30: Change in the oxidation state of gold at -68°C under reaction mixture ……..…..208

Chapter 6

Figure 6.1: XRD spectra of Au/CeO_2 catalysts prepared by co-precipitation and deposition-precipitation……..…….218
Figure 6.2: XRD spectra of calcined and uncalcined Au/TiO_2-CeO_2 catalysts....…220
Figure 6.3: The effect of reaction temperature on the calcined and uncalcined Au/CeO_2 prepared by co-precipitation……...222

Figure 6.4 The effect of reaction temperature on the calcined and uncalcined Au/CeO_2 prepared by deposition-precipitation……..…223
Figure 6.5: The effect of catalyst preparation method on uncalcined Au/CeO_2…...224
Figure 6.6: The effect of the mixed oxide support on the catalyst prepared by deposition-precipitation method……225
Figure 6.7: The effect of temperature on different catalyst for methane oxidation...226
Figure 6.8 The effect of catalyst calcination on methane oxidation……..228
Figure 6.9: The effect of temperature on uncalcined catalyst for methane oxidation ……...229

Chapter 1: General Introduction

1.1. Background

Some large cities had begun to experience problems of atmospheric pollution as early as the 1940s. The Los Angeles' basin in the U.S.A. was particularly affected, experiencing frequent natural ambient temperature inversions, which trap and recycle polluted air. Though the mass production of cars, powered by the internal combustion engine, was giving tremendous personal mobility, a very large number of cities were understood to be the major source of the man-made urban emissions (Haagen-Smith and Fox, 1956). Photochemical interactions between hydrocarbons and nitrogen oxides from car exhaust and oxygen occur in the lower atmosphere, forming ozone-containing "photochemical smog," (equation (i)) is identified as an important contributor to the pollution. The oxidation of fuel to carbon dioxide and water in engines, (equation (ii)) was incomplete. Unburnt hydrocarbons and partially combusted products, particularly carbon monoxide (CO) and to a smaller extent oxygenates, such as aldehydes, were present in the exhaust gases. Relatively high levels of CO were formed, (equation (iii)) and under the forcing conditions in the engine, nitrogen (N_2) and (O_2) reacted to establish a partial equilibrium with nitric oxide (NO), (equation (iv)). Appreciable amounts of NO and its oxidized form, nitrogen dioxide (NO_2) (together referred to as (NO_x) can be present in exhaust gas. The major pollutants in exhaust gas are therefore HC, NO_x and CO. Subsequent photo-induced reactions of the first two pollutants with oxygen forms ozone, which is strong irritant, as well as low levels of other compounds, notably peroxyacetyl nitrate, which is a very strong lachrymator irritant (Twigg, 1999 and Wayne, 1996).

$HC + NO_x + hv \rightarrow O_2 +$ other products (i)

$4H_mC_n + (m + 4n)O_2 \rightarrow 2_mH_2O + 4_nCO_2$ (ii)

$4H_mC_n + (m + 2n)O_2 \rightarrow 2_mH_2O + 4_nCO$ (iii)

$N_2 + O_2 \rightarrow 2NO$ (iv)

These problems resulted in an intensive research and the development of a catalyst system that could convert HC, NO_x, and CO into less harmful products such as carbon dioxide water and nitrogen.

1.2 Development of Three-Way Catalysts

From earlier experience with catalytic NO_x reduction with CH_4, Johnson Matthey had developed low light-off temperature Pt/Rh oxidation catalysts, which were used by some European car manufacturer (Acres, 1972). With them, if the engine was operated close to the stoichiometric point (air: fuel ratio corresponding to complete combustion), some NO_x control was obtained via reduction, even though oxidation reactions were also taking place. Suitable catalyst formulations were important in optimizing this behavior (Twigg, 1999). By 1979, oxygen sensors had been developed and placed in the gas close to the exhaust manifold to provide feedback control to the fueling, so conditions could be maintained around the stoichiometric point using electronic control. This enabled good consistent catalytic performance, and the use of Pt/Rh catalysts to simultaneously control HC, CO and NO_x became the preferred system. Since all three pollutants were controlled with one catalyst, the concept was named the "Three-Way Catalyst", (TWC). Early TWCs had a narrow operating "air: fuel" range over which all three pollutants were removed, and from about 1980 they were almost universally fitted to cars sold in the U.S.A. Since then effort has been directed towards improving catalyst performance: enhancing activity, thermal durability, selectivity and widening the air: fuel ratio operating window. Catalyst improvement took place in parallel with the development of increasingly

sophisticated fuel management systems; carburetors gave away to single point fuel injection and then multi-point injection into the inlet manifold, then latterly direct injection into the cylinder.

It has been reported that the "Three Way Catalyst" starts to be active at relatively high temperatures. However, at the time the catalyst reaches its operating temperature a lot of exhaust emissions have already been released into the atmosphere. This therefore, influenced the search for the catalyst which would be active for the removal of these emissions at or even below room temperature.

Unlike the platinum group metals, gold was regarded to be catalytically inactive, but the pioneering of Haruta *et al.* (1993) sparked an interest in gold as a heterogeneous catalyst and offered some promise for the substitution of the "Three Way Catalyst" in alleviating the car exhaust emissions. This "noble'' metal has since then been reported to be active for many reactions ranging from oxidation (Bond 1999 and references there in), reduction, hydrogenation (Schimpf *et al,* 2002 and Hutchings *et al,* 2002), epoxidation (Uphade *et al,* 2002; Haruta *et al,* 2003) etc.

Since the beginning of 1996 *Gold Bulletin* has reviewed the current status of gold science and technology in most its principal areas of application, including metallurgy and jewellery; pharmaceuticals and dentistry; chemistry and catalysis; analytical methods; and electronics and electrochemistry, plating and electro-catalysis, decoration of ceramic tableware and decorative plates. A striking outcome of all these recent articles is the emergence of a common theme of the unique nature of the properties of gold and its derivatives (Thompson, 1998).

1.3 Properties of gold

Catalysis is a surface science and is concerned mainly with reactions of the molecules on the surface of the catalyst. This means that the nature of surface atoms have an influence on the activity and selectivity in catalytic reactions. Because the surface atoms are directly bonded to the underlying atoms in the bulk, it is desirable to understand how the nature of these free valencies is related to the bonds that hold atoms together in the crystal. It is also necessary to understand the chemical and physical properties of gold compared to its neighboring elements in order to relate them to the unbelievable activity of the catalyst (Debeila, 2002).

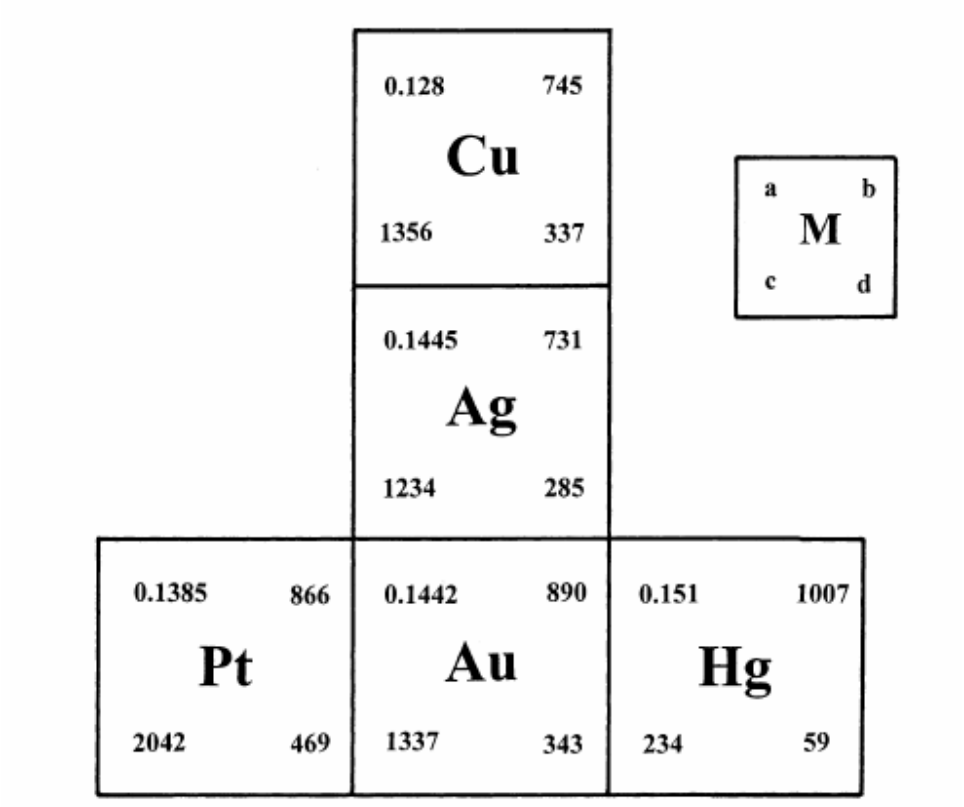

Figure 1.1: Some physical properties of platinum, mercury and the metals of Group II.

a: metallic radius (nm); b: first ionization potential (kJ mol^{-1}); c: melting temperature (K); d: sublimation enthalpy (kJ mol^{-1}).

Au lies between Pt (group 10) and Hg (group 12) in the periodic table and the effect brought about by the sequential increase in nuclear charge and the number of the electron shells have been compared by Bond and Thompson (1999) as shown in table 1.1. Except as observed in hydrochlorination reactions, mercury is regarded as a poison, while Pt is a versatile catalytic metal widely used in chemical processing and in pollution control systems.

Table 1.1: Properties of Au compared to those of Pt and Hg

Property	Pt	Au	Hg
Atomic number	78	79	80
Electron configuration	$[Xe]4f^{14}5d^{9}6s^{1}$	$[Xe]4f^{14}5d^{10}6s^{1}$	$[Xe]4f^{14}5d^{10}6s^{2}$
Structure	FCC	FCC	Hexagonal
Lattice constant (nm)	0.392	0.408	0.299
Metallic radius (nm)	0.1385	0.1442	0.151
Density ($g.cm^{-3}$)	21.41	19.32	13.53
Melting temperature (K)	2042	1337	234.1
Boiling temperature (K)	4443	3081	630
Sublimation enthalpy ($kJmol^{-1}$)	469	368	59.1
Ionization potential ($kJ.mol^{-1}$) 1st	866	890	1007

Au is also in the same group as Cu and Ag and their properties have previously been compared by Bartlett (1998) and Bond and Thompson (1999) as shown in table 1.2. Schwerdtfeger (1996) has indicated the many apparent anomalies in the physical properties of gold compared with those of the other elements of Group 11 (IB), i.e.

silver and copper, including color specific resistivity, electrical heat capacity, melting point and boiling point. It is evident from the table that the trends that are normally shown within a given group in the periodic table are not uniformly found in this group. For instance, measurement of the atomic radius shows that the Au atom is slightly smaller than that of an Ag atom (Rapson, 1996) and the same is true for Au(I) and Ag(I) ions (Bayler *et al,* 1996). This was previously attributed to the so called Lanthanide contraction resulting from inadequate shielding of s, p, and d electrons from increasing charge by f electrons.

Table 1.2: Properties of Au compared to those of Cu and Ag

Property	Cu	Ag	Au
Atomic number	26	47	79
Electron configuration	$[Ar]3d^{10}4s^{1}$	$[Ar]4d^{10}5^{s1}$	$[Xe]4f^{l4}5d^{10}6s^{1}$
A-A distance in FCC cell (A)	-	2.8894	2.8840
Structure	FCC	FCC	FCC
Lattice constant (nm)	0.361	0.409	0.408
Metallic radius (nm)	0.128	0.14447	0.14420
Density ($g.cm^{-3}$)	8.95	10.49	19.32
Melting temperature (K)	1356	1234	1337
Boiling temperature (K)	2843	2428	3081
Sublimation enthalpy ($kJmol^{-1}$)	337	285	368
Electron affinity (eV)	-	1.202	2.039
Heat of atomization ($kJmol^{-1}$)	-	285	368
Ionization potential ($kJmol^{-1}$) 1st	-	730	890
Ionization potential ($kJmol^{-1}$) 2nd	-	2073	1980

The parameters, which reflect the strength of inter-atomic bonding in a crystal, are melting temperature and energy of vaporization. Values in table 1.2 suggest that the inter-atomic bonding is stronger in Au than in Ag. Other anomalies of Au are:

(i) It is the most electronegative metal, and only slightly more electropositive than sulfur and iodine, and

(ii) Its electron affinity is greater than that of oxygen (Bond and Thompson, 1999)

Atoms in group 11 exhibit a number of oxidation states. For example, the +2 state (Cu^{+2}) is known and the +3 and +4 states are only seen in the fluoride ions $[CuF_6]^{2+}$ and $[CuF_6]^{3+}$. Only the +1 state is known for Ag. Au has access to wide range of oxidation state. For example the +1 and +3 states are common and the +5 state is seen in $[AuF_6]^-$ complexes. The existence of aurides (Cs^+Au^-), which are non-metallic semiconductors, is also to be noted (Spicer *et al,* 1959).

Metallic Au quickly dissolves in liquid anhydrous hydrogen fluoride (HF) in the presence of alkali fluoride to form an alkali salt of the anion AuF_4^- according to the following reaction (Lucier *et al,* 1996):

$$Au(s) + F^- + 3/2F_2 \longrightarrow AuF_4^- \qquad (v)$$

If F_2 is photo-dissociated to atoms, AuF_4^- is further oxidized to AuF_6 (Bartlett, 1998):

$$AuF_4^-(solv) + 2F(solv) \longrightarrow AuF_6^-(solv) \qquad (vi)$$

Under the conditions in reaction (v), Ag only forms AgF_2 (+2 state), and AgF_4^- is only formed under the conditions of reaction (vi). These differences in the ionization

of Au and Ag under similar conditions were attributed to the stronger binding of Ag 4d electrons than Au 5d electrons (Bartlett, 1998). This is also shown by the value of the second ionization potential of Ag which is slightly greater than that of Au (table 1.2). The unique chemistry exhibited by Au is attributed to relativistic effects (Bond, 2002).

1.4 Relativistic effect

The uniqueness of gold can be rationalized in terms of its relativistic contraction. Figure 1.2 demonstrates the relativistic contraction for the 6s orbitals of the heavy elements as a function of the atomic number Z.

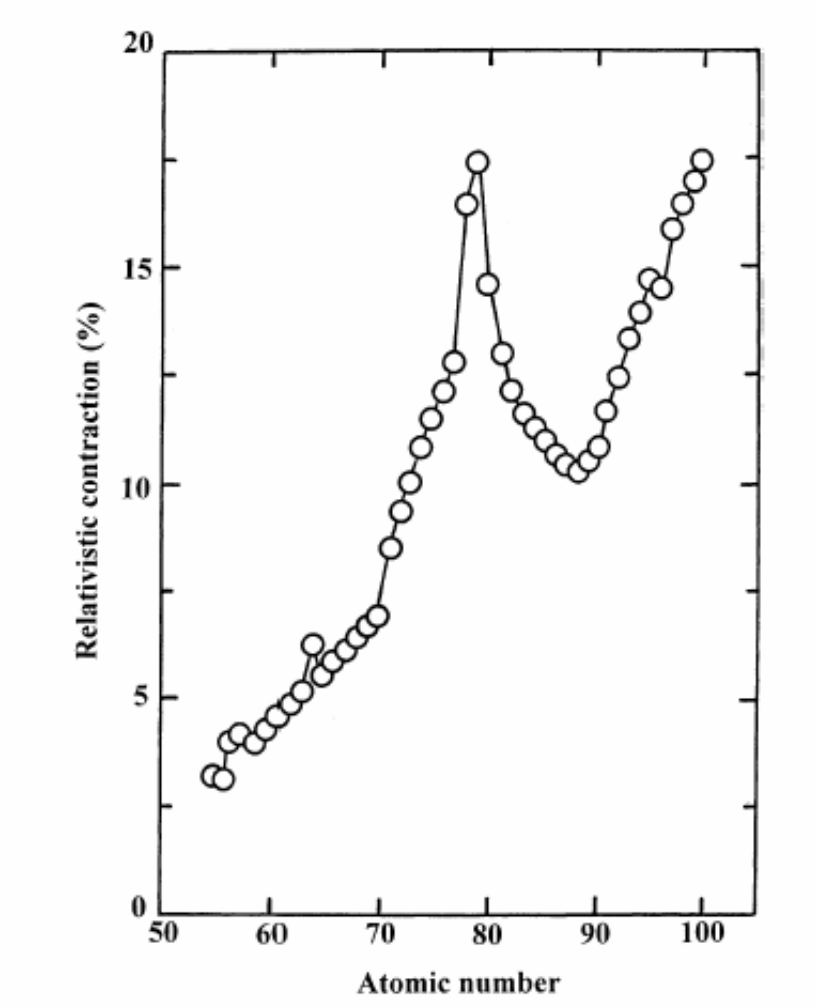

Figure 1.2: Relativistic contraction for the 6s orbitals of the heavy elements as a function of the atomic number Z.

It has been shown that as the mass of the nucleus increases, the speed of the innermost $1s^2$ electrons has to increase to maintain their position, and for gold they attain a speed which is about 60% that of light. There is then a relativistic effect on their mass and the 1s orbital contracts. All the outer "s" orbital has to contract in sympathy, but p and d electrons are much less affected. In consequence, the $6s^2$ pair is contracted and stabilized and much of the chemistry including the catalytic properties (Bond, 2002 and Pyykko, 1988) of the 5d elements is determined by the high energy and reactivity of the 5d electrons. Although, this idea is very helpful in understanding why gold differs so much from its neighbors, it only rationalizes the view held until recently that gold was almost useless as a catalyst (Bond, 2002).

The element gold (Z=79) is at a pronounced local minimum. Electrons in atoms with high atomic numbers are influenced by the increased nuclear point charge and reach speeds which are approaching the velocity of light and therefore must be treated according to Einstein's theory of relativity (Bond, 2002). These relativistic effects consist of three components i.e. s-orbital and, to a smaller extend p-orbital contraction, spin orbit coupling and f-orbital expansion. The unique colour of gold derives from the relativistic effect. The van der Waals interactions between gold atoms are correlation effects. The Au^+ ion is not noble in a classical sense – it is reactive, especially in the gas phase.

There is good agreement between the various methods of calculating the relativistic contraction in Au_2. Relativistic effects lead to increased van der Waals interaction and increased physisorption energies on gold surfaces. Schwerdtfeger (1996) has rationalized the structures of AuX_3 and Au_2X_6.

Most areas of gold science are at an earlier stage of evolution than that already attained for neighboring elements in the periodic table, and although some of the potential applications are at an early stage of development, many significant developments can be anticipated in the future. In earlier studies, gold had been regarded a useful promoter in some catalytic reactions, but it has now been demonstrated that in some circumstances supported gold catalyst systems themselves can be the most active and this has been rationalized *via* theoretical concepts.

It has been demonstrated that gold systems are the best for both the synthesis of vinyl chloride from acetylene (Haruta and Daté, 2001 and Hutchings, 1996) and in the low temperature oxidation of carbon monoxide (Costello *et al,* 2002, Oh *et al,* 2001, Bond and Thompson, 2000 and references therein).

Recent results indicate that further investigation could lead to new applications for gold catalyst systems in both the chemical processing and environmental fields. Although much more research is required in order to identify and realize the full potential of the catalysts studied to date, use in such important areas of application as fuel cells and some forms of vehicle pollution control can be foreseen as possibilities, as well as in gas masks for removing toxic gases such as carbon monoxide. Initial results in both homogeneous and supported homogeneous catalysis indicate that the field of gold catalysis as a whole is beginning to progress and is worthy of closer examination (Thompson, 1998).

1.5 Application of Highly dispersed gold catalysts

Gold has been commercially used for bimetallic Pd-Au catalysts supported on SiO_2 in the production of vinyl acetate from ethylene and acetic acid. Other recent advances are the reduction of NO_2 with H_2 to form NO over Au/Al_2O_3 at round 300 ^oC and the oxidation-decomposition of odors, mainly amine-related compounds over Au/Fe_2O_3 carried on zeolite coated honeycombs in modern Japanese toilets. There are other several candidates which are technologically ready for commercial applications. These applications have been motivated by the interesting fact that supported gold catalysts are usually enhanced in their activities by moisture:

i) CO regeneration catalysts for sealed, unheated CO_2 lasers (Gardner *et al,* 1991).
ii) CO safety gas masks (Haruta, 1990).
iii) CO removal from air to produce high purity N_2 and O_2 gas (Haruta *et al,* 1991)
iv) CO gas sensors (Funasaki *et al,* 1993).

Although the above on-going applications of Au catalysts are a relatively limited area in comparison with those of Pt-group metals, there are many prospects for widening its capabilities and applications in the near future.

a) Chemical industries: it is desired to develop novel chemical process which can save energy and resources and can minimize burdens on the environment. Gold will make a significant contribution to the selective oxidation of hydrocarbons with oxygen and to the selective hydrogenation of unsaturated hydrocarbons.

b) Environmental protection and maintenance: in addition to indoor-air cleaning at ambient temperature, gold will be effective for the protection of the global environment involving, for example, decomposition of halogenated hydrocarbons, reduction and decomposition of NO and N_2O.
c) Chemical sensors: Semiconductor type gas sensors have already been developed. Optical gas sensors will provide a new technological advance because they are resistant to electrical noise and enable the recognition of gas molecules by using light with different wave lengths
d) Electrochemical processes: the electrochemistry of gold is also expected to find its application in fuel cells, batteries and some electrochemical sensors. One example is as an electrode material for fuel cells (Haruta *et al,* 1997 and references therein).

In order for the above mentioned possible applications to be a reality, a thorough investigation into different aspects of gold and its uses is needed. For over a decade, a number of aspects on the high activity of gold have been agreed upon by researchers. This includes a small gold particle size; preparation method etc. and the attractiveness of using gold-based catalysts for commercial applications will increase as the data continue to be accumulated on these factors (Thompson, 2003; Haruta *et al,* 1997). The following chapter (chapter 2), thoroughly reviews of the work reported on gold as a catalyst. These include the disputes and agreements concerning the activity, the structure and the mechanisms displayed by the gold catalysts studied by different research groups.

1.6 References

Acres G.J.K, *British Patent,* 1,390,182; 1971

Bartlett N., *Gold Bull.,* 31 (1998) 22

Bayler A, Schier A, Mawmaker G.A, Schmidbaur H, *J. Am. Chem. Soc.,* 118 (1996) 7006

Bond G.C and Thompson D.T, *Catal. Rev. Sci., Eng.,* 41 (1999) 319

Bond G.C., *Plat. Met.,* 44 (2000) 146

Bond G.C., *Catal. Today*, 72 (2002) 5

Costello C.K, Kung M.C, Oh H.-S, Wang Y, Kung H.H, *Appl. Catal., A*: 232 (2002) 159

Debeila M.A., PhD Thesis; "*A DRIFTS study of nitric oxide adsorption on Au/TiO_2"*; University of the Witwatersrand, (2000)

Funasaki N., Henmi A., Ito S., Asano Y., Yamashita S., Kobayashi T and Haruta M., *Sensors and Actuators B,* 13-14(1993) 536.

Gardner S.D., Hoflund G.B., Upchurch B.T., Schryer D.R, Kielin E.J. Schryer J.*, J. Catal.,* 129 (1991) 114.

Haagen-Smith A and Fox M, *Ind. Eng. Chem*., 48 (1959) 1484

Haruta M., *Hyomen (Surface),* 28 (1990) 333.

Haruta M., T. Takase and T. Kobayashi, in: S. Yoshida., Eds., *Catal. Sci. Technol. Vol. I,* Kodansha, 1991, pp. 331

Haruta M*,* Daté M, *Appl. Catal. A:* 222 (2001) 427

Haruta M, *Chem. Record,* 3 (2003) 75

Haruta M, Tsubota S, Kobayashi T, Kageyama H, Genet M.J, Delmon B, *J. Catal*., 144 (1993) 175

Hutchings G.J, *Gold Bull.,* 29 (1996) 123

Lucier G., Elder S., Chacow L., and Bartlett N., *Eur. J. Sol. St. Inorg. Chem.,* 33 (1996) 809

Oh H.-S, Costello C.K, Cheung C, Kung H.H, Kung M.C, *Stud. Surf. Sci. Catal.,* 139 (2001) 229

Pyykko P., *Chem. Rev.,* 88 (1988) 563

Rapson W.S, *Gold Bull.,* 29 (1996) 143

Schimpf S., Lucas M., Mohr C., Rodemerck U., Brückner A , Radnik J., Hofmeister H, Claus P., *Catal. Today,* 72 (2002) 63

Schwerdtfeger P, *Angew Chem.*, 108 (1996) 2973

Spicer W.E., Sommer A.H, and White J.G., *Phys. Rev*., 115 (1959) 57

Thompson D.T, *Appl. Catal. A.,* 243 (2003) 201

Thompson D.T., *Gold Bull.,* 31 (1998) 111

Twigg M, *Plat. Met. Rev.*, 43 (1999) 168

Uphade B, Akita T., Nakamura T., and Haruta M., *J. Catal.,* 209 (2002) 331

Wayne P, *"Chemistry of Atmospheres",* 2nd edn., Oxford University Pres, New York 1996

Chapter 2

Literature Review

2.1 Introduction

When gold is highly dispersed as nanosized particles on a metal oxide support it shows a high catalytic activity in several reactions such as the reduction of nitrogen oxides (Salama *et al,* 1996), the epoxidation of propene (Hayashi *et al,* 1998) and the low temperature oxidation of CO (Bond and Thompson, 1999; Haruta *et al,* 1993). The high catalytic oxidation of gold is unexpected as bulk gold is quite inert because of its $5d^{10}$ configuration and even reactive molecules like CO and H_2 do not adsorb on its surface (Tripathi *et al,* 1999, Grunwaldt *et al,* 1999). Over the past decade it has been established that a number of requirements must be met in order to produce a highly active catalyst for the reactions mentioned above. These include a suitable preparation method and preparation conditions, small particle size, and some pretreament conditions. However, certain issues concerning the activity of Au catalysts, such as the nature of the active site (Bond and Thompson, 2000; Triphati *et al,* 1999; Haruta *et al,* 1997 and Haruta *et al,* 2001) and a required particle size (Zanella *et al,* 2004) are still discussed controversially.

2.2 Preparation Method of Au nano-particles

2.2.1 Impregnation

The synthesis of highly dispersed small gold particles is highly sensitive towards the preparation method. It has been reported that the incipient wetness impregnation method is unsuitable for producing highly dispersed gold catalysts (Haruta *et al,* 1997 and Haruta *et al.* 1993). However; Bollinger and Vannice (1996) reported a high activity with catalysts prepared by impregnation after high temperature and low temperature treatment for CO oxidation. The impregnation method involves filling of the pores of the support with a solution of gold salt. Alternatively, a support can be suspended in a large volume of a solution of gold salt, from which the solvent is removed. These are the traditional and simplest methods for dispersing gold and the other metals into the support. These methods are still used today. For example, Au/SiO_2 was recently prepared by suspending silica (Cab-O-SIM5) in a solution containing $HAuCl_4$ after which the solvent was allowed to evaporate to dryness at 80 ^oC (Bailie *et al,* 1999). Supports such as silica (Ntais *et al,* 2004), alumina (Bond and Sermon, 1973), magnesia (Galvagno and Parravano, 1978) are common supports that have been used as a dispersing media. In addition, hematite (α-Fe_2O_3) (Haruta *et al,* 1993), magnesium hydroxide (Vogel *et al,* 1996) and titania (Lin and Vannice, 1991) have been used as supports in the impregnation method. Gold salts such as $HauCl_4$ have been used as a source of gold (Galvano and Parravano, 1978) typically dissolved in water. However, aqua regia has also been used to dissolve $HAuCl_4$ (Nkosi *et al,* 1991). It is to be noted that aqueous solutions of chloroauric acid are sufficiently acidic and capable of dissolving alumina and magnesia (Bond and Thompson, 1999). After drying, the catalyst is typically calcined at high temperature and even temperatures as high as 1073 K (Blick *et al,* 1999) has been used. The gold particles formed in the impregnation method are relatively large compared with those prepared

by other methods. Table 2.1 shows typical particle size values that have been measured and reported. The data shows that particles size range from < 3 nm to > 100 nm. The particle size depends on (i) Au concentration, (ii) pretreatment conditions (e.g. air, vacuum, hydrogen) and (iii) the nature of the gold source used.

Table 2.1: Gold particle sizes in catalysts prepared by impregnation. [a, b, c, d, e]

Support	Au (wt%)	Au source	Size range (nm)	Method used to estimate particle sizes	References
SiO_2	0.19	$KAu(en)_2$	< 3	WAXS	Galvagno, 1978
SiO_2	1.46	$HAuCl_4$	< 100	WAXS	Galvagno, 1978
SiO_2	1.8	$AuCl_3$	30	XRD	Lin, 1993
η-Al_2O_3	10	$HAuCl_4$	(5-10)[a]	TEM	Delgass, 1968
η-Al_2O_3	10	$KAu(CN)_2$	(10-200)[b]	TEM	Delgass, 1968
γ-Al_2O_3	1.25	$HAuCl_4$	26	TEM	Bond, 1973
γ-Al_2O_3	0.06	$[Au(en)_2]Cl_3$	< 3	WAXS	Galvagno, 1978
γ-Al_2O_3	1.62	$HAuCl_4$	>100	WAXS	Galvagno, 1978
MgO	0.67	$KAu(CN)_2$	< 3[b]	WAXS	Galvagno, 1978
MgO	10	$KAu(en)_2$	500	TEM	Delgass, 1968
MgO	4.39	$HAuCl_4$	63	WAXS	Galvagno, 1978
MgO	10	$HAuCl_4$	(10-120)[a]	TEM	Delgass, 1968
MgO	1.5-15	$HAuCl_4$	5-10	TEM	Blick, 1998
$Mg(OH)_2$	5	$HAuCl_4$[c]	0.6-4	XRD, EXAFS	Cunningham, 1998
TiO_2(A)[d]	3.3	$HAuCl_4$	3.5±0.8	TEM	Iizuka, 1997
TiO_2(D)[e]	2.3	$AuCl_3$	25	XRD	Lin, 1993
α-Fe_2O_3	1	$HAuCl_4$	20-30	TEM	Haruta, 1993

[a:] Heated to 413 K

[b:] Heated to 643 K

[c:] Reduced with magnesium citrate

[d:] Anatase,

[e:] Degussa, P-25

Source: Based on Bond and Thompson (1999) and Bailie *et al,* (1999)

2.2.2 Suspension spray reaction method

In this method, the support is suspended in distilled water by ultrasonic treatment; then the aqueous solution of $HAuCl_4$ is added to obtain a spray suspension with the required concentration. The suspension is atomized by means of an ultrasonic device to produce a mist without separation of components. This process is followed by calcination in an air flow under the suction of an aspirator. The product fine particles are collected on a glass filter at the outlet (Fan *et al,* 2003). This preparation method has not been as widely studied as the other methods described in this Chapter. However, Fan *et al.* (2003) have used it to prepare three Au/TiO_2 samples at different spray reaction temperatures viz; 673, 873, and 1073 K. The CO oxidation catalytic activity increased with increasing suspension spray temperature. They reported that for the catalysts prepared at high spray temperatures, the gold particles are highly dispersed on the TiO_2 support because agglomeration could be prevented by the strong interaction between the gold and the support during the preparation process. The deposition of gold on the support increased with increasing spray temperature.

2.2.3 Co-precipitation

This preparation method can produce small Au particles below 10 nm in size, which are strongly attached to the metal oxide support. In addition, co-precipitation of Au and transition metal oxide consumes large amounts of Au solution and creates low surface area supports. Co-precipitation is usually performed by adding an aqueous solution of $HAuCl_4$ and a metal nitrate into an aqueous solution of Na_2CO_3. This manufacturing route is not easy to control. For example, variables include extent of mixing, as well as order and mode of addition of the various compounds, temperature, and ageing period of precipitate in the mother liquor, filtering and washing procedures. High surface area catalysts provide better utilization of expensive catalysts (Wolf and Schuth, 2002). Co-precipitation on the other hand results in some gold particles being encapsulated into the support matrix and hence unavailable to the reacting molecules, whereas deposition precipitation (section 2.2.4) is the preferred method since it results in smaller gold particles supported on the surface of the catalyst.

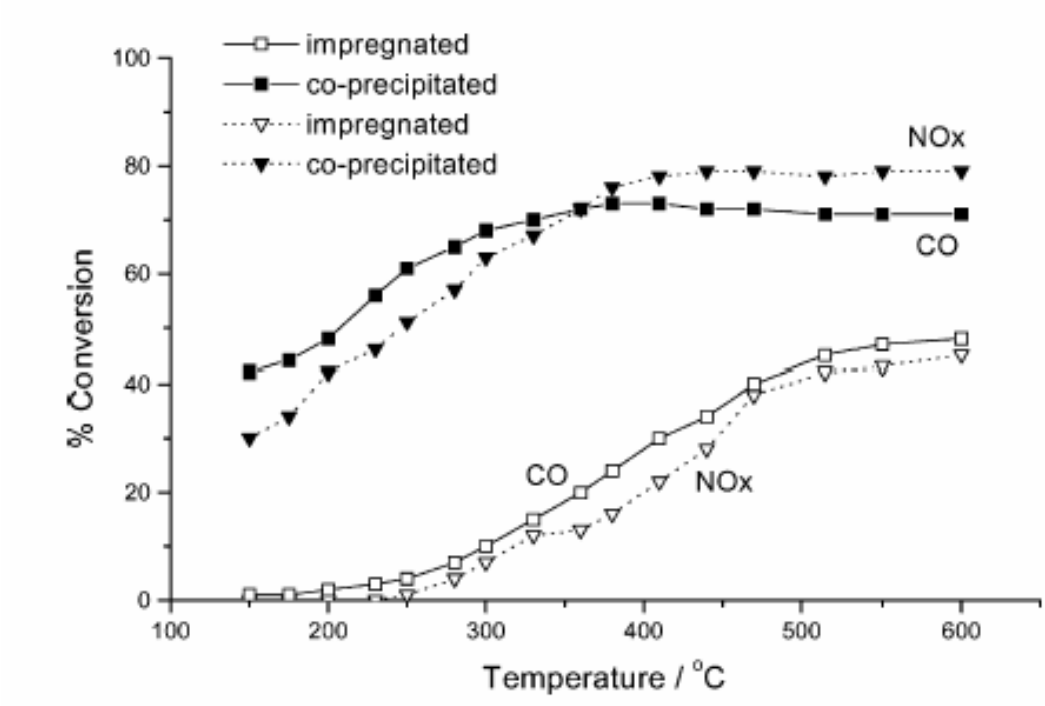

Figure 2.1: Comparison of the activity of Au/CeO_2 catalyst prepared by co-precipitation with that prepared by impregnation method for CO oxidation and NO_x reduction (Golunski *et al,* 2002)

The figure above shows that catalysts prepared by co-precipitation are more active than those prepared by impregnation. There may be several reasons for this behavior, but it has already been reported that the impregnation-derived catalysts contain more chlorine ions which facilitate the agglomeration of Au particles resulting in undesirable larger particles on the surface of the support. Chlorine has also been shown to be a poison for gold catalysts. Luengnaruemitchai *et al.* (2004) also reported the highly selective CO oxidation activity of Au/CeO_2 prepared by co-precipitation compared to those catalysts prepared with impregnation and by sol-gel method. The higher activity of the co-precipitated catalyst was due to the smaller gold particles of less than 5 nm whereas the impregnated catalyst and sol-gel prepared catalyst had particles of sizes 29 and 30 nm respectively. This data also shows the significant effect the preparation method has on particle size which in turn has an

effect on the catalytic activity. It has also been reported that the co-precipitation method results in the encapsulation of some gold particles in the support matrix; therefore unavailable for the adsorption of reacting molecules (Bond and Thompson, 2000) and catalyst calcination is necessary in order to create porosity on the surface of the support by removing chemisorbed water and other molecules during preparation, so that the Au species can be exposed to the reacting molecules. On the other hand, calcination at high temperatures has been reported to alter the Au particle size due to the formation of larger bigger clusters. An increase in the catalytic activity with increasing calcination temperature with catalysts prepared by co-precipitation was reported. However, there was an optimum temperature of calcination required Wang *et al,* (2003). Haruta *et al,* (1993) obtained the rate of $2.6x10^{-3}$ mol CO $(molAu^{-1})s^{-1}$ with 11.5% Au/Fe_2O_3 and observed the higher activity with $0.66\%Au/Fe_2O_3$ catalyst prepared by co-precipitation whereas Wagner *et al.* (1997) and Visco *et al,* (1997) obtained $3.4x10^{-2}$ and $3.4x10^{-1}$ mol $CO(molAu^{-1})s^{-1}$ respectively with 0.56% Au/Fe_2O_3. This data shows that other than the support, other factors such as gold loading are also very important.

2.2.4 Deposition precipitation

Deposition precipitation is the mostly preferred preparation method, because it is believed to produce hemispherical metal particles with their flat planes strongly attached to the support (figure 2.2 below), while other methods such as impregnation and photo catalytic decomposition yield spherical particles which are only loosely bound to the support and need higher temperatures for the CO oxidation and propylene epoxidation reactions to occur (Haruta and Daté, 2001).

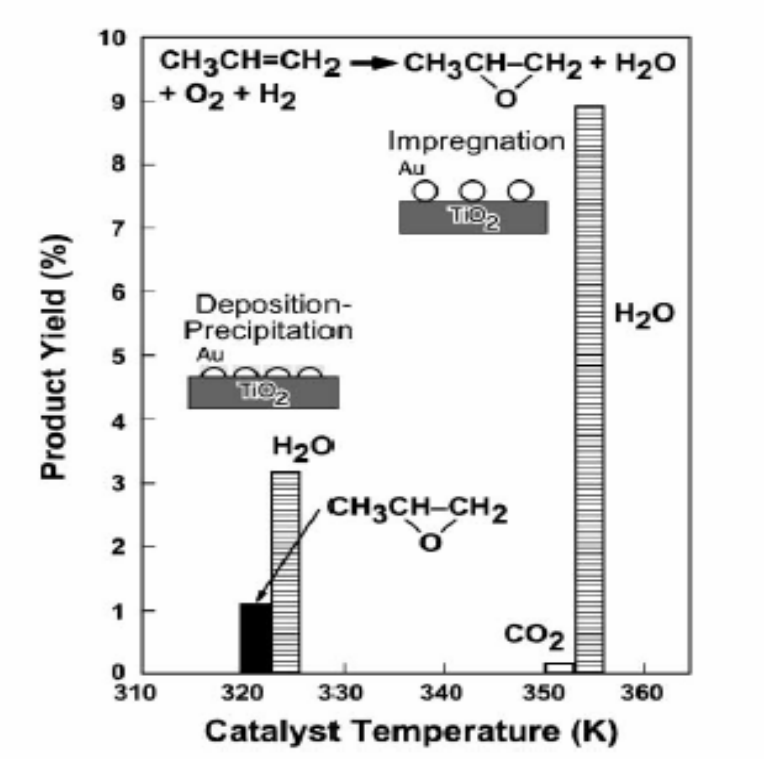

Figure 2.2: Interaction of gold particles with TiO_2 support prepared with different methods (Haruta and Daté, 2001)

In the deposition precipitation method, the Au precursor is brought out of solution onto a suspension of the support. The pH of the solution is raised in order to precipitate Au, typically as a hydroxide. The surface of the support acts as the nucleating center and this leads to a greater part of the active Au precursor being attached to the support. Thus, when the pH of a solution of gold chloride is raised to a value within the range 6-10, hydrolyzed species such as $[Au(OH)nCl_{4-n}]^-$ (n = 1-3) react with the surface of the support. Adhesion of negatively charged gold complexes to the positive support matrix takes place. This procedure is in general applicable to supports with high and medium values of the isoelectric point (point of zero charge = PZC) (Okumura *et al,* 1998). For example, Al_2O_3 with PZC of pH 8 and TiO_2 of pH 5 can be used to deposit gold hydroxide. The pH values below the PZC of the support generate an oxide, which will be positively charged in water and adhesion of

negatively charged colloid/clusters with good dispersion can then occur. SiO_2 has a PZC of pH 2 (Okumura *et al,* 1998) and thus cannot be used as a support with this procedure. This method has been applied to the preparation of Au catalysts supported on TiO_2 (Tsubota *et al,* 1995), Al_2O_3 (Chang *et al,* 1998), Ti-MCM-41 (Kalvacher *et al,* 1999), (Dekkers *et al,* 1999), and iron hydroxide (Boccuzzi *et al,* 1999). Deposition-precipitation has an advantage over co-precipitation in that all of the active components remain on the surface of the support and none is buried within. The method gives rise to a narrow particle size distribution (Bond and Thompson, 1999). The rate of adsorption of $[Au_nCl_{4-n}]^-$ onto a support and the particle sizes generated have been found to depend on the temperature and the value of n, which increases with the increasing pH. Above a pH of 6, particles smaller than 4 nm are formed (Haruta *et al,* 1997 and Haruta *et al,* 1993). The effect of the pH of the starting solution on the particle sizes and the amount of Au deposited onto TiO_2 has been studied by Tsubota *et al,* (1995). The authors reported that in acidic solution (below pH 6) gold particles larger than 10 nm in diameter were formed, while alkaline solutions gave particles with diameters smaller than 5 nm. It was shown that within the pH range 6-8, the number of Au particles is approximately constant. The particle size of Au was found to gradually increase with increasing temperature of calcination in air, but smaller particles were formed in a reducing atmosphere, e.g. CO/He, and H_2/He (table 2.3 below).

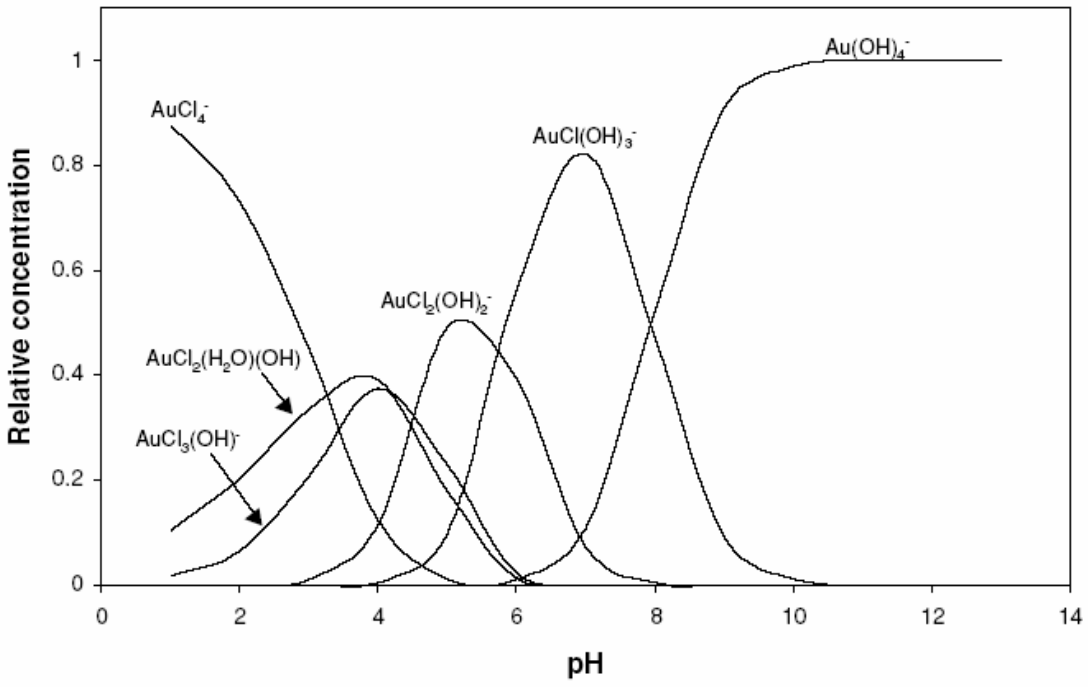

Figure 2.3: Relative equilibrium concentration of gold complexes in $2.5x10^{-3}$ M $HAuCl_4$ solution, calculated with adsorption constants reported by Nechayev and Nikolenko (1999).

In Au catalysts the particle size depends on the value of n in $[Au(OH)_nCl_{n-4}]^{-1}$ which in turn varies with the pH as shown in figure 2.3. The hydrolysis of the $[AuCl_4]^-$ ion has been investigated in detail (Nechayev and Nikolenko, 1999) and $AuCl_3(H_2O)$, $[AuCl_3(OH)]^-$, $[AuCl_2(OH)_2]^-$, $AuCl(OH)_3]^-$ and $[Au(OH)_4]^-$ have been postulated to form in a stepwise manner. Their relative concentrations are dependent on Cl^- and H^+ concentrations as well as the temperature. Reaction 1-6 shows the hydrolysis process for $AuCl_4$.

$[AuCl_4]^- + H_2O \leftrightarrow AuCl_3(H_2O) + Cl^-$ [1]

$AuCl_3(H_2O) \leftrightarrow [AuCl_3(OH)]^- + H^+$ [2]

$[AuCl_3(OH)]^- + H_2O \leftrightarrow AuCl_2(H_2O)(OH) + Cl^-$ [3]

$AuCl2(H_2O)(OH) \leftrightarrow [AuCl_2(OH)_2] + H^+$ [4]

$[AuCl_2(OH)_2]^- + H_2O \leftrightarrow [AuCl(OH)_3]^- + Cl^- + H^+$ [5]

$[AuCl\ (OH)_3]^- + H_2O \leftrightarrow [Au(OH)_4]^- + Cl^- + H^+$ [6]

Lee and Graviilidis (2002) observed an increase in the catalyst activity with increasing pH of precipitation with the Au/γ-Al_2O_3 catalyst with the gold precursor aged for 240 minutes at different pH before loading on the support. They reported that for Au/γ-Al_2O_3, increasing the pH of the solution up to pH 7 increases the concentration of strongly adsorbing complexes ($AuCl_2(OH)_2$ and $AuCl(OH)_3$ and therefore the optimum value of pH is expected where the concentration of the strongly adsorbed species is maximized.

2.2.5 Grafting

In this method a gold complex in solution reacts with the surface of the support forming a catalyst precursor. Okumura *et al.* (2003) described a liquid-phase grafting method, which was used to deposit gold onto TiO_2, Al_2O_3, and SiO_2 oxide supports using $Me_2Au(acac)$ as the gold precursor. This gold salt was dissolved in acetone, and a weighed quantity of metal oxide support was introduced. The mixture was stored in a refrigerator overnight. The solvent was then removed by filtration, and the metal oxide support with gold adsorbed precursor was calcined in air at 673 K. The mean diameters of gold particles were found to be comparable with those prepared using gas-phase grafting and other methods. This method was described as being applicable

to metal oxide supports commercially available and not necessarily only to freshly-prepared metal hydroxide supports. In their earlier study, Okumura *et al.* (2002) observed a higher activity for the hydrogenation of 1,3 butadiene over Au/Al_2O_3 prepared by the liquid-phase grafting method over that prepared by gas-phase grafting.

2.2.6 Ion exchange

This is a technique in which the protons (H^+) or other cations associated with a support exchange for Au^{n+} ions. Gold was dispersed into HY zeolite by cation exchange using $[Au(en)_2]^{3+}$, followed by thermal decomposition at 423 K (Guillemont *et al,* 1997). In this method, the majority of particles have diameters in the range 1-4 nm with the smallest being determined by the cavities of a zeolite. Larger particles (> 5nm) can be found on the outside of the zeolite. An alternative exchange method has been reported. This involves grinding a mixture of Au_2Cl_6 and NaY zeolite together followed by heating of the ground mixture in a vacuum. The volatile salt moves into the zeolite pores (Salama *et al,* 1994). The presence of water was said to cause reduction of Au^{3+} to Au^+ ions. In a similar fashion, when NaY powder was mechanically mixed with $AuCl_3$ crystals and heated in vacuum at 353 K for 16 h in a nitrogen atmosphere, a pale yellow sample denoted as $AuCI_3$ /NaY was found (Qiu *et al,* 1992). The absence of crystalline $AuCl_3$ (from XRD data) was interpreted to mean that $AuCI_3$ was present in the zeolite pores at monolayer dispersion.

2.2.7 Chemical vapour deposition (CVD)

In this method, a volatile gold compound is transported onto the support by means of a carrier (inert) gas to form a precursor to the active species. This method is suitable for a support such as silica were deposition precipitation is not suitable. For example, the method has been used to prepare gold supported catalysts using MCM-41, Al_2O_3 and TiO_2 (Okumura *et al,* 1998) as support. Organo-gold complexes are generally used as gold sources, e.g. β-diketonate, goldacetylacetone dimethylgold (111).

Lai *et al,* (1998), studied the nucleation and the growth of Au nanoclusters, which were vapour deposited onto TiO_2 (110) under ultra high vacuum conditions, using scanning tunneling microscopy (STM). The authors observed two different stages of Au cluster growth on TiO_2. At low Au coverage the formation of small quasi-2D clusters with varying shapes were observed and the formation of semi-spherical 3D clusters was observed as Au coverage increased. With increasing Au coverage the cluster size steadily increased while density remained constant. Similar observations were earlier reported by Zhang *et al.* (1997) for the growth of ultra-thin Au films on TiO_2 (110) surfaces using low energy ion scattering spectroscopy (LEIS), X-ray photo-electron spectroscopy (XPS) and low energy electron diffraction (LEED).

2.2.8 Iwasawa method

The Iwasawa group has developed a new method of obtaining dispersed Au particles on oxide surfaces (Yuan *et al,* 1996; Yuan *et al,* 1997; Kozlova *et al,* 1998; Kozlov *et al,* 1999). In this method, the as-prepared wet metal hydroxide $M(OH)_x$ is first prepared by hydrolysis of the corresponding nitrate (M=Fe, Mn, Ni, Co, Ce, Zn, Mg, Cu, La, etc.) or an alkoxide (M=Ti) with an aqueous solution of Na_2CO_3, NH_4OH or H_2O. The precipitates are therefore washed with distilled water to neutral pH and used as supports for Au phosphine complexes. The acetone solution of the gold complex is impregnated onto the freshly precipitated support, $M(OH)_x$ to form $Au/M(OH)_x$ catalyst after evaporation of the solvent in vacuum at room temperature.

The key issues of preparation are: (i) choice of suitable Au complexes as precursors for Au particles, (ii) use of as-precipitated wet metal hydroxides as precursors for oxide supports which have many surface OH groups reactive to the Au complexes and (iii) simultaneous transformation of both precursors of gold particles and oxides under their chemical interactions by temperature programmed calcination (Kozlov *et al,* 1999). Au phosphine complexes are good candidates of metal precursors because they are thermally decomposed to Au metal in a temperature range similar to that used for the transformation of wet metal hydroxides to oxides, and the phosphine ligands are expected to retard the growth of Au to large metallic particles (Yuan *et al,* 1996; Kozlov *et al,* 1999). The steady–state rate of CO oxidation of 0.5wt% Au/Fe_2O_3 catalyst prepared from $Au(PPh_3)(NO_3)$ and as-precipitated wet iron hydroxides was $3.9x10^{-2}$ mol CO/mol Au/s at 252 K. The rate was higher than that of

corresponding co-precipitated catalysts calcined under the identical conditions by a factor of >3. Activities of conventional impregnation catalysts were lower by at least two orders of magnitude compared with the catalysts prepared by the Iwasawa method. Highly active catalysts were also obtained when $[Au_9(PPh_3)_8(NO_3)_3]$ and $Au(NO_3)(CNBu^t)$ were used as precursors by Yuan *et al.* (1997) and Mathieson *et al.* (1998) respectively. In the case of titania-supported Au catalysts the preparation method gave a Ti oxide-supported Au catalyst with an activity of $9.6x10^{-3}$ mol CO/mol Au/s at 300 K (Yuan *et al,* 1998). It is now documented that the activity of gold catalysts for CO oxidation is sensitive to the nature of support, the size of gold particles and the properties of the gold support interface. The low melting point of gold results in difficulty preparing gold catalysts in highly dispersed state. The possibility of fast Au agglomeration during catalyst preparation may be one of the main reasons why choice of a preparation method has profound effects on the catalytic activity of gold to a much greater extent than in the cases of other noble metal catalysts (Liu *et al,* 1999).

Kozlov *et al.* (1999) have reported that a very high catalytic activity of gold can be achieved when as-precipitated wet metal hydroxides $M(OH)_x$ are used as support precursors and $AuPPh_3NO_3$ is used as a gold precursor. The $Au=M(OH)_x$ ($M=Mn^{2+}$, Co^{2+}, Ni^{2+}, Fe^{3+}, Zn^{2+} and Ce^{4+}) exhibited remarkably high activities for CO oxidation and achieved 100% CO conversion at 273 K or even lower as shown in table 2.2 below. On the other hand, supporting this precursor on $Al(OH)_3$ did not produce significant activity.

Table 2.2: Catalytic oxidation with various $Au/M(OH)_x$ (Kozlov *et al,* 1999)

Catalyst	Support Precursor	Au Precursor	$T_{50\%}$(K)	$T_{100\%}$(K)
$Au/Mn(OH)_2$	$Mn(NO_3)_2$	$AuPPh_3NO_3$	<203	273
$Au/Co(OH)_2$	$Co(NO_3)_2$	$AuPPh_3NO_3$	<203	273
$Au/Ni(OH)_2$	$Ni(NO_3)_2$	$AuPPh_3NO_3$	230	273
$Au/Fe(OH)_3$	$Fe(NO_3)_2$	$AuPPh_3NO_3$	206	273
$Au/Fe(OH)_3$	$Fe(NO_3)_2$	$[Au_9(PPh_3)_8](NO_3)_3$	240	273
$Au/Fe(OH)_3$	$Fe(NO_3)_2$	$AuPPh_3Cl$	673	>773
$Au/Zn(OH)_2$	$Zn(NO_3)_2$	$AuPPh_3NO_3$	248	273
$Au/Ce(OH)_2$	$(NH_4)_2Ce(NO_3)_6$	$AuPPh_3NO_3$	263	283
$Au/Mg(OH)_2$	$Mg(NO_3)_2$	$AuPPh_3NO_3$	250	>373
$Au/Mg(OH)_2$	$Mg(NO_3)_2$	$[Au_9(PPh_3)_8](NO_3)_3$	300	673
$Au/Ti(OH)_4$	$Ti(i\text{-}OC_3H_7)_4$	$AuPPh_3NO_3$	304	433
$Au/Cu(OH)_2$	$Cu(NO_3)_2$	$AuPPh_3NO_3$	334	443
$Au/La(OH)_3$	$La(NO_3)_2$	$AuPPh_3NO_3$	335	503
$Au/Al(OH)_3$	$Mn(OH)_2$	$AuPPh_3NO_3$	606	>633

Note: $T_{50\%}$: temperature for 50% conversion; $T_{100\%}$: temperature for 100% conversion; reaction conditions: 200 mg of catalyst, SV=20 000 ml $h^{-1}g^{-1}$ at atmospheric pressure, CO=1% balanced with air.

2.2.9 Other recently developed methods for the synthesis of Au nano-particles

The deposition of nano-sized metals can also achieved through electrochemical methods, e.g. under potential deposition (UPD) (Gilbert *et al,* 1996), and deposition using the tip of a STM (Kolb *et al,* 1997). These methods require direct contact between the substrate and the metal ions in solution to affect electron transfer for the reduction of metal ions.

Another method was also described by Sumida *et al.* (1999) for preparing gold nano-particles on a self assembled organic monolayer on Au(111) in an organic solvent, (e.g. acetonitrile or ethanol,) containing $AuCI_4^-$ ions under photo-irradiation (Sumida *et al,* 1999). In this method, the solvent molecules (e.g. EtOH and DMF) not only act as coordinating ligands, but also as electron donors to reduce gold ions. Changing the type of solvent and irradiation time varied the size and the shape of these particles.

Meldrum *et al.* (2000) prepared porous gold structures using echinoid skeletal plates, followed by organic matter removal (by a hot air gun). The sample was then annealed in a furnace at 400 ºC for 36 h. This class of material can serve as a catalyst support, due to its well defined pore size and the material is similar to a zeolite. Attempts to produce micro porous TiO_2 structures through the use of sol-gel methods have also been attempted (Meldrum *et al,* 2000).

Nano-particles of Au (and also Pt, Pd and Ag) supported on Al_2O_3 have been synthesized by combustion methods (Bera *et al,* 1999). This approach involves

dissolving $Al(NO_3)_3$ and $HAuCl_4$ in a minimum volume of water. The solution was then introduced into a muffle furnace at 500 ºC and allowed to boil; the solid underwent dehydration. At the point of complete dehydration, the surface foam ignited, burning with a flame and yielding a solid product. The new materials were characterized by XPS, XRD, and TEM. The catalytic activity of these materials for CO oxidation and CO + NO reactions was high.

Nano-size Au particles supported on TiO_2 were recently synthesized by a "surface sol-gel" method. $HAuCl_4$ was reduced by $NaBH_4$ in methanol/acetic acid in the presence of $[(OH(CH_2)_{11}S)_2]$ as stabilizer. A resonator covered by a thin layer (~8 Å) of TiO_2 was immersed into a gold colloidal solution in methanol. The material was then washed in methanol and then underwent ultra-sonification. The resulting deposited particles were characterized by SEM and UV-VIS spectroscopy and were reported to be uniform in size and spherical in shape. Physical and chemical methods for preparing metal nano-particles were applied to various other single metals and bimetallic nano-particles (Rao *et al,* 2000), (Debeila, 2000).

Hoflund *et al.* (1995) attempted to mount Au/MnOx co-precipitates on a monolith by immersing it in a mixture of $HAuCl_4.XH_2O$ and $Mn(NO_3)_2$ solutions while adjusting the pH, but the resulting monolith was not active at temperatures below 100 ^oC. A possible reason was suggested to be low loading of Au/MnO_x, since Au/MnO_x co-precipitates were observed in the solution but not in the monolith.

2.3 Catalyst synthesis and pretreatment conditions

The preparation of active gold catalysts depends on various synthesis and pretreatment conditions. For example, variables include extent of mixing, as well as order and mode of addition of the various compounds, temperature, and ageing period of precipitate in the mother liquor, filtering and washing procedures (Wolf and Schuth, 2002).

Zanella *et al.* (2004) have investigated the effect of using NaOH and urea as a precipitating agent. They observed slightly bigger particles with the catalyst precipitated with NaOH and reduction of Au particle on this catalyst began at a calcination temperature of 100 ^{o}C, whereas of that catalyst precipitated with urea began to reduce at 150 ^{o}C. Another study by Wang *et al.* (2003) revealed that the presence of Na^{+} ions in the precipitating agent results in enhanced catalytic activity and stability. They have observed a very low initial activity of 15% CO conversion with the catalysts precipitated with NH_4OH whereas catalysts precipitated with Na_2CO_3, NaOH, and $(NH_4)_2CO_3$ showed a total conversion. However, the life time of Au/ZnO/P (P= Na_2CO_3, NaOH, or $(NH_4)_2CO_3$) is different following the sequence of Au/ZnO/Na_2CO_3> Au/ZnO/NaOH> Au/ZnO/$(NH_4)_2CO_3$. Thus Na_2CO_3 was found to be the best precipitant. The authors ascribed the low activity of Au/ZnO/NH_4OH to the bigger gold particles (observed by XRD) that resulted during synthesis whereas other catalysts were found to have smaller gold particles and concluded that precipitating agent has a significant effect on the gold particle size. This can be supported by the study conducted by Uphade *et al.* (2002) who investigated the effect of the precipitating agent in Au/Ti-MCM-48 for the epoxidation of propene. They observed high activity with the catalyst precipitated with NaOH. This precipitation agent was found to be the best compared with other bases of the group 1 elements and the activity was in the sequence of NaOH > KOH > RbOH > LiOH > CsOH. In contrast, a different sequence of Li > K > Na, as carbonates rather than as hydroxide

on Au/MnO_x catalyst was reported by Hoflund *et al.* (1995). It was also noted that the alkali metal ions are often used as promoters in partial and complete oxidation catalysts (Hoflund *et al,* 1995, Gardner *et al,* 1991, Gardner *et al,* 1991 (a)).

Most researchers have been investigating the effect of catalyst calcination and there are some disputes concerning this matter. Haruta *et al.* (1989) suggest that an active catalyst is that which is calcined at 300 ^oC for Au/TiO_2 to produce well reduced gold particles whereas Zanella *et al.* (2004) reported that a catalyst only needs to be calcined at 200 ^oC, where they observed a total reduction into metallic gold species. These results, agree with those of Tsubota *et al.* (1995 a) who observed higher activity with increasing calcination temperature with 1% Au/TiO_2 prepared from a mechanical mixture of colloidal gold and TiO_2 powder. They suggested that the increase in activity is due to the formation of a stronger interaction between the two phases during calcination. Wang *et al.* (2003) observed an improved stability with Au/ZnO catalyst calcined at 240 ^oC whereas catalysts calcined at lower temperatures and at higher temperature deactivated faster. Surprisingly, all the catalysts except the one calcined at 50 ^oC achieved total initial conversion. It is shown that (table 2.3) an increase in calcination temperature results in an increased Au particle size.

Table 2.3: Mean particle diameters determined by TEM observation of samples prepared by deposition precipitation and calcined under a variety of conditions. [a, b, c]

Temperature (°C) (Calcination)	medium	(nm)
200	air	2.95 ± 0.95
300	air	3.08 ± 0.75
400	air	3.58 ± 0.67
500	air	4.33 ± 0.96
600	air	6.68 ± 1.35
250	air[b]	3.27 ± 0.59
250	N_2[b]	2.72 ± 0.63
250	10%/CO/He[b]	2.64 ± 0.54
250	10%H_2/He[b]	2.13 ± 0.49

a: Based on Tsubota *et al,* (1995)

b: Prepared at pH 7; calcined for 4 h; Au loading = 1.4 atom %; Support: TiO_2

c: flowing gases; 20ml/min

The improved catalyst activity noted with increasing calcination temperature was also reported by Kozlov *et al.* (1999) with Au/$Fe(OH)_3$ catalysts prepared by the Iwasawa method.

Examination of catalysts prepared by mixing colloidal Au particles with TiO_2 showed that under low temperature calcination conditions (~ 200 °C) Au particles retained their original sizes and were well dispersed (Tsubota *et al,* 1995). However, Au particle sizes grew with increasing calcination temperature up to (~ 600 °C). The particle sizes increased with increasing temperature and the effect was greater than that observed using deposition-preparation. It was also noticed that not only did the

size of the particles increase, but the shape also changed with temperature. For example, catalysts calcined at 200 ^{o}C had particles with spherical shape while those calcined at 600 ^{o}C were close to hemi-spherical in shape. On contrary, Park and Lee, (1999) and Wolf and Schuth (2002) observed the decrease in catalyst activity with increasing calcination temperature in both the presence and absence of water in the reactor. It is believed that during calcination a fraction of Au ions will auto-reduce, as oxygen is lost. If the model suggested by Bond and Thompson (2000) is to be taken into consideration, where the active catalyst is that which contains both metallic and ionic gold, the uncalcined catalyst in most reported studies (Costello *et al,* 2002; Oh *et al,* 2001; Zanella *et al,* 2004) contain ionic gold particles, mainly Au^{III}, which is believed to form the chemical glue between the metallic gold and the support. If higher calcination temperatures are used, all the ionic gold species are reduced to metallic gold, hence the chemical glue is lost from the interface and sintering can occur easily (Park and Lee, 1999 and Bond and Thompson, 2000). Triphati *et al.* (1999) observed an inhibited adsorption of both CO and O_2 by IR on Au/Fe_2O_3 at higher calcination temperature which in turn decreased the activity of the catalyst.

Wolf and Schuth (2002) reported that the highest activity with Au/TiO_2 and Au/Co_3O_4 catalysts calcined at 200 ^{o}C compared to samples calcined at 300, 400, and 500 ^{o}C. The activity decreased with increasing calcination temperature, and the authors attributed this to the corresponding increase in gold particle size. They note also that the reason for the decrease in catalytic activity could be the change of oxidic gold to metallic gold that occurs with increasing calcination temperature. However, they argue that after 400 ^{o}C all the gold should be metallic, yet these samples still exhibit activity for CO oxidation, implying that metallic gold is the active species. Similar results were obtained by Park and Lee (1999), who observed that for both Au/TiO_2 and Au/Fe_2O_3 the activity decreased with increasing calcination temperature. The highest activity was observed for catalysts calcined at 100 ^{o}C. Investigation by XPS showed that these samples contained the largest amount of

oxidic gold and that the ratio of oxidic to metallic Au decreased with increasing calcination temperature, indicating that oxidic gold is responsible for high CO oxidation activity. This agrees with the results of other research groups (Visco *et al,* 1997; Finch *et al,* 1999; Minaco and Scire, 1997) who also found that the catalysts exhibiting the highest activity were those containing the largest ratio of oxidic to metallic gold.

The pH at which the catalyst is precipitated has a very important role in determining activity of the catalyst. As described above, the pH determines the nature of the Au particles deposited on the surface of the support. An increase in catalytic conversion with increasing pH was observed by Uphade *et al.* (2002) with Au/Ti-MCM-48 catalysts used for the epoxidation of propene at 150 ^{o}C reaction temperature. Conversion increased from a pH of 6.0 reaching an optimum at pH 7 above which conversion stared to decrease. Wolf and Schuth (2002) observed decreasing gold particle size with increasing pH value and correlated it with the decreasing amount of gold. Haruta *et al.* (1997) reported that for Au/TiO_2 in the pH range 6-10, the particle size was below 5 nm in diameter and did not change significantly. On the other hand, Wolf and Schuth (2002) reported the most active catalyst based on TiO_2 being that precipitated at pH 8. These differences can be due to the different isoelectric point of different supports.

Various pretreatment conditions lead to different activities of catalysts. This is because; the catalyst structure is altered during pretreatment. For instance, pre-treating the as-prepared catalyst in air, at 100 ^{o}C removes the adsorbed water molecules, which may hinder the adsorption of reacting molecules on the surface of the catalyst. Park and Lee (1999) observed a decreased activity with Au/TiO_2 catalysts pretreated in reducing medium (H_2) relative to that seen when the catalyst was treated in N_2.

The best activity was achieved with the catalyst pretreated in air. It was reported that, treatment of the catalyst in H_2 medium result in the formation of Au^0 at the expense of Au^+ species and it was also reported that the treatment of a catalyst with hydrogen and oxygen at higher temperatures results in the removal of chlorine ions on catalyst prepared by impregnation (Pestryakov *et al,* 2002). On the other hand, high temperature reduction was reported to reduce the agglomerated Au particle size during calcination in air at 400 ^oC of $Au/Fe_2O_3/Y$ (Kang and Wan, 1995). The reduced catalyst was reported to have the highest dispersion than those of other treatments, but its activity was not the highest and this was ascribed to the sever adsorption competition between the CO and O_2 on the active site.

It was also reported that pretreatment with the stream of He containing some trace amount of water followed by thermal treatment at 400 ^oC had the highest activity at 40 ^oC reaction temperature than those pretreated in reductive medium after calcination in oxygen and this was ascribed to the reduction and removal of OH groups from the ionic Au species (Kang and Wan, 1995). Hoflund *et al.* (1995) observed no difference in the catalyst activity between the catalyst pretreated in a stream of helium at 125 ^oC and the untreated catalyst, but they conceded that water adsorbed is removed during this pretreatment which means that the presence of adsorbed water had no effect. In their earlier study (Gardner *et al,* 1991 (a)), they observed an improvement in catalytic activity with treatment in 5 vol.% CO in He at 50 ^oC. A similar pretreatment at higher temperature did not result in any further activity improvement, but a mild pretreatment of the catalyst in an oxidizing environment resulted in a poorer performance.

2.4 Effect of Support

For CO oxidation, many oxides other than the materials such as SiO_2 and activated carbon can be used as support and induce activity even below 300 K. Semi-conductive metal oxides such as TiO_2, Fe_2O_3 and NiO provide more stable Au catalysts than do insulating metal oxides such as SiO_2 (Haruta, 2003). The difference also appears in the moisture effect. Alumina (Oh *et al,* 2001, Daté and Haruta, 2001) and silica (Daté and Haruta, 2001) supports require a concentration of water 10 ppm greater than that for TiO_2 for CO oxidation to proceed at room temperature. Alkaline earth metal hydroxides such as $Be(OH)_2$ and $Mg(OH)_2$ are excellent choices for demonstrating high activity at a temperature as low as 196 K. In contrast, when an oxidic material such as SiO_2, WO_3 or activated carbon is used as a support, gold exhibits poor activity even at temperatures above 473 K, the conversions being below 100% (Haruta, 2003). However, the presence of activated carbon on $Au/Fe_2O_3/ACF$ (ACF = Activated carbon fiber) produced higher CO oxidation activity than that of $Au/Fe_2O_3/Al_2O_3$ and was beneficial for Au particle dispersion (Bulushev *et al,* 2002). The type of support used for a gold catalyst has a very significant effect on the Au particle size. For instance, Haruta *et al.* (1993) produced 6-7 nm of gold particles supported on Co_3O_4 by deposition precipitation and 2nm of gold particles on TiO_2 using the same preparation method. On the same study they also produced 4 nm of gold particles on γ-Fe_2O_3 by co-precipitation whereas Bollinger and Vannice (1996) reported 33 nm on TiO_2 using the same preparation method.

Structural complexity in the support also occurs during preparation and pretreatment. This is exemplified by ferric oxide. Co-precipitation using sodium carbonate leads to the formation of ferrihydrite, a structurally disordered material having the composition $Fe_5HO_8.4H_2O$, and FeO(OH) (goethite), which after calcination

transforms into α-Fe_2O_3 (hematite) (Bond 2002; Finch *et al.* 1999). Kozlov *et al.* (1999) compared the effect of supporting Au on $Fe(OH)_3$ and on Fe_2O_3 by the Iwasawa method. It was reported that Au/$Fe(OH)_3$ catalyst calcined at 400 ^oC was more active than Au/Fe_2O_3 calcined at the same temperature. This difference was attributed to the particle sizes obtained after calcination. Au particles were found to increase to 12 nm on Au/Fe_2O_3 whereas Au/$Fe(OH)_3$ still contained an average of 2.6 nm sized Au particles. This shows the effect of the support on stabilizing the smaller Au particles at high temperature.

Grunwaldt *et al.* (1999 a) emphasized a strong support effect on the activity of the catalysts. They prepared Au/TiO_2 and Au/ZrO_2 catalysts by adsorption of gold colloid onto the support. Here Au/TiO_2 achieved 21% and 100% conversions at 305 and 353 K respectively whereas the Au/ZrO_2 catalyst was inactive at both temperatures. This study also shows the strong effect the support has on the gold particles. Wolf and Schuth (2002) observed the best activity with Au/TiO_2 catalyst with the PZC of 6, giving $T_{1/2}$ at -60 ^oC whereas supporting gold on SiO_2 gave the lowest activity as shown in the table below. The low PZC of the support makes it difficult to make a good catalyst with precipitation methods. However, appreciable activity was reported with the catalyst prepared by CVD.

Table 2.4: Temperature of 50% conversion obtained for the best catalysts

Sample	PZC	$T_{1/2}$ (°C)
Au/TiO_2	~6.0	-60
Au/ZrO_2	~6.7	-20
Au/Al_2O_3	~9.0	-44
Au/Co_3O_4 (DP)[a]		-62
Au/Co_3O_4 (CP)[b]		~10
$Au/CoAl_2O_3$		-32
Au/SiO_2	1.0–2.0	>200

[a] DP: deposition–precipitation.

[b] CP: co-precipitation.

Based on Wolf and Schuth (2002)

It has been reported that small gold particles can also be stabilized by inserting them into the cages of zeolites. Different kinds of zeolites have been used as supports for Au, for catalyzing different reactions. For instance, type Y zeolite was used as a support for Au for the oxidation of CO (Lin *et al,* 2002, Lin *et al,* 2003). Qui *et al.* (1994) used Au_2Cl_6 as a precursor to prepare Au^I/NaY via solid-vapor reaction. Guillemot *et al.* (1996) used $[Au(en)_2]Cl_3$ to prepare Au/NaHY via cation exchange method. Au/NaY catalysts were prepared by impregnation method and found to be active for the reduction of NO by H_2. The rates of N_2 and N_2O formation on Au(I)/NaY catalyst were almost twice those found for Au^0/NaY catalyst in the temperature range of 433 – 623 K (Salama *et al,* 1996). Horvath *et al.* (2001) compared the activity of Au/HY and that of Au-Fe/HY and observed better activity with the bimetallic catalyst on CO oxidation. On the other hand; Kang *et al*. (1995) compared Au/Y and Au/Fe/Y on CO oxidation and observed a higher activity in the catalyst containing Fe. Other zeolite-supported catalysts and zeolite containing

catalysts, such as Au/Ti-MCM-41 (Sinha *et al,* 2003), Au/Ti-MCM-48 (Haruta, 1997 (i)), have been used for propylene oxidation. However, chlorine contamination was also a problem in these catalysts as it is for the catalysts with transition metal oxide supports. High temperature treatment is therefore required to activate these catalysts which in turn results in sintering (Lin *et al,* 2002).

The use of composite oxides has not been widely studied as the support for gold nano-particles to investigate the effect of the second support on the catalyst. Wang *et al,* (2003) has investigated the effect of the presence of the second metal oxide on Au/Al_2O_3 catalyst for CO oxidation reaction. They observed a lower $T_{100\%}$ with $Au/FeO_x/Al_2O_3$ than with Au/Al_2O_3. Grisel *et al.* (2002) observed a lower particle size of 2.6 nm for $Au/MgO/Al_2O_3$ catalyst compared to 3.6 nm of Au/Al_2O_3. In their earlier study, they reported the stabilization of Au particle size in the presence of MgO on Au/Al_2O_3 catalyst (Grisel *et al,* 2001). In contrast, Mallik *et al.* (2003) observed a lower catalytic activity with Au/TiO_2-ZnO than with Au/TiO_2. The data shows that the catalytic activity of the catalyst depends on both the particle size and the nature of the support.

2.5 Effect of Particle Size

It is widely accepted that small gold particle size is desirable for the high activity of gold catalysts for CO oxidation (Grisel *et al,* 2002), methane oxidation (Grisel *et al,* 2000), and selective CO oxidation (Grisel *et al,* 2001). What is not clear is the optimal diameter of the gold particles and whether this diameter differs with different supports or pre-treatment conditions. As the size of a metal particle is decreased, a number of things happen: (i) obviously the fraction of surface atoms increase, and because these vibrate more freely the melting temperature falls and surface atom

mobility rises. (ii) Because the overlap of electron orbitals decreases as the average number of bonds between atoms becomes less, the band structure is weakened, and surface atoms in particular start to behave more as individuals than as members of the club. (iii) At the same time, a greater fraction of the atoms comes into contact with the support, and the length of the periphery per unit mass of metals rises (Haruta and Daté, 2001). However, some authors have observed higher activities with Au particles of about 3 nm (Haruta, 2003, Valden *et al,* 1998, Akita *et al,* 2001).

Okumura *et al.* (1998) used a CVD method to prepare Au/TiO_2, Au/SiO_2 and Au/Al_2O_3 catalysts. The average gold particle diameters of 3.8, 6.5 and 3.5 nm respectively, and the turnover frequencies were 0.02, 0.02 and 0.01 s^{-1} respectively. Small differences suggest that similar activities were obtained over a range of gold particles and different supports. Bollinger and Vannice (1996) compared a catalyst prepared by impregnation with 25 nm and that prepared by co-precipitation with 4.5 nm and observed similar activities. Different preparation methods result in different activities of the catalysts. It is generally accepted that traditional incipient wetness (impregnation) method results in bigger gold particles, and chlorine can not be removed from the catalyst other than by treatment at high temperature which in turn increases the gold particle size. Zanella *et al.* (2004) observed an increase in the activity of the catalyst with increasing particle size from 1.1 nm to about 2.2 nm, but activity decreased with gold catalysts containing particles larger than 2.2 nm, in Au/TiO_2 catalysts synthesized by deposition precipitation using urea as a precipitation agent. This study shows that there is an optimum particle size of ~ 2 nm required for the high activity of Au catalysts.

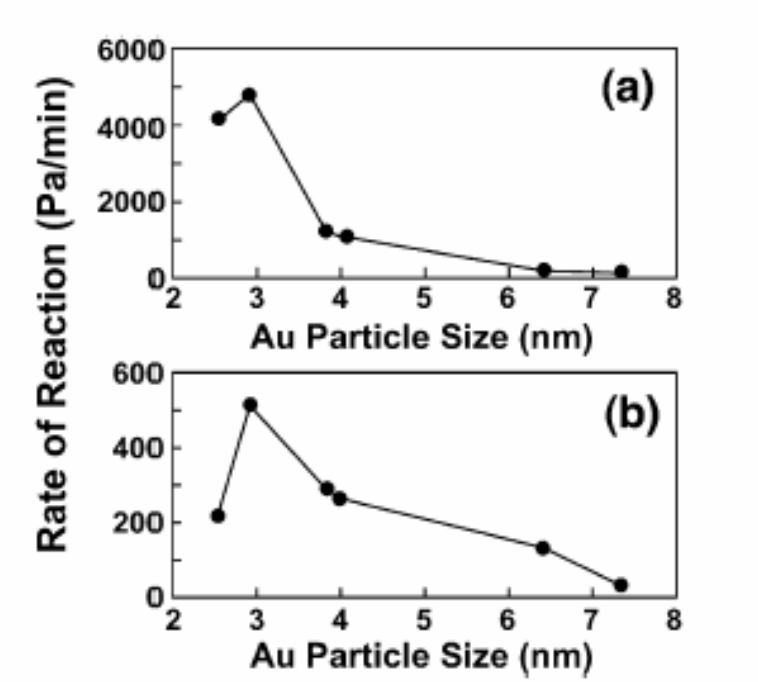

Figure 2.4: Dependence of the catalytic activity of (a) CO oxidation (b) acetylene hydrogenation on particle diameter (Haruta and Daté, 2001, Jia *et al,* 2000).

The figure above shows in an increase in the activity of the catalyst with increasing particle size, but the optimum activity was observed with the catalyst containing 3 nm Au particle size. An increase in the particle size to 4 nm and above decreases the activity of the catalyst on both CO oxidation and acetylene hydrogenation. Generally it has been agreed in the literature that small gold particles are required for the higher activity of the catalysts, but there is still a contradiction in the optimum particle since some reported 3 nm (Valden *et al,* 1998) and others about 2 nm (Zanella *et al,* 2004). Kang and Wan (1995) reported that the catalyst containing smallest particle size and the highest dispersion was less active than those that contained bigger particles and this was attributed to the different catalyst pretreatment. It therefore becomes clear that the particle size is not the only aspect to consider since these catalysts are prepared with different supports and this brings about the effect of the support on the

oxidation state of Au particles which has also been discussed with sharp differences in the literature.

2.6 Oxidation State of Gold

It was claimed that the effect of the Au oxidation state is as important as that of the size of gold particles (Park and Lee, 1999). It has been suggested that the role of the metal oxide is to stabilize the gold nano-particles and that the reaction takes place on the gold surface (Haruta *et al,* 1997; Haruta *et al,* 1989; Valden *et al,* 1998).

It has also been proposed that the reaction takes place at the gold/metal oxide interface and that the metal oxide could act as a source of oxygen (Kozlov *et al,* 1999). On the other hand researchers proposed that the active species is metallic gold because they found no evidence of the presence of ionic gold species on their active catalysts (Griesel *et al,* 2002 and Guczi *et al,* 2000). Grisel *et al.* (2001) and Grisel *et al,*(2002) argue that due to the high activity of the pre-reduced catalysts over those that are pre-oxidized, Au^{I} species does not exist in such catalysts and even if they do, they are not necessary for the high activity of the catalysts on CO oxidation. High activity of the pre-reduced catalysts was also observed by Bulushev *et al.* (2002). Zanella *et al.* (2004) observed an increased activity with the increasing amount of metallic gold species on Au/TiO_2 catalysts, of which the highest activity was achieved with the catalyst calcined at 200 ^{o}C which according to their XANES results contained 100% Au^{0} species. Even though most of the authors believe that their active catalysts only contain Au^{0} species, and it is the only species responsible for the high activity of gold catalyst, some are beginning to concede that there is a possibility of the existence of oxidic Au species, probably in the form of $Au(OH)_3$ or Au(OH) at the perimeter interfaces at the conditions where water is present at concentration

above 1 ppm, but still dispute their involvement in the CO oxidation reaction (Haruta, 2003).

Based on the spectroscopic analysis indicating the presence of ionic gold in the most active catalysts, some researchers proposed the ionic gold to be necessary for high CO oxidation activity although there is no consensus on whether Au^{III}, Au^{I} or both, are important. However, other groups have reported that their as prepared catalysts containing mainly Au^{III} species were not active for CO oxidation and activity increases with the increasing reduction of these species (Costello *et al,* 2002; and Zanella *et al,* (2004). Several groups have observed the presence of ionic gold in active catalysts by Mössbauer (Soares *et al,* 2003 and Finch *et al,* 1999), XPS (Park and Lee, 1999), XANES (Guzman and gates, 2002) and FTIR Minaco *et al,* (1997). Visco *et al,* (1997) observed much larger catalytic activity with their uncalcined catalysts than with calcined ones and proposed that the oxidized Au species are the most active for low temperature CO oxidation with Au/Fe_2O_3 catalysts.

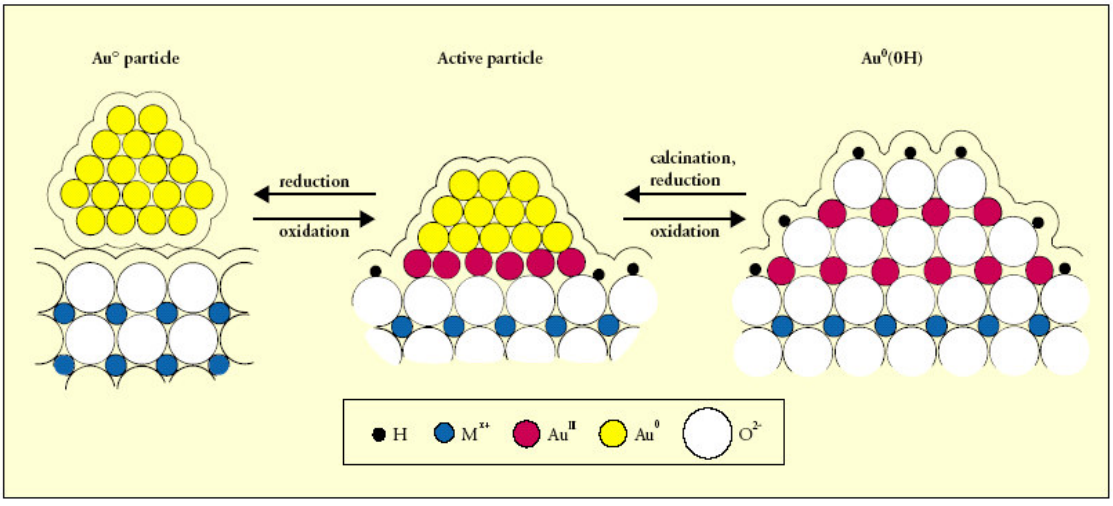

Figure 2.5: Pictorial representation of supported gold catalyst indicating possible changes under conditions giving oxidation or reduction of the active gold particles (Bond, 2000)

After extensively reviewing the available literature on gold catalysis, Bond and Thompson (2000) proposed that the active site consists of an ensemble of $Au(OH)_3$ and metallic gold (figure 2.5), where ionic gold species are believed to be the chemical glue between the metallic gold species and the support. At high temperature treatment, these species would be reduced to metallic gold and result in the agglomeration of gold on the surface of the support. This theory was confirmed by Costello *et al.* (2002), where they reported that a Au(OH) species is responsible for the adsorption of CO molecule and an oxygen atom would be adsorbed on the surface of the metallic gold particle.

Guzman and Gates (2002) observed the simultaneous presence of Au^I and Au^0 gold clusters with an average diameter of about 30 Å in MgO supported catalysts was demonstrated by XANES of the functioning catalysts during steady-state CO oxidation. The initial dispersion and oxidation state of the gold in the catalyst were found not to affect the properties of the catalysts functioning at steady state. The data is consistent with the postulate that the catalytically active species consist of Au^0 gold clusters interacting with cationic gold at the cluster-support interface.

2.7 CO Oxidation Reaction Proposed Mechanisms

Several publications in the literature have proposed different reaction mechanism according to the active site proposed. For example, as described in the figure 2.5 above, Bond and Thompson (2000) suggested that an active site is comprised of both the ionic and the metallic Au species. Here, a CO molecule is adsorbed on the surface of metallic Au species (Au^0---CO). This is therefore attacked by the hydroxyl group either from the support cation or from the peripheral Au^{III} ion, forming the

carboxylate group attached to the Au^{III} ion. This is therefore attached by the superoxide, which must be responsible for oxidizing two carboxylate ions; the hydroxyl group returns to where it came from and is ready to re-engage in the catalytic cycle as shown in the reactions (1)-(6) below.

$$Au^{0} + CO \rightarrow Au^{0}...CO \quad (1)$$

$$Au^{III} + OH_s \rightarrow Au^{II}...OH \quad (2)$$

$$Au^{0}...CO + Au^{II}...OH \rightarrow Au^{II}...COOH + Au^{0} \quad (3)$$

$$O_2 + \Delta_s^{-} \rightarrow O_2^{-}...\Delta_s \quad (4)$$

$$Au^{II}...COOH + O_2^{-}...\Delta_s \rightarrow Au^{II} + CO_2 + HO_2^{-}...\Delta_s \quad (5)$$

$$Au^{II}...COOH + HO_2^{-}...\Delta_s \rightarrow Au^{II} + CO_2 + 2\,OH_s^{-} + \Delta_s \quad (6)$$

$$Au^{II} + \Delta_s \rightarrow Au^{III} + \Delta_s^{-} \quad (7)$$

The mechanism described above was proposed for magnesium support and it was suggested that different reaction mechanisms are possible on different Au catalyst supports (Bond and Thompson, 2000; Kozlov *et al,* 1999).

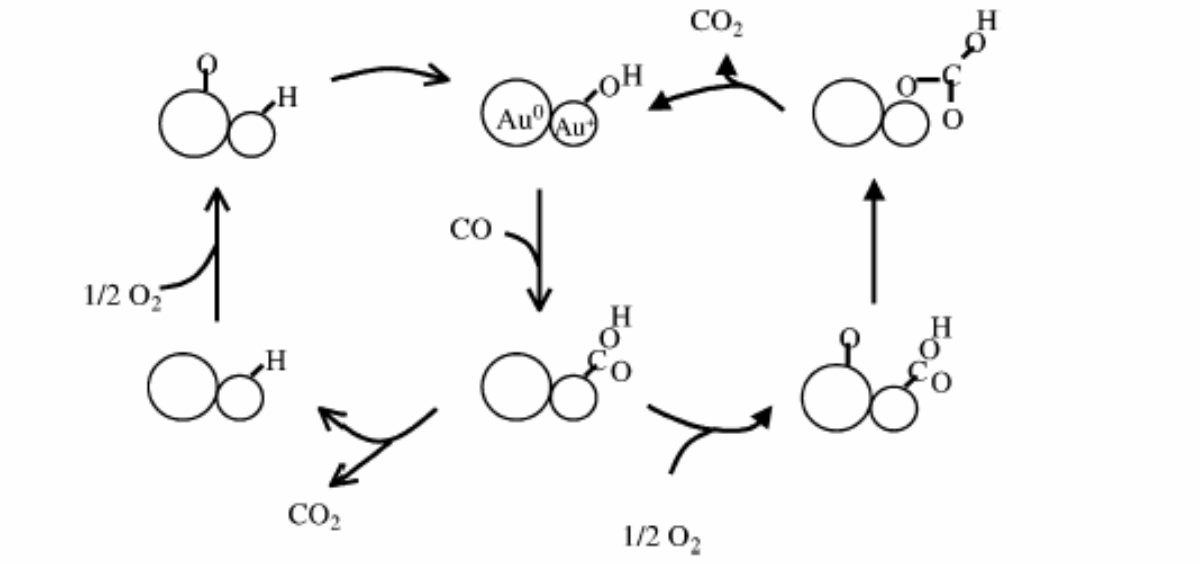

Figure 2.6: Proposed mechanism for CO oxidation by Au catalysts (Costello *et al,* 2002; Oh *et al,* 2001)

A mechanism for Au/Al_2O_3 catalyst was also suggested (Costello *et al,* 2002; Oh *et al,* 2001). In this proposed mechanism, the reaction proceeds by insertion of an adsorbed CO into an $Au^+–OH^-$ bond to form a hydroxycarbonyl. There are two possible reaction pathways for the hydroxycarbonyl. In one pathway, the hydroxycarbonyl is oxidized to bicarbonate, which is then decarboxylated to $Au^+–OH^-$ and CO_2. Another one is decarboxylation of the hydroxycarbonyl to CO_2 and Au–H, and the latter is oxidized to $Au^+–OH$. The difference between this mechanism and that proposed by Bond and Thompson (2000) is that the CO molecule is adsorbed on the Au^+-OH and the metallic Au species seems to be only necessary for the adsorption of an oxygen atom. This proposed cycle does not involve participation by OH radical-like species (Cunningham *et al,* 1999) or superoxide (Haruta *et al,* 1993) or direct participation of the support (Buccozzi *et al,* 1999), as suggested by others. The mechanism describe above is similar to that proposed earlier by Knell *et al,* (1992) on Au/ZrO_2 catalyst.

As for the mechanism of CO oxidation on the active Au catalysts, the active oxygen species and the role of lattice oxygen atoms have not been clarified. There is still some controversy on whether molecular oxygen or atomic oxygen contributes to CO oxidation. To explain the high activity of co-precipitation and deposition-precipitated Au catalysts, a scheme that involves catalysis at the boundary of small Au particles and the metal oxide support, Iizuka *et al.* (1997) proposed a mechanism which involves reversible adsorption of CO on the surface and parameter of Au particles and irreversible adsorption of oxygen at the boundary to form an OC-Au-O intermediate via oxygen dissociation, followed by CO_2 formation at the boundary. Boccuzzi *et al.* (1999) claimed that adsorption of oxygen changed CO stretching frequencies, which may indicate the adsorption of CO and oxygen in the neighborhood of each other on a gold particle, supporting the formation OC-Au-O species. Further, the information of atomic oxygen species on deposition precipitated Au/TiO_2 and co-precipitated Au/ZnO was also suggested by noticeable oxygen scrambling in the reaction of $C^{16}O + {}^{18}O_2$.

The existence of other independent, slower pathways involving oxygen atoms of the oxides supports was also demonstrated. Knell *et al.* (1992) suggested that CO oxidation on the co-precipitated Au/ZrO_2 catalysts involve interaction of CO with surface OH groups to form surface formates that can be oxidized by atomic oxygen activated on the surface of Au metallic particles. Kozlov *et al.* (1999) suggested in their proposed mechanism that the CO molecule is adsorbed on the surface of the metallic Au and the react with molecular oxygen species adsorbed on defect sites of the oxide support near the periphery of the Au particle in the $Au/M(OH)_x$ catalysts.

2.8 CO oxidation reaction kinetics

A unique feature of Au catalysts is that apparent activation energies (Ea) are very low. At temperatures below 300 K, the value of Ea is 20-40 kJ/mol and is nearly zero at temperatures below zero. This is in contrast to the Pt group metals that have a value ranging from 80 to 170 kJ/mol and are more active that the gold but only at temperatures higher that 500 K. However at room temperature, Au is more active by four orders of magnitude (Haruta and Daté, 2001). As much as the activity of the catalyst depends on the preparation method, this factor also influences the activation energy. The activation energy of Au/TiO_2 catalyst prepared by impregnation was found to lie between 49 and 60 kJ/mol, whereas that catalyst prepared by deposition precipitation was found to be between 18 and 27 kJ/mol (Haruta, 1997).

The rate of CO oxidation over Au/TiO_2, Au/Fe_2O_3, and Au/Co_3O_4 is independent of the concentration of CO but is slightly dependent on the concentration of O_2. Over unsupported Au powder with average particle size of 17 nm, the rate is almost independent of the concentrations of CO and O_2. This independence suggests that these molecules are adsorbed on the catalyst surface to saturation and the reaction of the two adsorbed species is the rate determining step. It is clear from the table 2.5 below that the rate of CO conversion is very dependent on the diameter of Au particles. Small Au particles have higher activity of CO conversion. A plot of TOF at 300 K versus average Au diameter appears to suggest that there is a dramatic dependence on the Au particle size with a sharp maximum at around 2.9 nm (Okumura *et al,* 2002). However, since the activation energy is different for different samples, the activity of the 2.5 nm sample became similar to the 2.9 nm sample at 236 K. Kinetics also depends on other variables such as the support and the preparation method used (Okumura *et al,* 2002). Higher rates have been reported with

catalysts prepared with deposition precipitation (Schimpf *et al,* 2002) whereas impregnation method (Haruta and Daté, 2001) was reported to produce catalysts that have lower rates and TOF.

Preparation methods have been described above as very crucial for the higher activity of the catalyst. This indicates the small Au particles have more active sites that the bigger particles (Lee and Graviilidis, 2002). When the rate is high, it means that more reacting molecules are adsorbed on the surface of the catalyst where they are converted into products.

Table 2.5: Rate of CO conversion by Au catalysts with different particle diameters and supports

Support	Method	Diameter (nm)	*tos*	T (K)	Rate (molCO.molAu^{-1}.s^{-1})	TOF (s^{-1})	Reference
TiO_2	CP	4.5	First 30 min	313	2.5 X10^{-2}	0.11	Bollinger, 1996
	DP	n/r	First 30 min	313	6.93X10^{-2}	n/r	Bollinger, 1996
	DP	1.7	>40 min (ss)	273	3.29x10^{-3}	1.3	Okumura, 1998
	DP	2	-	278	~4.0x10^{-2}	0.16	Zanella, 2004
	DP	3.5	-	278	~5.6x10^{-2}	0.077	Zanella, 2004
	CVD	3.8	>40 min (ss)	273	4.91x10^{-3}	0.02	Okumura, 1998
$Ti(OH)_4$	IAH	3	Ss	300	9.6x10^{-3}	0.03	Kozlov, 1999
Fe_2O_3	CP	n/r	3 h (ss)	293	3.4x10^{-1}	n/r	Visco, 1997

	CP	3.6	n/r	203	$2.6x10^{-3}$	n/r	Haruta, 1993
$Fe(OH)_3$	IAH	2.6	Ss	203	$6.4x10^{-3}$	0.02	Kozlova, 1998
Al_2O_3	IM	7.5	60 min	298	0	-	Lee, 2002
Al_2O_3	IM	n.d	60 min	298	$5.4x10^{-6}$	-	Lee, 2002
Al_2O_3	CP	3.5	>40 min (ss)	273	$1.6x10^{-3}$	0.006	Okumura, 1998
	DP	2.4	>40 min (ss)	273	$7.78x10^{-3}$	0.02	Okumura, 1998
	DP	3-5	>40min(ss)	295	$3.10x10^{-2}$	0.17-0.46	Costello, 2002
	CVD	3.5	>40 min (ss)	273	$2.6x10^{-3}$	0.01	Okumura, 1998
SiO_2	CVD	6.6	>40 min (ss)	273	$2.8x10^{-3}$	0.02	Okumura, 1998

n.d = not detected;

ss = steady state

2.9 Deactivation and stability of Au catalysts

Catalyst deactivation is one of the main problems to circumvent for practical catalysts. It is caused by some changes in chemical composition and structure of surface or bulk of the catalyst which is assumed to be occurring during the reaction. For gold catalyst systems in CO oxidation the change may be due to phase transitions such as the formation of carbonates and/or blocking the active sites (Kanova *et al,* 2004). It has also been demonstrated that thermal treatments of the catalyst in dry He at 100 ^{o}C or higher deactivated the catalyst (Oh *et al,* 2001 and Costello *et al,* 2002). This treatment is believed to modify the catalyst by removing the hydroxyl groups from the ionic Au species and from the surface of the support. Hydroxyl groups are believed to be crucial for the activity of the catalyst (Bond and Thompson, 2000; Oh *et al,* 2001 and Costello *et al,* 2002). Thermal treatment also leads to the agglomeration of Au particles which is not desirable for the high activity. The activity of Au/Al_2O_3 catalyst decreases rapidly initially with time-on-stream, followed by a much lower decrease once most of the initial activity has been lost (Costello *et al,* 2002). For example, the CO conversion decreased from about 50 % to 20 % over 5 min and then decrease more slowly until it reach a pseudo steady state of about 8% over the following 25 minutes. This pseudo steady-state activity corresponds to a turnover frequency of about 0.26 s^{-1} for this catalyst which contains an average gold particle size of about 4 nm. When hydrogen was co-fed in the reaction mixture, as in selective CO oxidation (SCO), no deactivation was observed over several hours of catalyst testing (Costello *et al,* 2002; Costello *et al,* 2003). This is because the CO oxidation reaction removes the hydroxyl groups from both the support and Au particles and during H_2-SCO, the presence of H_2 restores them by hydrolyzing the Au-carbonate bond formed during the reaction.

Kanova *et al.* (2004) witnessed a constant decrease in the activity of Au/TiO_2 catalyst with increasing time from 100 % to about 25% conversion of CO in the period of 30 h and no steady state was reached over this period. Similar results were observed by Sihna *et al,* (2003) with Au/Ti-MCM-41 catalyst for the vapor-phase epoxidation of propylene over a period of 4 h. In contrast to Kanova`s *et al.* (2004) observation, Zanella *et al.* (2004) have observed a steady state after 1,5 h of time-on-stream reaction which persisted until the end of the reaction (5 h) with the same catalysts system Au/TiO_2, calcined at 300 ^{o}C. Similar results were observed by Salama *et al.* (1996) with Au/NaY catalyst for the conversion NO at different reaction temperatures. Lin *et al.* (2002) observed a very good stability of Au/Y catalyst, which exhibited 100% conversion for over 2 days of reaction. The support may have a very important role to play in the stability of the catalyst. It was reported that the support stabilizes the small gold particles against agglomeration. It was demonstrated that 0.6% $Au/FeO_x/Al_2O_3$ deactivated very rapidly and substantially from 60% to about 20% whereas 0.5% Au/Fe_x/ACF (ACF = activated carbon fiber) showed a better stability with a slowly decreasing CO conversion from 100% to 80% (Bulushev *et al,* 2002).

The effects of water are the subjects of some controversy in the literature. A constant stability of about 63 % conversion was achieved for over 2 days with 1% Au/CeO_2 catalysts for H_2-SCO in the presence of water (Luengruemitchai *et al,* 2004). On the other hand, running CO oxidation with Au/Al_2O_3 in the presence of traces of water was found to have lead to a much faster deactivation of the catalyst after about 75 minutes of time-on-stream whereas dry conditions resulted in a pseudo-steady state activity which only to a decrease from 100% to about 90% conversion over 250 minutes of time-on-stream (Lee and Graviilidis, 2002).

Catalyst deactivation is ascribed to the drying out of the catalyst during the reaction and it is reversible. It was reported (Costello *et al,* 2002 and Costello *et al,* 2003) that, deactivated catalysts can be regenerated by flowing a stream of hydrogen or H_2O for given period of time. The regenerated catalysts could achieve about 90 % of the initial activity of the catalyst. The presence of water is believed to replace the hydroxyl groups lost during catalyst deactivation by thermal treatment. It was also shown that the deactivated catalyst can be regenerated by the flow of SCO reaction feed leading to the restoration of initial activity.

2.10 The effect of moisture on CO oxidation

The addition of water on the reaction stream was found to be beneficial to the activity of the catalysts (Buccozzi *et al,* 2001; Daté *et al,* 2002). Depending on the partial pressure of water, its effect could be to enhance or suppress the activity of the catalyst. Water can remove chloride poisoning by hydrolyzing the Au-Cl bond. The presence of water was also found to prevent the deactivation of Au/Al_2O_3 catalyst (Oh *et al,* 2001). In the chemical mechanism of the active site proposed by Costello *et al,* (2002), (figure 2.6 above), the Au-OH which actively participates in the reaction can be easily removed thermally leading to the deactivation of the Au/Al_2O_3 catalyst. Regeneration can be achieved by exposure of the catalyst to water vapor at room temperature (Kung *et al,* 2003).

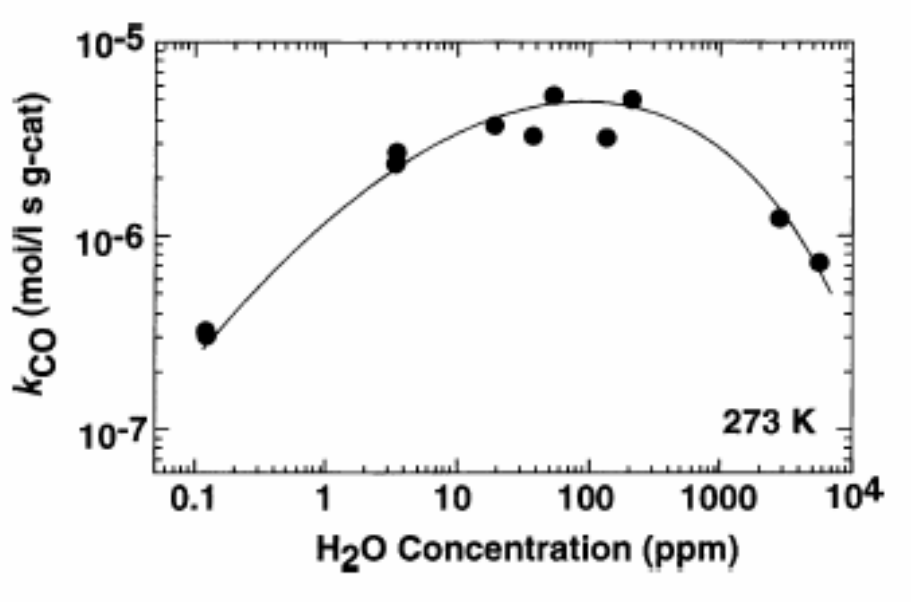

Figure 2.7: Dependence of CO oxidation rate at 273 K over Au/TiO_2 on the moisture concentration of the reactant gas. Catalyst sample: 50 mg of 1 wt.% Au/TiO_2. Reactant gas: 1 vol.% CO in air, 67 ml/min (Daté *et al,* (2002).

Daté *et al.* (2002) observed an increase in the CO oxidation rate with increasing concentration of moisture yielding a maximum reaction rate at 200 ppm with Au/TiO_2 as shown in figure 2.7 above. They reported that the activity is determined mainly by the amount of moisture accumulated in the catalyst sample and the reaction mechanism is not significantly influenced by the moisture. Enhanced activity by in presence of water was found to be reversible since the removal of water resulted in the attainment of original activity obtained before the water was added. Au/Co_3O_4 catalysts have been reported to be insensitive to water vapor concentrations between 6.5×10^{-4} Torr and 4.6 Torr, and this behavior was ascribed to the absence of adsorption of H_2O on Au surfaces (Cunningham *et al,* 1993). It has been recently noticed that the reaction with Au/Fe_2O_3 catalyst does not proceed at 273 K when the reactants are completely dry, but a total conversion was achieved at the same temperature when the moisture was present (G.J Hutchings personal communication; Bond and Thompson, 2000).

Contrasting results have been presented by Bollinger and Vannice (1996) reported that the addition of 4.5 Torr water vapor at 313 K deactivated the 1.0% Au/TiO_2 catalyst. The deactivation was ascribed to the adsorption of H_2O on the TiO_2 surface, since water is known to adsorb both associatively and dissociatively (as OH^-) on reduced Ti cations and to oxidize the surface thus, blocking the titania inter-facial sites. The activity of this catalyst was not restored by removing the water vapor from the feed stream and this indicated an irreversible adsorption. However, some activity was obtained after heating at 393 K for 30 min, and complete regeneration was obtained after calcination and low temperature reduction at 473K (Bollinger and Vannice, 1996). This is consistent with the DRIFTS results which suggest that partial, but not complete, water removal could occur after heating at 393 K for 30 min. This pretreatment should also decompose carboxylate species which have been associated with the initial activity decrease in Au/TiO_2 catalysts (Haruta *et al,* 1993). The catalyst poisoning in the presence of water was also observed by Kang *et al.* (1995) on Au/Fe/Y catalyst thermally pretreated in reductive and oxidative media.

2.11 Other reactions catalyzed by gold nano-particles

2.11.1 Selective CO Oxidation in the presence of hydrogen (H_2-SCO)

Over the last decade, the preferential oxidation of CO (PROX) in H_2-rich gas (Mann *et al,* 1993) has spurred new interest owing to its application in fuel cell technology, where it may be used to purify H_2 produced via steam reforming [e.g., of methanol (Donitz *et al*, 1997)]. The selective oxidation of CO is particularly promising for vehicle applications since it allows small-scale operation. Next to offering reasonably

high rates for CO oxidation, the most important requirement of the catalyst is a high selectivity, S, with respect to the undesired H_2 oxidation side reaction. From a process perspective (reformer, PROX, fuel cell), there are two temperature levels that are particularly convenient for PROX: either the fuel cell operating temperature (80-100 ^{o}C) or the temperature level of the methanol reformer unit (250-300 ^{o}C) (Kahlich *et al,* 1999). Oxide supported Au catalysts (Au/MeO_X) have been shown to exhibit an outstanding activity already at low temperatures for several hydrogenation and oxidation reactions, in particular CO oxidation. Consequently, gold catalysts, such as Au/MnO_X or Au/ α-Fe_2O_3 (Schubert *et al,* 2001; Schubert *et al,* 1999) were also suggested as suitable candidates for the selective (preferential) CO oxidation in H_2 rich gases (PROX) at low temperatures. This reaction is employed for the purification of feed as gas streams for PEM (polymer electrolyte membrane) fuel cells produced *via* methanol steam reforming; the so-called reformate gas (Sanchez *et al,* 1996). It was suggested that the high activity observed on Au/MeO_X catalysts with easily reducible oxides supports results from cooperative effects of the support material, i.e., its propensity for facile adsorption and storage of oxygen which would result in a Mars-van Krevelen type reaction mechanism. So far, however, systematic, comparative studies on the influence of the support material for different Au/MeO_X catalysts and under identical conditions, exists only for the pure CO oxidation reaction. For the envisaged employment as PROX catalysts, not only the CO oxidation activity, but also the selectivity S($S = r_{CO}/[r_{CO} + r_{H2}]$, with r_X being the rates for CO and H_2 oxidation respectively) and the long-term stability (approximately 5000 h lifetime are commonly assumed to be necessary mobile applications) are important key features (Kahlich *et al,* 1999).

Schubert *et al.* (2001) reported the results of a comparative study on the catalytic properties of various supported gold catalysts for the PROX reaction in methanol reformate. Catalysts include Au/α-Fe_2O_3, Au/TiO_2, Au/CoO_x, Au/NiO_X, $Au/Mg(OH)_2$, Au/CeO_2, Au/SnO_2, Au/MnO_X, and Au/γ-Al_2O_3. Bethke *et al.* (2000) investigated the

selective oxidation of CO in a hydrogen rich stream over Au/Al_2O_3 catalysts and found that the presence of Magnesium citrate in the preparation solution had a significant effect on the properties of the catalyst. The catalyst prepared without citrate contained larger gold particles which were less catalytically active and less selective for CO oxidation. They suggested that the optimal average Au size of about 5-10 nm was required for the best activity and selectivity and the presence of Magnesium citrate served to remove the residual chlorine. The same group (Oh *et al,* 2002) investigated the effect of the presence of chlorine in the catalyst by deliberately adding some chlorine to the catalyst and observed the resulting enlarged Au particle size. The catalysts to which chlorine was added showed a decreased activity and selectivity towards the formation of CO_2. Grisel *et al.* (2001) reported higher selectivity towards CO_2 in the presence of H_2 at temperatures below 50 ^oC with $Au/MgO/Al_2O_3$ and $Au/MnO_x/MgO/Al_2O_3$ catalysts. This was because of the high amount of CO adsorbed on the surface of the catalyst. However at temperatures higher that 50 ^oC, CO desorption increases which results in the commencement of H_2 oxidation. The decrease in the amount of CO coverage of the surface of Au catalysts was also observed by Schubert *et al.* (1999) by DRIFTS. It was observed that a decrease in CO partial pressure decreases the reaction probability for CO oxidation. The relatively high selectivity towards CO oxidation of Au catalysts particularly at high CO partial pressures can be rationalized by the very low dissociative sticking probability for H_2 on the Au surface. Assuming low CO coverage under preferential selective CO oxidation conditions, hydrogen dissociation would be expected not to be essentially unperturbed by adsorbed CO, so that the H_2 oxidation rate (at constant oxygen partial pressure) should be independent of the CO oxidation reaction rate (Schubert *et al,* 1999; Kahlich *et al,* 1999; Luengnaruemitchai *et al,* 2004; Grisel *et al,* 2002). The CO conversion increased with increasing O_2 concentration while the CO selectivity decreases with increasing O_2 concentration. In the presence of water, the CO conversion decreased at temperatures lower than 373 K and this was ascribed to the strong adsorption of water on the active sites. However, at higher temperatures, water favored the CO conversion since it provides the hydroxyl groups on the surface

of the catalysts which are implicated in catalysis by gold (Luengnaruemitchai *et al,* 2004).

2.11.2 Hydrochlorination of ethyne

The heterogeneously catalyzed addition of hydrogen chloride to ethyne is a synthetic route for the production of vinyl chloride. Mercuric chloride, supported on activated carbon, is often used as a catalyst commercially (Hutchings and Grady, 1985) but, its drawback is the rapid deactivation with time-on-stream. The high rate of deactivation, together with the toxicity associated with mercury compounds, has prompted many studies involving the search for alternative catalysts. In this respect, one of the most extensive studies of metal chloride catalysts was carried out by Shinoda (1975). One unfortunate observation for all the supported metal chloride catalysts is that they all deactivate with time on stream when used in a standard fixed bed reactor. Gold was reported to be the most active catalyst for ethyne hydrochlorination (Hutchings, 2002; Hutchings and Grady, 1985).

Supported Au catalysts deactivate much less rapidly than other supported metal catalysts but further deactivation can be minimized by the use of high gold loadings (≥1 wt.%). Interestingly, the deactivation with Au catalysts for ethyne hydrochlorination was found to be temperature dependent, and high rates of deactivation were observed at both high and low temperatures. The low temperature deactivation was reported to be caused by coke deposition (Nkosi *et al,* 1991), probably as a result of surface polymerization reactions of vinyl chloride and ethyne. The high temperature deactivation was probed using ^{197}Au Mössbauer spectroscopy (Nkosi *et al,* 1991) and it was found that this deactivation was due to the reduction of Au^{III} to Au^{0}. Although deactivation was observed to be a problem with gold catalysts,

in common with other supported metal chloride catalysts, it was found that gold catalysts could be reactivated by treatment off-line with hydrogen chloride or Chlorine (Nkosi *et al,* 1991 (a)).

2.11.3 Epoxidation of propelyene

The direct gas-phase synthesis of propene oxide, by the use of molecular oxygen, has long been desired. Highly dispersed Au/TiO_2 catalysts show an extraordinary selectivity in the oxidation of propene to the corresponding epoxide (>99%), using a combination of H_2 and O_2 as oxidation mixture (Hayashi *et al,* 1998). Additional studies of the epoxidation reaction indicated several drawbacks of the Au/TiO_2 catalyst. Firstly, the low conversion (1–2%) obtained under typical reaction conditions (atmospheric pressure, 323–423 K) cannot be improved by increasing the reaction temperature, because this leads to extensive by-product formation. Secondly, the low efficiency of hydrogen (relatively large amounts of water are formed) is hard to prevent. Finally, significant deactivation of Au/TiO_2 catalysts within several hours on stream has been observed. Deactivation can be partly prevented by using dispersed TiO_2 supports, such as TiO_2/SiO_2 and titanium-silicalite-1 (TS-1) (Nijhuis *et al,* 1999 and Clarck *et al,* 1999) and Ti-MCM (Uphade, 2000). For industrial applications, the efficiency of hydrogen should be increased not only to favor process economics, but also decrease the amount of heat released in the reactor (Zwijnenburg *et al,* 2002).

Zwijnenburg *et al.* (2002) have investigated the effect of the addition of the second metal on Au/TiO_2 catalysts. However the monometallic catalyst (Au/TiO_2) was found to be more selective to the formation of propylene oxide, whereas the bimetallic catalyst had lower selectivities as shown in the table below.

Table 2.6: Product yield for bimetallic catalysts compared to Au-only at 373 K (Zwijnenburg *et al,* 2002)

Metal	PO (%)	Propane (%)	H_2O/PO (-)
Au-only	1.2	<0.1	29
Au-Pd	<0.01	10	∞
Au-Pt	1.0	0.1	9.3

2.11.4 Water Gas Shift reaction (WGS)

Fuel cell power generation is currently undergoing rapid development both for stationary and transportation applications (Fu *et al,* 2003). A renewed interest in the water gas shift reaction has occurred, arising from the need of pure hydrogen in conjunction with the development of fuel-cell power station (Andreeva *et al,* 2002). A number of research groups are engaged in the investigation of the use of gold as a catalyst for this reaction. The mostly used support reported are CeO_2 (Andreeva *et al,* 2002, Fu *et al,* 2003, Tabakova *et al,* 2003), α-Fe_2O_3 (Venugopal and Scurrell, 2003, Andreeva *et al,* 1998). In contrast to the situation found for CO oxidation, the activity of these catalysts on WGS reaction at room temperature seems not to be attainable. However, Mahomad *et al.* (2000) reported some activity with Au/NaY catalyst prepared by co-precipitation at a reaction temperature of 50 ^oC. Most activities reported in the literature however are at reaction temperatures above 100 ^oC (table 2.7). For instance, Luengnaruemitchai *et al.* (2003) did not observe any conversion with Au/α-Fe_2O_3 catalysts prepared by both co-precipitation and deposition precipitation at 120 ^oC reaction temperature whereas, Venugopal *et al.* (2003) reported only 8% CO conversion with Au/α-Fe_2O_3 prepared by deposition precipitation at 120 ^oC reaction temperature. Andreeva *et al.* (1998) reported a higher

activity of 19% conversion with the same catalyst, and in their later report, Venugopal *et al,* (2003 (a)) observed an increase in activity to 20% when they supported gold on hydroxyapatite (HAP) at 100 ^{o}C reaction temperature. Among the gold catalysts, Au/TiO_2 showed the highest reaction rates. While the reaction rate at 373 K increased with increasing Au loading for a series of Au/TiO_2 catalysts prepared by the deposition precipitation method, but the same catalyst prepared by co-precipitation showed a lower rate despite the higher metal loading and the smaller gold particles. This may be attributed to differences in exposure of gold particles on the surface and the crystalline nature of TiO_2 depending on the preparation method (Sakurai *et al,* 1997).

As shown in the table below, various reports mention different partial pressure of water and it seems to have a significant effect on the conversion of CO. The CO conversion increases with increasing partial pressure of water, but there seems to be an optimum amount of water, for instance, an increase in the amount of water from 60:5 to 60:10 resulted in the increase in the rate of CO_2 formation from 0.26 μmol/g.s to 0.31 μmol/g.s with Au/NaY catalyst at 100 ^{o}C reaction temperature (Mohamed *et al,* 2000). However, a further increase to 60:17 resulted in a massive drop in activity to 0.09 μmol/g.s.

Table 2.7: Summary of activities of different catalysts on WGS reaction

nr: not reported

Au wt%	Support	Method	Particle size (TEM) nm	Reaction temperature	$CO:H_2O$	Activity % or rate(µmol/.g.s)	Reference
1	α-Fe_2O_3	CP	2.0	120 ^oC	10:7	9%	Andreeva, 1998
2	α-Fe_2O_3	DP	2.0	120 ^oC	10:7	19%	Andreeva, 1998
5	NaY	CP	nr	50 ^oC	12:1	0.2	Mahomed, 2000
3.4	TiO_2	DP	4.4	100 ^oC	1:2	$1x10^{-1}$	Sakurai, 1997
3	CeO_2	DP	5.5	140 ^oC	-	11%	Andreeva, 2002
3	TiO_2	DP	nr	-	-	-	Buccozzi, 1999
1	CeO_2	CP	4.0	120 ^oC	4:2.6	0%	Luengnaruemitchai, `03
3	α-Fe_2O_3	CP	nr	120 ^oC	4:2.6	0%	Luengnaruemitchai, `03
3	α-Fe_2O_3	DP	nr	120 ^oC	4:2.6	0%	Luengnaruemitchai, `03
3	HAP	DP	nr	100 ^oC	1:11	20%	Venugopal, 2003
3	α-Fe_2O_3	DP	nr	120 ^oC	1:2.2	8%	Venugopal, 2003 (1)
4.5	CeO_2-La	DP	5 .0	150 ^oC	2:10.7	22%	Fu, 2003
5	ZnO	CP	4.9	100°C	1:2	$9x10^{-3}$	Bond, 1999
3.4	TiO_2	DP	4.4	100°C	1:2	$0.1x10^{-1}$	Bond, 1999
10	TiO_2	DP	4.4	100°C	1:2	$0.3x10^{-1}$	Bond, 1999
33	TiO_2	CP	2.8	100°C	1:2	$6.4x10^{-2}$	Bond, 1999
5	Al2O3	CP	3.7	100°C	1:2	$3.4x10^{-2}$	Bond, 1999
5	Fe_2O_3	CP	3.3	100°C	1:2	$2.2x10^{-2}$	Bond, 1999

2.11.5 Methane Oxidation

Natural gas, which consists primarily of methane, had been receiving much attention as an alternative fuel for motor vehicles and power plants (Sekizawa *et al,* 2001). Catalytic oxidation is an important method to remove methane from the systems where it appears as an undesirable contaminant or waste product. Methane is one of the most difficult hydrocarbons to oxidize catalytically (Waters *et al,* 1995).

Methane combustion at sufficiently low temperatures can be achieved only by the application of highly active noble metal catalysts. Palladium has been well known as the most active material for the oxidation of methane (Rebeiro *et al,* 1994; Hicks *et al,* 1990). From the point of view of fundamental research and practical application, it is still highly desirable to develop a catalyst with higher activity to initiate methane oxidation at a temperature as low as possible.

Conversional noble metal supported catalysts (Pt or Pd on Al_2O_3) have been previously reported to show reasonable activity only above 300 ^oC. However, Rebeiro *et al.* (1994) reported some activity of methane oxidation at temperatures below 300 ^oC.

Miao and Deng (2001) reported the activity of Au–Pd/Co_3O_4 at higher temperatures to be a little enhanced in comparison with Au/Co_3O_4 (entry 3) (table 2.8, below), but slightly reduced in comparison with Pd/Co_3O_4 (entry 7) and concluded that gold may inhibit the Pd activity for methane oxidation when they are combined together, on the other hand the temperatures of light-off and 100% methane conversion were further

decreased with increasing Au and Pt loading (entries 9 and 10) and seemed to reach a minimum value (entry 10), i.e. methane could be oxidized at ca. 218 °C and could be completely oxidized at ca. 360 °C. It can be concluded that there exists synergism between Pt and Au, which could enhance the activity of methane combustion. Moreover, the activity for methane oxidation would be slightly reduced when the Au loading reached ca. 5 wt.% (entry 11), indicating that there may exist an optimized ratio for Au and Pt loading (Miao and Deng, 2001).

Table 2.8: Catalytic performances for methane combustion over supported noble metal catalysts

Entry	Catalyst	Au content (%)	Pt or Pd content (%)	BET (m^2/g)	Catalytic activity (°C)			
					$T_{light-off}$	T_{50}	T_{90}	T_{100}
1	Co_3O_4	–	–	57.1	250	325	376	420
2	Au/Co_3O_4	0.18	–	55.3	241	317	370	420
3	Au/Co_3O_4	1.91	–	52.2	241	314	369	418
4	Pt/Co_3O_4	–	0.21	64.5	238	312	358	400
5	Pt/Co_3O_4	–	1.96	72.6	235	308	348	385
6	Pd/Co_3O_4	–	0.19	62.3	228	307	350	392
7	Pd/Co_3O_4	–	1.92	66.2	224	304	338	376
8	$Au–Pt/Co_3O_4$	0.38	0.23	59.2	228	305	340	379
9	$Au–Pt/Co_3O_4$	1.90	0.19	59.8	232	303	338	368
10	$Au–Pt/Co_3O_4$	1.92	1.63	61.0	218	295	332	360
11	$Au–Pt/Co_3O_4$	4.76	1.67	64.1	222	296	336	364
12	$Au–Pd/Co_3O_4$	1.90	1.48	48.5	241	317	363	388
13	Pd/Al_2O_3	–	1.58	139.8	264	338	367	387
14	Pd/Al_2O_3	–	3.70	132.5	251	313	339	358

Grisel and Nieuwenhuys (2001) (a) reported that the addition of a metal oxide to Au/Al_2O_3 catalyst improved the catalytic activity in both the low temperature CO oxidation and methane oxidation, though the extent was low for the latter. The measured oxidation activity of methane oxidation over $Au/MOx/Al_2O_3$ decreased in the order: $CuO_x > MnO_x > CrO_x > FeO_x > CoO_x > NiO_x > ZnO_x$. In this project, our main objective was to establish if the catalyst which is good for CO oxidation could also be good for methane oxidation. This would shed light on the nature and preparation of a common catalyst for both reactions, which would be used to simultaneously remove these toxic products of the indoor cooling systems. For this purpose, the Au/TiO_2, and Au/TiO_2-MO_x (where MO_x is ZrO_2, and CeO_2) prepared by various methods.

Table 2.9: Summary of reactions catalyzed by gold catalysts

Type of Reaction	Reactant	Temperature (K)	Support	Notes	Reference
oxidation	CO	200-400	$Be(OH)_2$,TiO_2	Acidic metal oxide are excluded as supports	Cunningham, 1998
	CH_4	473-1013	Al_2O_3	To CO_2 + H_2O	Grisel, 2000
	succinic acid	463	TiO_2	To acetic acid	Besson, 2003
	HCHO	300-450	TiO_2	Regenerable by sun	Daté, 2000
	benzene	473-673	Au-V_2O_5/TiO_2	Total oxidation	Idakiev, 2003
	CH_3OH	300-450	TiO_2	Regenerable by sun	Daté, 2000
	CH_4,C_3H_8	450-650	Co_3O_4	as active as Pd, Pt catalysts	Haruta, 1992
	trimethylamine	330-500	Fe_2O_3, $NiFe_2O_4$	Commercialized for odour eater	Ueda, 1992
oxidative decomposition	chlorofluorocarbon	550-823	Co_3O_4, Al_2O_3,LaF_3	LaF_3 for HCN synthesis	Aida, 1990
	o-chlorophenol	450-550	Fe_2O_3	Other supports Pt/SnO_2+Ir/La_2O_3	Okumura, 2001

	Dioxin	400-500	Fe_2O_3	Intergrated with $Pt/SnO_2+Ir/La_2O_3$	Okumura, 2001
reduction	$NO + C_3H_6$	450-800	Al_2O_3	To N_2, mixed with Mn_2O_3	Ueda, 1996
decomposition	N_2O $(+O_2+H_2O)$	500-	Co_3O_4	To N_2	Yan, 2002
WGS	$CO + H_2O$	400-500	CeO_2	To $CO_2 + H_2$	Andreeva, 1998
reduction of CO_x	$CO + 2H_2O$	400-500	ZnO	To methanol	Sakurai, 1995
	$CO_2 + 3H_2O$	400-500	TiO_2	To CO	Sakurai, 1995
selective oxidation	Phenylmethane -1,2-diol	343-363	Carbon	Mandelic acid	Biella, 2003
	$C_3H_6 + H_2 + O_2$	300-500	TiO_2, $Ti-SiO_2$	To propylene oxide	Hayashi, 1998
	$C_3H_8 + O_2 + H_2$	300-400	TiO_2	To acetone	Hayashi, 1998
	$C_4H_{10} + O_2 + H_2$	300-400	TiO_2	To butanol	Hayashi, 1998
	glycerol	303	Carbon	To Sodium glycerate	Porta, 2004
selective hydrogenation	C_2H_2	400-500	Al_2O_3	To ethylene	Jia, 2000
	$CH_2CHCHCH_2$	400-500	Al_2O_3, SiO_2,TiO_2	To butenes	Bond, 1973

	crotonaldehyde	500-550	ZnO	To crotyl alcohol	Bailie, 2001
	crotonaldehyde	553	SiO_2	To crotyl alcohol[a]	Schimpf, 2002
	crotonaldehyde	523	ZrO_2	To crotyl alcohol[b]	Hutchings, 2002
	butadiene	513, 533	Al_2O_3	To butenes[a]	Schimpf, 2002
	acrolein	473	TiO_2	To allyl alcohol[a]	Schimpf, 2002
	acrolein	513	TiO_2	To allyl alcohol	Mohr, 2003
	cyclohexene	353	SiO_2	To cyclohexane[c]	Mukherjee, 2002
selective partial oxidation	propylene	323	TiO_2	To propylene oxide[d]	Haruta, 1997
hydrochlorination	C_2H_2	373-393	$AuCl_3$/activated carbon	To vinyl chloride	

Table based on Haruta (2001) except, [d] Haruta (1997)

2.12 Characterization of Au nano-particles

Characterization of catalysts is necessary in order to understand the reaction mechanism involved during the reaction and to understand the reason behind the high activity of these catalysts. It is important to determine the surface area, particle size, crystallinity and oxidation state of Au particles of the active catalysts. A number of characterization techniques have been used to characterize and elucidate the surface structure of Au catalysts. These techniques have assisted researchers to propose mechanisms for CO oxidation reaction even though there are still some differences in the proposed mechanisms probably due to different kinds of supports and preparation parameters used.

2.12.1 Surface area determination (Brunauer, Emmett, and Teller)

It is generally believed that high surface area is required for the high performance of the catalyst. Generally surface area determines the surface active sites on the surface of the catalyst. Brunauer, Emmet and Teller have developed a technique which determines the surface area and the average pore volume of the catalyst called BET. Here, the surface are is reported in m^2/g of the catalyst.

Several papers have been published which report the surface area of the gold catalysts. There has been little comment on the direct relationship reported between the surface area of gold catalysts and the activity. Even though the issue of particle size has been discussed intensively and there has been an agreement amongst the publications that small gold particle size is one of the requirements for high catalytic activity, the surface area of gold catalysts has not been directly related to the particle

size and it has not been a matter of thorough discussion amongst researchers involved in Au catalysis. Recently, Wang *et al.* (2003), reported different surface areas with different precipitating agents. It has been noted that the total surface area of the catalyst was significantly affected by the precipitant. Catalyst activity was reported to decrease in the following sequence: $Au/ZnO/Na_2CO_3$ >$AuZnO/(NH_4)_2CO_3$> Au/ZnO/NaOH>$Au/ZnO/NH_4OH$, and so does the surface area. The most active catalyst was found to have the surface area of 69.82 m^2/g and the least active had only 7.47 m^2/g. Kozlov *et al.* (1999) also found an increase of CO oxidation activity with increasing surface area, in the following order for the commercially available catalysts: Au/Fe_2O_3 (5 m^2/g)<$AuFe(OH)_3$(47 m^2/g)<Au/FeOOH (84 m^2/g). Similarly it was claimed that the use of titania with the surface are S_{BET} > 10 m^2/g was necessary in order to obtain active Au/TiO_2 catalysts by the deposition precipitation method (Haruta *et al,* 1993). On the other hand it was noted that a catalyst with a high catalytic activities $Au/Fe(OH)_3$-dried (57 m^2/g) had a similar S_{BET} as Au/Fe_2O_3 (55 m^2/g) catalyst which show a lower catalytic activity (Kozlov *et al,* 1999).

2.12.2 Transmission Electron Microscopy (TEM)

It has been agreed that for high catalytic activity, Au has to be dispersed as small gold particles on the surface of the support. TEM has been one of the mostly used techniques to estimate the gold particle size. TEM images usually depict Au particles as dark contrasts on the surface of the support. Oxide supports on the other hand exhibit different morphology. For instance TiO_2 were identified as small ordered microcrystals with sharp borders whereas ZrO_2 were found to have much broader size distribution and roundly shaped on the TEM images (Manzoli *et al,* 2003, Buccozzi *et al,* 2001). EDX can be used to identify and verify the presence of gold particles. It has been reported that gold particles of 5 nm or less are more desirable for the extremely high activity of Au catalysts. TEM was used to observe the changes in the

particle size of Au with change in calcination temperature (Buccozzi *et al,* 2001), preparation conditions (Wolf and Schuth, 2002; Lee and Graviilidis, 2002) and preparation methods (Golunsky *et al,* 2002). It has been noted however that the TEM technique has its drawbacks. For example, Guczi *et al.* (2003) reported the stripping off of the Au particles from Si substrates in 10-20 % hydrogen fluoride (HF) solution during the preparation of samples, which results in the unreliability of the TEM results. These authors mentioned their preference for Atomic force microscopy (AFM) over TEM. However most TEM users do not mention the use of HF during sample preparation; instead the catalyst is usually dispersed in an alcohol or acetone (Mabudafhasi *et al,* 2002, Mallick and Scurrell, 2003) before being mounted on the copper grid.

2.12.3 X-ray Diffractometer (XRD)

XRD is used to monitor the crystallinity of both the support and the metal particles of the catalyst. The morphology of the support (crystallinity) has a very significant effect on the surface Au atoms. It has been suggested that a crystalline support has a stronger interaction with the Au particles (Kozlov *et al,* 1999). The Scherrer equation ($B = 0.9\lambda/t\text{Cos}\theta$, where B is the crystallite size; λ is the synchrotron wavelength; t is the full-with at half maximum height) (Jung *et al,* 2004; Centeno *et al,* 2002) can be used to estimate the Au particle size from the width of the Au peak, however, if the catalyst, especially the Au particles are more amorphous, this may not be possible. Au peaks, Au (111), Au (200) and Au (220) have been identified and used to estimate the Au particle size. In the case of Au/TiO_2-P25, Au(111) was found to be shielded by the Ti(004) peak and has been not used for particle size determination, and Au(200) was used instead. Luengnaruemitchai *et al.* (2004) observed no XRD Au peak with Au/CeO_2 catalysts prepared by co-precipitation and estimated that the Au particle size in that catalyst was smaller that 5 nm. Au reflections were observed with

the catalyst prepared by both sol-gel and impregnation and their Au particle sizes were found to be 30 and 29 nm respectively. Ko *et al.* (2003) used XRD to monitor the change in the increase and crystallization of Au particle with increasing heat treatment of the catalyst from 100 ^{o}C where there was no Au peak detected due to the presence highly amorphous particles to 600 ^{o}C where the Au peaks are clearly evident of the bigger crystalline particles. This data shows that XRD is a very important characterization technique for estimating the particle size and crystallization of catalyst components. However, Bond and Thompson (2000) highlighted the danger of inferring to what species are catalytically active on the bases of what is revealed by XRD because irradiation used may change the electronic structure of the catalyst being examined, i.e. small, amorphous and ionic Au species may be reduced to metallic Au which in turn may result in agglomeration and crystallization.

2.12.4 X-ray Photoelectron Spectroscopy (XPS)

XPS has been used to identify the oxidation state of the Au particle on the surface of the support. Most of the reports showed that the Au particles are mostly metallic, but there have been a suspicion of in situ reduction of the Au ions by the photon beam. Bond and Thompson (2000) highlighted the danger of inferring to what species are catalytically active on the bases of what is revealed by XPS because irradiation used may change the electronic structure of the catalyst being examined, i.e. ionic Au species may be reduced to metallic Au by XPS irradiation. This technique can also be used to identify the atomic ratio of surface species of the catalyst, which can suggest whether the Au species are agglomerated or well dispersed, for example, Kozlov *et al.* (1999) observed the larger Fe/Au ratio for Au/Fe(OH)$_3$ calcined at 200 ^{o}C than that of uncalcined Au/Fe(OH)$_3$. The reason for this is that the Au species detected by XPS on the calcined catalyst are either agglomerated or they are located in relatively

deeper channels below the outer surface. A shift in the binding energy of Au $4f_{7/2}$ to the lower binding energy was observed with increasing calcination temperature and this suggests the formation of Au^0 from the ionic species (Kozlov *et al,* 1999). Similar results were also observed by Soares *et al.* (2003) with Au/TiO_2 catalysts

2.12.5 Mössbauer Effect Spectroscopy

Since Mössbauer is element selective and sensitive to the local surroundings of the atoms. It is an excellent probe for gold catalysts as it can provide information on the s-electron density at the gold nuclei from the Isomer shift (IS) and on the symmetry of the environment of the gold atoms from the quadrupole splitting (QS) (Stievano *et al,* 1998). This sensitivity makes it possible to resolve different metal sites within the catalyst particles and thereby differentiate between metal atoms at the surface and atoms in the inner-core of the particles (Goosens *et al,* 2002). This technique has been employed to assist the elucidation of the oxidation state in gold of active catalysts. The structural and bonding information on gold compounds is mainly derived from the IS and the QS of the Mössbauer line. The isomer shift is proportional to the electronic density of gold nuclei that increases with the oxidation state of the gold and the covalency of the bonds (Faltens, 1979; Parish, 1982). The quadrupole splitting is the measure of the asymmetry of the distribution of the electronic charge around the gold nucleus and reflects the covalency and asymmetry of the bonds. There is no QS for metallic gold which has a cubic structure and the Mössbauer spectra consists of one line (singlet). For gold compounds there is a correlation between IS and QS which is useful to distinguish between Au(I) and Au(III) and gives the indication of the number and type of the ligands bound to the gold atom (Griffie *et al,* 1996). Stievano *et al.* (1998) observed an additional quadupole splitting components attributed to surface atoms with gold particles less

than 6nm in diameter. These components became more dominant for the smallest particles. Mössbauer helps in shedding light on the fact that small gold particles which are known to be more active for CO oxidation may contain Au^{n+} species as will be shown later in chapter 4 of this document.

2.12.6 Infrared Spectroscopy (IR)

FTIR of adsorbed CO on different catalysts have been studied by different groups to correlate the pretreatment and the Au particle size effects on the adsorption behavior and on the catalyst performances. This technique has been employed and assists in elucidating the gold catalyst morphology by means of the different peaks observed after adsorption of species such as NO and CO on the surface of the catalysts. For example, Buccozzi *et al.* (2001) have observed an absence of the band at about 2100 cm^{-1} with the catalyst calcined at 873 K sample but this band is present on those catalysts calcined at 573 K and 473 K after chemisorbing CO on the catalysts and 90 K. The absorption at 2100 cm^{-1} is assigned to CO chemisorbed on metallic gold sites of the catalyst. This therefore means that the catalyst calcined at 873 K does not adsorb CO on terrace site which constitute a larger majority of exposed gold sites on this catalyst at 90 K. IR also reveals that only metallic Au species on the step site can chemisorb CO at 90 K. The lower intensity of the band at 2100 cm^{-1} was observed on the 473 K sample than on the 573 K sample, in spite of a smaller mean diameter of the metallic Au particles, was ascribed to the fact that on the 473 K sample a significant fraction of gold after preparation is still not in metallic but in an oxidized state (Buccozzi *et al,* 200; Manzoli *et al,* 2003).

2.12.7 X-ray absorption Fine Structure (XAFS)

XAFS spectroscopy is the only spectroscopic technique that provides information on the electronic and structural properties of catalysts under reaction conditions and in the presence of reactants. This is true because EXAFS is one of only a few probes that utilize photons exclusively. XRD is similar in this regard but requires long-range order and provides only geometric information. EXAFS explores the modulations of the X-ray absorption coefficient above the absorption edge of a given element and is caused by the scattering of the ejected photoelectron from neighboring atoms. Quantitative information is obtained regarding the structure of the first few coordination shells around the absorbing atom such as bond distances, coordination number and the Debye-Waller factions. Typically the EXAFS region extends from approximately 40 eV to about 1000 eV. In contrast to the XRD, EXAFS is very sensitive to the light backscattering atoms, and it is therefore very useful for the investigation of oxides and nitrides. This technique has been limited until recently to providing geometric information on systems with short range order. However, recent advances have extended it to also providing electronic structure (Koningsberger *et al,* 2000). EXAFS is used to identify the size of the Au cluster on the surface of the support by monitoring the number of neighboring atoms and the bond distance between two Au atoms. For instance, Guzman and Gates (2002) observed that a catalyst prepared from $[Au(CH_3)_2(acac)]$ adsorbed on MgO and subsequently treated in flowing He at 373 K for 2 h, initially contained gold predominantly in the form of extremely small clusters, modelled as Au_6 octahedral using EXAFS, showing first- and second-shell Au-Au coordination numbers of 4.0 ± 0.4 and 1.0 ± 0.1, respectively. Another catalyst prepared in a similar way but subsequently treated in flowing He at 573 K for 2 h, initially contained larger (aggregated) clusters, with an average diameter of about 30 Å (containing an average of about 100 Au atoms each)

as inferred from the EXAFS first- and second-shell Au-Au coordination numbers of 9.4 ± 0.9 and 3.5 ± 0.4, respectively.

2.12.8 X-ray Absorption Near Edge Structure (XANES)

For other experiments using the near edge region (up to 40 eV above the edge), the name XANES usually applies. XANES can provide information about vacant orbitals, electronic configuration and site symmetry of the absorbing atom. The absolute position of the edge contains information about the oxidation state of the absorbing atom. In the near edge region, multiple scattering events dominate. Theoretical multiple scattering calculations are compared with experimental XANES spectra in order to determine the geometrical arrangement of the atoms surrounding the absorbing atom. XANES provides information about the oxidation state of gold on fresh and used catalyst (Guzman and Gates, 2002). This technique was also used to monitor the change in the oxidation state of gold during an in-situ CO oxidation (Zanella *et al,* 2004). The use of this technique can provide information on the effect of CO/O_2 mixture (time-on-stream) on the oxidation state of the as-prepared catalyst at a certain temperature.

2.13 References

Aida T, Higuchi R, Niiyama H, *Chem. Lett.,* (1990) 2247.

Akita T, Lu P, Ichikawa S, Tanaka K, Haruta M, *Surf. Interf. Anal.* 31 (2001) 73.

Andreeva D., Tabakova T., Idakiev V., Ilieva L., Falaras P., *Appl., Catal., A*: 72 (2002) 51.

Andreeva D., Tabakova T., Idakiev V., Christov P., and Giovanoli R., *Appl., Catal., A*: 169 (1998) 9.

Bailie J.E. and Hutchings G.J., *Chem. Comm*., (1999) 2151.

Bailie J.E, Abdullah H.A, Anderson J.A, Roechester C. H, Richardson N.V, Hodge N, Zhang J.-G, Kiely C.J, Burrows A, Hutchings G.J, *Phys. Chem. Chem. Phys.,* 3 (2001) 4113.

Bethke G.K and Kung H.H, *Appl. Catal. A:* 194 –195 (2000) 43.

Besson M, Kallel A, Gallezot P, Zanella R, Louis C, *Catal. Comm.,* 4 (2003) 471.

Bera P, Partil K.C, Jayaram P, Hedge M.S, Subbanna G.N, *J. Mater. Chem.* 9 (1999) 1801.

Biella S, Prati L, Rossi M, *Inorg. Chem. Acta*, 349 (2003) 253.

Buccozzi F., Chiorino A., Manzoli M., Andreeva D., Tabakova T., *J. Catal.,* 188 (1999) 176.

Blick K., Mitrelias T.D, Hargreaves J.S.J, Hutchings G.J, Joyner R.W, Kiely C.J, Wagner F.E., *Catal. Lett,* 50 (1998) 211.

Bond G.C., *Catal. Today*, 72 (2002) 5.

Bond G.C and Thompson D.T, *Gold Bull*., 33 (2000) 41.

Bond G.C and Thompson D.T, *Catal. Rev. Sci. Eng*. 41 (1999) 319.

Bond G.C and Sermon P, *Gold Bull.,* 6 (1973) 102.

Bollinger M.A and Vannice M.A, *Appl. Catal.,* 8 (1996) 417.

Boccuzzi F, Chiorino A, Tsubota S, Haruta M, *J. Phys. Chem.*, 100 (1996) 3625.

Boccuzzi F, Chiorino A, Manzoli M, Lu P, Akita T, Ichikawa S, Haruta M, *J. Catal.,* 202 (2001) 256.

Bulushev D.A, Kiwi-Minsker L., Yaranov I., Suvorova E.I., Buffat P.A., Renken A, *J. Catal*., 210 (2002) 149.

Chang C.-Y, ChenY.-J, Yeh C.-T, *Appl. Catal. A:* 174 (1998) 13.

Clark H.W., Bowman R.G., Maj J.J., Bare S.B., Hartwell G.E., *US Patent* 5,965,754 (1999).

Centeno M.A., Paulis M., Montes M., Odriozola J.A., *Appl. Catal.,* 234 (2002) 65.

Costello C.K, Kung M.C, Oh H.-S, Wang Y, Kung H.H, *Appl. Catal., A*: 232 (2002) 159.

Cunningham D.A.H, Vogel W., Kageyama H., Tsubota S., Haruta M., *J. Catal.,* 177 (1998) 1.

Daté M, Ichihashi Y, Haruta M, *Jpn Pat. Appl.* 2000-158422.

Daté M, Haruta M, *J. Catal.,* 201 (2001) 221.

Dekkers M.P.A, Lippits M.J, Nieuwenhuys B.E, *Catal. Today*, 54 (1999) 381.

Delgass W.N, Boudart M., Parravano G., *J. Phys. Chem*., 72 (1968) 3563.

Donitz W., Gutmann G., and Urban, P., *in "Proceedings of the Second International Symposium on New Materials for Fuel Cell and Modern Battery Systems"* (O. Savadogo and P. R. Roberge, Eds.), pp. 14–26. Ecole Polytechnique de Montreal, Montreal, 1997.

Finch R. M., Hodge N.A, Hutchings G.J, Meagher A, Pankhurst Q.A, Rafiq M, Siddiqui H, Wagner F.E, Whyman R, *PCCP,* 1 (1999) 485.

Fu Q., Kudriavtseva S., Saltburg H., Flytzani-Stephanopoulos M., *Chem. Eng. Journal,* 93 (2003) 41.

Galvagno S., Parravano G., *J. Catal.,* 55 (1978) 178.

Gardner S.D, Huflund G.B, Davidson M.R, Laitinen H.A, Schryer D.R, Upchurch B.T, *Langmuir*, 7 (1991) 2140.

[a]Gardner S.D, Huflund G.B, Upchurch B.T, Schryer D.R, Kielin E.J, Schryer J., *J. Catal.*, 129 (1991) 114.

Gilbert S.E, Cavalleri O, Kern K, *J. Phys. Chem.,* 100 (1996) 12123.

Golunski S*,* Rajaram R, Hodge N, Hutchings G.J, Kiely C.J*, Catal. Today,* 72 (2002) 107.

Goosens A., Craje M.W.J, van der Kraan A.M, Zwijnenburg A, Makkee M., Moulijn J.A., de Jongh L.J., *Catal. Today,* 72 (2002) 95.

Grisel R.J.H, Weststrate K.-J, Gluhoi A., Nieuwenhuys B.E, *Gold Bull.,* 35 (2002) 39.

[a]Grisel R.J.H and Nieuwenhuys B.E., *Catal. Today,* 64 (2001) 69.

Grisel R.J.H and Nieuwenhuys B.E., *J. Catal*., 199 (2001) 48.

Grisel R.J.H, Kooyman P.J, Nieuwenhuys B.E, *J. Catal.,* 191 (2000) 430.

Grunwaldt J.-D and Baiker A., *J. Phys. Chem. B*:, 103 (1999) 1002.

Grunwaldt J.-D, Maciejewski M, Becker O.S, Fabrizioli P, Baiker A., *J. Catal.,* 186 (1999) 458.

Guczi L, Horvath D., Pastel Z., Toth L., Horvath Z.E, Karacs A., *J. Phys. Chem. B*., 104 (2000) 3183.

Guillemot D, Polisset-Thfoin M, Fraissard J., *Catal. Lett.,* 41 (1996) 143.

Guillemont D, Borovkov V.Y, Kazansky V.B, Polisset-Thfoin M, Frassard J, *J. Chem. Soc. Faraday Trans.,* 93 (1997) 3587.

Guzman J. and Gates B, *J. Phys. Chem., B:* 106 (2002) 7659.

Haruta M, *Now and Future,* 7 (1992) 13.

Haruta M, Tsubota S, Kobayashi T, Kageyama H, Genet M.J, Delmon B, *J. Catal*., 144 (1993) 175.

Haruta M., *Catal. Today*, 36 (1997) 153.

Haruta M., Tamada N., Kobayashi T and Iijima S., *J. Catal*., 115 (1989) 301.

Haruta M*,* Daté M, *Appl. Catal A:* 222 (2001) 427.

Haruta M, *Chem. Record,* 3 (2003) 75.

Hayashi T., Tanaka K., Haruta M., *J. Catal.,* 178 (1998) 566.

Hoflund G.B, Gardner S.D, Schryer D.R, Upchurch B.T, Kielin E.J, *Appl. Catal., B*: 6 (1995) 117.

Hutchings G. J., *Catal. Today* 72 (2002) 11.

Hutchings G.J, Grady D.T, *Appl. Catal.,* 16 (1985) 411.

Idakiev V, Ilieva L, Andreeva D, Blin J.L, Gigot L, Su B.L*, Appl. Catal., A*: 243 (2003) 25.

Iizuka Y., Fujiki H., Yamanchi N., Chijiika T., Arai S., Tsubota S., Haruta M., *Catal. Today,* 36 (1997) 115.

Jia J, Haraki K, Kondo J.N, Domen K, Tamaru K, *J. Phys. Chem. B* 104 (2000) 11153.

Jung C.R, Han J., Nam S.W., Lim T.-H, Hong S.-A., Lee H.-I., *Catal. Today*, 93-95 (2004) 183.

Kahlich M.J, Gasteiger H.A., and Behm R.J, *J. Catal*., 182 (1999) 430.

Kalvachev Y.A, Hayashi T, Tsubota S, Haruta M, *J. Catal.,* 186 (1999) 228.

Kang Y.-M, Wan B.-Z, *Appl. Catal. A:* 128 (1995) 53.

Knell A., Barnickel P., Baiker A. and Wokaun A., *J. Catal*., 137 (1992) 306.

Ko Y.Y.H, Mizuhata M., Kajinami A., Deki S., *J. Elect. Anal. Chem.,* 559 (2003) 91.

Kolb D.M, Ullmann R, Will T, *Science,* 275 (1997) 1097.

Koningsberger D.C, Mojet B.L, van Dorssen G.E, Ramaker D.E, *Topics in Catalysis* 10 (2000) 143.

Konova P, Naydenov A, Venkov Cv, Mehandjiev D, Andreeva D, Tabakova T, *J. Mol. Catal A:* 213 (2004) 235.

Kozlov A.I, Kozlova A.P, Liu H, Iwasawa Y, *Appl. Catal. A:* 182 (1999) 9.

Kozlova A.P, Sugiyama S, Kozlov A.I, Asakura K, Iwasawa Y, *J. Catal.,* 176 (1998) 426.

Kung H.H, Kung M.C, and Costello C.K, *J. Catal.,* 216 (2003) 425.

Lai X, St. Clair T.P, Valden M, Goodman D, *Prog. Surf. Sci.,* 59 (1998) 25.

Lee S.-J, and Gavriilidis A., *J. Catal*., 206 (2002) 305.

Lin S. and Vannice M.A., *Catal. Lett*., 10 (1991) 47.

Lin S, Bollinger M., Vannice M., *Catal. Lett.,* 17 (1993) 245.

Lin J.-N, Chen J.-H, Hsiao C.-Y, Kang Y.-M, Wan B.-Z, *Appl. Catal. B*: 36 (2002) 19.

Liu H, Kozlov A.I, Kozlova A.P, Shido T, Asakura K, Iwasawa Y, *J. Catal.,* 185 (1999) 252.

Luengnaruemitchai A, Osuwana S, Gulari E, *Int. J. Hydr. Energy,* 29 (2004) 429.

Luengnaruemitchai A., Asuwan S., Gulari E., *Catal. Comm.,* 4 (2003) 215.

Mabudafhasi M.L., Bodkin R., Nicolaides C.P., Liu X.-Y, Witcomb M.J., Coville N.J., *Carbon,* 40 (2002) 2737.

Mallick K., Scurrell MS, *Appl. Catal*., *A*: 253 (2003) 527.

Mann R. F, Amphlett J. C, Peppley B. A., *Frontiers Sci. Ser.,* 7 (1993) 613.

Mathieson T.J, Langdon A.G, Milestone N.B, Nicholson B.K, *Chem. Comm.,* (1998) 371.

Meldrum F.C, Seshadri R, *Chem. Comm.,* (2000) 29.

Miao S, Deng Y, *Appl. Catal. B:* 31 (2001) L1–L4.

Minaco S., Scire S., Crisafulli C, Visco A.M, Galvano S, *Catal. Lett*., 47 (1997) 273.

Mohamed M.M., Salama T.M., Ichikawa M., *J. Col. Int. Sci.*, 224 (2000) 366.

Mohr C, Hofmeister H, Claus P, *J. Catal.,* 213 (2002) 85.

Mukherjee P., Patra C.R, Ghosh A., Kumar R., Sastry M., *Chem. Mater.,* 14 (2002) 1678.

Nechayev Y. A., and Nikolenko N. V., *Geochem. Intl.,* 23 (1986) 32.

Nijhuis T.A., Huizinga B.J., Makkee M., Moulijn J.A., *Ind. Eng. Chem. Res*. 38 (1999) 884.

Nkosi B, Coville N.J, Hutchings G.J, Adams M.D, Friedl J, Wagner F.E, *J. Catal. ,* 128 (1991) 366.

[a]Nkosi B, Adams M.D, Coville N.J, Hutchings G.J., *J. Catal.,* 128 (1991) 378.

Ntais S, Dracopoulos V, Siokou A, J. Mol. Catal., A: 220 (2004) 199.

Oh, H.-S., Costello, C. K., Cheung C., Kung, H. H., and Kung, M. C., *Stud. Surf. Sci. Catal.,* 139 (2001) 229.

Oh H.-S, Yang J.H, Costello C.K, Wang Y.M, Bare S.R, Kung H.H, Kung M.C, *J. Catal.,* 210 (2002) 375.

Okumura H., Tsubota S., Haruta M., *J. Mol. Catal. A:* 199 (2003) 73.

Okumura M., Akita T., Haruta M., *Catal. Today,* 74 (2002) 265.

Okumura M, Haruta M, Wang X, Kajikawa O, Okada O, *Abstract 3rd Intern. Conf. Environ., Catal., Tokyo Dec.* (2001), p 15.

Okumura M., Tsubota S., Iwamoto M., and Haruta M., *Chem. Lett.*, (1998) 315

Park E.D. and Lee J.S., *J. Catal.,* 186 (1999) 1.

Pestryakov A.N, Lunin V.V, Kharlanov A.N, Kochubey D.I, Bogdanchikov N, Stakheev A.Y, *J. Mol. Str.,* 642 (2002) 129.

Porta F and Prati L., *J. Catal*., 224 (2004) 397.

Qui S, Ohnishi R, Ichikawa M, *J. Phys. Chem.* 101 (1994) 2719.

Qui S, Ohnishi R, Ichikawa M, *J. Chem. Soc., Chem. Commun.* (1992) 1425.

Rao C.N.R, Kulkarni G.U, Thomas P.J, Edwards P.P, *Chem. Soc. Rev.,* 29 (2000) 27.

Robeiro F.H, Chow M, Betta R.A.D, *J. Catal.,* 146 (1994) 537.

Sakurai H., Ueda A., Kobayashi T., Haruta M., *Chem. Comm.,* (1997) 271.

Sakurai H, Haruta M, *Appl. Catal. A:* 127 (1995) 93.

Salama T.M., Ohnishi R, Shido T., Ichikawa M., *J. Catal.,* 162 (1996) 169.

Salama T.M, Ohnishi R, Shido T, Ichikawa M, *J. Chem. Soc., Chem. Comm.,* (1994) 2749.

Sanchez R.M.T, Ueda A, Tanaka K, Haruta M, *J. Catal.* 168 (1996) 125127.

Schubert M.M, Hackenberg S, van Veen A.C, Muhler M, Plzak V, Behm R.J, *J. Catal.* 197 (2001) 113.

Schimpf S., Lucas M., Mohr C., Rodemerck U., Brückner A , Radnik J., Hofmeister H, Claus P., *Catal. Today,* 72 (2002) 63.

Schubert M.M, Kahlich M.J, Gasteiger H.A, Behm R.J, *J. of Power Sources*, 84 (1999) 175.

Sekizawa K, Wadjaja H, Eguchi K, *Proc. Inc. Workshorp Catal. Combust*, 4 (1999) 79.

Sermon P.A, Bond G.C, Wells P.W, *J. Chem. Soc., Faraday Trans. I,* 75 (1979) 385.

Sinha A.K, Seelan S, Akita T, Tsubota S, Haruta M, *Appl. Catal A:* 240 (2003) 243.

Shinoda K., *Chem. Lett*., (1975) 219.

Soares J.M.C, Morrall P., Crossley A, Harris P, Bowker M., *J. Catal.,* 219 (2003) 17.

Stievano L., Santucci S., Lozzi S, Calogero S, Wagner F.E, *J. Non-Crystal. Sol.,* 232-234 (1998) 644.

Sumida T, Murakoshi K, Yanagida S, *Chem. Lett.,* 28 (1999) 599.

Tabakova T, Boccuzzi F, Manzoli M, Andreeva D, *Appl. Catal. A:* 252 (2003) 385.

Tripathi A.K., Kamble V.S., and Gupta N.M. *J. Catal.*, 187 (1999) 332.

[a]Tsubota S, Cunningham D, Bando Y, Haruta M, *Stud. Surf. Sci. Catal.* 91 (1995) 227.

Tsubota S, Cunningham D, Bando Y, Haruta M., in Poncelet G., *et al.* (Eds.), Preparation of Catalysts VI, Elsevier, Amsterdam, 1995, 275 pp.

Ueda A, Haruta M, *Appl. Catal. B:* 285(1996)81.

Ueda A, Haruta M, *Shigen Kankyu Taisaku (Res. and envir. Tech.),* 28(1992)1035.

Uphade B.S, Akita T., Nakamura T., Haruta M., *J. Catal.,* 209 (2002) 331.

Uphade B.S., Okumura M., Tsubota S., Haruta M., *Appl. Catal.* A 190 (2000) 43.

Valden M, Pak S, Lai X, Goodman D.W, *Catal. Lett*., 56 (1998) 7.

Venugopal A., and Scurrell M., *Appl., Catal., A*: 245 (2003) 137.

[1]Venugopa A, Aluha J., Mogano D., Scurrell M., *Appl., Catal., A*: 245 (2003) 149.

Visco A, Donato A, Milone C, Galvagno S, *Reac. Kinet. Catal. Lett.,* 61 (1997) 219.

Vogel W., Cunningham D.A.H, Tanaka K., and Haruta M., *J. Catal*., 40 (1996) 175.

Wagner F.E, Galvagno S, Milone C, Visco A.M, Stievano L, Calogero S, *J. Chem. Soc., Faraday Trans.* 93 (1997) 3403.

Wang D, Hao Z, Cheng D, Shi X, Hu C, J. *Mol. Catal A,* 200 (2003) 229.

Waters R.D, Weimer J.J, Smith J.E, *Catal. Lett.,* 30 (1995) 181.

Wolf A and Schuth F. A., *Appl. Catal*., 226 (2002) 1.

Yan L, Zhang X, Ren T, Zhang H, Wang X, Suo J, *Chem. Comm.,* (2002) 860.

Yuan Y, Asakura K, Wan H, Tsai K, Iwasawa Y, *Catal. Lett*., 42 (1996) 1520.

Yuan Y., Kozlova A. P, Asakura K., Wan H., Tsai K., Iwasawa Y., *J. Catal*. 170 (1997) 191.

Yuan Y, Asakura K, Kozlova A.P, Wan H, Tsai K, Iwasawa Y, *Catal. Today,* 44 (1998) 333.

Zanella R, Giorgio S, Shin C.-H, Henry C.R, Louis C, *J. Catal.,* 222 (2004) 357.

Zhang L, Persuad R, Madey T, *Phys. Rev. B* 56 (1997) 10549.

Zwijnenburg A, Saleh M, Makkee M, Moulijn J.A, *Catal. Today,* 72 (2002) 59.

Chapter 3

Experimental Procedures

3.1. Catalyst preparation

3.1.1. Preparation of 2wt% Au/TiO_2-ZrO_2 catalysts

3.1.1.1. Zirconia introduction by deposition precipitation

The appropriate amounts of $ZrO(NO_3)_2.xH_2O$ and TiO_2 (P25 Degussa) were measured in such a way that they make a 1:1 ratio by mass. These were mixed with distilled water (1.5 l) and stirred with an overhead stirrer for about 20 min. A solution of $HAuCl_4.xH_2O$ (Johnson Matthey) in 250 ml of distilled water was prepared and added to the support solution in a drop wise manner (approx. 1 drop in 2 seconds). When all the gold solution had been added to the support suspension, the mixture was stirred for about 15 to 20 min. before precipitation with 10% NH_4OH solution, which was also added in a drop wise manner at approximately the same dropping rate as that used for the gold solution. The ammonia solution was added until the mixture reached a required pH. The precipitates were aged in the mother solution for 24 h (unless

otherwise mentioned), after which they were filtered, washed and dried at 120 ^{o}C overnight and calcined for 5 h at selected temperatures between 100 and 500 ^{o}C).

3.1.1.2. Zirconia introduction by impregnation

Catalyst A (Au/TiO_2-ZrO_2)

$ZrO(NO_3)_2.xH_2O$ was dissolved in water and impregnated onto TiO_2. Various amounts of ZrO_2 were impregnated on the TiO_2 surface as shown in table 1. The product was dried at 120 ^{o}C for 16 h and calcined at 400 ^{o}C for 5 h, after which it was ground into a fine powder and suspended in 1 litre of distilled water. This was stirred with an overhead stirrer for 40 minutes. Deposition of gold, drying and calcination of these catalysts followed the procedure as described above.

Table 3.1: Varying the amount of ZrO_2 on Au/TiO_2-ZrO_2 catalyst

Catalyst	(% ZrO_2 by mass %)
A1	50
A2	30
A3	15
A4	5
A5	0

3.1.2 Preparation of 2wt% Au/TiO_2 Catalysts

3.1.2.1 Deposition-precipitation: Method 1

TiO_2 (Degussa P25) (5.06 g) was mixed with distilled water (1 l) and stirred for 10 min. A solution of $HAuCl_4.xH_2O$ with distilled water was added drop wise after which the ammonium solution was added drop wise to precipitate the catalyst until a certain pH was reached. The catalyst was aged, filtered and washed with distilled water (~ 3 l). The catalyst was dried at 120 ^oC for 16 h and then calcined at 400 ^oC for 5 h. Various pH and ageing times were investigated as shown below.

The catalysts were precipitated at different pH and aged for 12 h:

- pH 5 (AT 5)
- pH 7 (AT 7)
- pH 9 (AT 9)
- pH 11 (AT 11)

AT = Au/TiO_2 at a certain pH

The catalysts were aged for different periods and precipitated at pH 9

- Age 0 (Unaged) (A 0)
- Age 6 (A 6)
- Age 12 (A 12)

A = ageing for a certain period

3.1.2.2 Deposition-precipitation: Method 2

An appropriate amount of $HAuCl_4.xH_2O$ was dissolved in distilled water and hydrolyzed by 0.2 M NaOH solution until pH 6 (pH 7 for some catalysts) with constant stirring. This pH was maintained for 24 h to ensure complete hydrolysis of the gold chloride complex. 2 g of TiO_2 (P-25 or rutile) was added into the solution with continued stirring. The temperature of the mixture was raised to 80 ^oC and the stirring was stopped. The catalyst was aged at this temperature for 1 h after which it was cooled to room temperature, suction filtered and washed. This was followed by drying at room temperature. No further catalyst pre-treatment was done before the reaction was carried.

Catalysts Prepared and studied:

- Au/TiO_2 (rutile) (pH 6)
- Au/TiO_2 (rutile) (pH 7)
- Au/TiO_2 (P25) (pH 7)

3.1.2.3 Sol-gel catalyst preparation method

Au/ZrO_2 (2 wt%)

Zirconium isopropoxide (2 g) was weighed and mixed with 8 ml of n-propanol in a two necked round-bottomed flask. This mixture was refluxed at 82 ^{0}C for about 90 min. No total dissolution of zirconium isopropoxide in n-propanol was observed. A solution of $HAuCl_4.xH_2O$ in distilled water (1 ml) was added drop wise to the propoxide suspension. After about 5 min, 7 drops of 10% NH_4OH was added to increase the pH of this solution. The contents of the flask were stirred at the same temperature (80 ^{o}C) for about 24 h. About half of the contents of the flask had gelled whereas the rest of the mixture remained in a liquid form. No filtering or washing of the catalyst was carried out; the contents of the flask were dried (120 ^{o}C/16 h), and a portion of it was subsequently calcined (400 ^{o}C/5 h)

Au/TiO_2 (2 wt%)

A similar method (as described above) was used to synthesize this catalyst with the titanium isopropoxide being used instead of zirconium isopropoxide.

3.1.2.4 An attempt to control the size of the gold particles by means of pH

Au/TiO_2 (2 wt%)

Titanium isopropoxide (4.03 g) was weighed and mixed with 16 ml of n-propanol in a two-necked-round bottomed flask. This mixture was refluxed at 80 ^oC for about 90 min. A solution of $HAuCl_4.xH_2O$ in distilled water was adjusted to pH 9 with 10% NH_4OH before being added drop wise to the titanium- containing solution. Some precipitation of gold was observed, probably because pH 9 was too high. No further base was added into the round-bottomed flask. The contents of the flask were stirred at the same temperature (80 ^oC) for about 24 h. About half of the contents of the flask had gelled whereas the rest of the mixture remained in a liquid form. This solid was washed with distilled water, even though contact with water produced a very thick gel. The contents of the flask were dried at 120 ^oC for 16 h; a portion of it was calcined at 400 ^oC for 5 h.

3.1.2.5 Synthesis of the support by sol-gel method and deposition of gold

Equivalent masses of titanium isopropoxide and zirconium isopropoxide were weighed and mixed with 16 ml of n-propanol in a two-necked round-bottomed flask. This mixture was refluxed at 80 ^oC overnight to ensure the dissolution of zirconium isopropoxide. 7 drops of 10% NH_4OH were added to increase the pH of this solution. The solution gelled to some extent and was washed with distilled waster even though contact with water made it a very thick gel. The thick gel was dried for 16 h in the oven and then calcined for 5 h at 400 ^oC.

The support was crushed and re-dispersed in distilled water followed by the deposition of gold solution as described before, then dried and calcined.

3.1.3 Catalyst synthesis of ceria-containing catalysts

3.1.3.1 Preparation of CeO_2 from $Ce(NO_3)_3 \cdot 6H_2O$

$Ce(NO_3)_3 \cdot 6H_2O$ (30 g) was dissolved in 1 l of distilled water and stirred for 10 min. to ensure complete dissolution. 10% NH_4OH solution was added drop wise to precipitate $Ce(OH)_4$ out of the solution. This occurred when the pH reached 9, and the colour of the precipitate turned brown. The precipitates were aged for 1 h to allow complete precipitation. After filtration, the precipitate was washed with cold distilled water (ca. 8 liters) until the pH of the filtrate reached 7. The precipitate was dried in the oven for 16 hours at 120 ^oC, after which the colour had changed from brown to yellow. The mass of the dried product were ca. 10 g. The calcined (400 ^oC) material (CeO_2) was still yellow in colour and the mass was 9.8 g.

3.1.3.2 Au/CeO_2 by deposition-precipitation

CeO_2 (8.0 g) prepared as described above was crushed and mixed with 1 l of water. The mixture was heated slightly to increase the degree of dissolution which was found to be difficult at room temperature. A solution of $HAuCl_4 \cdot xH_2O$ in distilled water was added drop wise into the support dispersion after which 10% NH_4OH was used to precipitate the catalyst up to pH 9. The colour remained yellow during precipitation. The catalyst was aged for 12 h after which the precipitate was filtered

and washed with cold distilled water. The catalyst was dried for 16 h at 120 ºC. Another batch of this catalyst was synthesized in a similar manner and was calcined at 400 ^{o}C for 5 h.

3.1.3.3. Au/CeO_2 by co-precipitation

$Ce(NO_3)_3 \cdot 6H_2O$ (20 g) $HAuCl_4.xH_2O$ were mixed with distilled water (1 l) and stirred for about 15 minutes to ensure complete mixing. NH_4OH (10%) was used to precipitate the catalyst by a drop wise addition from pH 3.81 to pH 9.04. Once a few drops of the base were added, the solution changed from light yellow (gold solution colour) to brown black. The pH increased very slowly from 8 to pH 9 and in this region of pH, a lot of base was consumed. The catalyst was aged for 16 h after which it was filtered and washed. It was dried for 16 h at 120 ºC in an oven. No calcination was carried out.

3.1.3.4. Au/TiO_2 – CeO_2 by deposition- precipitation

Equivalent masses of TiO_2 and CeO_2 were mixed with distilled water (1.5 l) CeO_2 was first heated in water to about 50 ºC to increase dissolution of CeO_2 which was difficult to achieve at room temperature. These solutions were stirred for about 10 min at room temperature. A solution of $HAuCl_4 \cdot xH_2O$ with distilled water was prepared and added drop wise to the support suspension. A solution of 10% NH_4OH was added drop wise to precipitate the solid. The solid was aged for 12 h after which the suspension was filtered and washed with cold distilled water. The catalyst was dried for 16 h at 120 ºC.

3.2 Catalyst Characterization

Catalyst characterization is an essential part of all investigations in surface chemistry and a number of characterization techniques is required to complement each other with information on the surface structure of the catalyst (Mpholle, 2002). There are many techniques available for this purpose and the choice depends on the information required. Techniques that have been used in the present work are listed and described below.

3.2.1 Surface area determination – BET

The surface areas of the fresh and used catalysts were determined using a Micromeritics ASAP 2010 porosimeter. The catalyst was placed in the sample holder and first degassed by passing a mixture of N_2 and He over the catalyst while it was heated at 120 ^oC until the pressure reached 0.004 μm Hg (about 3 h) in order to remove any adsorbed water or other volatile materials from the surface of the catalyst. The catalyst was then allowed to cool to room temperature. The sample holder was then moved from the degassing pot to the analysis pot containing the thermocouple. The mixture of N_2 and He (70/30 ratio) was passed over the catalyst and the level of N_2 leaving the reactor was continuously monitored using gas chromatography. The volumes of N_2 detected were then used in surface area calculation in order to obtain pore volume, pore diameter and surface areas.

3.2.2 Mössbauer Effect Spectroscopy

For the ^{197}Au Mössbauer spectroscopy measurements, three sources of ^{196}Pt have been irradiated separately in the "A-East" hydraulic system position #2, at the SAFARI-1 research reactor at NECSA (Pelindaba) for 24 h. Total neutron flux at this position is expected to be ~3×10^{14} n/cm^2/s for the reactor power of 16 MW. This corresponds to ~30 mg/cm^2 of Au in the sample. The platinum foil that constituted the source had dimensions of 4 mm x 4 mm x 60 μm. This was first encapsulated in a titanium holder so that it may be easily handled and also does not become highly radioactive upon irradiation. Secondly the source was encapsulated in an aluminium container to permit handling after irradiation and connection to the probe. By irradiating Pt with thermal neutrons, a fraction of the atoms is transformed into ^{197}Au by the nuclear reaction, $^{196}\text{Pt} \longrightarrow {}^{197}\text{Pt}$, then followed by

$$^{197}\text{Pt} \longrightarrow {}^{197}\text{Au} + e^- + V_e + 0.6\ \text{MeV}$$

Where e^- and V_e are electron and antineutrino respectively.

After ^{197}Pt decays, the ^{197}Au is formed and is in an excited state, decaying with a half life of 18 h, and emitting a photon energy of 77.34 keV. Typical measuring times were in the range 15 – 25 h. Source and sample were first loaded into a liquid helium cryostat 6-10 hours after the irradiation time, and kept at ~6 K for the duration of the Mössbauer measurement. Powdered sample (ca. 3 g) was compacted into a teflon sample holder. A high-resolution Ge detector, cooled to 80 K, was used in the experiment to detect the ~ 77 keV resonance radiations.

3.2.3 X-ray Photon Spectroscopy (XPS)

For this study, a Quantum 2000 Scanning ESCA Microprobe was used. The catalyst was ground and pressed into the sample holder to remove all the air trapped in between the catalyst powder particles. The area of analysis for each catalyst was 500 x 500 μm. A monocromized aluminium K_α source was used as an X-ray source to produce a beam of 100 μm diameter with 20 W power. The base vacuum was 8 x 10^{-9} torr. A charge neutralizer to produce a low flood of electrons and argon ions was used. The carbon 1s peak at 285.0 eV was used for the peak position correction. The pass energy of 117 eV was used for the wide scan, while charge energy of 27 eV was used for a narrow scan. XPS is primarily a surface technique, as the escape depth of the photo-electrons ranges from 2 to 5 nm. The detection limit of XPS is approximately 0,1 at%.

3.2.4 High Resolution Transmission Electron Microscope (HRTEM)

The JEM-100S Transmission Electron Microscope operating at 80 kV was used to establish the dispersion and the particle size of the metal on the catalyst surface. The catalyst was ground and mixed with methanol to make a liquid mixture. A droplet of methanol solution was placed onto the carbon-film-coated copper grids. The sample was left at room temperature for a few minutes to dry before being loaded into the microscope.

3.2.5 X-ray Absorption Near Edge Structure (XANES)

In-situ XAS experiments were carried out at Beam line 5-BMD of the Dupont Northwestern Dow Collaborative Access team at the Advanced Photon Source at Argonne National Laboratory in Argonne, IL. All spectra were collected in a transmission mode at the Au L_{III} edge (11.919 keV) during CO oxidation or in flowing He at –68°C. A flow-through stainless steel sample cell equipped (Figure 3.2) with Al windows was used for the in-situ XAS measurements. About 0.15 g of sample was used to make a self-supporting pellet and was placed at the end of a stainless steel tube between two layers of quartz wool and two nylon grids. The tube was placed in another stainless tube, and a thermocouple was located between them. In order to keep the temperature below –68°C, the outer surface of the cell was in contact with a copper block that was cooled with a mixture of dry ice and ethanol. CO oxidation reaction was conducted at -68°C with a feed of 1% CO, 2.5% O_2, and the balance He with a flow rate of 50 mL min-1 at STP. The CO and O_2 concentrations in the effluent were monitored by a HP 6890 gas chromatograph with a molecular sieve column.

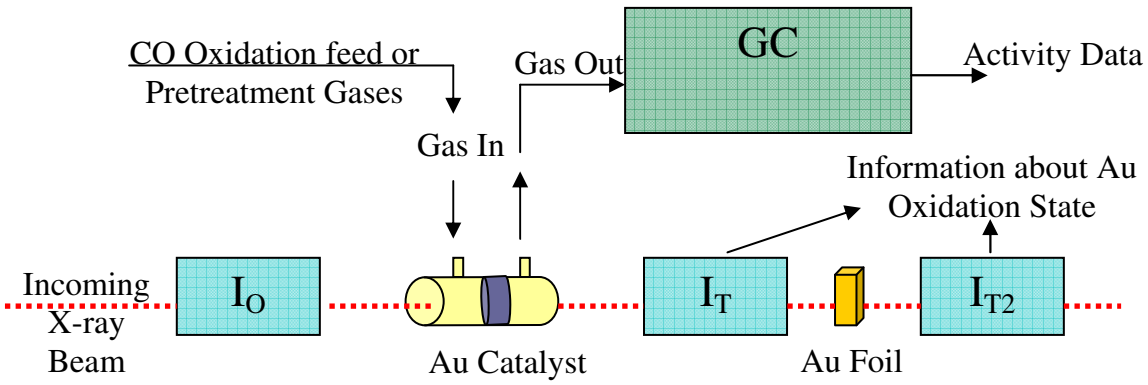

Figure 3.1: Flow diagram of gases and X-ray beam during the XANES experiment

The x-ray source used is the synchrotron which provides a full range of wavelengths and a monchromator was used to select a suitable wavelength. The absorption was measured directly by measuring what is transmitted through the sample by the detector (I_T) using the equation:

$$I = I_o e^{\mu t}$$

Where: I = x-ray transmitted through the sample

Io = incident ray

μ = absorption coefficient

t = sample thickness

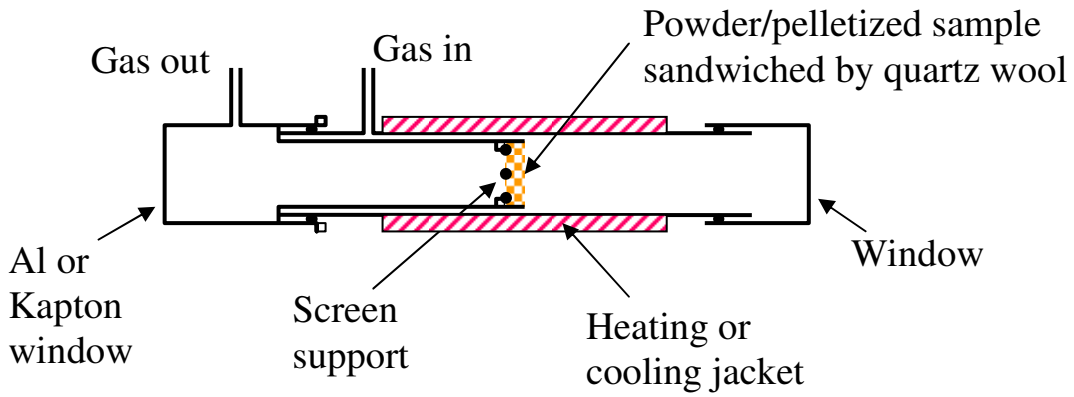

Figure 3.2: Schematic representation of a XANES cell

The sample was purged with 200 ml/min of helium gas at room temperature and cooled to -75 ^{o}C with continuous purging and a XANES scan was taken under the helium atmosphere. The reactor was thereafter allowed to warm up to -60 ^{o}C and maintained at that temperature where CO oxidation reaction was conducted at atmospheric pressure. The flow into the reactor was switched to a by-pass mode and

the reaction mixture of 1% CO and 2.5% O_2 balanced by helium with the total flow rate of 50 ml/min was allowed to flow for calibrations of CO and O_2. The concentration of the gases was monitored by a GC (HP6890) equipped with the molecular sieve column and a TCD detector. The GC was controlled by a PC with Chemstation software. After calibrations, the reactants were allowed into the reactor and the actual activity of the catalyst was monitored. When the CO conversion was constant, the reaction was stopped and the catalyst was purged with 200 ml/min flow of helium, cooled to -75 ^{o}C and another XANES scan was taken. This cycle was repeated until no change in the extent of reduction of the catalyst was observed and when there was also no change in the activity of the catalyst.

3.2.6 Temperature Programmed Reduction (TPR)

An uncalcined Au/P-25 sample was loaded into a u-tube quartz reactor and held between two quartz wool plugs and purged with 200 ml/min flow of helium at room temperature. The reactor was then cooled to -77 ^{o}C with liquid nitrogen. The liquid nitrogen Dewar was emptied and the catalyst was subjected to a flow of 5 vol% H_2/Ar. With the reactor in the emptied, cold Dewar the system was allowed to warm up by a controlled blowing of the air into the Dewar such that the warming was at 3 ^{o}C/min until room temperature, where the Dewar was removed and the reactor was heated at the same rate of 3 ^{o}C/min until 300 ^{o}C. The catalyst temperature was monitored by a K-type thermocouple attached on the outside of the reactor with its tip right next to the catalyst.In another experiment an uncalcined catalyst was first treated in 1% CO/He mixture at room temperature and then subjected to the procedure described above.

3.2.7 Thermogravimetric Analysis (TGA)

TGA of different sol-gel-prepared catalysts was performed using a Pyris 1 TGA-DTA (Perkin Elmer) in order to establish the catalyst mass loss upon temperature increase. These experiments were performed under air atmosphere to assess the temperature at which the adsorbed surface species such as the organic material from the support precursor are burnt off from the catalyst. About 10 mg of the catalyst was placed on the sample holder (aluminium pan). The heater was elevated to completely cover the sample holder. An air flow rate was adjusted to 30 ml/min. The heater was started from room temperature at the heating rate of 10 ^{o}C/min up to 900 ^{o}C. The TGA plots were constructed using an origin 6.0 program.

3.2.8 Inductively Coupled Plasma-Optical Emission Spectrometer (ICP-OES)

The ICP-OES Ciros CCD machine was used to determine the gold loading of the catalysts. Before analysis, 100 mg solid of the sample was first digested with the mixture of 3 ml hydrogen fluoride (HF) and 5 ml nitric acid (HNO_3) for 60 minutes or until complete digestion was achieved in a multi-wave 3000 (solvent extraction) microwave oven (Anton Paar Co.) The digested sample after suitable dilution was then injected into the ICP machine equipped with a 1300 W plasma power and a wavelength of 201.200 nm is used.

3.3 The leaching process of Au/TiO_2 catalysts

Selected catalysts were leached with potassium cyanide (KCN) at different concentration. The simplified equation for gold leaching is:

$$Au + 2CN^- \longrightarrow [Au(CN)_2]^-$$

Thus two moles of CN^- are needed to leach one mole of Au.

The concentrations used for leaching were:

i) 6 mol CN^- : 1 mol Au
ii) 2 mol CN^- : 1 mol Au
iii) 1 mol CN^- : 1 mol Au

10 ml KCN solution was added to 1.0 g Au/TiO_2 catalyst and stirred with a magnetic stirrer. 2.5 ml of NaOH (pH 9) was then added to the leaching mixture drop wise. With the first trial the mixture was stirred for 1 h, but with the subsequent trials, the leaching process was carried out for 5 min. The leached catalyst was filtered and washed with 1 l of distilled water.

The catalysts were leached at different conditions as indicated below.

i). Leached with distilled water only
ii) Leached with the base only (no cyanide)
iii) Leached with cyanide and no base
iv) Another sample was leached with excess base

The leached catalysts were dried in the oven for 16 h and sieved (150-250 µm).

3.4 Activity measurement

3.4.1 Catalysts prepared by deposition-precipitation (method 1) and by sol-gel method

The CO oxidation reactions were carried out in tubular quartz reactor. The temperature was measured by a thermocouple placed in the thermo-well (figure 3.3), which extended down to the catalyst bed. About 200 mg of the catalyst was loaded and treated in 20% oxygen in helium at 100 ^{o}C. The reaction mixture consisted of 10% CO and 5% O_2 balanced by helium at a total flow rate of 40 ml/min. This flow rate corresponded to a space velocity of 2500 h^{-1}. A GC equipped with a Porapak column and a thermal conductivity detector (TCD) was used to analyze the reaction products.

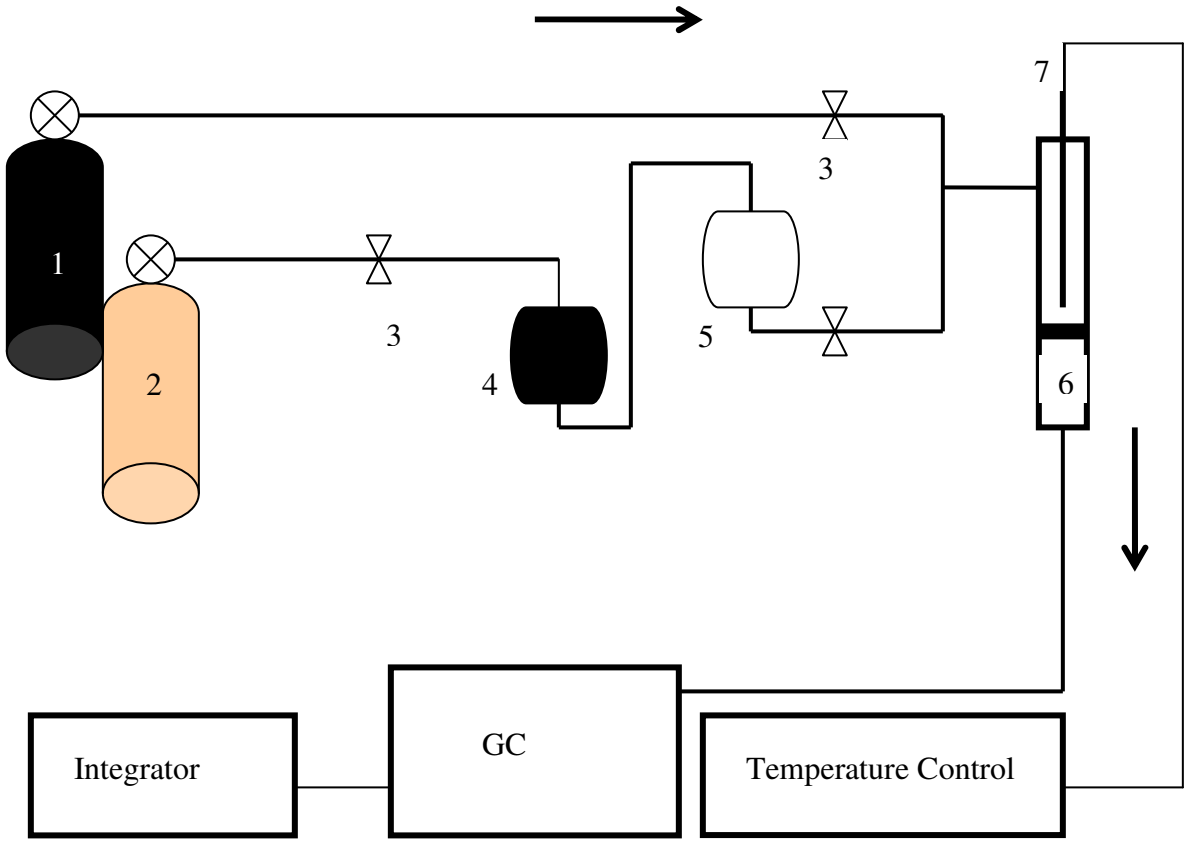

Figure 3.3: Schematic representation of the reactor used for both CO and methane oxidation

Where: 1 = O_2 Gas cylinder; 2 = CO/CH_4 gas cylinder; 3 = shut off valve; 4 = Activated carbon trap; 5 = NaOH trap; 6 = reactor and catalyst bed; 7 = thermocouple; arrow = direction of flow.

3.4.2 Catalysts prepared by deposition-precipitation by method 2

A batch of 0.1 g catalyst was loaded in the u-tube quartz reactor and purged with 200 ml/min flow of He for 30 minutes. It was then cooled to dry ice temperature in a bath of dry ice and acetone and tested for CO oxidation at -58 ^{o}C or -78 ^{o}C. The reaction mixture comprised 1% CO, 2.5% O_2 balanced by helium and the total flow rate was either 50 ml/min or 200 ml/min. The reactants and products of the reaction were separated by a GC equipped with a molecular sieve column and a TCD detector.

3.5 Calculations

$$\%CO\ Conversion = \frac{CO_{in} - CO_{out}}{CO_{in}}\ X\ 100\%$$

$$\%wt\ Au = \frac{M_{Au}}{M_{Au} + M_{\sup}}\ x\ 100\%$$

Where: M: - is the molecular weight

Sup: - support

CO_{in}: - moles of carbon monoxide fed into the reactor

CO_{out}: - moles of carbon monoxide unreacted

3.6. Reference

Mpholle L.J, PhD Thesis, University of the Witwatersrand, Johannesburg 2000.

Chapter 4

The effect of zirconia on Au/TiO_2-ZrO_2 catalyst for CO oxidation

4.1. Introduction

When gold is highly dispersed as nano-sized particles on a metal oxide support it shows a high catalytic activity in several reactions such as the reduction of nitrogen oxides (Salama *et al,* 1996), the epoxidation of propene (Hayashi *et al,* 1998) and the low temperature oxidation of CO (Bond *et al,* 1999; Haruta *et al,* 1993). The high catalytic oxidation of gold is unexpected as bulk gold is quite inert because of its $5d^{10}$ configuration and even reactive molecules like CO and H_2 do not adsorb on its surface (Tripathi *et al,* 1999; Grunwaldt *et al,* 1999).

Although the catalytic activity of gold catalysts in the low temperature CO oxidation has been intensively studied during the last decade, the nature of the active species is still discussed controversially. It has been suggested that the role of the metal oxide is to stabilize the gold nano-particles and that the reaction takes place on the gold surface (Haruta *et al,* 1997; Haruta *et al,* 1989; Valden *et al,* 1998). Other authors proposed that the reaction takes place at the gold/metal oxide interface and that the metal oxide could act as a source of oxygen (Kozlov *et al,* 1999). Other researchers

however proposed that the active species is the metallic gold because they found no evidence of the presence of ionic gold species on their active catalysts (Griesel *et al,* 2002; Guczi *et al,* 2000).

Based on the spectroscopic analysis indicating the presence of ionic gold in the most active catalysts, some researchers proposed the ionic gold to be necessary for high CO oxidation activity although there is no consensus on whether it is Au^{III} or Au^{I}, which is important. Several groups have observed the presence of ionic gold in active catalysts by Mössbauer effect spectroscopy (Soares *et al,* 2003, Finch *et al,* 1999), XPS (Park and Lee, 1999) and XANES (Guzman and Gates, 2002; Oh *et al,* 2001). Minaco *et al.* (1997) have observed the presence of Au^{I} on their active Au/Fe_2O_3 using FTIR. After extensively reviewing the available literature on gold catalysis, Bond and Thompson (2000) proposed that the active site consists of an ensemble of $Au(OH)_3$ and metallic gold.

The synthesis of highly dispersed small gold particles is highly sensitive with respect to the preparation method. It has been reported that the incipient wetness impregnation is unsuitable to produce highly dispersed gold catalysts (Haruta, 1997 and Haruta *et al,* 1993), and that in order to obtain high activity gold catalysts, the materials have to be prepared via co-precipitation (Fu *et al,* 2003) or deposition-precipitation (Wolf and Schuth, 2002; Grisel *et al,* 2000) .On the other hand, Grunwaldt *et al* (1999) emphasized a strong support effect on the activity of the catalysts. They prepared Au/TiO_2 and Au/ZrO_2 catalysts by adsorption of gold colloid onto the support. In their work, Au/TiO_2 achieved 21% and 100% conversions at 305 and 353K respectively whereas the Au/ZrO_2 catalyst was inactive at both temperatures. Their study reports the strong effect the support has on the gold particles.

The use of composite oxides has not been widely studied as supports for gold nano-particles. Wang *et al.* (2003) have investigated the effect of the presence of the second metal oxide on Au/Al_2O_3 catalyst for CO oxidation reaction. They observed a lower $T_{100\%}$ with $Au/FeO_x/Al_2O_3$ than with Au/Al_2O_3. Grisel *et al.* (2002) observed a lower particle size of 2.6 nm for $Au/MgO/Al_2O_3$ catalyst compared with 3.6 nm found with Au/Al_2O_3. In their earlier study, they reported the stabilization of Au particles in the presence of MgO on Au/Al_2O_3 (Grisel *et al*, 2001). In contrast to the increased activity with the composite oxide supports, Mallick and Scurrell (2003) observed a lower catalytic activity with Au/TiO_2-ZnO compared with Au/TiO_2. Composite catalysts were also investigated for the benzene oxidation reaction. The $V_2O_5/Au/TiO_2$ sample was reported to exhibit the highest catalytic activity in comparison with the other samples showing 100% benzene conversion at temperature of 250 ^oC compared to pure titania and zirconia supported catalysts which achieved total conversion of benzene only at 400 ^oC (Idakiev *et al,* 2003). This data shows that the catalytic activity of the catalyst depends on both the particle size as well as the nature of the support. In this chapter, the effect of ZrO_2 in Au/TiO_2-ZrO_2 catalysts prepared by deposition-precipitation will be reported.

4.2 Results and Discussion

4.2.1 Catalyst Characterization

Catalyst characterization is very important in understanding the catalyst structure and in attempting correlation with the possible mechanism of the reaction. In this chapter, the catalysts were characterized with various techniques and the results were found to agree with each other. These are mixed support-based catalysts and the characterization sheds light on the role of the second metal oxide both on the surface structure of the catalyst as well as its activity. For instant; in the literature, it was observed that the addition of MnO_x to Au/Al_2O_3 catalyst leads to the decrease in the agglomeration of Au particles (Grisel *et al,* 2000 and Grisel *et al,* 2001) and improved the activity of the catalyst.

4.2.1.1 Surface Area (BET)

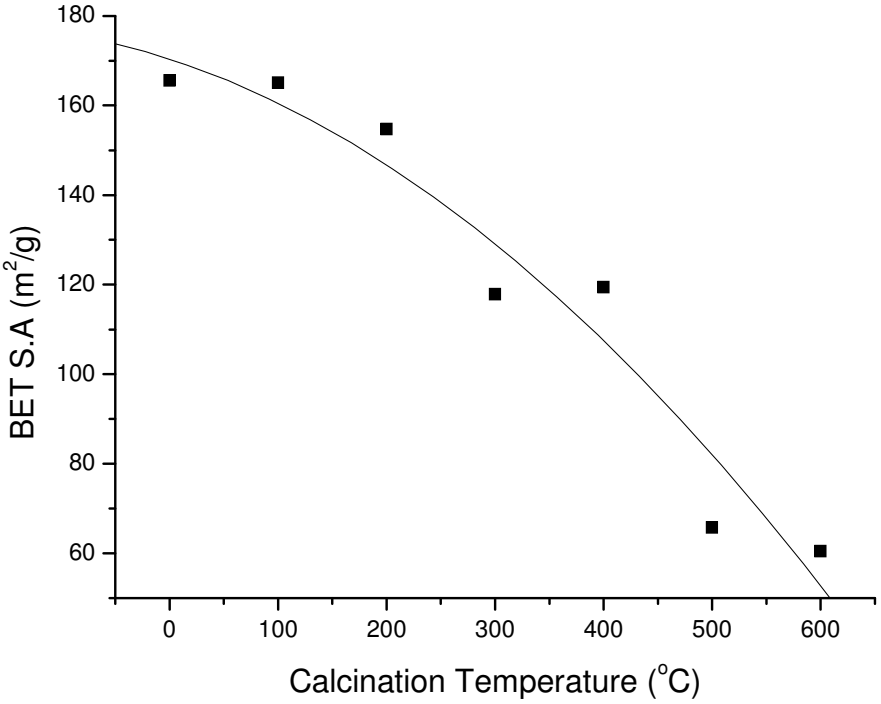

Figure 4.1: The effect of calcination temperature on BET surface area of Au/TiO_2-ZrO_2 catalyst

Figure 4.1 indicates that the surface area of an uncalcined sample is very high (165.6 m^2/g) compared to those of the calcined samples. The surface area collapse to 60.5 m^2/g upon calcination at 600 ^{o}C. Shashri *et al.* (1984) reported that such a decrease in surface area is not caused by the phase transformation of anatase to rutile. Gold is believed to have a retarding effect on this transformation (Shashri *et al,* 1984). Debeila (2000) also observed a retarding effect of gold on the transformation of TiO_2 from anatase to rutile at 700 ^{o}C. However, most of the decrease in the surface area is attributed to the crystallization of zirconia particles which occurred and increased

with calcination temperature, and this was confirmed by XRD. During this study we have observed that crystalline zirconia has a lower surface area compared with amorphous zirconia.

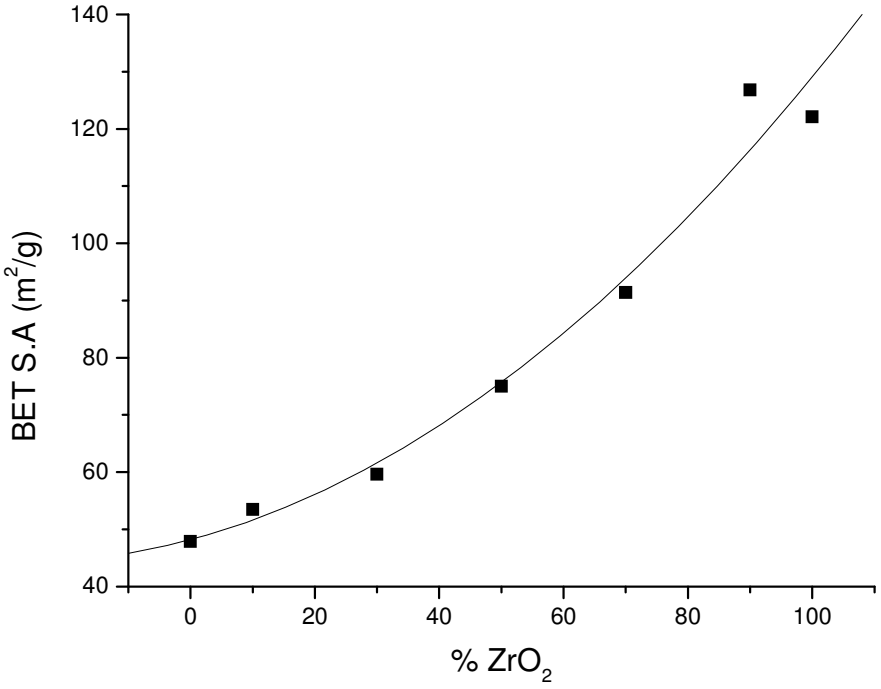

Figure 4.2: The effect of the amount of ZrO_2 on BET surface area of Au/TiO_2-ZrO_2 catalyst

The above graph shows that an increase in ZrO_2 content increases the surface area of the catalysts. The single support catalysts indicate that Au/ZrO_2 (122 m^2/g) has a higher SA compared to Au/TiO_2 (47.9 m^2/g) catalyst. In these catalysts, the ZrO_2 is deposited on the surface of TiO_2 and as its fraction increases; its surface area becomes more predominant on the expense of that of TiO_2 due to the surface shielding.

Au/TiO_2-ZrO_2 catalysts were prepared by deposition-precipitation method under varied conditions, such as pH, ageing period, and calcination temperature. An increased gold particle size was observed by high resolution transmission electron microscopy (as will be shown later in this chapter) with increasing calcination temperature. XRD was also used to inspect the change in the crystallinity of gold with increasing pH of precipitation and increasing ageing period.

Except for that precipitated at pH 5, the catalyst specific surface area seems to decrease with increasing pH of precipitation e.g. 105 m^2/g for the catalyst precipitated at pH = 9 and 95.5 m^2/g of the catalyst precipitated at pH 11. The reason for the low surface area on the catalyst precipitated at pH 5 could be that gold particles are bigger and there is a poor dispersion of these particles on the surface of the support. The average pore diameter (APD) of these catalysts does not seem to be influenced by an increase in the pH of precipitation. The single point total volume (SPTV), on the other hand, is slightly influenced wherein it increases from 0.13 cm^3/g of the catalyst precipitated at pH 5 to 0.15 cm^3/g of the catalyst precipitated at pH 9 and pH 11.

The BET surface area of the catalysts decrease with increasing period of catalyst ageing (before filtering and washing) from unaged catalysts with 94.1 m^2/g decreasing to 72.1 m^2/g for the catalyst aged for 12 h. However, the catalyst aged for 24 hrs has an increased BET surface area of 84.0 m^2/g and APD of 6.4 nm. With other catalysts, the APD increases from 6.5 nm of the unaged catalyst to 7.8 nm of the catalyst aged for 12 h. The table below also shows that an increase in the period of catalyst ageing decreases the SPTV.

Table 4.1: BET surface areas of Au/TiO_2-ZrO_2 catalysts prepared at deferent conditions

Catalysts	**BET SA m^2/g**	**APD (nm)**	**SPTV (cm^3/g)**
Uncalcined	165	4.3	0.18
Cal 200 ^oC	155	4.2	0.16
Cal 300 ^oC	118	4.9	0.14
Cal 400 ^oC	119	5.4	0.16
Cal 500 ^oC	66.7	8.4	0.14
Cal 600 ^oC	60.5	8.5	0.13
pH 5	82.3	6.4	0.13
pH 7	105	5.5	0.14
pH 9	102	6.1	0.15
pH 11	95.5	6.3	0.15
Age 0	94.1	6.5	0.15
Age 6	83.5	7.3	0.15
Age 12	72.1	7.8	0.14
Age 24	84.0	6.4	0.13

Cal 200 ^oC denotes calcinations at 200 ^oC etc

Age 0 denotes ageing for 0 h etc

4.2.1.2 Mössbauer Effect Spectroscopy

Since Mössbauer is element selective and sensitive to the local surroundings of the atoms. It is an excellent probe for gold catalysts as it can provide information on the s-electron density at the gold nuclei from the IS and on the symmetry of the environment of the gold atoms from the quadrupole splitting (QS) (Stievano *et al,* 1998). This sensitivity makes it possible to resolve different metal sites within the catalyst particles and thereby differentiate between metal atoms at the surface and atoms in the inner-core of the particles (Goosens *et al,* 2002).

Nano-phase gold particles in gold-based catalysts are of potential interest as a carbon monoxide oxidation ($CO \rightarrow CO_2$) system. It is still uncertain as to which species of gold, metallic (Au^0) or the ionic variants Au^I or Au^{III}, is the active site for CO oxidation. If this is elucidated and the chemistry/reactivity of nano-sized gold particles is better understood, it will aid in optimum catalyst design. A batch of four Au/TiO_2-ZrO_2 catalyst samples was analyzed with ^{197}Au Mössbauer effect spectroscopy in an attempt to determine the amount and kind of Au species (ionic state) on the surface of different catalysts.

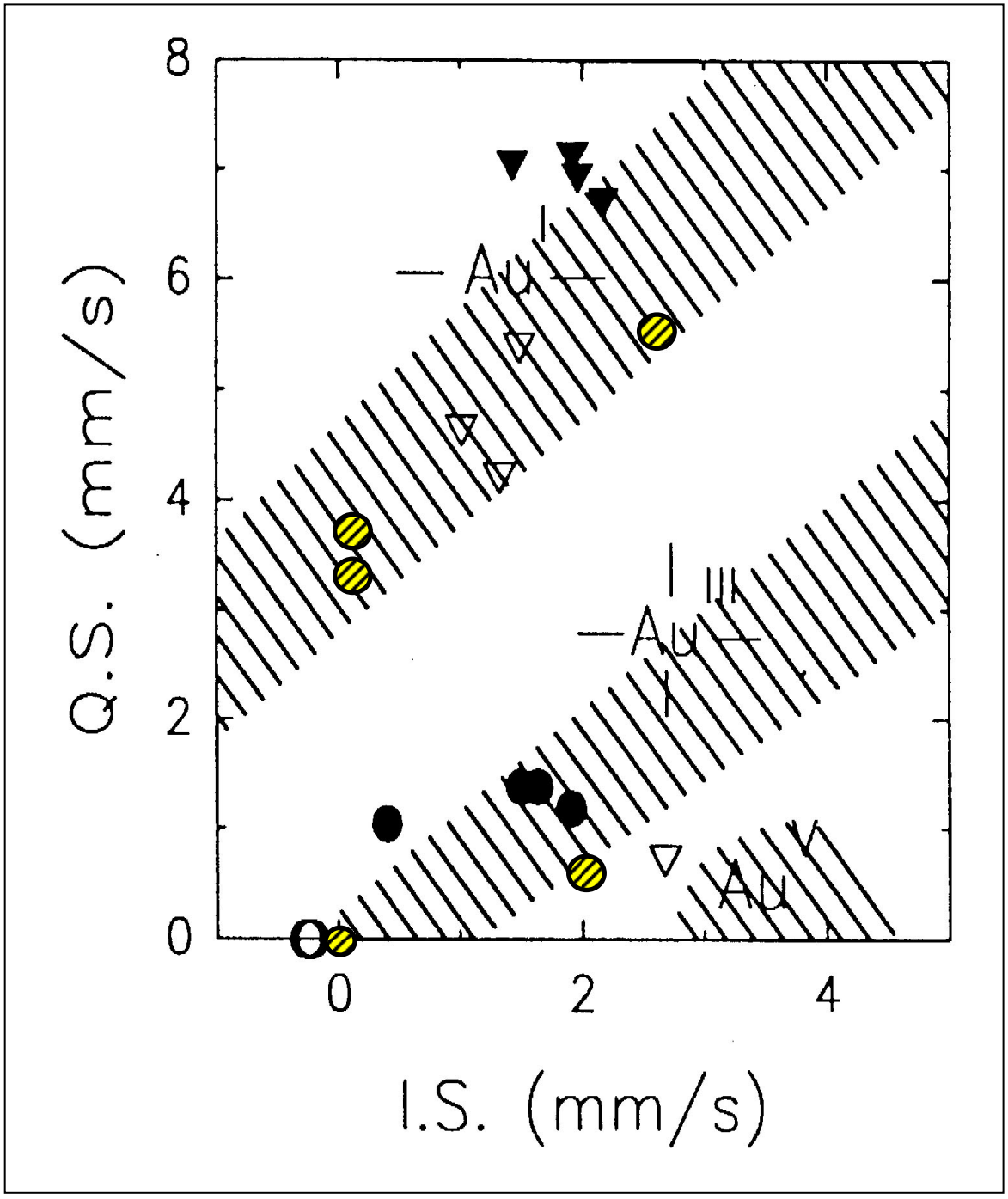

Figure 4.3: Correlation plot of quadrupole splitting (QS) versus isomer shift (IS) (Mulder, 1994).

In the figure above the shaded bands encompass parameters for most gold compounds measured to date. Symbols are for the various sites of different Au_{55} clusters. Bulk gold metal is at the origin. The parameters of the fitted spectral components listed in table 4.3 and shown in figure 4.3 for the nano-Au/TiO_2-ZrO_2 samples are the cross-hatched circles.

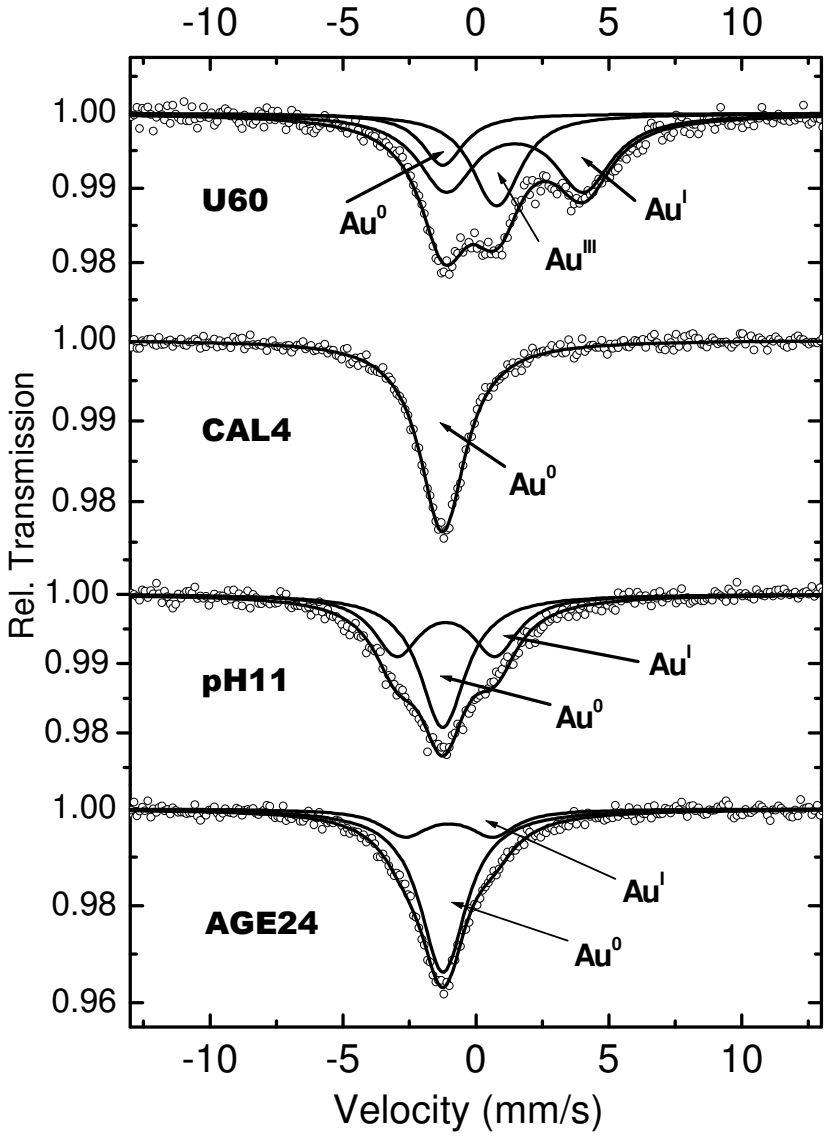

Figure 4.4: Isomer shift quoted with respect to Au metal at 6 K.

The following has been deduced from the theoretical fits to the data, based on the nuclear hyperfine interaction parameters of table 4.3.

U60: Au/TiO_2-ZrO_2

As shown in figure 4.4, attempts to use only two components (*i*.e. two doublets) to fit the spectrum showed glaring discrepancies between the overall theoretical curve and the spectrum. Therefore three spectral components i.e., two singlet (for Au^{III} and Au^0) and one doublet (for Au^I) have been used in the fitting, each representing the different typical oxidation states of Au. It is clear that this catalyst contain all three ionic state of Au. Since this catalyst is not calcined, it is not surprising that some of the Au species are Au^{III}. It has been reported that the as prepared catalysts contain mostly Au^{III} species and there is usually no evidence of metallic Au (Yang *et al,* – in preparation). The presence of metallic Au on this catalyst is considered to be brought about by the drying process.

Cal 4: Au/TiO_2

This sample exhibit a typical singlet spectrum essentially identical to that found with bulk gold metal. No other species of gold is evident. The line width of Γ=2.1 mm/s is typical of these source conditions and sample thickness (*i*.e. gold content) of ~30 mg/cm^2. This catalyst was analyzed to indicate the effect of the presence of ZrO_2 on Au/TiO_2-ZrO_2. The Mössbauer spectrum of this catalyst reveals that calcining the Au/TiO_2 catalyst results in the reduction of most of the Au species. The unreduced species, if any, are in a very low concentration and probably below the detection limit of this technique. This catalyst and "Age 24" catalyst below were prepared under the same conditions except for the absence of zirconia in "Cal 4" catalyst. This demonstrates that the presence of zirconia retards the reduction of Au species since "Age 24" catalyst still contains Au^I species after calcination at 400 ^oC.

pH 11: Au/TiO_2-ZrO_2

A minimum of two components (singlet and doublet) were required for a satisfactory fit of the data. Two chemical species of gold, viz, Au^0 (singlet) and Au^I (doublet) are evident in the spectrum.

Age24: Au/TiO_2-ZrO_2

Initial attempts to fit this spectrum as a singlet gave a very broad line width Γ=2.8 mm/s. This suggests that a second spectral component is masked in the resonance envelope. Indeed, fitting with two components (singlet and doublet) gave an optimum fit to the data, thus suggesting the presence Au^0 and Au^I but in different relative abundances compared to sample precipitated at "pH 11".

The above results show that the presence and increase of Au^I species on the catalyst results in the high activity on CO oxidation reaction. Mössbauer effect spectroscopy shows that the catalysts that have a poor activity are those that contain a higher content of metallic gold species. Table 4.3 also indicates that the uncalcined catalyst contain all three gold species including the Au^0 gold. It is also evident that catalyst calcination results in the reduction of Au^{III} species either into Au^I and/or Au^0 species since none of the calcined catalysts contain any Au^{III} species. Such observation was also reported by Goosens *et al.* (2002) who observed a gradual formation of metallic gold species at the expense of ionic gold species with increasing calcination temperature. Such calcined catalysts with zero or lower amounts of ionic gold show lower activity for CO oxidation. However, this study reveals that calcination temperature is not the only factor determining the formation of metallic gold species, since the catalyst that have been calcined at the same temperature have different abundances of metallic gold species, due to other preparation conditions such as ageing and precipitation temperature.

In contrast, the Mössbauer study of Lee *et al.* (2001) revealed only metallic gold species with the samples analyzed just after co-precipitation of Au-Mn and this was also confirmed by their XPS results.

Table 4.2: Activity of different catalysts containing various amounts of Au^I species

Catalyst	% CO Conversion	Rate (mol CO(mol Au)$^{-1}$.s^{-1})	% Au^I
Au/TiO_2	10	0.01	0
Au/TiO_2-ZrO_2	38	0.05	24
Au/TiO_2-ZrO_2 (Uncalcined)	100	0.12	57

Table 4.3: Hyperfine interaction parameters of each of the sub-components in the overall fit to each of the spectra measured in this study. *The parameters are line width Γ, isomer shift δ, quadrupole splitting QS, and abundance obtained from the integrated area under the sub-component.*

Sample	**Γ ▽ mm/s**	**δ/Au # mm/s**	**QS mm/s**	**Abundances♦ %**	**Attribution**
Au/TiO_2	2.1	0	0	100	Au^0
Au/TiO_2-ZrO_2	2.1	0.2	3.2	24 ± 5	Au^I
	2.1	0	0	75	Au^0
Au/TiO_2-ZrO_2	2.0	2.0	0.5	29 ± 5	Au^{III}
(Uncalcined)	2.0	2.7	5.2	57	Au^I
	1.9	0	0	14 ± 5	Au^0

♦ *Typical relative error is ~10% of the quoted abundance value (e.g. 24 ± 3 %), unless specified explicitly in the table;*

▼ *Fixed value of the line widths caused by strongly overlapping sub-spectra. Fixed line width values are primarily based on the amount of gold in the sample (Viegers, 1976). Line width value obtained for sample Au/TiO_2 was extracted as a free parameter from the fitting;*

\# *Isomer shift quoted with respect to Au metal at 6 K.*

4.2.1.3 X-ray Photoelectron Spectroscopy (XPS)

The presence of zirconia on the catalyst results in higher amount of gold particles detected by XPS on the surface of the catalyst. In the absence of zirconia as shown in the table 4.4, more agglomeration of gold particles occurs. This implies that during calcination, zirconia stabilizes the gold particles against agglomeration and/or reduction. An explanation for this could be that during preparation, both zirconia and gold particles are deposited on the surface of titania and zirconia particles hinders the movement of one gold particle towards its nearest gold particle neighbor resulting in the well dispersed gold particles on Au/TiO_2-ZrO_2 catalyst compared with Au/TiO_2 hence no or less agglomeration and reduction occurs when the gold particles are relatively immobile. The broader FWHM of the peaks observed on the catalysts containing zirconia is the evidence that more than one Au species may exist even after calcination. This agrees with the Mössbauer observations where, calcined Au/TiO_2 catalysts were found to be all-metallic whereas some Au^I species were detected on calcined Au/TiO_2-ZrO_2. The uncalcined Au/TiO_2-ZrO_2 has a very broad (FWHM = 2.45 eV) suggesting more than one Au species, which also complies with the Mössbauer data that reveals three different Au species (Au^0, Au^I and Au^{III}) in this catalyst. However, due to low detection limits of XPS, species other than metallic Au species were not detected as can be seen by a low binding energy (table 4.4). This

seems to indicate that the catalyst consists only of metallic species. However, the possibility of beam induced reduction of gold species can not be excluded since XPS was reported to have this effect (Bond and Thompson, 2000).

Table 4.4: Binding energies of gold and percentage composition of different species on the surface of the catalysts.

Catalyst	**Au/B.E (eV)**	**FWHM (eV)**	**% Au**	**% C**	**% Ti**	**% Zr**	**%O**
Au/TiO_2 (400°C)	83.26	0.96	0.2	7.8	29.3	0	62.6
Au/TiO_2-ZrO_2(400° C)	83.56	1.29	0.5	9.1	21.2	5.9	63.3
Au/TiO_2-ZrO_2 uncalcined	83.44	2.45	0.6	10.5	21.1	4.9	62.9

Effect of catalyst treatment on XPS

An increase in the calcination temperature of the catalyst increases the extent of agglomeration of gold species on the surface of the support as shown by the amount of gold species detected on the surface of the catalyst and this result in the decrease in catalytic activity with increasing calcination temperature. The agglomeration of gold species was confirmed by HRTEM as will be shown later in this chapter. As far as the binding energy is concerned, there is no significant consistent change.

Catalyst ageing also has an effect on the content of gold species on the surface of the catalyst. The gold content increased from 0.3% of the unaged catalyst to 0.5% of the catalyst aged for 24 h. FWHM increased with decreased ageing from 1.43 to 1.29, which suggests that the number of different gold species decreased with an increasing

period of ageing. This also suggests that some extent of reduction may have occurred during the preparation and ageing steps.

The amount of gold detected on the surface of the catalyst is very low (0.2%) on the catalyst precipitated at pH 5, while increasing the pH from 7 to 11 does not actually change the surface abundance of gold which remains at 0.5% according to XPS. Though there is no systematic change in the B.E of gold species with changing pH, the catalyst with the highest B.E of 83.51 eV (pH 9) is the one that has shown the highest catalytic activity. An increase in the pH at which the catalyst is precipitated increases the amount of zirconia precipitating on the surface of titania covering its surface; hence the amount of titania exposed decreases with increasing pH.

Table 4.5: The binding energies of gold on different catalysts and surface abundances of elements.

Catalyst	Au/B.E (eV)	FWHM (eV)	% Au	% Ti	% Zr	%O
pH 5	83.35	0.98	0.2	23.2	4.2	62.8
pH 7	83.2	1.42	0.5	23	4.7	63.6
pH 9	83.51	1.17	0.5	22.8	5.7	62.5
pH 11	83.39	2.36	0.5	21.1	5.8	62.8
Age 0	83.53	1.43	0.3	21.4	6.1	63.2
Age 6	83.54	1.31	0.4	22.8	5.3	63.9
Age 12	83.31	1.06	0.4	21.6	6	62.2
Age 24	83.56	1.29	0.5	21.2	5.9	63.3
Uncalcined	83.44	2.45	0.6	21.1	4.9	62.9
Cal 200 ^oC	83.75	1.33	0.5	20.8	5.6	62.3
Cal 300 ^oC	83.38	1.55	0.5	21.1	6	63.2
Cal 400 ^oC	83.47	1.14	0.5	21.4	5.7	62.0
Cal 500 ^oC	83.49	1.67	0.4	19.6	7.4	62.4
Cal 600 ^oC	83.23	1.49	0.3	20.7	6.4	62.7

Cal 200 ^oC denotes calcinations at 200 ^oC etc.

Age 0 denotes ageing for 0 h etc.

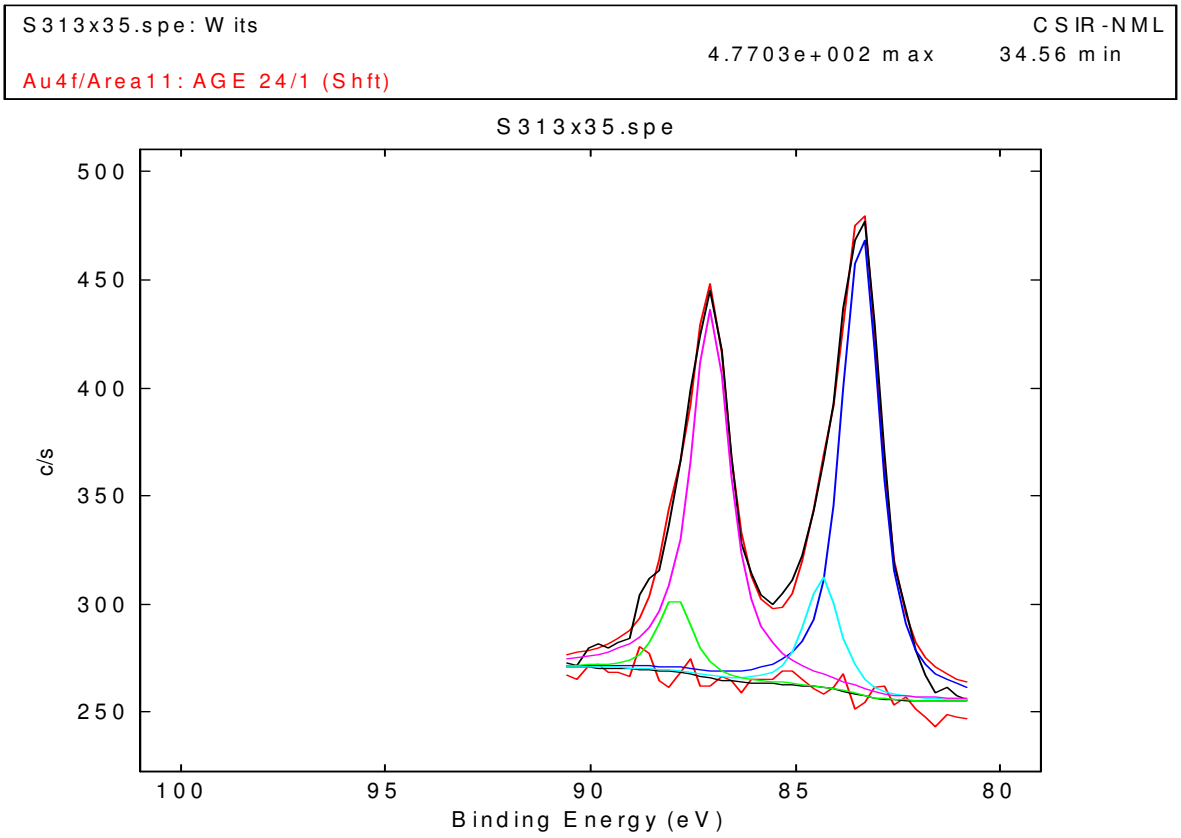

Figure 4.5: Deconvoluted Au XPS spectrum of Au/TiO_2-ZrO_2 calcined at 400 ^oC

Even though it was shown in table 4.5 by the binding energy that the catalyst is comprised of metallic gold, the figures 4.5 and 4.6 show that after peak deconvolution, some shoulder peaks at higher binding energies are present, which is evident of the presence of a differently charged gold species probably the slightly electron deficient. This data agrees with that of Mössbauer effect spectroscopy where the catalyst calcined at 400 ^oC was found to still contain Au^I after calcinations at 400 ^oC.

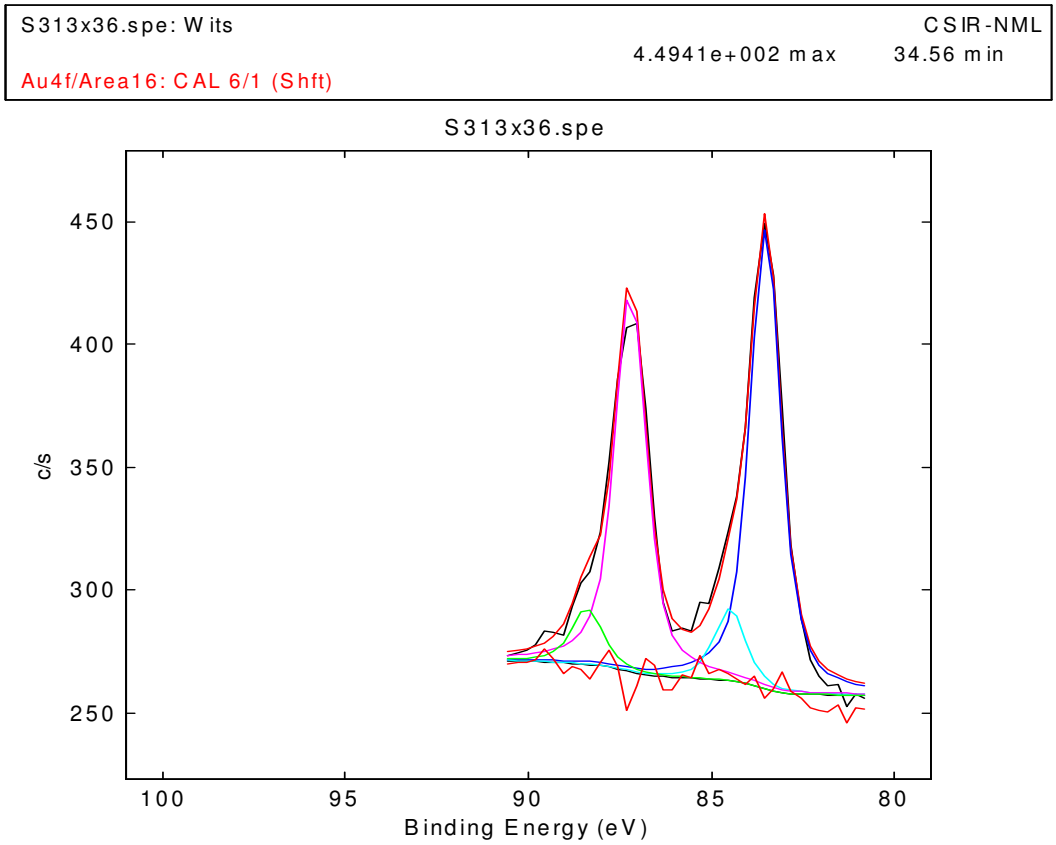

Figure 4.6: Deconvoluted Au XPS spectrum of Au/TiO_2-ZrO_2 calcined at 600 ^oC

The deconvoluted $Au4f_{7/2}$ and $Au4f_{5/2}$ peaks in figure 4.6 are less intense compared to those in figure 4.5. The height of the peaks in the catalyst calcined at 600 ^oC are 30 and 23 respectively compared to 51 and 34 for the catalyst calcined at 400 ^oC, indicating the effect of calcinations temperature on the intensity or reduction of the number of these species upon increased temperature treatment.

4.2.1.4 High Resolution Transmission Electronic Microscopy

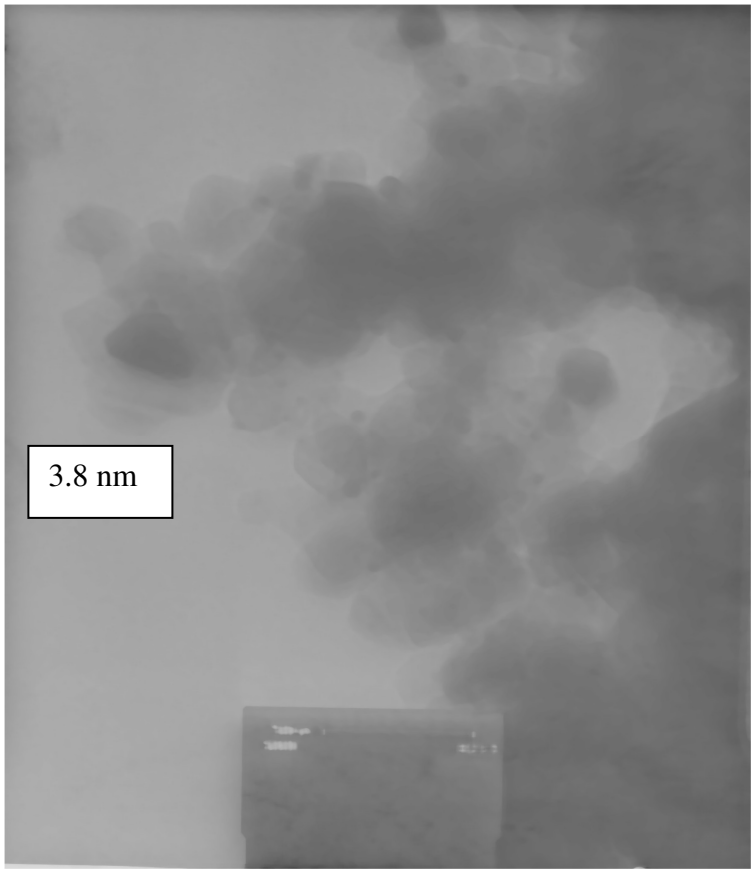

Figure 4.7: HRTEM picture of an uncalcined Au/TiO_2-ZrO_2 catalyst (deposition-precipitation)

Figure 4.7 shows that the uncalcined catalyst has well-dispersed small gold particles with an average diameter of 3.8 nm. The micrographs also reveal that gold and TiO_2 particles have preferred interaction relative to that displayed by gold and ZrO_2 particles, i.e. Au tends to associate with titania rather than with zirconia.

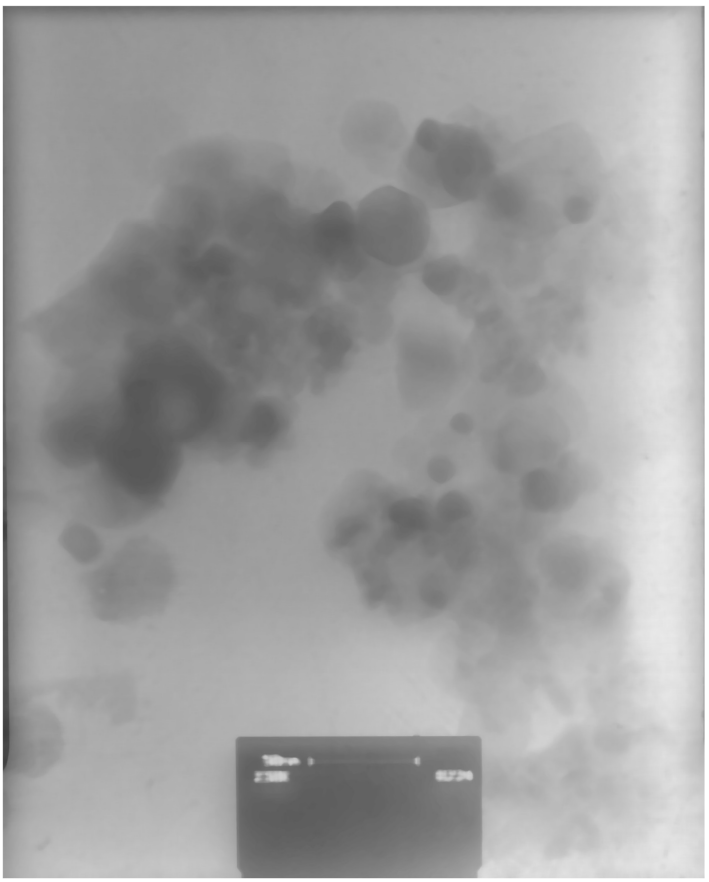

Figure 4.8: HRTEM picture of Au/TiO_2-ZrO_2 (deposition-precipitation) catalysts calcined at 600 ^oC.

Figure 4.8 shows that this catalyst has larger particles with an average diameter of 14 nm dispersed on the TiO_2 particles. This picture also shows a good interaction between gold and TiO_2 particles rather than between the gold and ZrO_2 particles. These results contradict those of Maciejewski *et al.* (2001), who observed no significant sintering at calcination temperatures below 600 ^oC, with both 20% Au/TiO_2 and 20% Au/ZrO_2 catalysts which is probably because the Au particles size of these catalysts are already large due to the high loadings used. However, these authors observed an increase in gold particles size after calcining the catalyst at 800 ^oC. HRTEM of this study (fig. 4.8) generally shows that increasing the calcination temperature leads to the agglomeration of gold particles on the support system. At

higher calcination temperatures, the interaction between the gold and the support weakens due to the reduction of gold ions to metallic gold leading to the agglomeration of metallic gold particles (Bond and Thompson, 2000). As will be shown by the reactor studies of these catalysts (Figure 4.18), agglomeration of gold particles results in the poor performance of the catalyst in CO oxidation. Therefore the decrease in catalytic performance may also be attributed to the increase in the ZrO_2 particle size, which may also tend to shield the gold-TiO_2 interface.

4.2.1.5 X-ray Powder Diffraction (XRD)

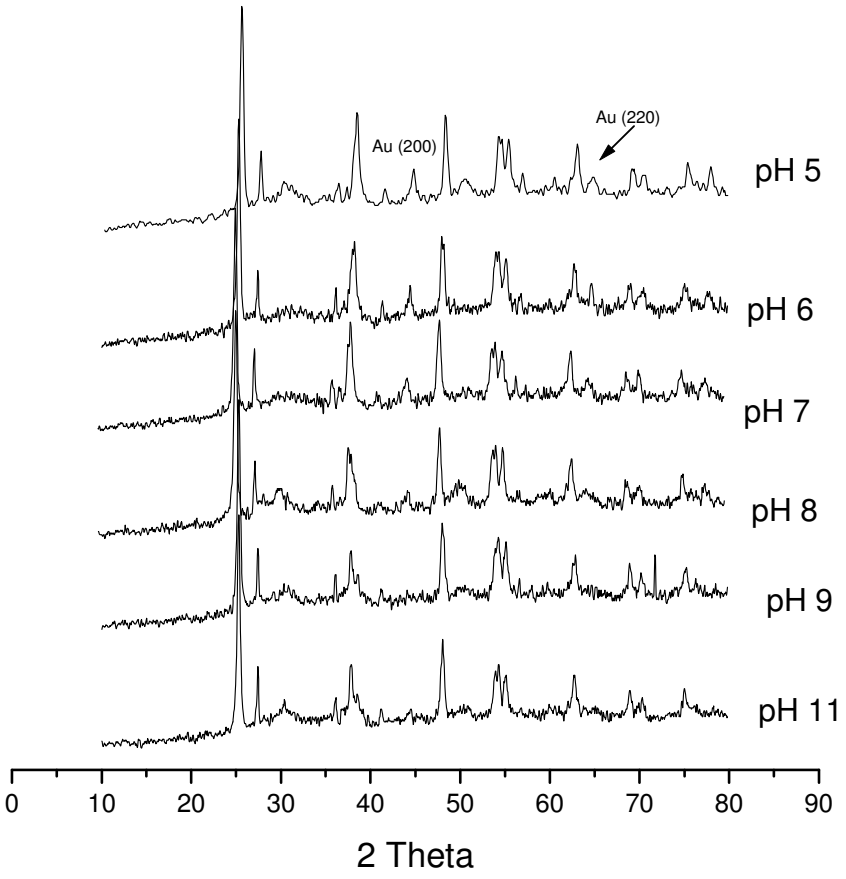

Figure 4.9: XRD spectrum of Au/TiO_2-ZrO_2 catalyst precipitated at different pH

Figure 4.9 shows little difference in the intensities and shapes of the TiO_2 and ZrO_2 peaks with an increasing pH. Of more interest is a decrease in the intensity and broadening of the Au(200) and Au(220) gold peaks at 44.8° and 64.8° respectively with increasing pH of precipitation. These results agree with those of Wolf and Schuth (2002) who observed a decrease in the amount of gold and broadening of Au(111) and Au(200) with increasing pH. A decrease in the gold loading increases the dispersion and size of gold particles on the surface of the support and leads to an improved catalytic activity.

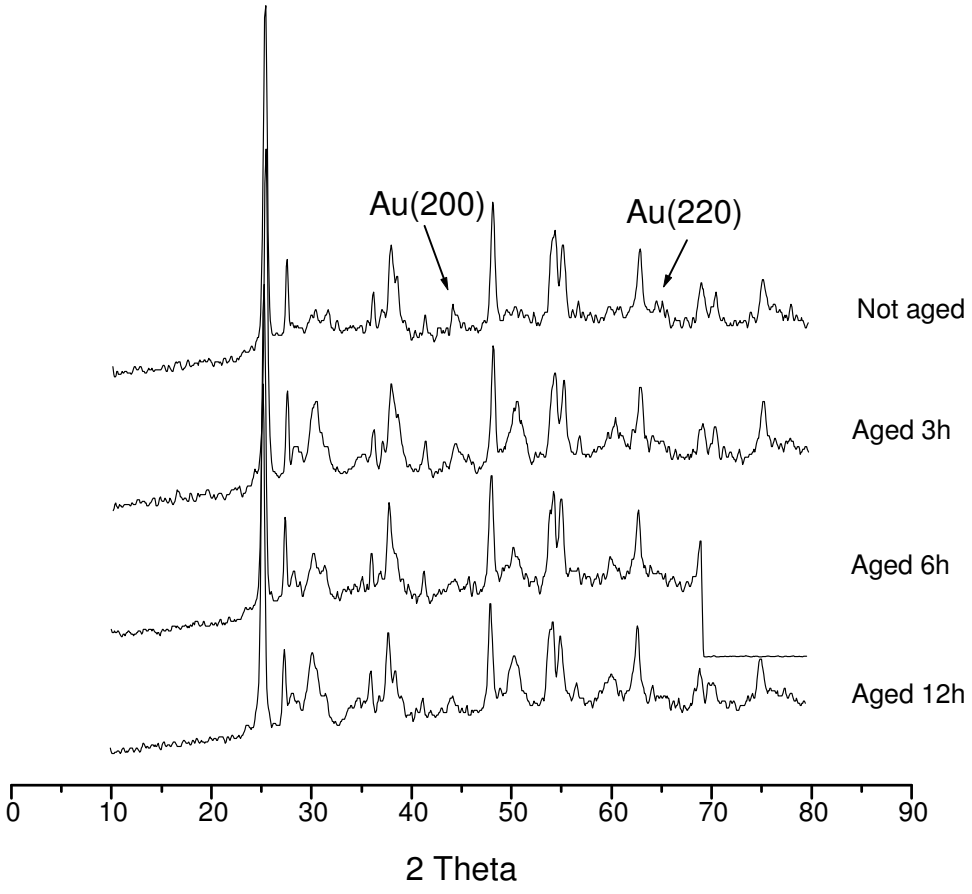

Figure 4.10: XRD spectra of Au/TiO_2-ZrO_2 (deposition-precipitation) catalysts aged at for different periods

Figure 4.10 shows that ZrO_2 particles crystallize with increasing period of ageing. The figure depicts a slight broadening of the Au(200) peak with the catalyst aged for 3 hrs. However, the figure shows smaller Au particles (less crystalline) with higher period of ageing. During ageing, more time is allowed for $HAuCl_4$ particles to be hydrolyzed into smaller $Au(OH)_3$ particles which have a stronger interaction with the support and the chlorine ions which are believed to be the catalyst poison are removed from the catalyst surface into the mother liquor.

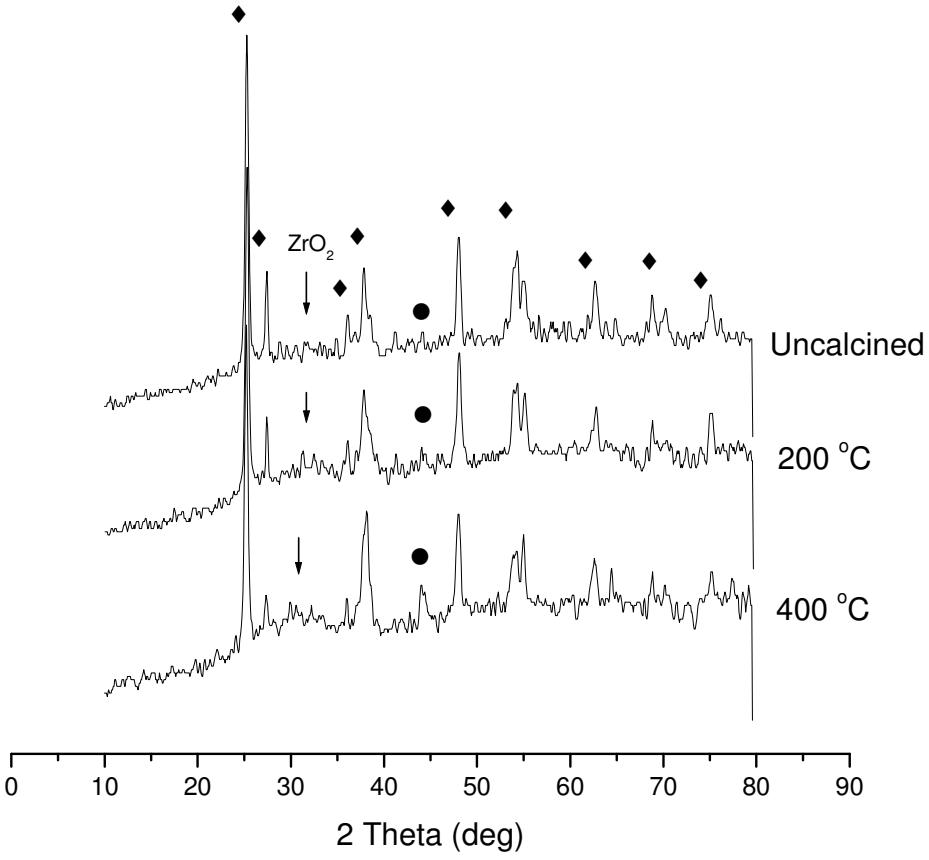

Figure 4.11: XRD spectra of Au/TiO_2-ZrO_2 (deposition-precipitation) catalyst calcined at different temperatures

Figure 4.11 above shows the effect of calcinations temperature on Au/TiO_2-ZrO_2 catalyst. The gold reflections are not clearly visible on an uncalcined catalyst and can not be distinguished from noise. This shows that Au particles are dispersed as small particles on the surface of the support. An increase in the intensity of gold peaks is visible as the calcinations temperature increases leading to a much prominent Au(200) peak at $2\theta = 44.2^{o}$. This is an indication of the presence of bigger gold particles on the catalyst and as will be shown later, this lead to a decrease in the activity of the catalyst. An increase in calcinations temperature to 400 ^{o}C also has an effect on the crystallization of ZrO_2 particles. This can be seen by the slight appearance of a broad ZrO_2 peak at the area of $2\theta = 30^{o}$ whereas it was not observed on the uncalcined catalyst.

4.3 Catalytic Activity

An uncalcined Au/TiO_2-ZrO_2 catalyst (200 mg) was loaded in the reactor and pre-treated in the oxidizing atmosphere in 100 ^{o}C for 60 minutes. The oxygen gas was stopped and the reactor was then cooled to room temperature (25 ^{o}C) whereafter the reaction was run. At this temperature, a gas cylinder containing equal amounts of CO and oxygen (1% each) with the balance of helium was opened and the flow was set to the required rate.

4.3.1 Au/TiO_2-ZrO_2 catalysts prepared by deposition-precipitation

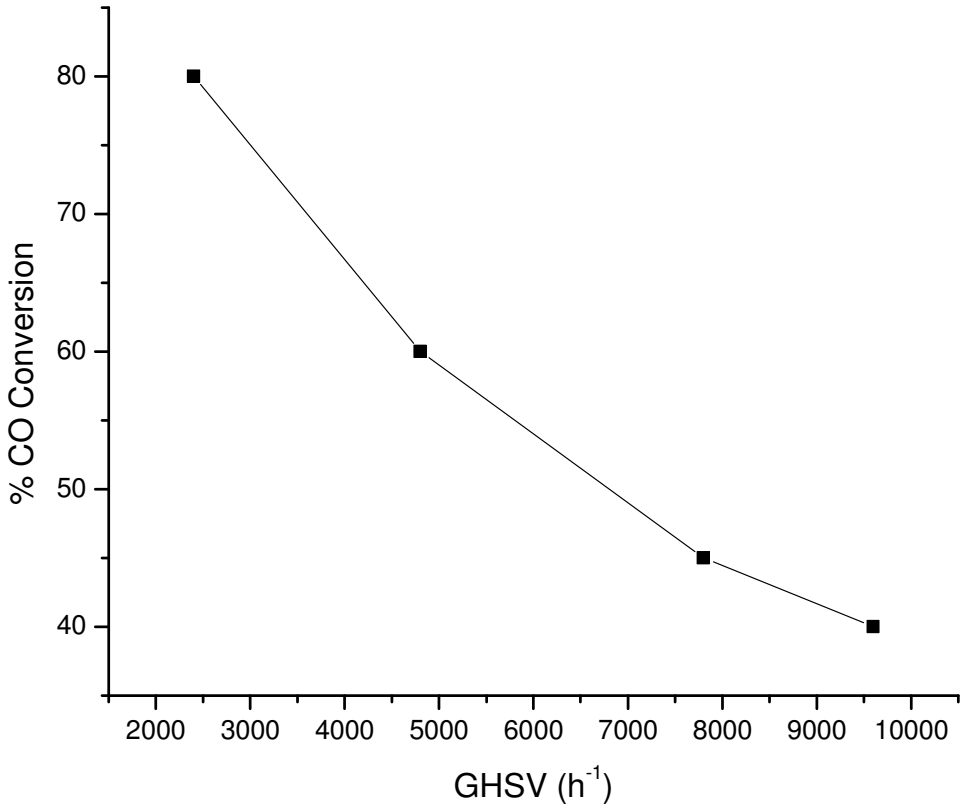

Figure 4.12: The effect of GHSV on the uncalcined Au/TiO_2-ZrO_2 catalyst at 25 ^oC reaction temperature and the CO/O_2 ratio of 1.

The figure above shows that low flow rate of the reacting gases gives a higher CO conversion (80%) even at room temperature. However as the space velocity increases the conversion decreases, giving about 40% conversion at a space velocity of 9600 h^{-1}.

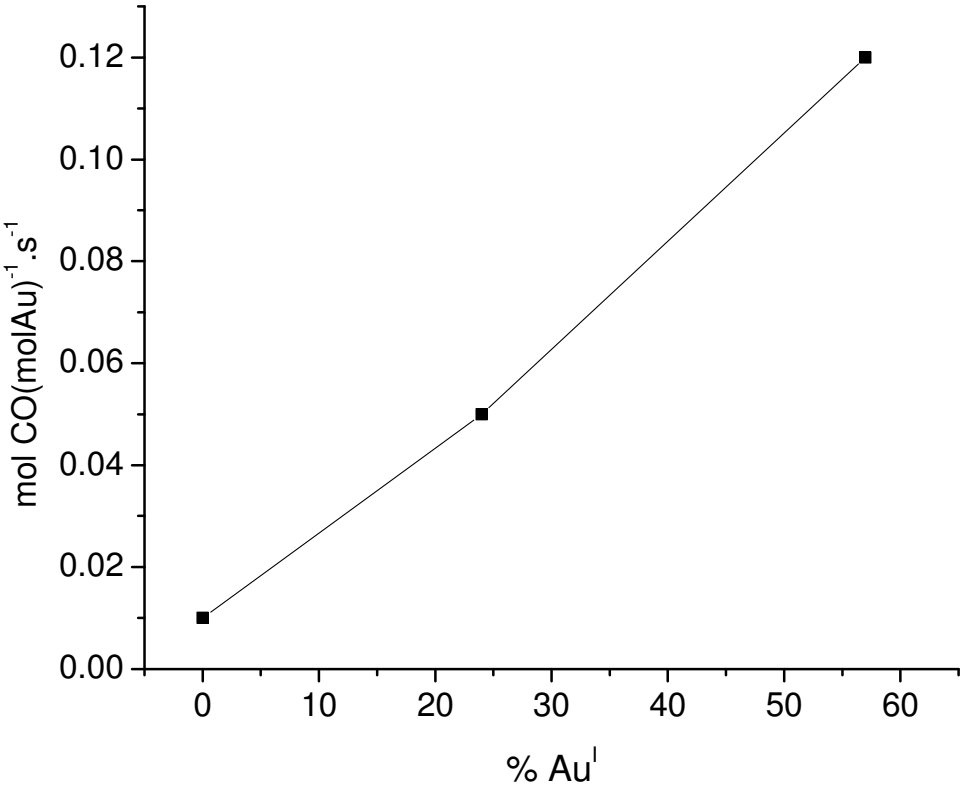

Figure 4.13: The effect of the amount of Au^I (as determined by Mössbauer spectroscopy) on Au/TiO_2-ZrO_2 catalyst on the rate of CO conversion

The figure above reveals the importance of Au^I species in CO oxidation. This is shown by the high activity of the catalyst, which contains the high number of these species. The most active catalyst is the one which contains the highest number of Au^I species and it is uncalcined. Therefore, as much as it is not disputed the fact that metallic Au particles may be necessary for CO oxidation as suggested by other authors (Haruta, 1997; Haruta *et al,* 1989; Valden *et al,* 1998), This study suggests that Au^I species constitute an important part of the active site of these catalysts. This is evident since an increase in the number of these species increases the rate of reaction and this may suggest their importance as part of the active site (figure 4.13).

A calcined Au/TiO_2 catalyst shows very low activity and Mössbauer effect spectroscopy shows that it contains mostly metallic Au species and this suggests that metallic gold species cannot alone provide an active site for CO oxidation; a certain proportion of partially reduced gold species are also required.

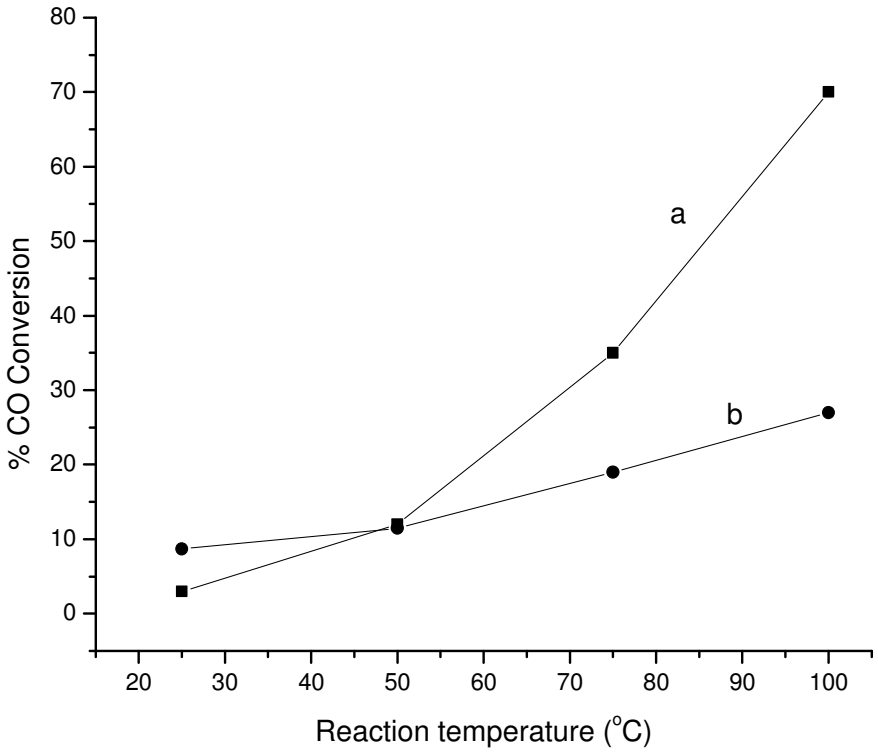

Figure 4.14: The effect of temperature on (a) Au/TiO_2-ZrO_2 and (b) Au/TiO_2: catalysts precipitated at pH 9, calcined at 400 ^oC (5 h) and aged for 12 h

The figure above shows a higher activity of Au/TiO_2 catalyst at room temperature compared with that of Au/TiO_2-ZrO_2. This trend is however short lived since the activity of the composite catalyst increases more as the reaction temperature increases. This may be due to the sintering of gold species or (more probably) due to an increased rate of gold reduction on Au/TiO_2 catalysts. The presence of ZrO_2 in the

catalyst seems to stabilize the gold particles against sintering and reduction. This data correlates with Mössbauer results where the catalyst containing ZrO_2 seems to contain a higher proportion of Au^I species even after treatment at high temperature.

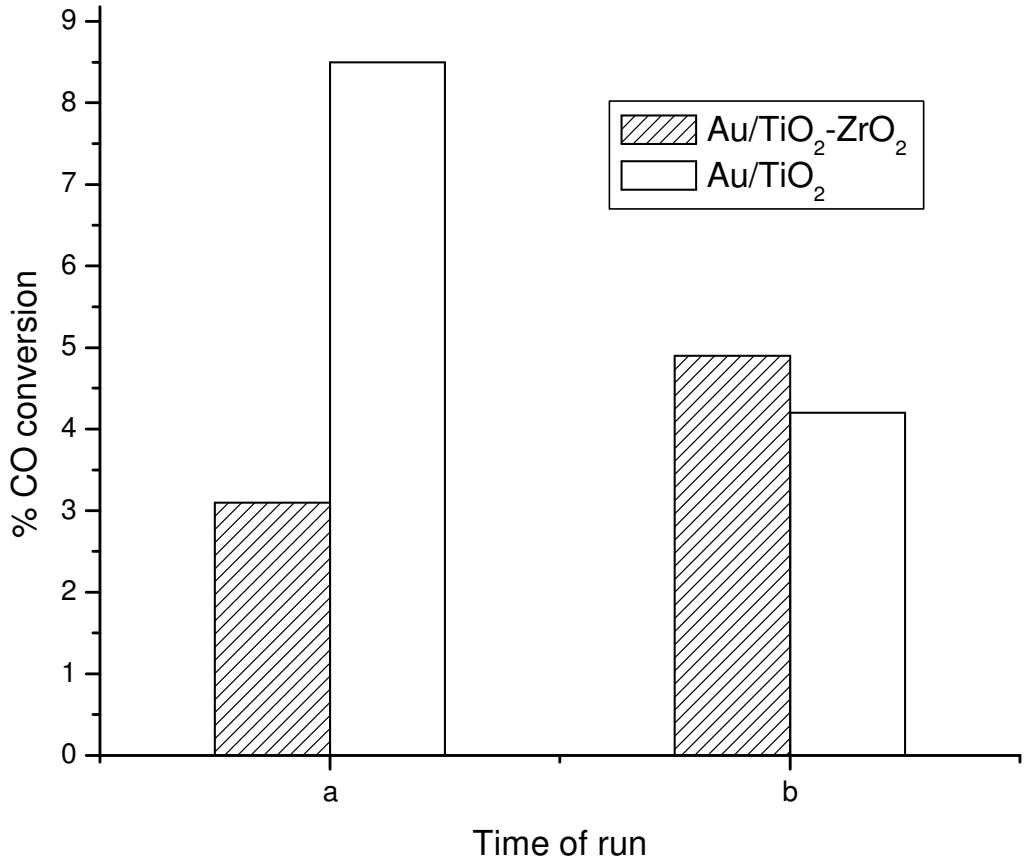

Figure 4.15: CO oxidation activity of the above catalysts (figure 4.14) at room temperature: (a) initial activity (b) after CO oxidation at 100 ^oC for 3 minutes.

The positive effect of ZrO_2 is also shown in figure 4.15 where a catalyst was cooled to room temperature after a few minutes of CO oxidation at 100 ^oC. This is evident by almost two-fold decrease in the activity of Au/TiO_2 at room temperature after being subjected to 100 ^oC of reaction. However, such behavior was not observed with

Au/TiO_2-ZrO_2 catalyst; instead, a slight increase of 2% conversion was achieved. This behavior provides further evidence that the presence of ZrO_2 hinders the agglomeration and/or reduction of Au species on the surface of TiO_2.

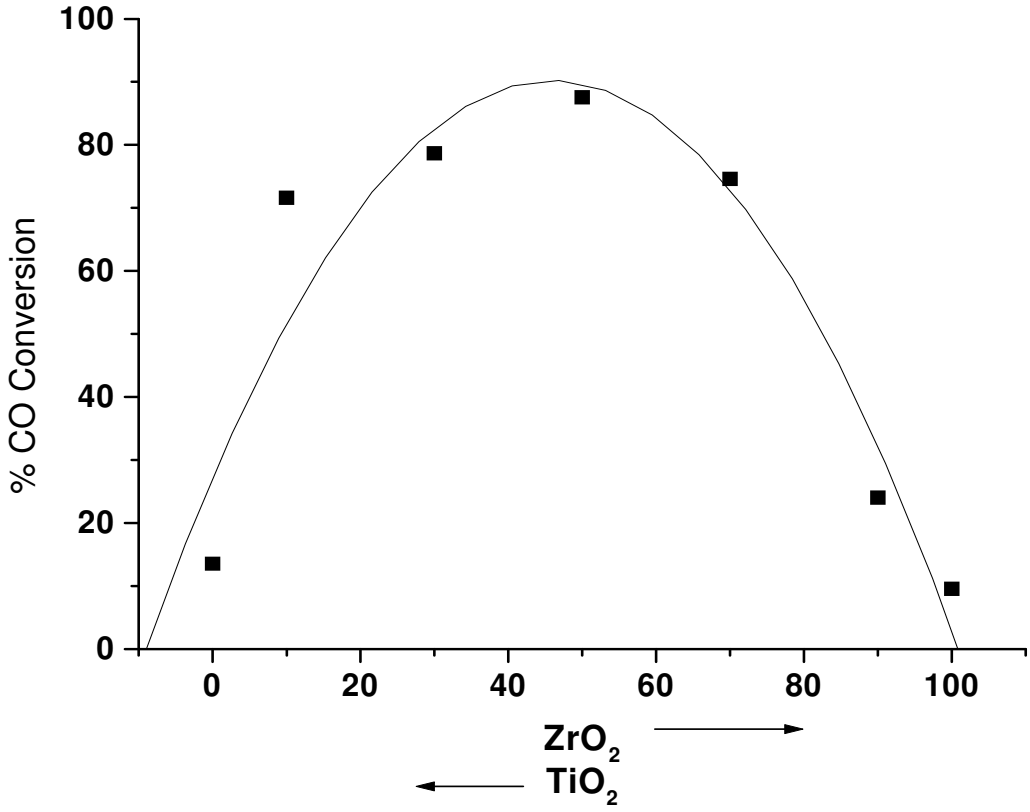

Figure 4.16: Effect of the amount of ZrO_2 on calcined Au/TiO_2-ZrO_2 (deposition precipitation)

Elsewhere, zirconia is believed to play an integral role in auto-catalysts providing oxygen storage and improved thermal stability which broadens conversion efficiency for all three pollutants during the rich/lean perturbations associated with the feedback control regulating the air-to-fuel ratio used by the engine (Fernandez-Garcia *et al,* 2000 and Sahu and Rao, 2000).

The effect of the amount of ZrO_2 on Au/TiO_2-ZrO_2 catalyst was therefore investigated and we observed that the optimum amount of ZrO_2 required about 50% (figure 4.16).

As shown by both Mössbauer and XPS such catalyst containing 50% ZrO_2 has a higher number of Au^I particles and a higher dispersion than Au/TiO_2. However, it was found that at higher ZrO_2 content, the CO conversion decreases to as low as 20%. This was probably due to the shielding of both gold particles on the surface of TiO_2 and the gold-TiO_2 interface, which is believed to play a necessary role in CO oxidation catalysis.

Other than deposition precipitation, impregnation of titania surface with zirconium nitrate solution was employed to introduce zirconia before gold was deposited. This was done in an attempt to maximize the interaction between two supports.

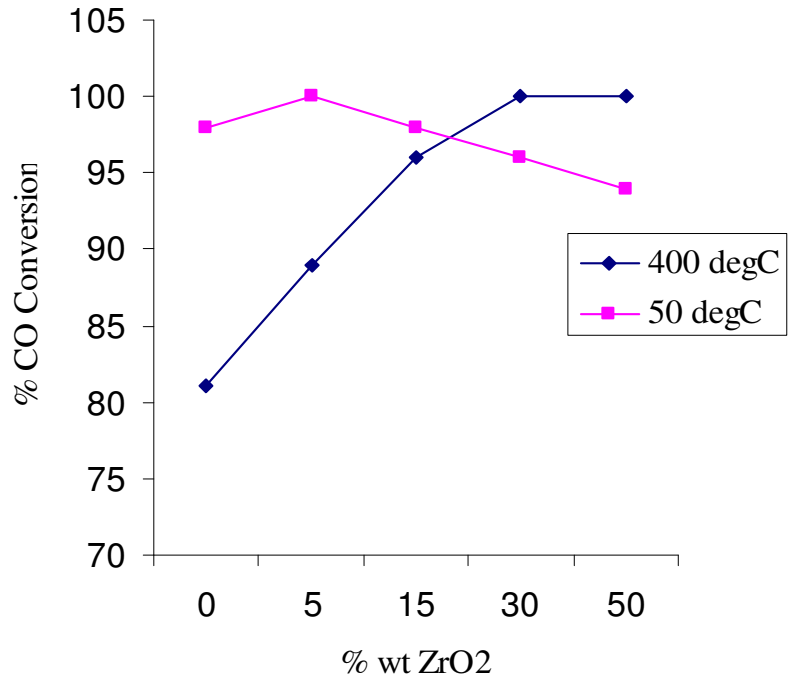

Figure 4.17: Effect of the amount of zirconia impregnated on Au/TiO_2-ZrO_2

Figure 4.17 shows that impregnating zirconia results in a more active catalyst compared to the one in which the zirconia was introduced by deposition-precipitation. At 400 ^{o}C, the reaction trend is similar to that in figure 4.16 where the activity of the catalyst increases with increasing amount of zirconia. At such a high temperature, Au/TiO_2 suffers deactivation due to a higher degree of agglomeration of Au particles. But it seems from figure 4.16 that, an increase in the amount of zirconia impregnated on the surface of titania might hinder that agglomeration process and the Au particles are still fairly dispersed. Furthermore, Au ions still exist as was shown by Mössbauer effect spectroscopy in figure 4.4 above (catalyst "age 24") hence higher activity. At low reaction temperature, the activity is slightly affected by an increase in the amount of zirconia, where we observed a slight decrease in the activity of the catalyst from total conversion to about 94% with increasing amount of zirconia.

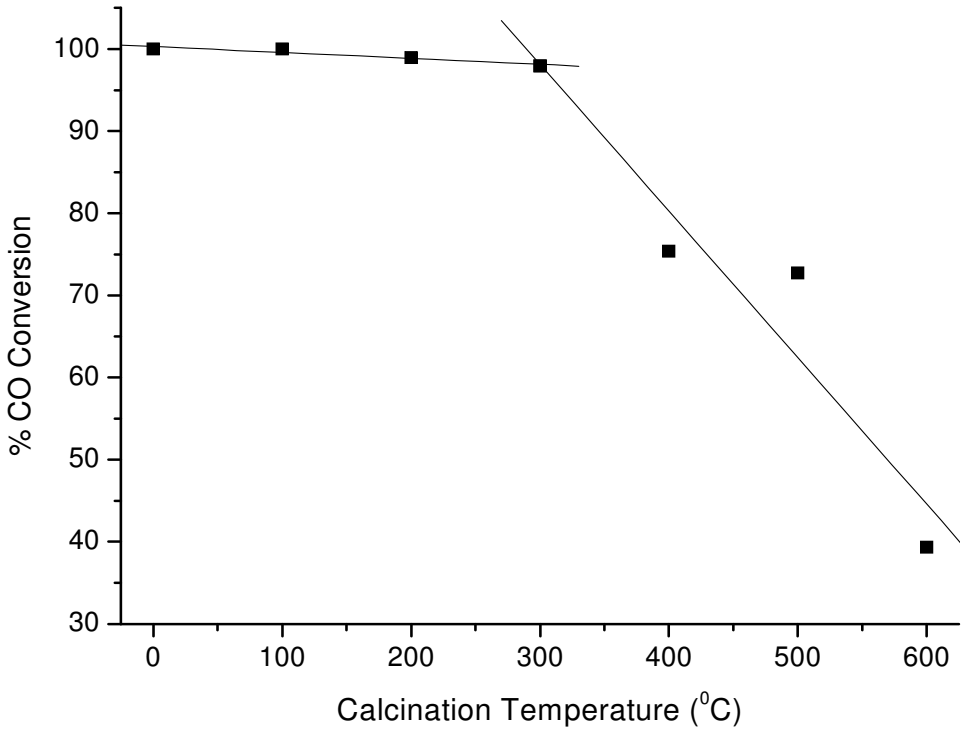

Figure 4.18: The effect of calcination temperature on Au/TiO_2-ZrO_2 catalyst prepared by deposition-precipitation.

Catalyst calcination is generally believed to be a necessary step of catalyst activation because it creates porosity by loss of water molecules from the pores of the catalysts prepared by co-precipitation, with improved access to the gold particles by the reacting molecules. In the disordered zone of the support it may also be easier to create anion vacancies into which oxygen molecules can be chemisorbed (Bond and Thompson, 2000). Figure 4.18 above however reveals that calcination of the catalysts prepared by deposition-precipitation is not necessary and it can in fact be harmful. Here we see that the conversion decreases with increasing calcination temperature. An uncalcined catalyst gives a total conversion of CO whereas the catalyst calcined at 600 ^{o}C gives ~40% conversion. This observation agrees with those of Park and Lee

(1999) and Wolf and Schuth (2002) who also observed a decrease in catalyst activity with increasing calcination temperature in both the presence and absence of water in the reactor. During calcinations, a fraction of Au ions will auto-reduce, as oxygen is lost. If the model suggested by Bond and Thompson (2000) is to be taken into consideration, where the active catalyst is that which contains both metallic and ionic gold, the uncalcined catalyst in this study may contain sufficient gold ions to form the chemical glue between the metallic gold and the support hence high activity. During calcination, these gold ions are reduced to metallic gold with an increase in temperature, hence the chemical glue is lost from the interface and sintering can occur easily (Park and Lee, 1999 and Bond and Thompson, 2000). These results, however contradict those of Tsubota *et al.* (1995) who observed higher activity with increasing calcination temperature with 1% Au/TiO_2 prepared by a mechanical mixture of colloidal gold with TiO_2 powder. They suggested that the increase in activity is due to the formation of a stronger interaction between the two phases during calcination. Elsewhere, Idakiev *et al.* (2003) observed a beneficial effect of calcination on V_2O_5-Au/TiO_2 and V_2O_5-Au/ZrO_2 catalysts at higher temperature (400 ^oC) for the benzene oxidation reaction. Catalysts calcined at lower temperatures (250 ^oC) were found to have lower activities (Idakiev *et al,* 2003).

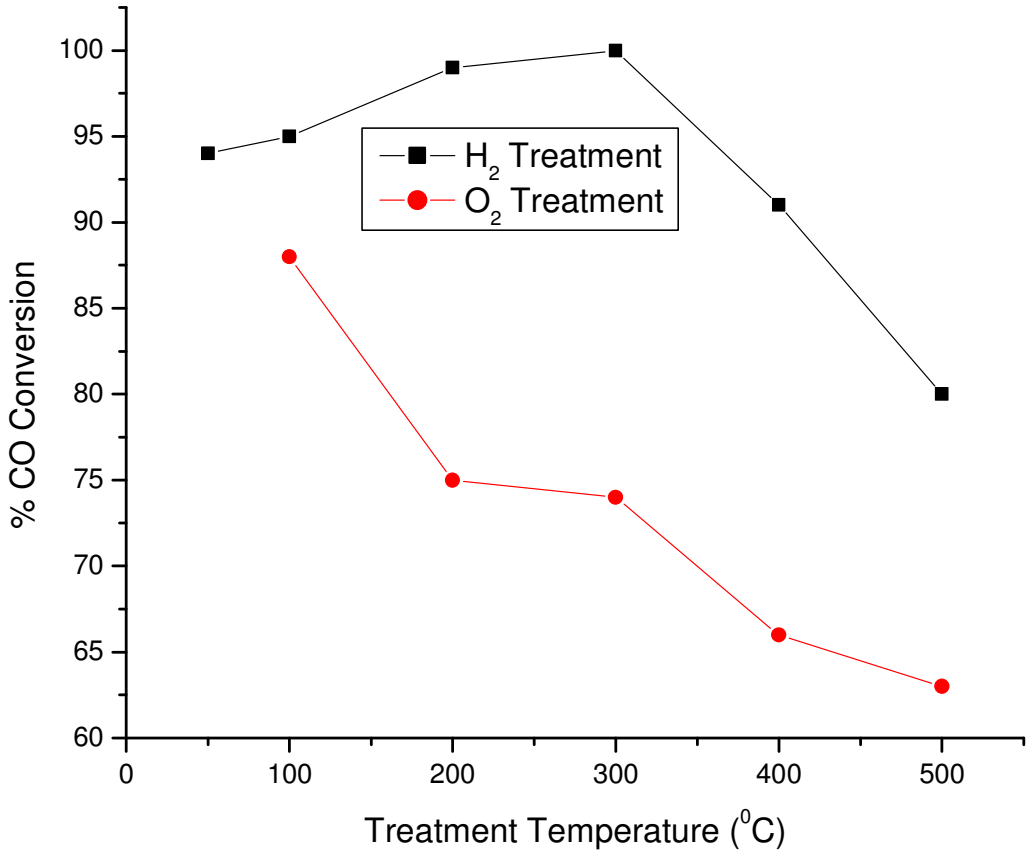

Figure 4.19: The effect of catalyst pre-treatment at different temperatures on a calcined Au/TiO_2-ZrO_2 catalyst prepared by deposition-precipitation.

Figure 4.19 shows that pre-treating the catalyst by reducing gives higher conversion than pre-treating it in oxidizing medium. The above figure also revealed that the optimum temperature for reduction is 300 ^{o}C which leads to total CO conversion. The increase in activity with increase in reduction temperature may arise from the formation of metallic gold from gold ions. At temperatures above 300 ^{o}C, the concentration of gold ions ($Au(OH)_3$) which are believed to constitute the glue between the Au^0 and the support system might fall, resulting in the loose contact between the two, hence increase the chance for sintering (Bond and Thompson,

2000). It is therefore conclusive that the decrease in activity at temperature higher than 300 ^oC may therefore be arising from the massive increase in metallic gold and sintering as was shown in figure 4.11 by an increase in the intensity of gold reflections after catalyst calcinations at higher temperatures. Cunningham *et al.* (1998) suggested that for 5 %wt Au/$Mg(OH)_2$ prepared by deposition precipitation method, 25% of gold is present in the metallic phase at 200 ^oC and at 280 ^oC all the gold present has crystallized with. However, this does not seem to be the case with the catalysts of our study since those pre-reduced at temperatures higher than 300 ^oC still shows some activity, and we speculate that it is an indication of the presence of some ionic Au species. XPS results show that the Au particles are mostly metallic; however, after peak deconvolution another set of $Au4f_{7/2}$ and $Au4f_{5/2}$ peaks appear at slightly higher binding energies, indicating the presence of electron deficient (ionic) species after calcination temperatures of 400 ^oC (figures 4.5) and 600 ^oC (figure 4.6). XPS technique has been reported to be having a disadvantage of in-situ reduction by an X-ray beam (Bond and Thompson, 2000), suggesting the possible unreliability of the results compared to those of Mössbauer. Tripathi *et al.* (1999) observed a decrease in the activity with increasing reduction temperature of the catalyst with the highest conversion achieved with the catalysts pre-reduced at 200 ^oC and the lowest with that pre-reduced at to 300 ^oC and that pre-reduced at 250 ^oC achieved an intermediate activity. When comparing the activity of these catalysts, it was beared in mind the different supports and their effects on the Au particles i.e. the extent of reduction and sintering of Au particles may not be the same for the catalysts with different supports and preparation procedures.

Catalytic activity decreases from 87% at 100 ^oC to 65% at 500 ^oC with increasing pretreatment temperature in oxidizing medium. Increasing the pretreatment temperature seems to be similar to calcining the catalyst at higher temperatures and it was shown in figure 4.18 that calcining the catalyst at higher temperatures is harmful because it leads to sintering of Au particles (figure 4.8).

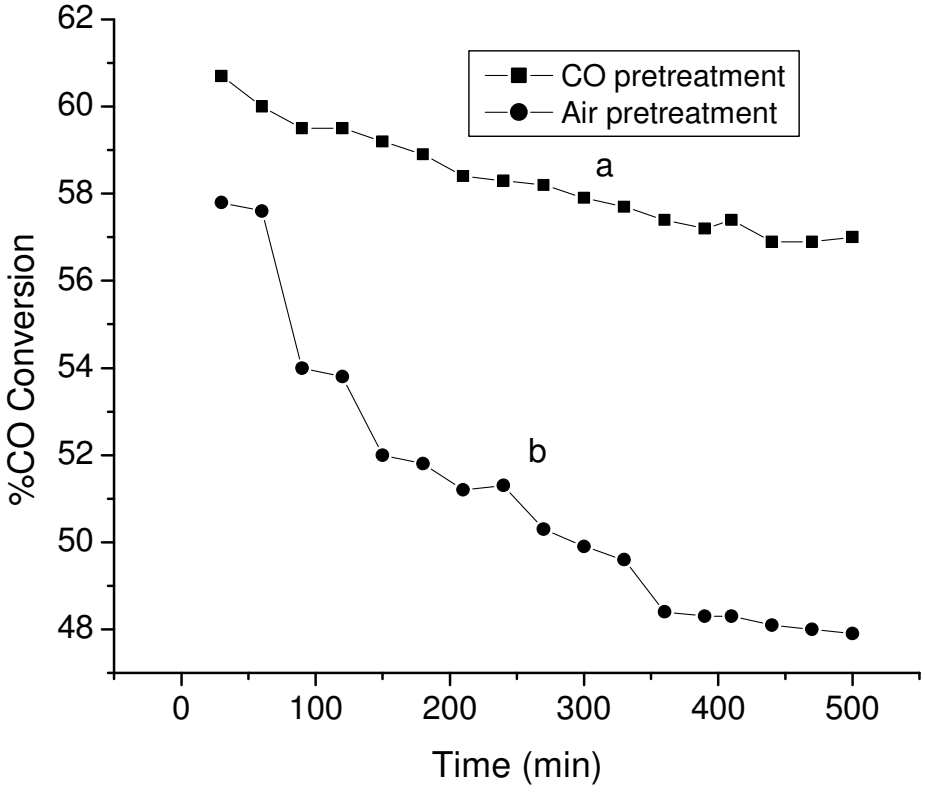

Figure 4.20: Effect of catalyst pre-treatment gas on calcined Au/TiO_2-ZrO_2 catalyst prepared by deposition-precipitation.

The catalyst pre-activated in air shows a lower activity than that pre-activated in a CO medium. The lower activity of this catalyst is probably due to the oxidation of more Au species which leads to lower amount of CO adsorbing during the reaction. Bond and Thompson (2000) proposed an ensemble of both ionic and metallic species for an active catalyst. So pre-activating the catalyst in a reducing medium increases the number of metallic species whereas the oxidizing medium results in more of ionic species. A certain ration is probably required.

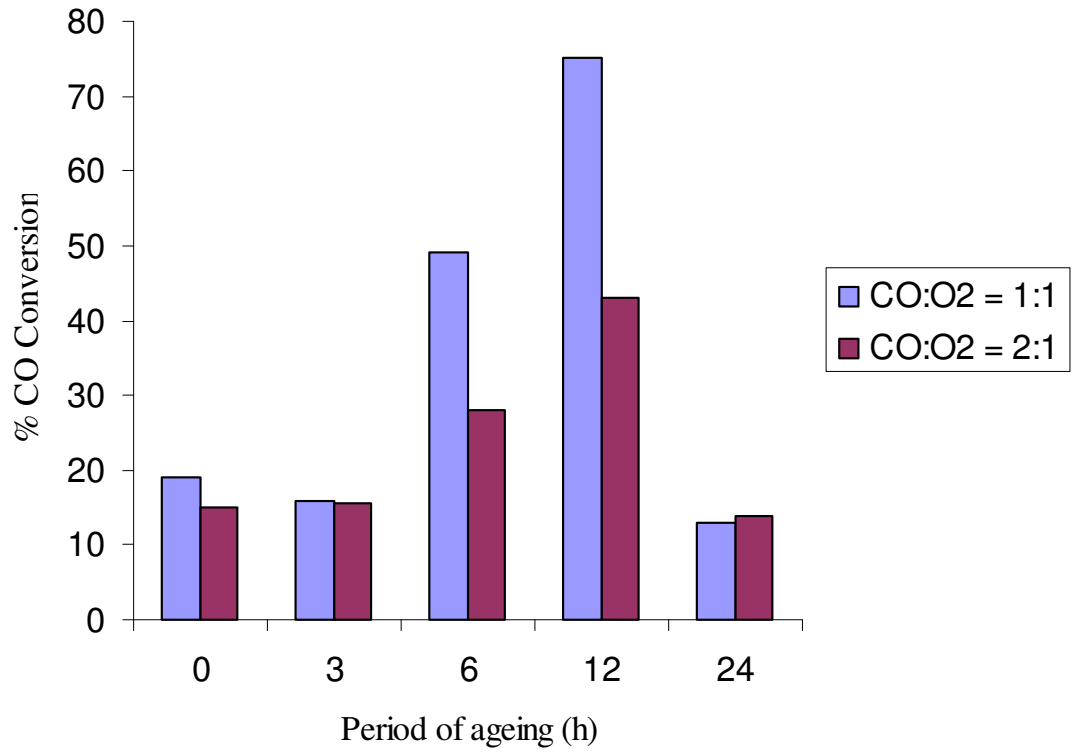

Figure 4.21: The effect of ageing period on calcined Au/TiO_2-ZrO_2 (deposition precipitation) and different ratios of CO and Oxygen at room temperature.

An unaged catalyst seems to have a higher activity than that of the catalyst aged for 3 h. However, a general trend is that the activity of the catalyst increases with an increasing ageing period up to 12 h which has a very high activity corresponding to about 75% conversion. This is probably because as the ageing period increases, more gold particles precipitate with the support particles while the chloride ions are being hydrolyzed out of the $AuCl^-_4$ to form $Au(OH)_3$ which strongly interacts with the support, whereas, at no or less ageing period, some of the gold particles remain in the mother solution during filtering. It is speculated that as the catalyst is aged for the

period longer than 12 hours, its activity decreases due to the fact that gold particles probably tend to grow into larger particles which are less active than the smaller particles. As revealed by figure 4.21 above, the use of oxygen in excess of the stoichiometric amount is beneficial for CO oxidation, as the ratio of 1:1 of the reacting molecules gives higher activity than the stoichiometric amount. This behavior was also observed by Lee and Graviilidis (2002) with Au/γ-Al_2O_3 having the precursor aged for different periods at pH 9.

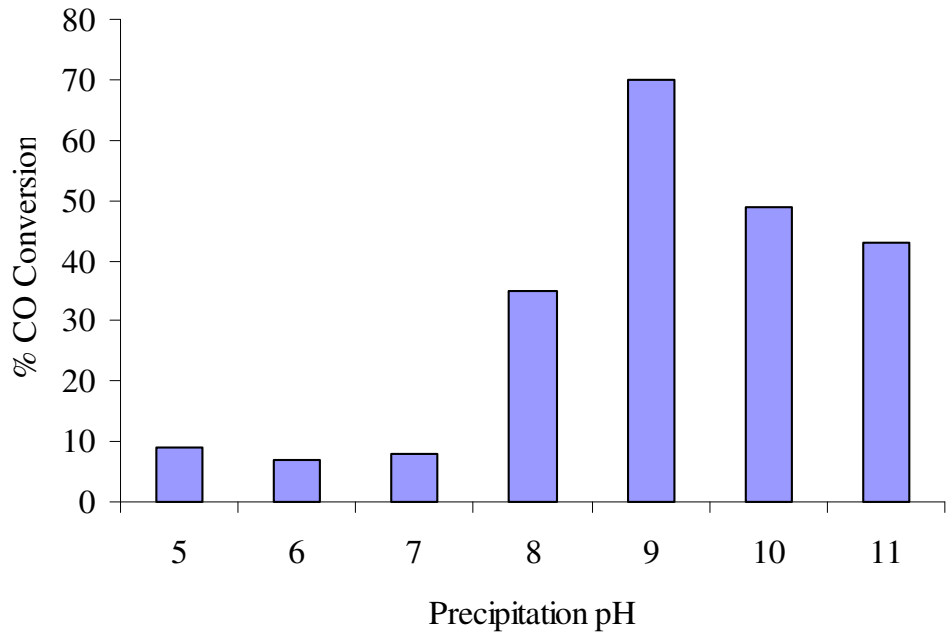

Figure 4.22: Effect of the precipitation pH of Au/TiO_2-ZrO_2 (deposition precipitation) on CO oxidation at 25 ^oC.

Figure 4.22 shows that the catalysts aged at pH 5 to pH 7 have very low activities (< 10% conversion). However, the catalyst aged at pH 9 has a higher activity and at higher pH the activities of such catalysts decrease. These results agree with those of

Lee and Gavriilidis (2002) who also observed similar behavior with the Au/γ-Al_2O_3 catalyst with the gold precursor aged for 240 min at different pH before loading on the support. The pH also has an effect on growth of the gold particles. With increasing pH values, a broadening of the Au(200) and Au(220) XRD reflections (figure 4.9) can be observed and this clearly indicates that higher pH during precipitation lead to a smaller gold particles. Lee and Gavriilidis (2002) reported that for Au/γ-Al_2O_3, increasing the pH of the solution up to pH 7 increases the concentration of strongly adsorbing complexes ($AuCl_2(OH)_2$ and $AuCl(OH)_3$) and therefore the optimum value of pH is expected where the concentration of the strongly adsorbing species is maximized.

The XPS data (table 4.5) shows that no chlorine detected on the surface of our catalysts which strongly suggests that the adsorbed gold species are in the form of $[Au(OH)_4]^-$ as well as $Au(OH)_3$ and the increase in the pH affects the gold loading and the particle size which in turn affects the catalyst activity. However, we do not rule out the presence of chloride ions in the form of $AuCl(OH)_3$ on the surface at concentrations which are smaller than the lower detection limits of the XPS technique. With increasing pH, the fraction of gold dispersed on the support increases probably due to the hydrolysis of $HAuCl_4$ into species such as $Au(OH)_3$ which interact strongly with the support. When Wolf and Schuth (2002) observed decreasing gold particle size with increasing pH value they correlated it with the decreasing amount of gold present. This study shows a similar trend (figure 4.9) on the XRD peak intensity of gold but believe that it indicates good dispersion of gold particles on the surface of the support and a decrease in particle size. Haruta (1997) reported that for Au/TiO_2 prepared in the pH range 6-10, the particles diameter was below 5 nm and did not change significantly in that pH range, whereas our results show that an increase in the pH has a significant role to play in the size of gold particles with the most active system was that precipitated at pH 9. On the other hand, Wolf and Schuth (2002) reported the most active catalyst being that precipitated at pH 8.

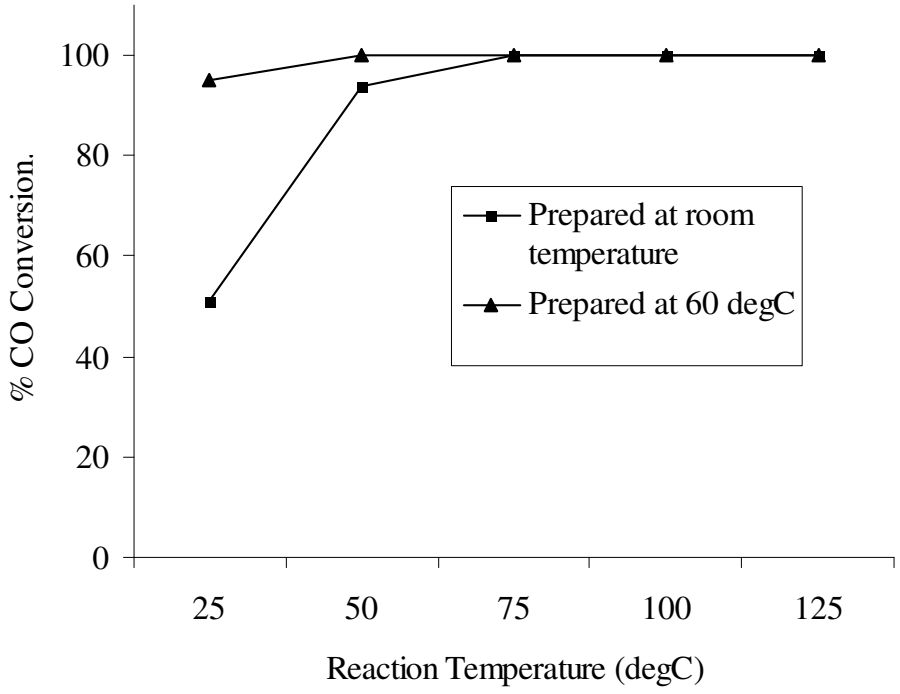

Figure 4.23: The effect of Reaction temperature on the uncalcined catalyst.

The catalyst prepared at higher temperatures was found to be more active than that prepared at room temperature giving 95% conversion at ambient reaction temperature and total conversion of CO at 50 ^{o}C whereas the catalyst prepared at room temperature gave only 51% conversion at room temperature and a total conversion at 75 ^{o}C. These results show the significant role that temperature may play during the catalyst preparation.

It has been reported that catalyst preparation by deposition–precipitation at higher temperature is desirable because interaction of the support with $Au(OH)_{4-x}Cl^-$ is by ligand substitution which is temperature dependent (Oh *et al,* 2002; Che, 1993).

4.3.2 Sol-gel method prepared catalysts

The periodic mesoporous materials are ideal candidates as templates to synthesize nano-crystals with controlled size and shape. Although the direct deposition-precipitation (DP) method can be used to prepare gold nanoparticles on titanium oxide substrates, it is difficult to synthesize gold nanoparticles (<30 Å) on silica materials with such a methodology. This difficulty can be attributed to the low Point of zero charge (PZC) of silica-based supports (PZC = ~2). Dai *et al.* (2004) reported an alternative technique to accomplish the formation of gold nano-particles on ordered mesoporous silica materials via the DP method without the constraint of the low IEP of SiO_2 surfaces. The essence of this methodology involves the introduction of a high-IEP oxide component on mesoporous silica surfaces to decrease the negative charges of silica surfaces. Sol-gel prepared catalysts were also used for the different reactions. For instance, Watson and Ozkan (2002) prepared a Gd-Pd/TiO_2 catalyst for the reduction of nitric oxide with methane. Recently, the new Au(0) sols were obtained by reducing $AuCl_3$, $NaAuCl_4$, and $HAuCl_4$ with $H_2C_2O_4$, $SnCl_4$ and $NaBH_4$ in the presence of protective agents such as pollyvinylalchohol (PVA) and Poly(diallylmethylammonium chloride (PDDA) Porta *et al.* (2002). These catalysts were used for the liquid-phase oxidation of ethylene glycol.

The recent breakthrough in the synthesis of mesoporous materials by sol-gel methodology has led to a new class of the materials with a high degree of control of pore size, shape, and lateral distribution of nanostructures (Kresge *et al.* 1992) and

this prompted us to use the sol-gel methodology for the preparation of Au/TiO_2-ZrO_2 catalysts in an attempt to develop a strong interaction between the two supports.

4.3.2.1 Characterization of Sol-gel Synthesized Catalysts

4.3.2.1.1 Thermogravimetric Analysis (TGA)

Thermogravimetric analysis was performed with a Perkin Elmer 1 TGA thermogravimetric analyzer using nitrogen as a purge gas and a heating rate of 10 $^{o}C/min^{-1}$.

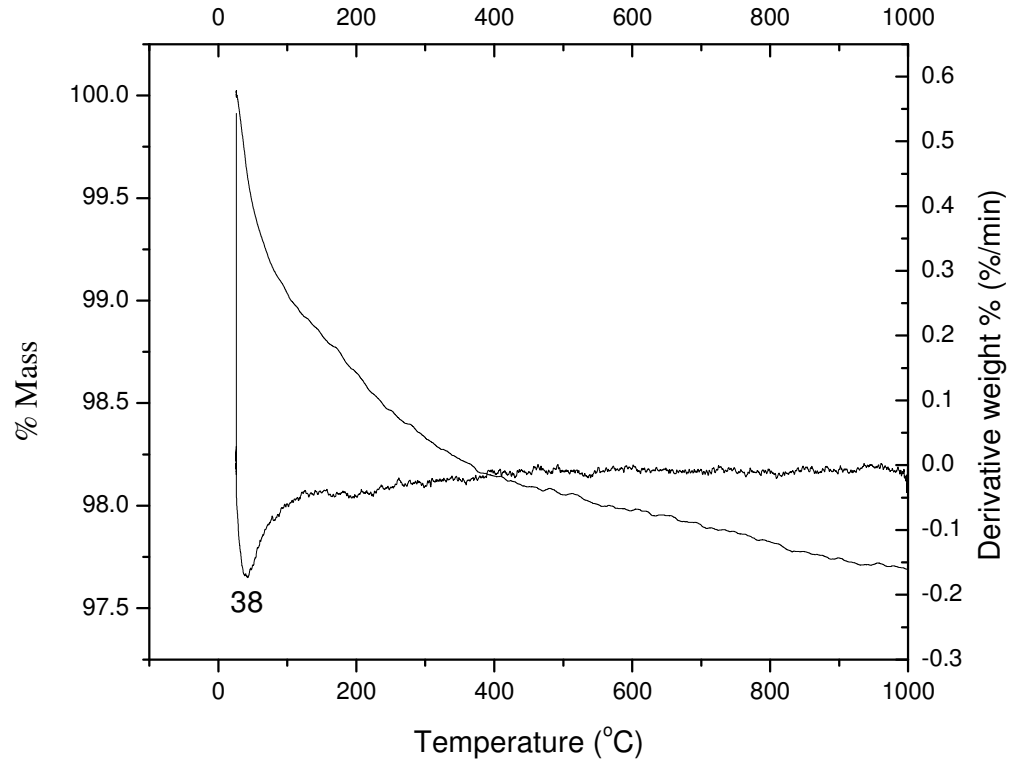

Figure 4.24: TGA profile of uncalcined Au/TiO_2 (P-25)

The most significant feature of the figure above is due to the loss of adsorbed water in the temperature range 50 °C - 120 °C.

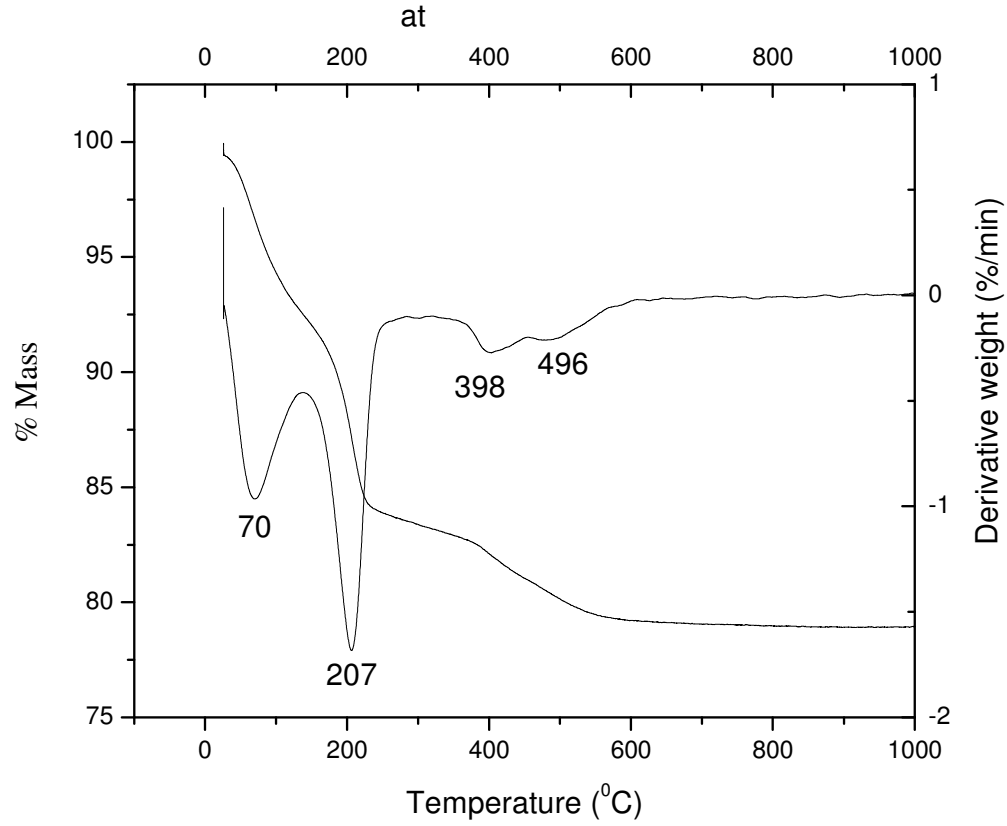

Figure 4.25: The TGA profile of sol-gel uncalcined Au/TiO_2 (uncalcined)

The figure above reveals the loss of adsorbed water at the temperature range of 50 - 150 ^oC, followed by the loss of the organic groups between 150 ^oC and 300 ^oC from the propanol solvent. The two peaks at 398 ^oC and 496 ^oC can be assigned to the loss of water molecules as a result of condensation of the internal hydroxyl groups and more organic groups from the titania isopropyl molecules. It has been proposed that the hydroxyl groups are essential in the CO oxidation mechanism (Costello *et al,* 2002). However, even if this catalyst contains more hydroxyl groups, it is not more active than the catalyst prepared by deposition-precipitation on P25, of which the TGA spectrum only shows the loss of water molecules in the region between 50 ^oC and 120 ^oC (Figure 4.24).

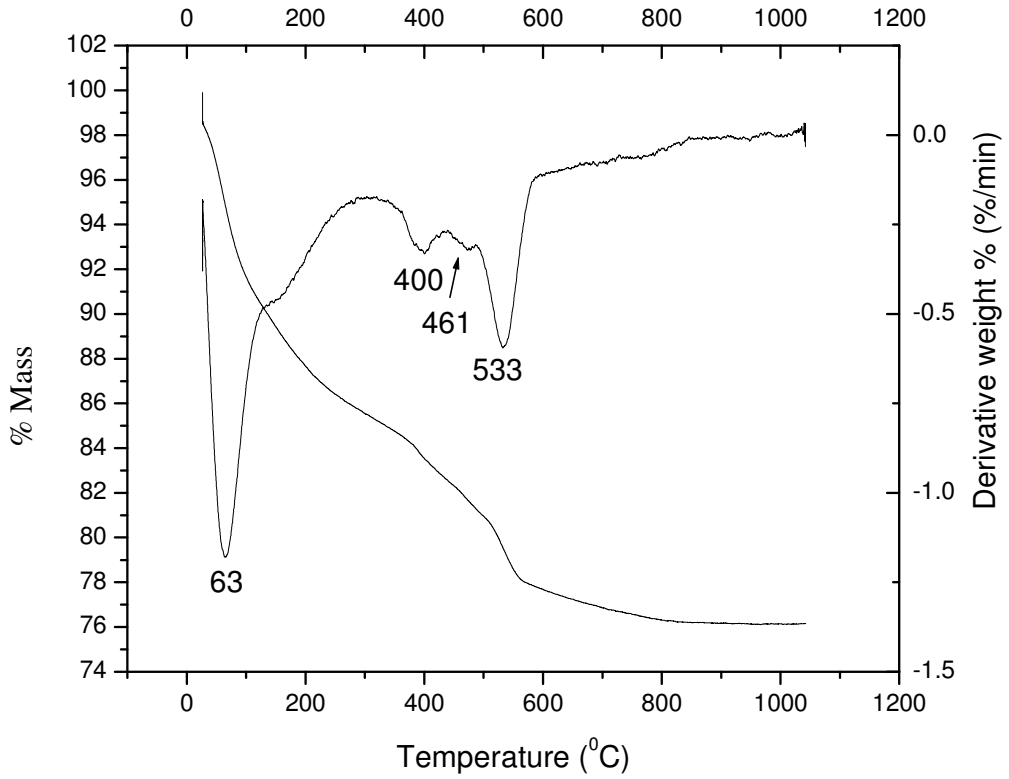

Figure 4.26: TGA profile of sol-gel uncalcined Au/ZrO_2 (uncalcined)

The figure above reveals the loss of adsorbed water at the temperature range of 50 - 150 ^{o}C. The peak at ~ 200 ^{o}C is very small which may indicate that there is little loss of carbonyl groups from the propanol solvent and those from the zirconia isopropyl may be lost between 400 ^{o}C and 533 ^{o}C. At this temperature range water is also lost due to the condensation of internal hydroxyl groups.

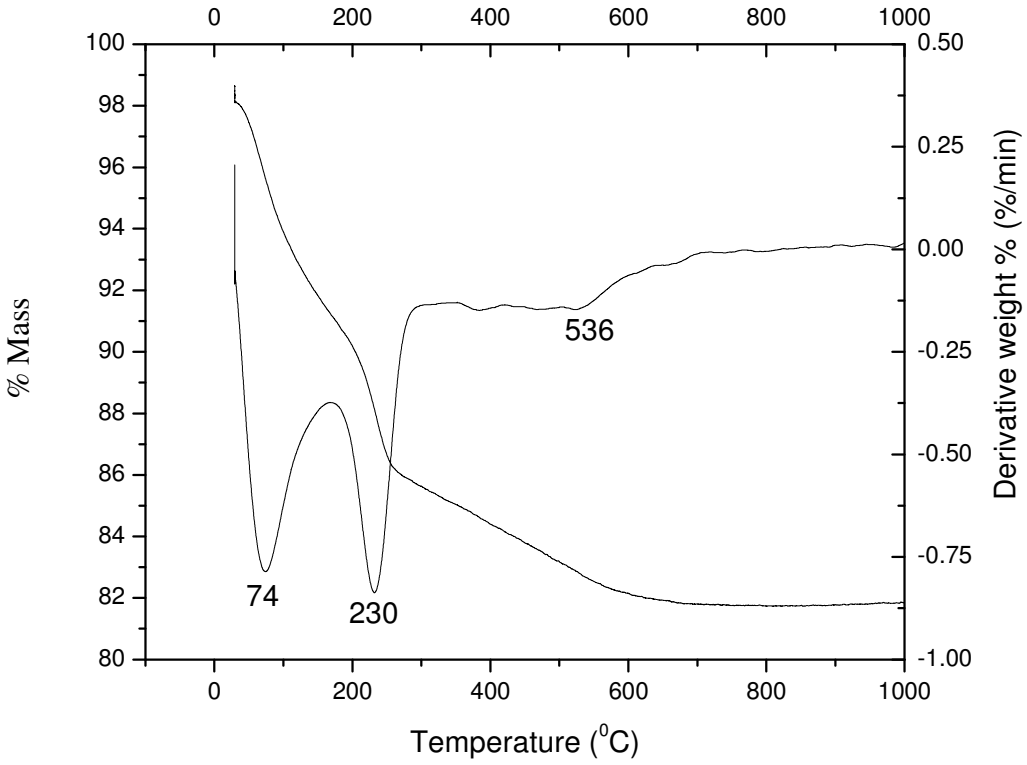

Figure 4.27: TGA profile of sol-gel Au/TiO_2-ZrO_2 (uncalcined) catalyst

The figure above reveals the loss of adsorbed water at the temperature range of 50 - 150 ^{o}C, followed by the loss of the organic groups between 150 ^{o}C and 300 ^{o}C. The broad peak from 300 ^{o}C to 600 ^{o}C can be assigned to the loss water molecules as a result of condensation of the internal hydroxyl groups and the loss of carbonyl groups from the isopropyl molecules of titania and zirconia.

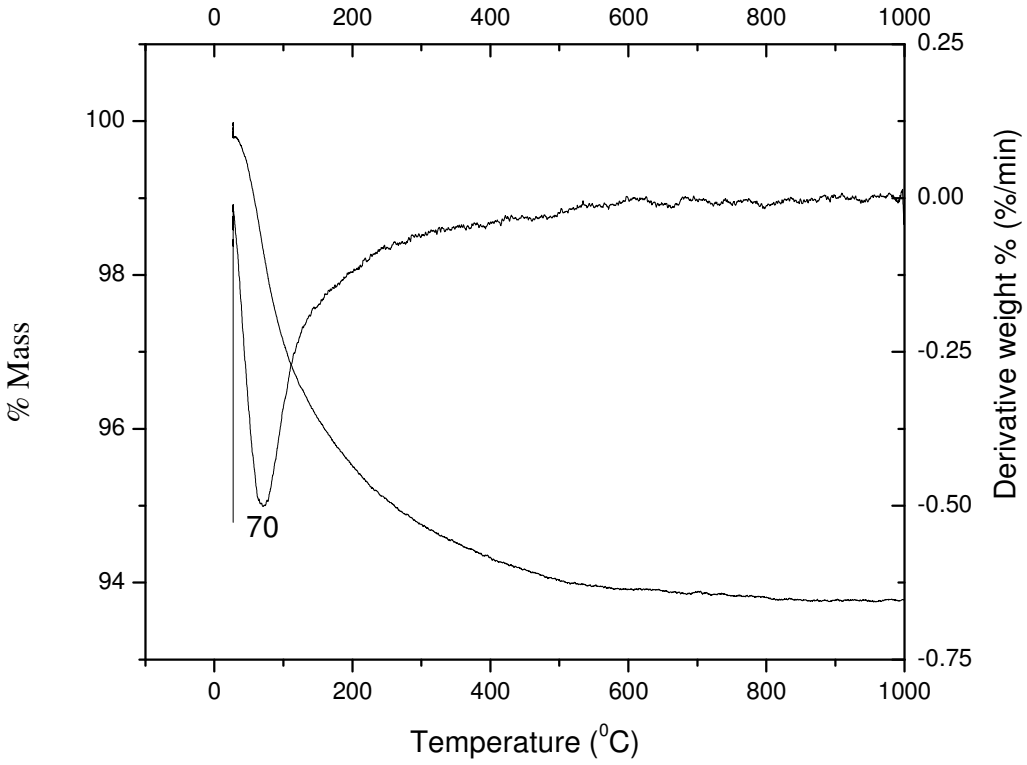

Figure 4.28: TGA profile of Au/TiO_2-ZrO_2 (with the support pre-calcined at 400 ^{o}C)

The support (TiO_2-ZrO_2) synthesized by sol-gel was calcined at 400 ^{o}C for 5 h during which all the organics were burnt and internal hydroxyl groups reacted. Only adsorbed water was found to be lost from this catalyst in the temperature range of 50 - 100 ^{o}C.

4.3.2.2 Results and discussion

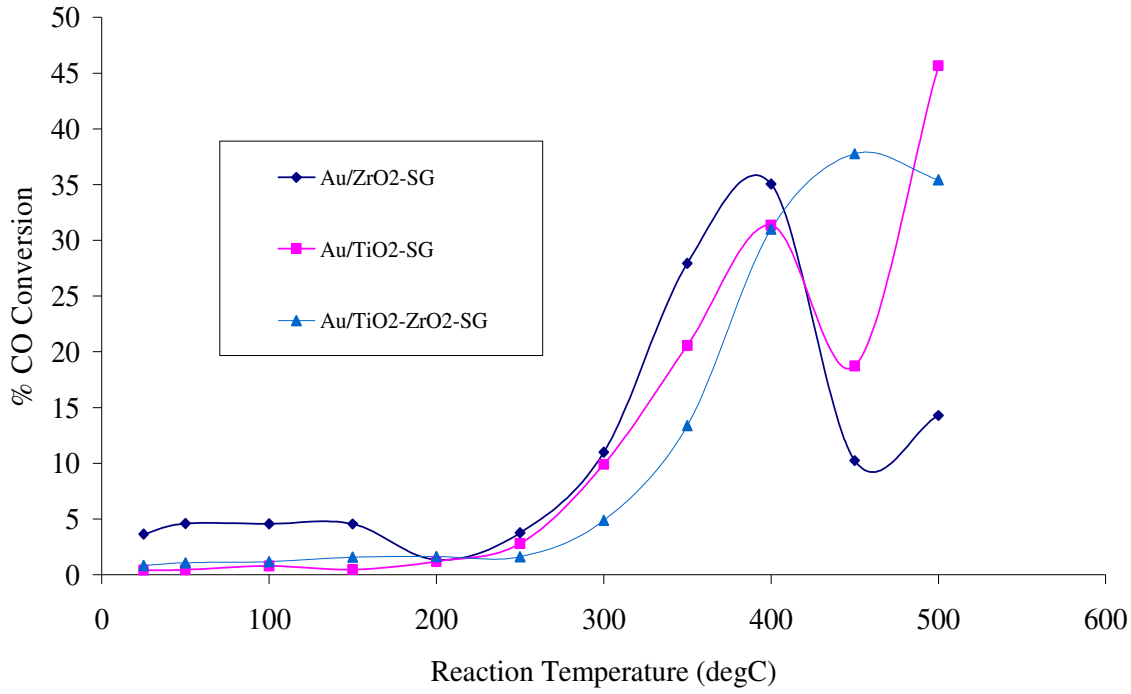

Figure 4.29: The effect of reaction temperature on the uncalcined catalysts

As shown by the figure above, sol-gel catalysts have a very low activity with Au/ZrO_2 having a higher activity of only 5 % conversion with the other catalyst being almost inactive for reaction temperatures below ca. 300 ^{o}C. Above this temperature the activity of these catalysts starts to increase with Au/ZrO_2 catalyst being the most active catalyst and the least active catalyst being Au/TiO_2-ZrO_2. This contrasts with the high activity of Au/TiO_2-ZrO_2 prepared by deposition-precipitation. However, it is the catalyst which is shown not to lose its activity at 450 ^{o}C, whereas the other catalysts show a decrease in the activity which was however regained at 500 ^{o}C. The reason for the loss of the activity with these catalysts at 450 ^{o}C has not been established.

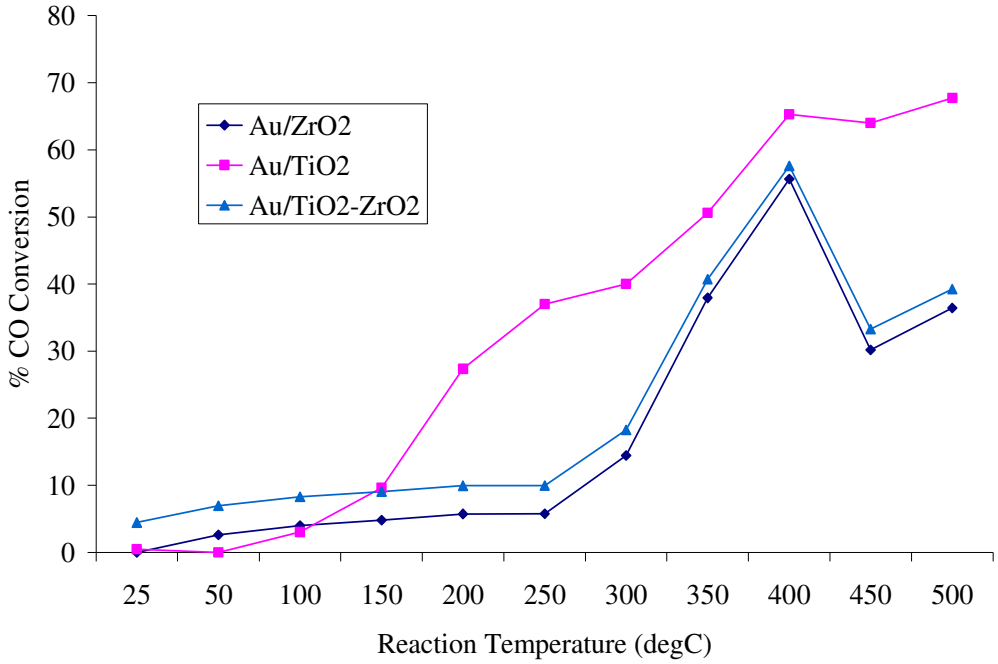

Figure 4.30: The effect of reaction temperature on the calcined catalysts

The calcined catalysts show a higher activity than the uncalcined catalysts as shown by comparing figures 4.29 and 4.30. The lower activity of the uncalcined catalyst may be due to the prevention of the reacting molecules from adsorbing on the active sites of the catalyst by the organic species which are believed to be on the surface of the catalyst. This trend contrasts with that found for the catalysts prepared by deposition precipitation, where uncalcined catalysts were found to be more active than the uncalcined.

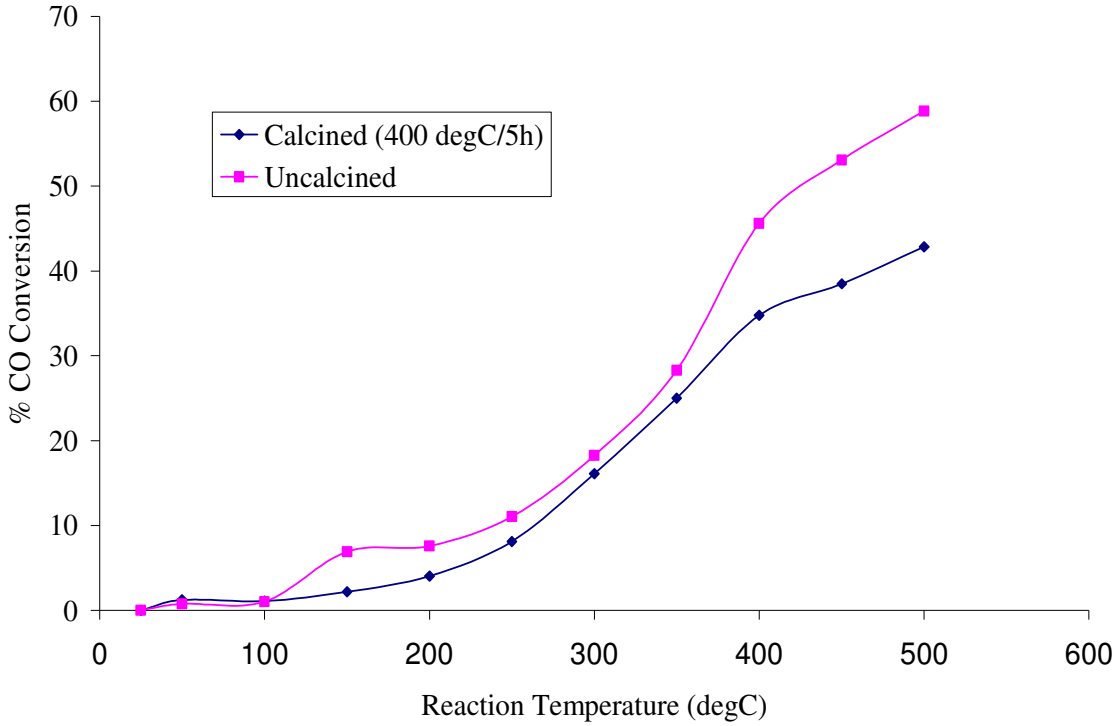

Figure 4.31: The effect of reaction temperature on the catalysts with $HAuCl_4$ solution adjusted to pH 8 before being added to the solution.

Figure 4.31 shows an increase with increasing reaction temperature with the highest conversion being 60 % for the uncalcined catalyst and only 43 % for the calcined catalyst. These activities however, are lower that those of the catalysts shown in figure 4.30. This result indicates than the gold particle size control was not so successful maybe because of the precipitation of the gold solution when it was increased to pH 8 before being added to the support gel. This precipitation may have resulted in the gold particles being deposited on the support as larger particles, which resulted in sintering, and low activity.

As for most of the catalysts we have tested, figure 4.30 also reveals that catalyst calcination has a deleterious effect on activity.

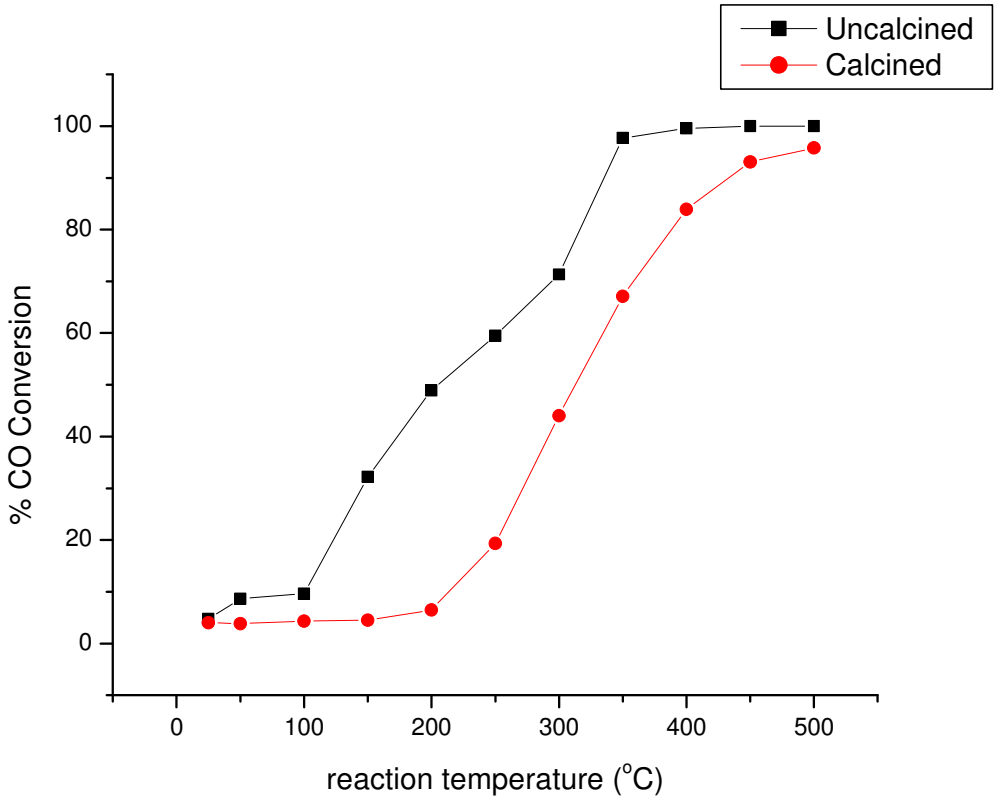

Figure 4.32: The effect of temperature on the calcined and uncalcined catalyst with its support prepared by sol-gel method.

The activities of the catalysts depicted in the Figure 4.32 above are very high compared to those of the catalysts whose supports we prepared simultaneously with the addition of gold solution during sol-gel. The support of this catalyst was synthesized first by sol-gel, dried and calcined before the addition of gold by deposition-precipitation. The organic species that are on the support are burnt out

during the calcination step, and it is suspected that during this step, an intimate interaction between the two supports occurs and during the deposition of gold the latter is evenly dispersed on the surface of both supports. It can be concluded that the poor activity of the other catalysts is due to the inhibition of gold particles from interacting strongly with the surface of the support by the organic groups that could also be filling the pore of the support.

Of more interest is that the catalyst synthesized in this manner could achieve total conversion of carbon monoxide (even if it is at higher temperatures compared to those of the catalysts prepared by deposition-precipitation), whereas other sol-gel catalysts could not, highest conversion being found to be about 70 % conversion. The difference between the calcined and the uncalcined catalyst could be due to the sintering of the gold particles on the surface of the support as was seen with other catalysts we have reported (figures 4.7 and 4.8).

4.4 Conclusions

When calcination has a detrimental effect on the catalysts, it emerges from the results of this study that the presence of zirconia seems to decrease such effect. It is evident in figure 4.18 that even the catalyst that is calcined at 600 ^oC still has a considerable conversion of about 40%. Figure 4.6 shows that deconvolution of an Au XPS peak of this catalyst reveals the presence of some electron deficient gold species, leading to the conclusion that there is still some Au^I ions presence in the catalyst. Mössbauer effect spectroscopy (figure 4.4) revealed that zirconia-containing catalysts still contain Au^I species even after calcination at high temperature (400 ^oC) whereas those that do not contain zirconia were found to be having none of the ionic species. It is speculated that the presence of zirconia, which is known to be good oxygen storage, increases the number of hydroxyl groups on the surface of the catalyst, which are known to be crucial for the catalytic activity. Even if they are calcined, the composite catalyst still possesses substantial amount of Au^I species. Activity test shows that the rate of CO oxidation is dependent on the amount of the Au^I species on the surface of the catalyst hence the presence of these species on the catalyst is crucial for CO oxidation.

In this study, a decrease in the activity of the catalyst with an increasing calcination temperature was observed. This was accompanied by sintering of the Au particles verified by HRTEM and a decrease in the surface area of the catalysts. The nature of pretreatment gas also has an effect on the catalyst activity, where reductive pretreatment conditions were found to be more beneficial that the oxidizing medium. The pH at which the catalyst is precipitated is also crucial. Poor activity was achieved with those catalysts precipitated at pH lower than 9. For this catalyst system it does not seem to be ideal to age the catalyst in the mother liquid for the period shorter than 12 h.

It is evident that sol-gel method is not an ideal preparation method for Au catalysts. The TGA results show the presence of organic molecules which are removed during calcinations but the activity is not as good as that of the catalysts prepared by deposition precipitation. Even though calcination removes the organic species from the surface of the catalyst, it results in the agglomeration of Au particles hence low activity.

4.5 References

Bond G.C, Thompson D.T, *Gold Bull*., 33 (2000) 41.

Bond G.C and Thompson D.T, *Catal. Rev. Sci., Eng.,* 41 (1999) 319.

Cunningham D.A.H, Vogel W., Haruta M., *J. Catal.,* 177 (1998) 1.

Che, M., *in "Proceedings, 10th International Congress on Catalysis, Budapest,* 1992" (L. Guezi, F. Solymosi, and P. Tetenui, Eds.), p. 32. Akad´emiai Kiad ´ o, Budapest, 1993.

Dai S, Yan W, Chen B, Mahurin S, Overbury S, *Proceedings of the international conference in catalysis, Paris, 11-16 July 2004.*

Debeila M.A, PhD Thesis, University of the Witwatersrand, 2000.

Fernandez-Garcia M., Martinez-Arias A., Iglesias-Juez A., Belver C, Hungria A.B, Conesa J.C, Soria J, *J. Catal*., 194 (2000) 385.

Finch R.M., Hodge N.A, Hutchings G.J, Meagher A, Pankhurst Q.A, Rafiq M, Siddiqui H, Wagner F.E, *PCCP* 1 (1999) 485.

Fu Q, Kudriavtseva S, Saltsburg H, Flytzani-Stephanopoulos M., *Chem Eng J*., 93 (2003) 41.

Goosens A., Craje M.W.J, van der Kraan A.M., Zwijnenburg A., Makkee M., Moulijn J.A., de Jongh L.J, *Catal. Today,* 72 (2002) 95.

Grisel R.J.H, Weststrate C., Goosens A., Craje M.W.J, van der Kraan A.M, Nieuwenhys B.E, *Catal. Today. 72* (2002) 123.

Grisel R.J.H, Nieuwenhuys B.E., *J. Catal*., 199 (2001) 48.

Grunwald J.-D., Keener C., Wogerbauer C., Baiker A., *J. Catal*., 181(1999) 223.

Grunwaldt J.-D, Maciejewski M, Becker O.S, Fabriozioli P, and Baiker A., *J. Catal*., 186 (1999) 458.

Guczi L, Horvath D., Pastel Z., Toth L., Horvath Z.E, Karacs A, Peto G, *J. Phys. Chem., B*. 104 (2000) 3183.

Guzman J. Gates B.C, *J. Phys. Chem., B*: 106 (2002) 7659.

Haruta M., *Catal. Today.,* 36 (1997) 153.

Haruta M., Tamada N., Kobayashi T and Iijima S., *J. Catal*., 115 (1989) 301.

Haruta M, Yamada N, Kobayashi T, Kageyama H, Genet M.J, Delmon B, *J. Catal*., 144 (1993) 175.

Hayashi T., Tanaka K., Haruta M., *J. Catal.,* 178 (1998) 566.

Idakiev V, Ilieva L, Andreeva D, Blin J.L, Gigot L, Su B.L, *Appl. Catal* A: 43 (2003) 25.

Kresge C, Leonowicz M, Roth W, Vartuli J, Beck J, *Nature*, 359 (1992) 710.

Kozlov I.A., Kozlova A.P, Liu H, Iwasawa Y, *Appl. Catal. A,* 182 (1999) 9.

Lee S.-J, Gavriilidis A., J. Catal. 206 (2002) 305.

Lee S.-J, Gavriilidis A., Pankhurst Q.A, Kyek A, Wagner F.E, Wong P.C.L, Yeung K.L, *J. Catal*., 200 (2001) 298.

Maciejewski M., Fabrizioli P., Grunwaldt J.-D., Becker O.S., Baiker A., *PCCP*, 3 (2001) 3846.

Mallick K., Scurrell M.S, *Appl. Catal., B*: 253 (2003) 527.

Minaco S., Scire S., Crisafulli C, Visco A.M, Galvano S, *Catal. Lett*., 47 (1997) 273.

Mulder F.M., *Mössbauer Spectroscopy on Metal Cluster Compounds and on Gadolinium Intermetallics under High Pressure*, PhD Thesis (1994), Leiden-Netherlands.

Oh H.-S., Costello C. K., Cheung C., Kung H. H., and Kung M. C., *Stud. Surf. Sci. Catal.,* 139 (2001) 229.

Park E.D., Lee J.S., *J. Catal.,* 186 (1999) 1.

Porta F, Prati L, Rossi M, Scari G, *J. Catal,* 211 (2002) 464.

Sahu H.R., and Rao R.G., *Bull. Mater. Sci.,* 232 (2000) 349.

Salama T.M., Ohnishi R., Ichikawa M., *J. Catal.,* 162 (1996) 169.

Shastri A.G., Datye A.K., Schwank J., *J. Catal.,* 87 (1984) 265.

Stievano L., Santucci S., Lozzi S, Calogero S, Wagner F.E, *J. Non-Crystal. Sol.,* 232-234 (1998) 644.

Soares J.M.C, Morrall P, Crossley A, Harris P, Bawker M, *J. Catal.,* 219 (2003) 17.

Tripathi A.K., Kamble V.S., and Gupta N.M., *J. Catal*., 187 (1999) 332.

Tsubota S, Cunningham D, Bando Y, Haruta M, *Stud. Surf. Sci. Catal.* 91 (1995) 227.

Valden M., Pak S., Lai X., Goodman D.W, *Catal. Lett.,* 56 (1998) 7.

Viegers T, *^{197}Au Mössbauer Spectroscopy Hyperfine Interactions and Dynamical Behavior of Gold in Molecular Crystals and Small Particles*, PhD Thesis (1976), Nijmegen-Netherlands.

Watson J, and Ozkan U, *J. Catal*., 210 (2002) 295.

Wang D, Hao Z, Cheng D, Shi X, Hu C, *J. Mol. Catal., A*: 200 (2003) 229.

Wolf A. and Schuth F. A., *Appl. Catal*., 226 (2002) 1.

Yang J.H, Miller J.H, Henao J, Wang Y, Raphulu M.C, Kung M.C, Kung H.H, *"In-situ Genesis of Catalytic Activity in Au/TiO_2"* ***in preparation.***

Chapter 5
CO Oxidation with Au/TiO_2

5.1 Introduction

It is widely accepted that a small gold particle size is desirable for the high activity of gold catalysts. What is not clear however, is the optimal diameter of the gold particles and whether the size differs with different support or pre-treatment conditions (Wolf and Schuth, 2002), (Zanella *et al,* 2004).

Okumura *et al.* (1998) used CVD method to prepare Au/TiO_2, Au/SiO_2 and Au/Al_2O_3 catalysts. The average gold particle diameters were 3.8, 6.5 and 3.5 nm respectively, and the turnover frequencies were 0.02, 0.02 and 0.01 s^{-1} respectively. Small differences suggest that similar activities were obtained over a range of gold particle size and different supports.

It has been proposed that the metal oxide support serves as the oxygen supplier, and the active support materials such as TiO_2 (Schumacher *et al,* 2004; Daté *et al,* 2002; Konova *et al*, 2004) and Fe_2O_3 (Haruta *et al,* 1993) among others, which can supply oxygen to the Au particles (Schubert *et al,* 2001), have been reported to be very active for support for CO oxidation and supports such as Al_2O_3 (Schubert *et al*,

2001), and SiO_2 (Bailie and Hutchings, 1999) which cannot supply oxygen to the Au particles, were found to need more severe activation (Costello *et al,* 2002) for high activity. Although such an effect may contribute to the activity of gold catalysts, the fact that Au on the inert $MgAl_2O_4$, SiO_2 and Al_2O_3 support has a catalytic activity as well (Mavrikakis *et al*, 2000; Grunwaldt and Teunissen, 2002; Lee and Graviilidis, 2002) indicates that even if the support effect is important, it is not the only reason behind the high activity of gold catalysts. Grunwaldt *et al.* (1999) reported a strong support effect on the activity of the catalysts. They prepared Au/TiO_2 and Au/ZrO_2 catalysts by the adsorption of gold colloid onto the support. Au/TiO_2 achieved 21 % and 100 % conversions at 305 and 353 K respectively whereas the Au/ZrO_2 catalyst was inactive at both temperatures. This data indicates the effect of different supports in stabilizing the gold particles.

The oxidation state of an active catalyst is another aspect of Au catalysis that has been controversially discussed in the literature. Many researchers proposed that the active species is metallic gold because they found no evidence of the presence of ionic gold species on their active catalysts (Griesel *et al,* 2002, Guczi *et al,* 2000). In contrast, others (Soares *et al,* 2003; Finch *et al*, 1999; Park and Lee, 1999; Guzman and Gates, 2002; Minaco *et al,* 1997) suggested ionic species to be a prerequisite for an active catalyst. On the other hand, Bond and Thompson (2000) proposed that the active site consists of an ensemble of $Au(OH)_3$ and metallic gold.

In this chapter, Au/TiO_2 catalysts were prepared by deposition-precipitation but in two different ways with conditions as described in Chapter 3. These catalysts were tested at and above room temperature, with the total flow rate of 40 ml/min of 10 % CO and 5 % O_2 balance with helium. Leaching with cyanide was also performed on these catalysts in order to assess the separate effects of bulk gold and residual gold (considered to be largely positively charged gold ions) on activity.

The second series of catalysts were prepared by a slightly different method, was coded “method 2”. CO oxidation was performed at dry ice temperature, with a total flow rate of 200 ml/min or 50 ml/min of 1% CO and 2.5% O_2 balanced with helium. With these catalysts the in-situ XANES was also performed.

The main objective of this study is to prepare gold catalysts that can to convert CO to CO_2 in the presence of oxygen at low temperatures and to identify the active species responsible for the high activity of gold catalysts.

5.2 Results and discussions

5.2.1 Method 1 catalysts (as described in Chapter 3)

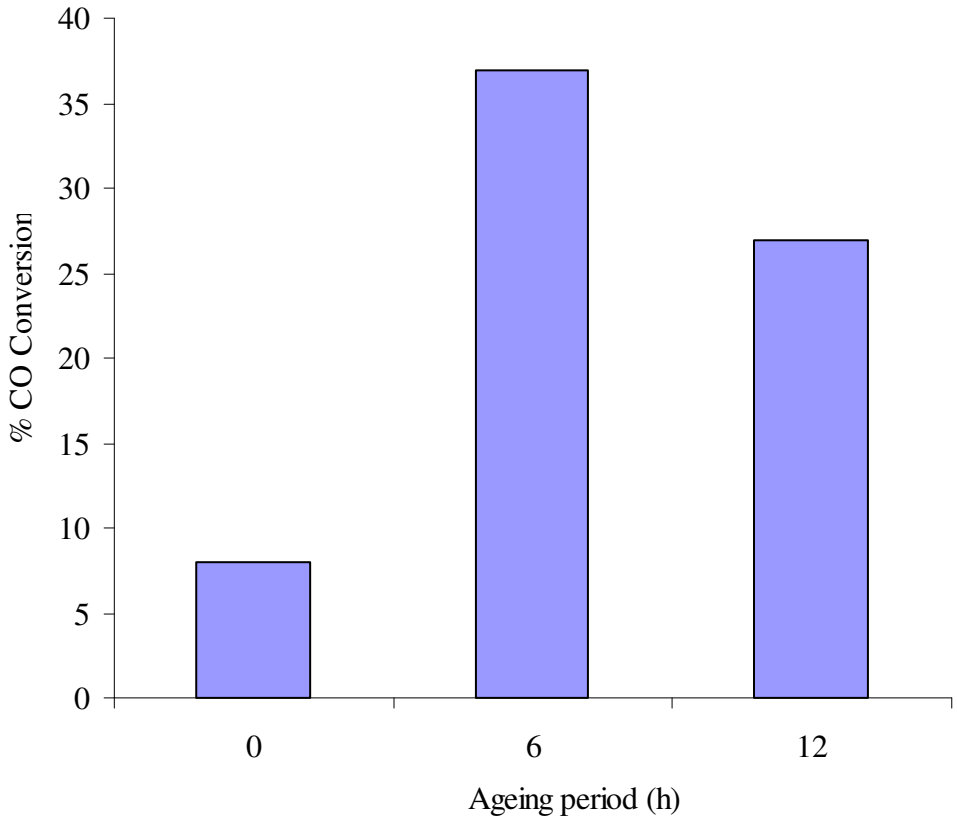

Figure 5.1: Effect of ageing period on Au/TiO_2 at 25 ^{o}C reaction temperature

The catalyst aged for 6 hrs was found to have the highest activity and it achieves its total activity at 150 ^{o}C, whereas other catalyst could not achieve total conversion (Figure 5.1). The catalyst which is not aged is believed to contain a higher content of Cl^- ions known to be responsible for catalyst poisoning (Kung *et al*, 2003; Oh *et al,* 2001). Ageing the catalyst for a longer period allows for the hydrolysis of these ions

from the $HAuCl_4$ complex into the mother liquid. More residual Cl^- ions are also removed during the washing process. Removal of the chlorine ions from the catalyst results in the deposition of small Au particles leading to higher dispersion and improved activity (Kung *et al*, 2003; Oh *et al,* 2001).

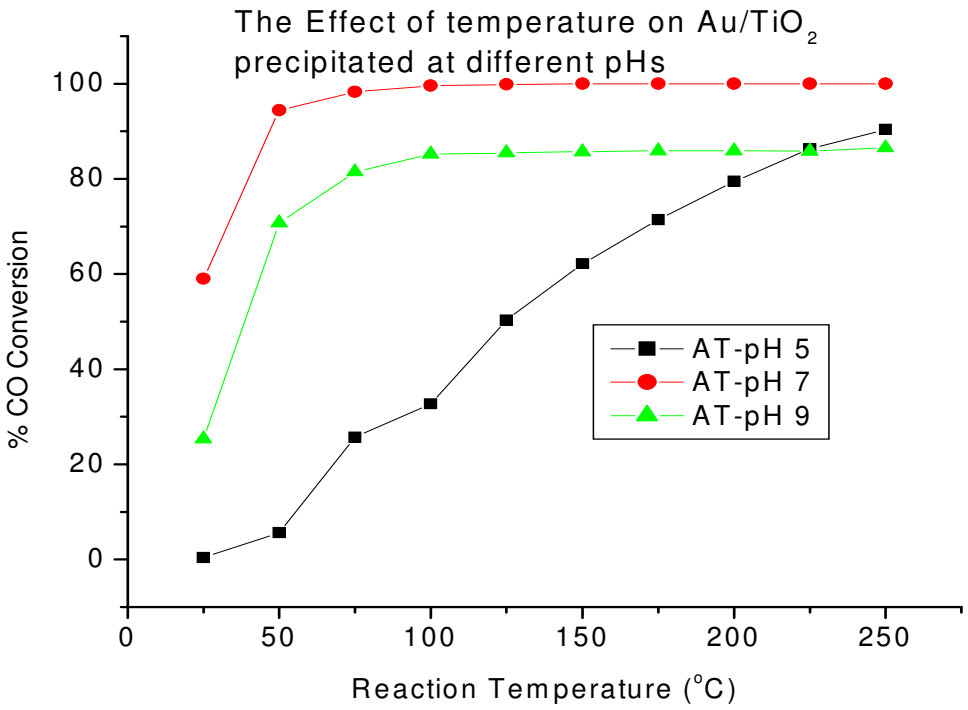

Figure 5.2: Effect of pH on Au/TiO_2 catalyst at 25 ^oC reaction temperature

Figure 5.2 shows that a high activity is obtained with the catalyst precipitated at pH 7 compared with the other catalysts. This catalyst achieves a total conversion at 75 ^oC and the conversion remains like that until 500 ^oC. The catalyst precipitated at pH 5 shows a very poor activity and never achieved a total conversion even at 500 ^oC. However the activity of this catalyst was found to increase with increasing reaction temperature. The catalyst precipitated at pH 9 shows an intermediate activity. It

reached its highest conversion of ~85% and leveled at that activity until the highest reaction temperature used.

The pH 5 catalyst shows a low activity due to a lack of hydrolysis of $HAuCl_4.XH_2O$ which is believed to occur at pH higher than 5. Therefore this catalyst may have some chlorine atoms attached to the gold species which increases the mobility of Au particles during calcinations and reaction at higher temperatures. In Au catalysts the particle size depends on the value of n in $[Au(OH)nCl_{n-4}]^{-1}$ with n being the function of pH as shown in figure 2.3 (Chapter 2). The hydrolysis of the $[AuCl_4]^-$ ion has been investigated in detail (Nechayev and Nikolenko, 1999) and $AuCl_3(H_2O)$, $[AuCl_3(OH)]^-$, $[AuCl_2(OH)_2]^-$, $AuCl(OH)_3]^-$ and $[Au(OH)_4]^-$ have been postulated to form in a stepwise manner. Their relative concentrations are dependent on Cl^- and H^+ concentrations as well as temperature. Lee and Graviilidis (2002) observed an increase in the catalyst activity with increasing pH of precipitation of Au/γ-Al_2O_3 catalyst with the gold precursor aged for 240 min. at different pH before loading on the support. They reported that for Au/γ-Al_2O_3, increasing the pH of the solution up to pH 7 increases the concentration of strongly adsorbing complexes $[AuCl_2(OH)_2]^-$ and $[AuCl(OH)_3]^-$ and therefore the optimum value of pH is expected where the concentration of the strongly adsorbed species is maximized.

Haruta (1997) also mentioned that such catalysts precipitated at lower pH contain larger particles of gold which decreases that activity of the catalyst. At pH 7, hydrolysis of $HAuCl_4.XH_2O$ is believed to be almost complete and such catalysts contain gold hydroxyl species ($Au(OH)_3$) which increases the activity of the catalyst by supplying the oxygen atoms to the CO molecules (Kung *et al*, 2003; Oh *et al,* 2001; Costello *et al,* 2002) adsorbed on metallic gold species (Nechayev and Nikolenko, 1999).

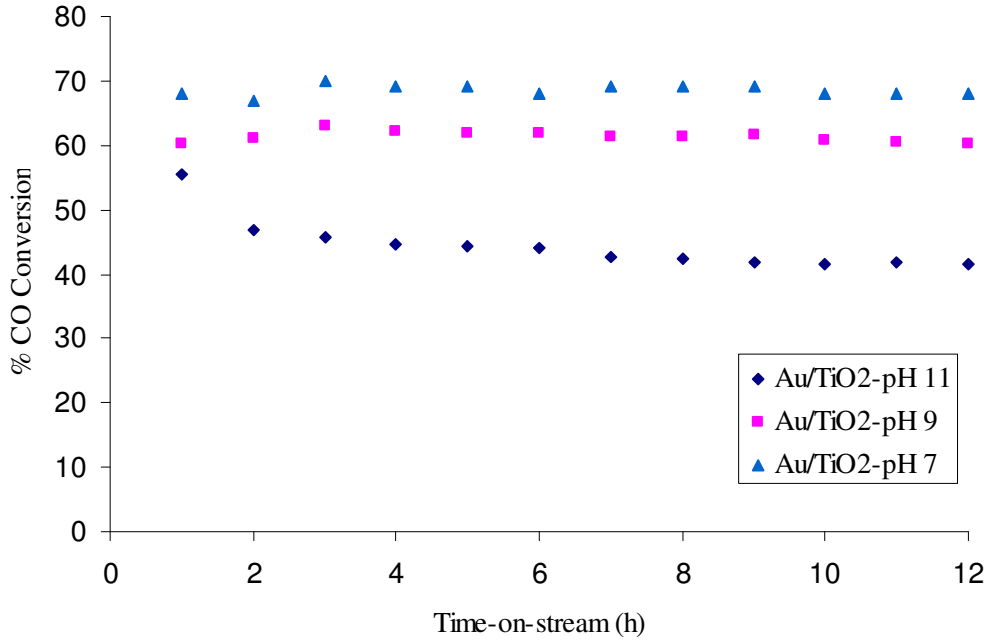

Figure 5.3: The effect of time-on-stream for different Au/TiO_2 catalysts precipitated at different pH: at 50 ^{o}C (reaction temperature), 100 ml/min, 0.1 g catalyst

The figure above shows a catalyst precipitated at pH 7 as having the highest activity followed by the one precipitated at pH 11, whereas that precipitated at pH 9 showed a poor activity and most deactivation with conversion initially at 40 % and decreasing to about 33 %. Catalyst Au/TiO_2 (pH 11) on the other hand shows a slight decrease during the first four hours but conversion remained steady at +/- 40 %. Generally, these catalysts show a very small and negligible deactivation as compared to Au/γ-Al_2O_3 reported by Costello *et al.* (2002) which started to show massive deactivation at the first few hours of the reaction. However, Costello *et al*. (2002) reported that a quasi-steady state activity was obtained when the feed contains 1.5 % water. The presence of chlorine on the surface of the catalyst has been reported to be one of the main reasons of catalyst deactivation.

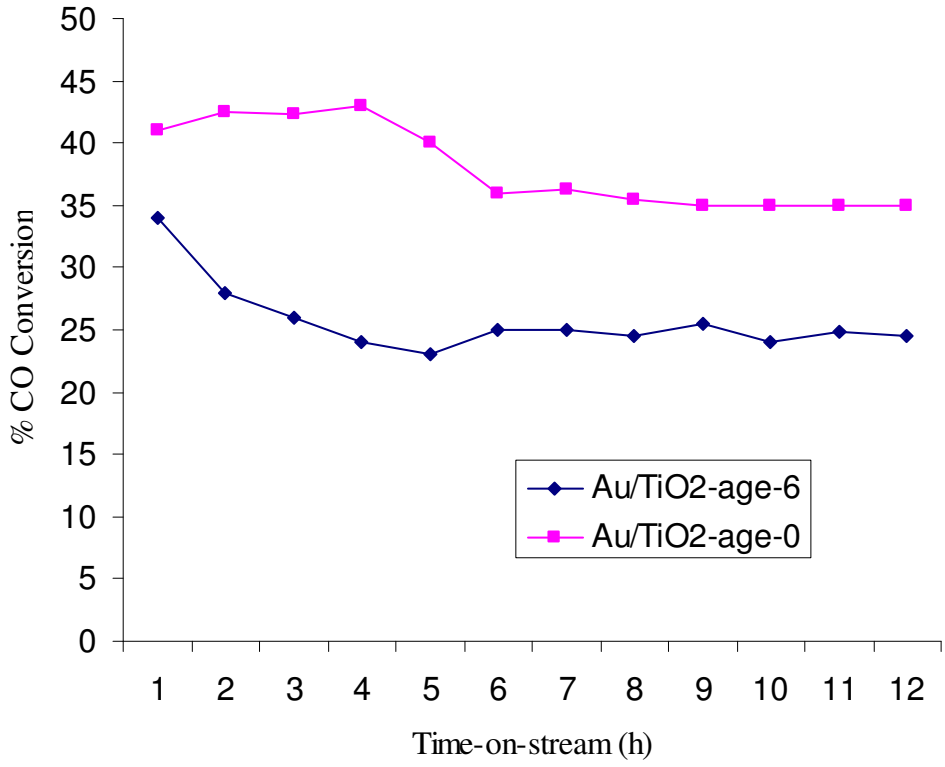

Figure 5.4: The effect of time-on-stream on CO oxidation over catalysts aged for different periods

The unaged catalyst suffered a severe deactivation during the first 5 hours of the reaction after which the steady state activity was observed. This suggests that lack of hydrolysis of $HAuCl_4$ complex and this catalyst contains a substantial amount of Cl^- ions which are known to be responsible for facilitating the movement of Au particles on the surface of the support leading to their agglomeration. After 5 hours, the movement of Au particles is minimal, and Au particles are more stable, leading to a more stable reaction (steady state). The catalyst aged for 6 hours is affected the same way, but its activity is higher than that of the unaged catalyst suggesting fewer

amounts of Cl^- ions. The catalyst aged for 12 hrs (figure 5.3), does not suffer any deactivation suggesting that the Cl^- ion content is very small.

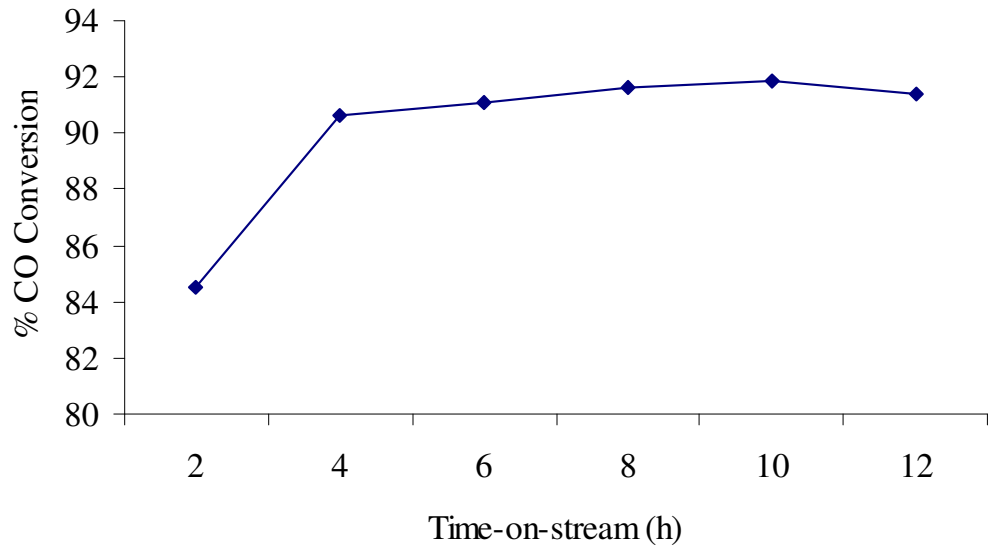

Figure 5.5: CO oxidation with uncalciend Au/TiO_2 catalyst as a function of time-on-steram at room temperature

The figure above shows that the as prepared uncalcined catalyst prepared by deposition-precipitation (method 1) has an induction period before it reaches its pseudo-steady state reaction. Before use, this catalyst contained mainly Au^{III} species, which are subsequently reduced to both Au^0 and Au^I species, which are also required for high activity of CO oxidation. It has been observed that reduction of Au^{III} species with CO/O_2 mixture occurs very quickly and a catalyst exposed to the reaction gas showed no sign of the presence of ionic species by XANES technique (Yang *et al,* in

preparation). This induction period therefore shows that even after 2 h of reaction, there is still some ionic species to be reduced by the reacting gas.

5.2.2 Leaching of Catalysts prepared by deposition-precipitation (method 1)

The confusion in the literature as to whether ionic or metallic gold is responsible for the catalytic activity of gold catalysts has aroused our interest in investigating the effect of gold catalysts freed of metallic gold species by leaching if the leaching process is successful in doing this.

The method of silver and gold extraction from their ores by dissolving them in a dilute solution of sodium cyanide or potassium cyanide is called "The McArthur-Forrest process,'' patented by McArthur *et al.* (1888) and it has been used by industry since the beginning of the 20th century. In cyanidation, metallic gold is oxidized and dissolved in an alkaline solution (more gold is recovered by cyanidation than by any other process). The oxidant employed is atmospheric oxygen which, in the presence of an aqueous solution of potassium cyanide, causes the dissolution of gold and the formation of cyanoaurite (reactions 2 and 3) (website 1).

The following chemical reactions can be used to represent the dissolution of gold by cyanide (Habashi, 1993 and 1987):

Oxidation of gold: $Au = Au^{+} + e^{-}$……..…..(1)

Complexation of gold: $Au^{+} + 2CN^{-} = Au(CN)_2^{-} + 4OH^{-}$…….(2)

Net reaction: $Au + 2CN^{-} = Au(CN)_2^{-} + e^{-}$……..(3)

The cyanidation process of materials is a heterogeneous reaction (i.e. a reaction driven by unlike components) and is corrosion process. The overall leaching of gold depends on the following reaction (McArthur *et al,* 1888; Jeffrey and Breuer, 2000):

$$4Au + 8CN^- + O_2 + 2H_2O = 4Au(CN)_2^- + 4OH^- \quad \ldots\ldots(4)$$

The reactivities of metallic and ionic gold on a support may well be sufficiently different that cyanide leaching could be selective (Fu *et al,* 2003 a, and b). The dissolution of metallic gold may be faster than that of ionic gold; hence metallic gold may be removed from the catalyst.

The leaching process

The catalyst (1 g) was leached with a solution of KCN in the presence of NaOH solution. The KCN concentration was varied in order to control the amount of Au removed from the catalyst. The pH of NaOH solution was also varied. A blank leaching process was first carried out in the absence of KCN and NaOH solution using only distilled water.

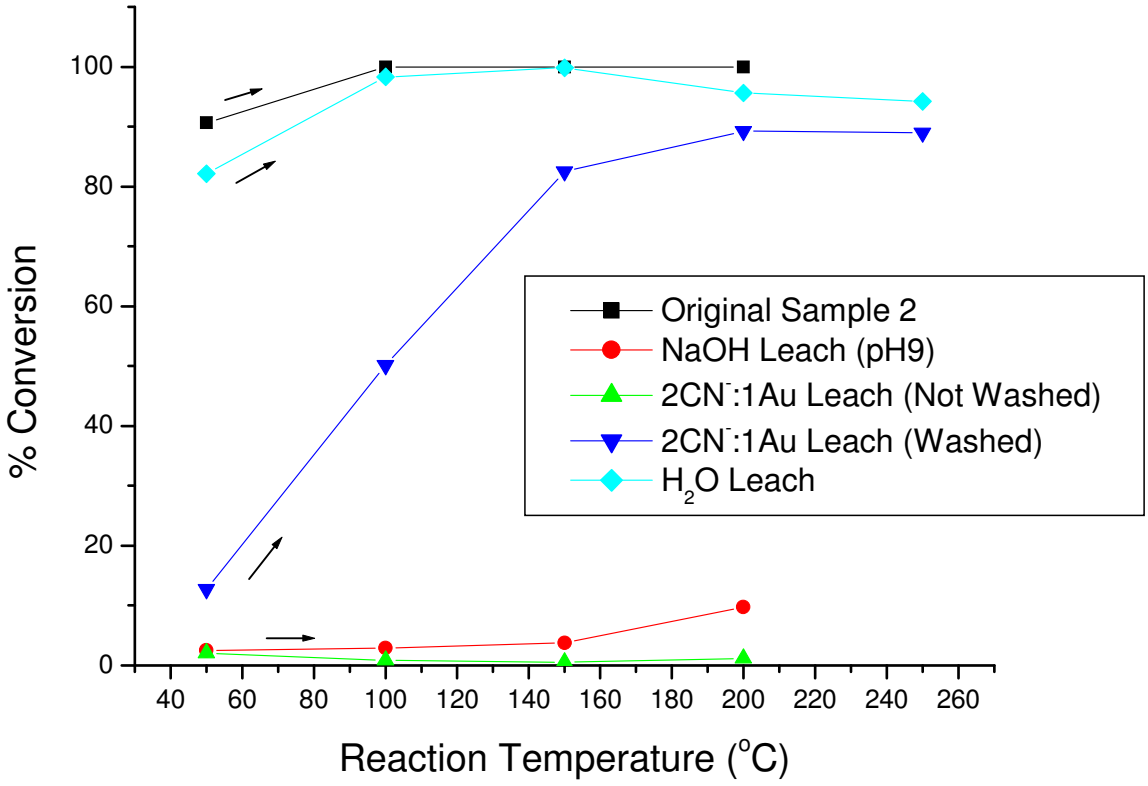

Figure 5.6: The effect of different leaching conditions on Au/TiO2 catalyst

The sample leached with 2 CN^- : 1 Au shows a very low activity at 50 °C (13 % conversion) which increases to 89 % at 200 °C. A sample leached under the same conditions but not washed after being filtered, shows an even lower activity of 2.0 % at 50 °C which decreased to 1.0 % at 200 °C. This could be due to the CN^- and Na^+ ions that were not washed out blocking most of the ionic gold particles and thereby preventing them from taking part in the reaction. The sample leached with only the NaOH base (without CN^-) does not show much improvement from the sample that was not washed after filtration. The catalyst appears to have been deactivated and only increased its activity to 9.7 % at 200 °C. The low activity could be due to sodium ions from the base solution adsorbing strongly on the surface of the catalyst

(which may have been removed by washing), thus competing for the active sites with the reacting molecules. Such ions were reported to increase the rate of CO oxidation (Hoflund *et al,* 1995; Zanella *et al,* 2004), but the optimum amount of these ions on the surface of the catalyst has not been thoroughly investigated.

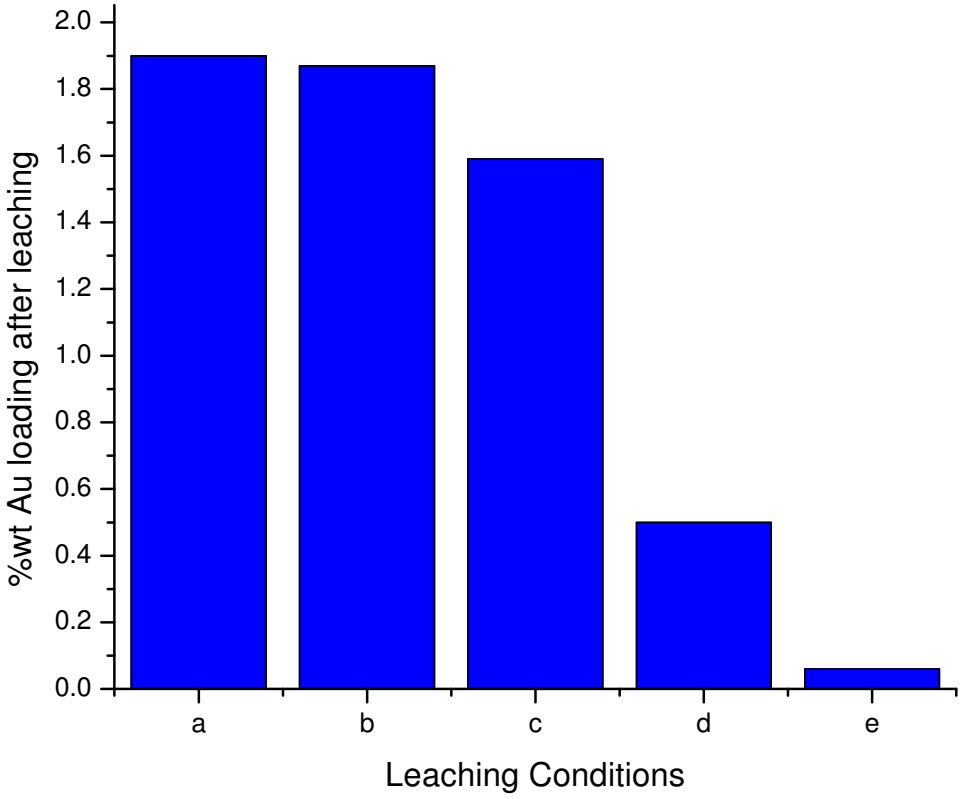

Figure 5.7: Effect of leaching conditions on Au loading obtained after catalyst leaching, where: a = fresh catalyst; b = water leached; c = NaOH only, d = KCN + NaOH and e = KCN only

The figure above shows that certain conditions for the leaching of gold catalysts need to be met in order to control the amount of gold remaining on the support. Leaching of the catalyst with NaOH solution removes a very small amount of Au from the

catalyst. The action of KCN solution results in an increased amount of Au leached. We have also observed that the Au content removed can also be controlled by the period over which the catalyst is leached. The longer the period, the more the gold was removed. We have leached all of the catalysts reported here for only 5 min.

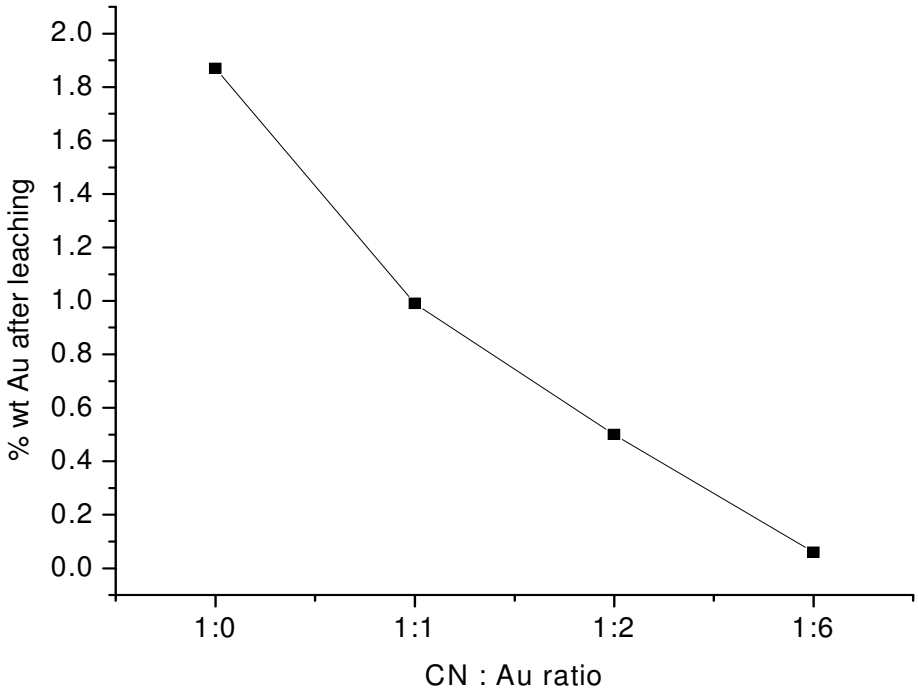

Figure 5.8: Effect of the amount of CN^- in the leaching solution on the Au loading obtained after leaching

Figure 5.8 shows the effect of the amount of CN^- ions on the amount of Au removed from the catalyst. An increase in the CN^- content leads to an increase in the Au content removed. With the highest content of CN^- ions, there is a severe leaching of Au from the catalyst with less than 0.1 % Au loading on the catalyst. According to the reaction schemes 2 and 3 above, this is due to the increase in the formation of $Au(CN)_2^-$ complex which removes the Au from the surface of the catalyst.

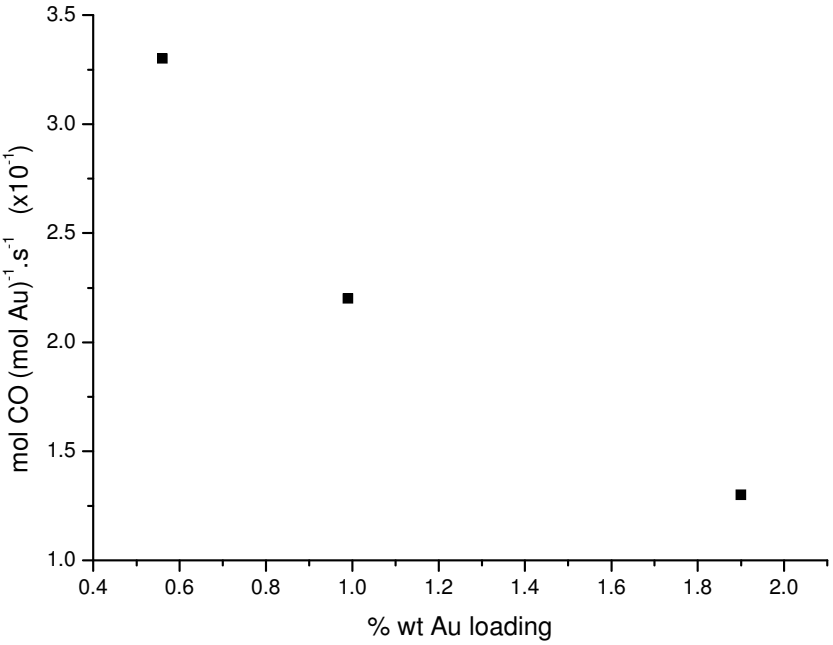

Figure 5.9: Effect of residual Au loading on the rate of reaction

Leaching removes the bulk Au from the surface of the catalyst, leaving small, well dispersed Au particles strongly interacting with the support (Fu *et al,* 2003 a and Davis, 2003). Minato *et al.* (2004) observed a decreased particle size with decreasing coverage of Au on the surface of TiO_2 using Scanning Tunneling Microscopy (STM). It has been reported that the CO oxidation reaction occurs on the steps, edges, and corners atoms, and these were found to increase in number with decreasing particle size (Lopez *et al,* 2004 a, and b). When leaching the catalysts (chapter 3), it was hoped that bulk Au^0 particles would be selectively removed leaving small, positively charged Au species. However, there is no spectroscopic evidence showing that this goal was achieved. At low loadings small gold particles may dominate. However, the catalyst which was leached down to 0.06% Au was found to be inactive for CO oxidation. This suggests that even if small Au particles are desired for a good Au

catalyst, there is an optimum particle size. This catalyst may also contain only small ionic Au particles while those with high gold loadings contain bigger particles.

Fu *et al.* (2003 a, and b) checked the oxidation state of Au before and after the leaching process with NaCN and observed the existence of both Au^{I} and Au^{III}, with the total removal of Au^{0} species. An interesting observation was that even after the reaction, the used catalyst could not be leached. As can be seen in figure 5.9 above, the activity increases with increasing the amount of Au removed from the catalyst, which is in contrast to the observations by Fu *et al.* (2003 b) who observed no change in the activity, before and after leaching, and concluded that metallic Au does not take part in the water-gas shift reaction.

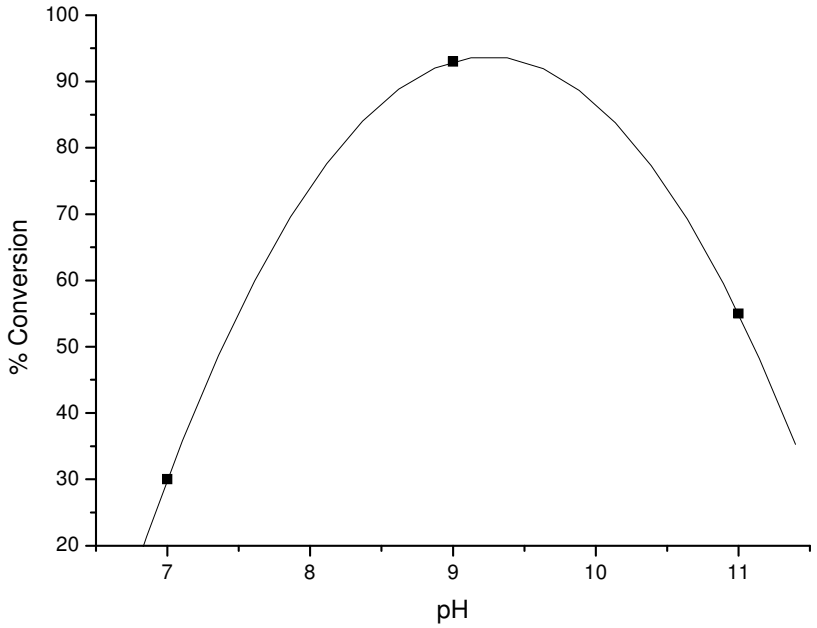

Figure 5.10: The effect of leaching pH on the activity of the catalyst

The pH of the NaOH solution in the leaching mixture has a significant effect on the activity of the catalyst. The figure above shows that pH 9 is an optimum pH for this purpose, whereas lower and higher pH lead to lower amount of CO converted.

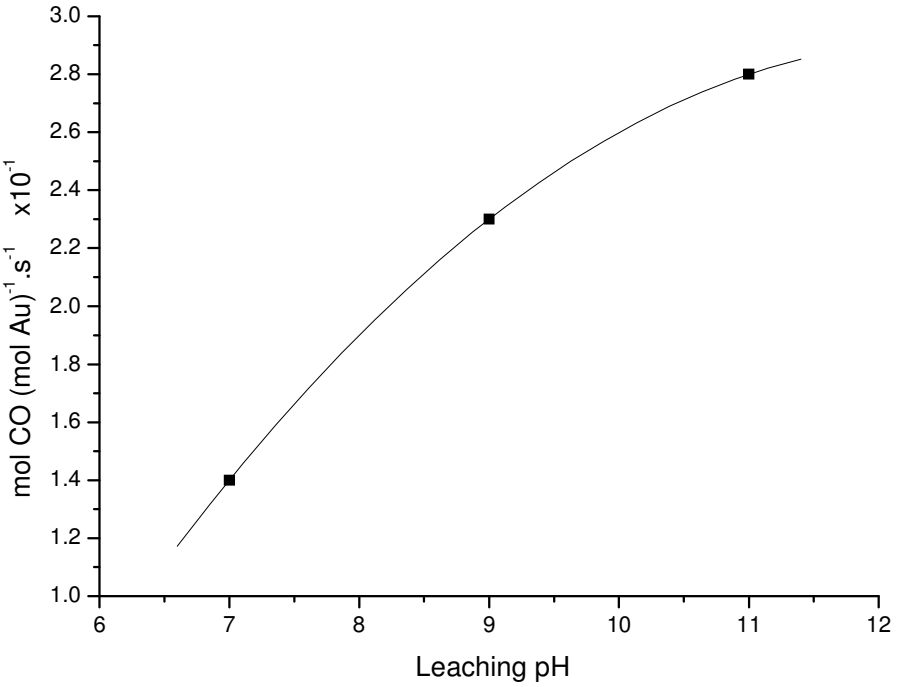

Figure 5.11: Effect of leaching pH on the rate of reaction on Au/TiO_2-ZrO_2

An increase in the pH of the NaOH increases the concentration of Na^+ ions present and these may not all be removed during the washing process. The effect of alkali metal ions in Au catalysts has been investigated and was found to increase the rate of CO oxidation reaction (Zanella *et al,* 2004; Hoflund *et al,* 1995). The mechanism by which the Na^+ ions exert this effect has not been proposed to date, but the alkali metals have been reported to act as promoters in gold-based catalysts (Hoflund *et al,* 1995; Gardner *et al,* 1991).

5.2.3 Deposition-precipitation (Method 2) preparation

5.2.3.1 CO Oxidation

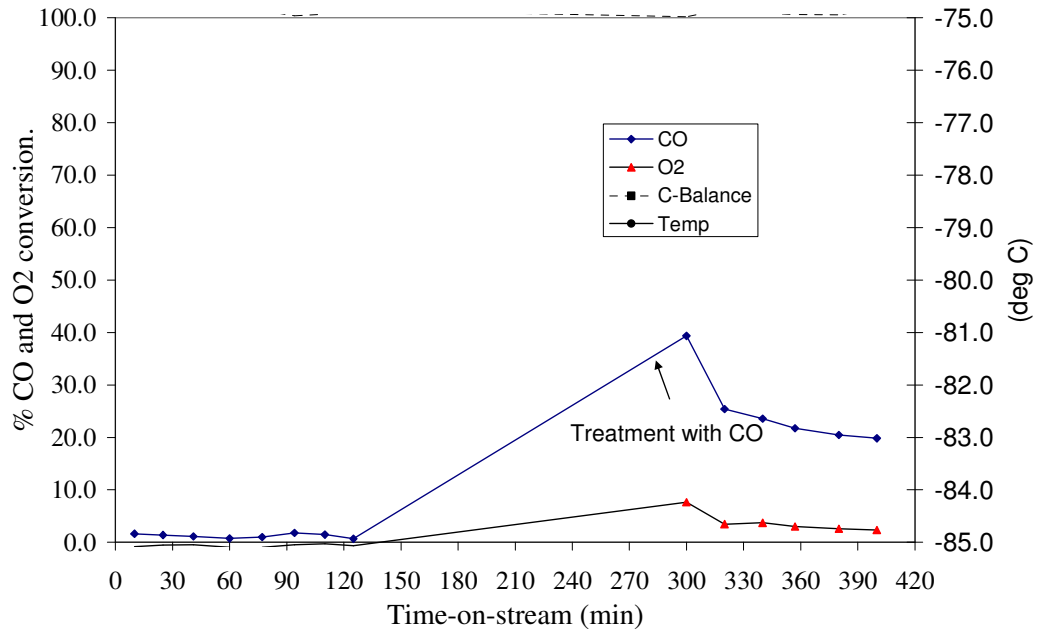

Figure 5.12: Effect of room temperature CO treatment on CO oxidation activity of the uncalcined Au/P25 (pH 7) catalyst at dry ice temperature

This catalyst shows no activity at dry ice temperature (Figure 5.12). Several research groups have reported that the uncalcined catalyst contain mostly ionic gold. Guzman and Gates (2000) in particular, have observed the presence of Au^{III} by XANES in the catalyst dried at 100 ^{o}C in helium. This agrees with the XANES data in Figures 5.27 (section 5.3.2), where no evidence of metallic gold species was observed on the as-prepared Au/TiO_2 catalyst. Costello *et al.* (2001) have suggested that both metallic and ionic species are necessary for high activity. They suggested that metallic gold species were necessary for the dissociation of oxygen molecules while the ionic species ($Au(OH)_x$) are responsible for the adsorption of CO. Treatment of the catalyst

with CO (figure 5.12) at room temperature reduces some of the ionic species into metallic species and more O_2 molecules are dissociated, according to the mechanism proposed by Oh *et al.* (2001) and Costello *et al.* (2002). The catalytic activity is seen to increase.

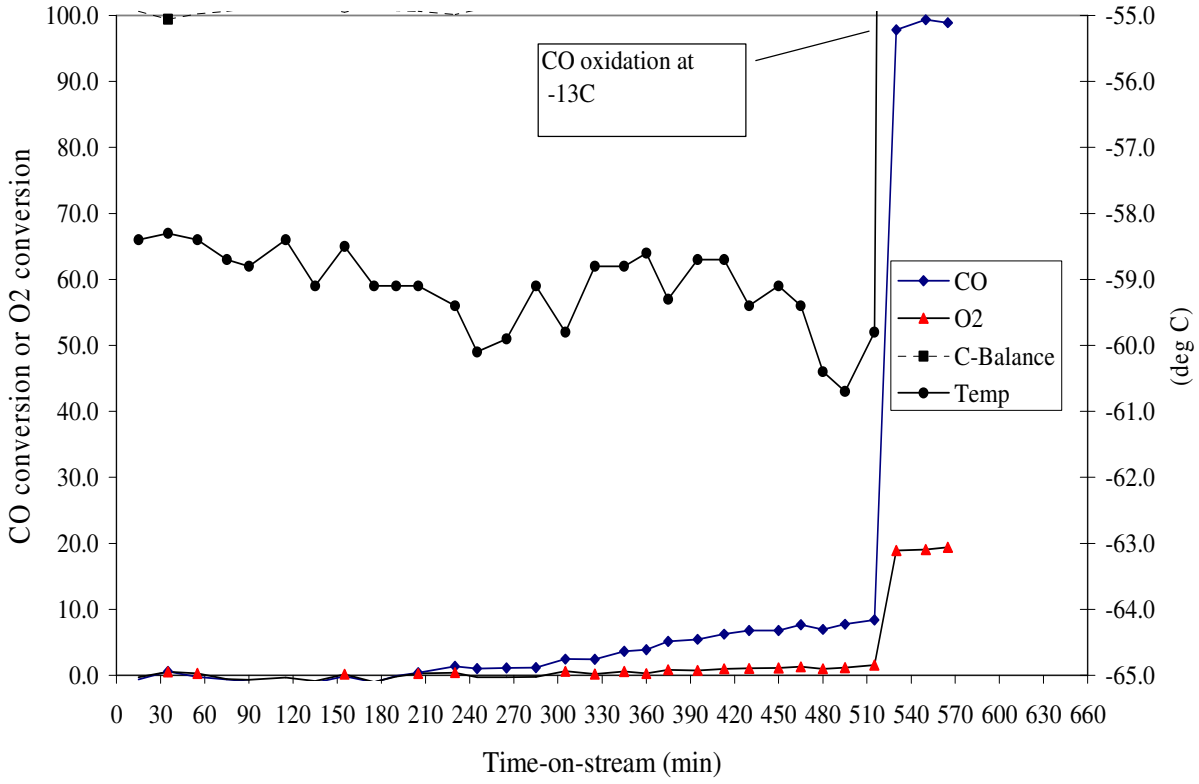

Figure 5.13: CO oxidation of Au/P25 (pH 7) catalyst at -59 ^{o}C and at -13 ^{o}C (no CO/He treatment), at 50 ml/min total flow rate.

Figure 5.13 above shows a long induction period of about 5 h, and then increases its activity to about 10% conversion. After a reaction at -59 ^{o}C, the catalyst was purged with 200 ml/min of helium at room temperature and the reactor was immersed in an ethylene glycol bath at -13 ^{o}C still with the reactor being purged with He (200 ml/min) The reactants were then admitted into the reactor. No induction period was

observed at this reaction temperature. The catalyst achieved its total conversion within the first few minutes of the reaction. This may suggest that at this temperature, CO/O_2 mixture reduces more of the ionic species of the catalyst within minutes or even seconds of reaction and the catalyst becomes more active. This suggests that at -59 ^oC, reduction of gold species occurs very much more slowly than at higher temperature, hence the longer induction period. This catalyst achieves a total conversion at -13 ^oC.

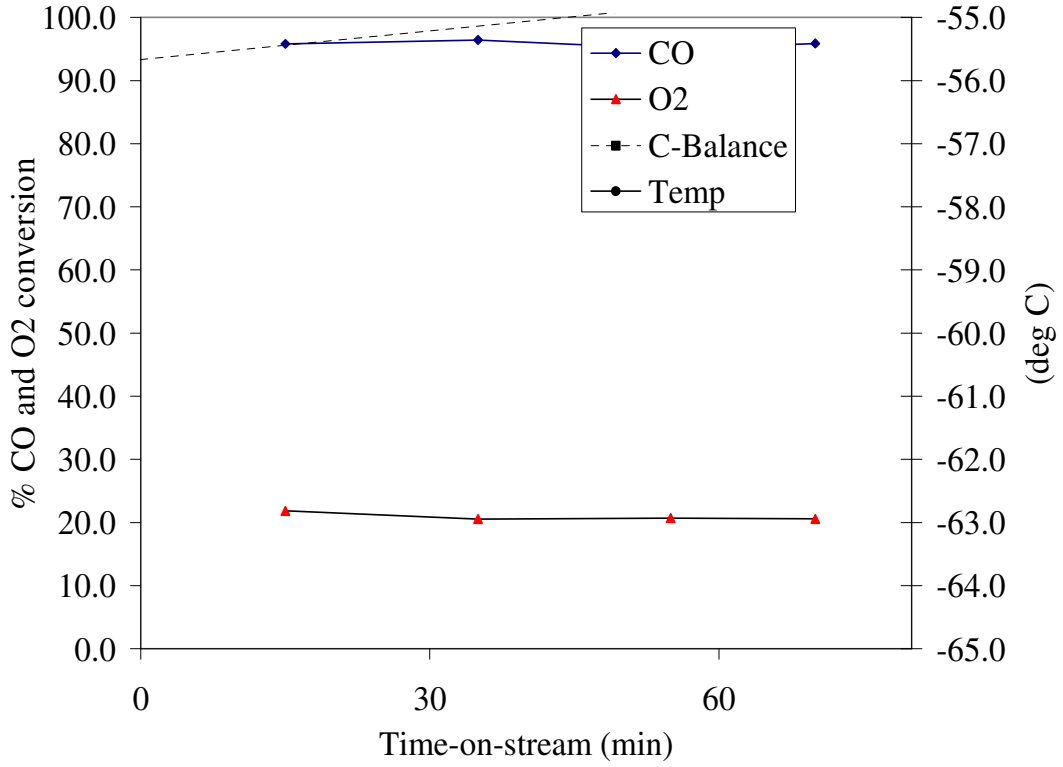

Figure 5.14: Activity of Au/P25 (pH 7) catalyst at -13 ^oC at 200 ml/min flowrate

Increasing the feed flow rate to 200 ml/min did not have much effect on the total conversion achieved with 50 ml/min. The conversion was constant for over an hour at 96%.

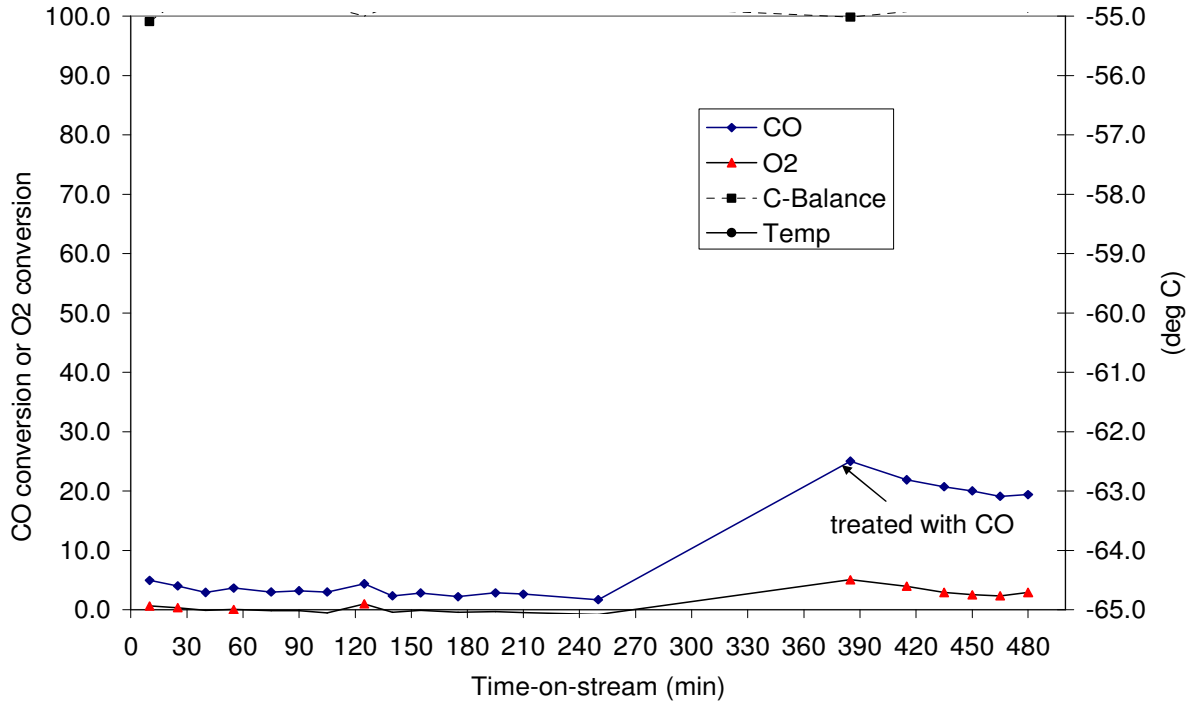

Figure 5.15: Effect of room temperature CO treatment in the activity of the Au/rutile (pH 7) catalyst at -77 ^{o}C at 50 ml/min.

The conversion of CO at dry ice temperature is very low (between 2 and 5%). At this temperature there is not much difference between the Au/P-25 (figure 5.13) and Au/rutile (figure 5.16). XANES data (section 5.3.2) reveals an as-prepared uncalcined Au/TiO_2 catalyst as mostly ionic, indicating the inability of ionic species to convert CO to CO_2 on their own without the presence of metallic species. However, when the catalyst was subjected to 1% CO/He (200 ml/min) treatment at room temperature for 1 h, the CO oxidation activity increases corresponding to a conversion of 20% at dry ice temperature. At room temperature, CO reduces Au^{III} species into metallic and probably Au^{I} species. TPR studies (section 5.3.1) of as-prepared catalysts reveal that treatement in 1% CO/He mixture at 200 ml/min for 1 h at room temperature does not lead to complete reduction. This was observed by running TPR (figure 5.26) on such

treated catalyst and the hydrogen consumption peak was still observed though it was small and broad, suggesting that the CO-treated catalyst still contains some reducible Au species. This evidence supports the Bond and Thompson theory of the active species being an ensemble of ionic and metallic gold species (Bond and Thompson, 2000).

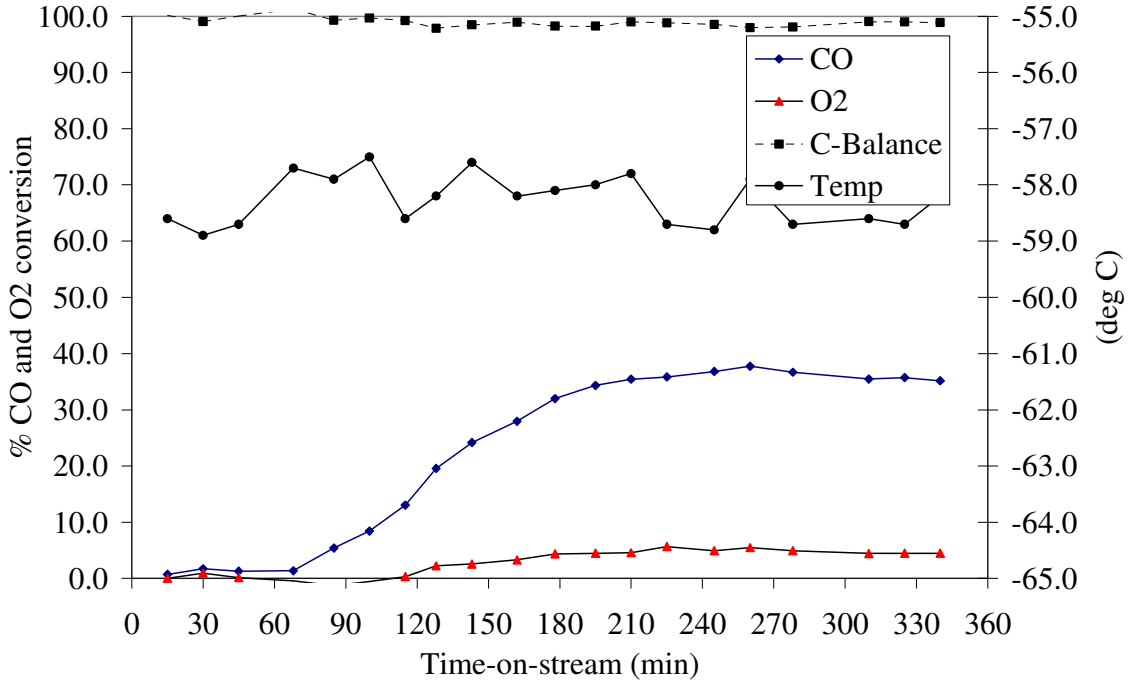

Figure 5.16: Effect of time on the activity of Au/TiO_2 (pH 7) catalyst at -58 ^oC

An induction period for Au/rutile at -58 ^oC is 70 min which is shorter than that of Au/P-25 (figure 5.13). The activity of this catalyst increases to the highest of about 38%, whereas the Au/P-25 increases to the highest activity of about 10% conversion. This clearly reveals the strong influence of the support on the dispersion, reduction and agglomeration of the gold species. Reduction of Au^{III} particles to Au^0/Au^I and probably some small extent of agglomeration occur faster on the surface of the rutile than on that of the anatase TiO_2 support.

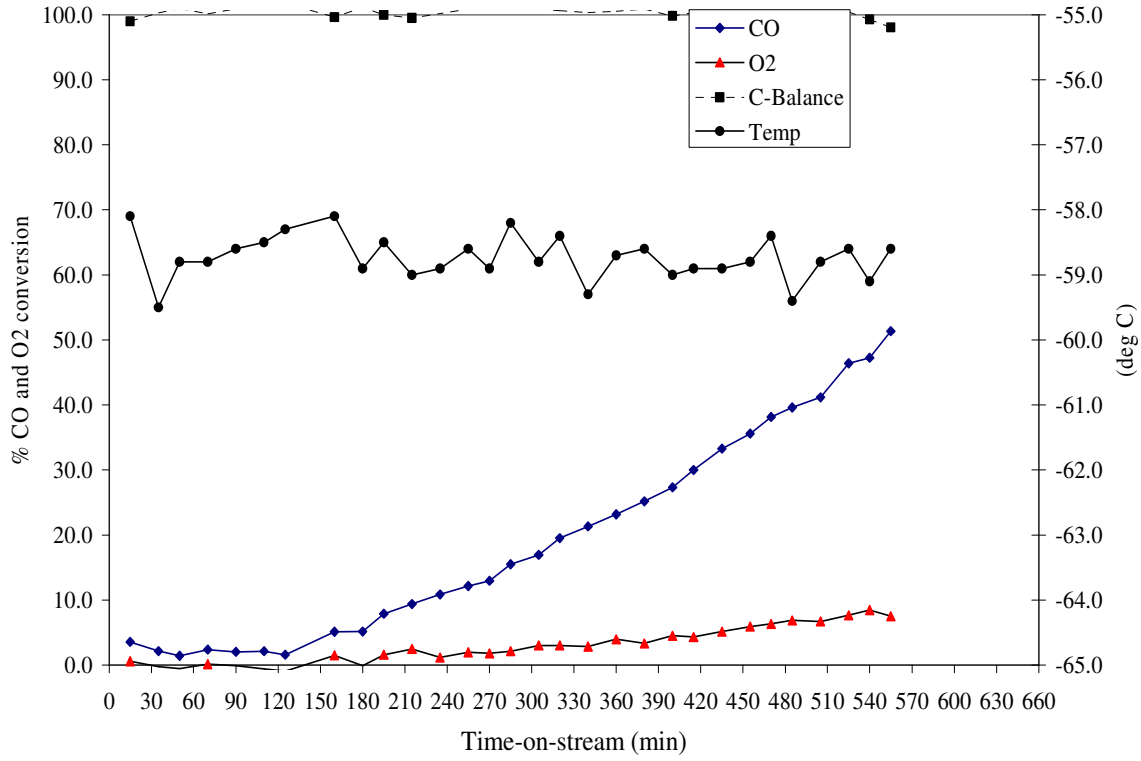

Figure 5.17: Effect of time on the activity of the Au/rutile (pH 6) catalyst at -58 ^{o}C

The figure above (Figure 5.17) also shows that the Au/TiO_2 (rutile) catalyst has a shorter induction period compared with that found with the catalyst based on P-25 support. This catalyst was found to contain 6% Au particles as compared to 3% Au on Au/P-25. This may suggest that at higher loadings, gold particles on the surface of the support agglomerate faster and auto reduces more to metallic and/or Au^{I} species, than at low gold loadings. However, contradicting evidence were observed when comparing two Au/rutile catalysts coded Au/rutile (pH 7) (figure 5.16) and Au/rutile (pH 6) (figure 5.17) containing 4wt% Au and 6wt% Au respectively. The induction period of the former (70 min) is shorter than that of the latter (2 h) though the amount

of gold on the surface of the support is lower. Therefore the amount of gold loading may not be the (only) factor governing the induction period. The pH at which these catalysts are prepared may be very crucial since Au/rutile (pH 7) was prepared at pH 6 and Au/rutile (pH 7) was prepared at pH 7. The catalyst prepared at lower pH may still contain some residual chlorine coordinated to both the gold particles and the support and the gold particles may not be as small as those of the catalyst prepared at pH 7 which contains little or no chlorine; agglomeration and reduction of the chlorine-containing gold particles might be faster.

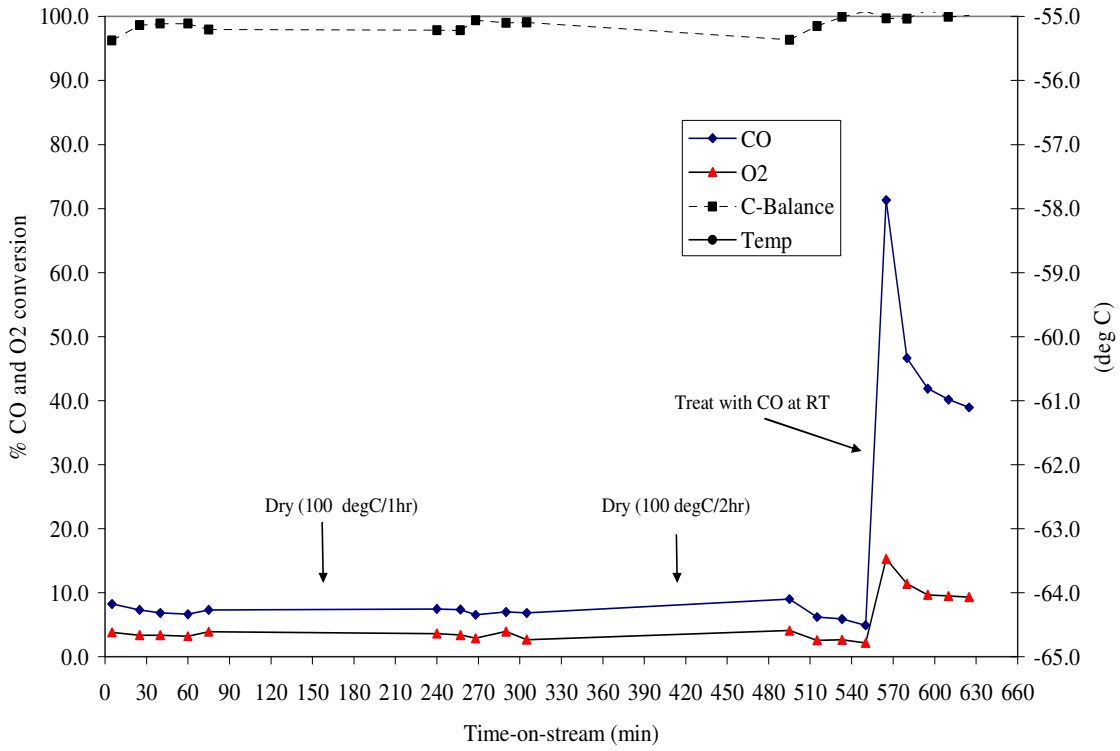

Figure 5.18: Effect of drying in helium on Au/rutile (pH 7) catalyst on CO oxidation at -77 ^{o}C

Drying this catalyst in an inert medium at 100 ^{o}C does not increase the activity of the catalyst. However, the catalyst shows activity of ~4%, which is not achieved without any drying. As XANES (section 5.3.2) reveals the presence of mostly ionic gold

species on uncalcined Au/TiO_2 catalysts, the slight activity achieved is due to the removal of hydroxyl groups in the form of water, leaving a very small proportion of ionic gold species autoreduced into metallic species. Increasing the period at which the catalyst is dried does not seem to improve its activity. A further treatment of this catalyst at room temperature with 1% CO/He resulted in an improved activity with the highest CO conversion being 70%. However the activity decreased with time to about 38% conversion. An improved activity after CO treatment suggests that more ionic species were reduced to metallic species which are also a necessary requirement for the high activity of the gold catalyst according to Bond and Thompson (2000); Costello *et al,* (2002) and Oh *et al,* (2001).

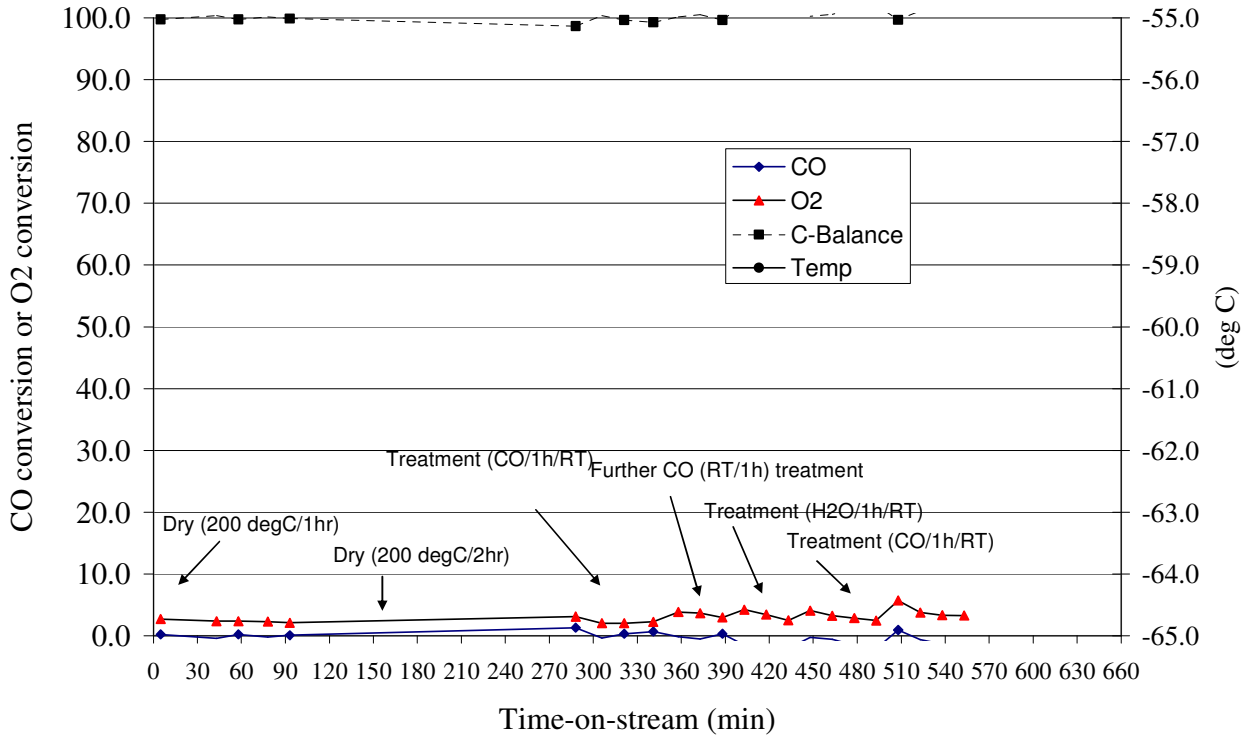

Figure 5.19: Effect of drying, CO and H_2O on Au/rutile (pH 7) catalyst on CO oxidation at -77 ^oC

Drying this catalyst at 200 ^oC also does not improve its activity but seems to deactivate it since not even the 8% conversion achieved after drying at 100 ^oC was achieved; the catalyst remains totally inactive. Interestingly, after being subjected to 200 ^oC drying the catalyst could not be activated by treatment with 1% CO/He at room temperature as was observed with the sample dried at 100 ^oC. The reason for this behavior could be that treatment at such high temperature removes all the hydroxyl groups from the ionic gold species, and according the mechanism suggested by Oh *et al.* (2000 and 2001) such $Au(OH)_x$ are required for the adsorption of CO which forms a hydroxycarbonly species. In the absence of $Au(OH)_x$, adsorption of CO does not occur and hence there is no activity. This catalyst could not be regenerated with water at room temperature either, but such treatment and a further treatment by 1% CO/He resulted in an increase in oxygen conversion. This may suggest that oxygen is somehow being adsorbed by this catalyst, probably by metallic gold according to the mechanism proposed by Oh *et al.* (2000 and 2001) and Costello *et al.* (2002).

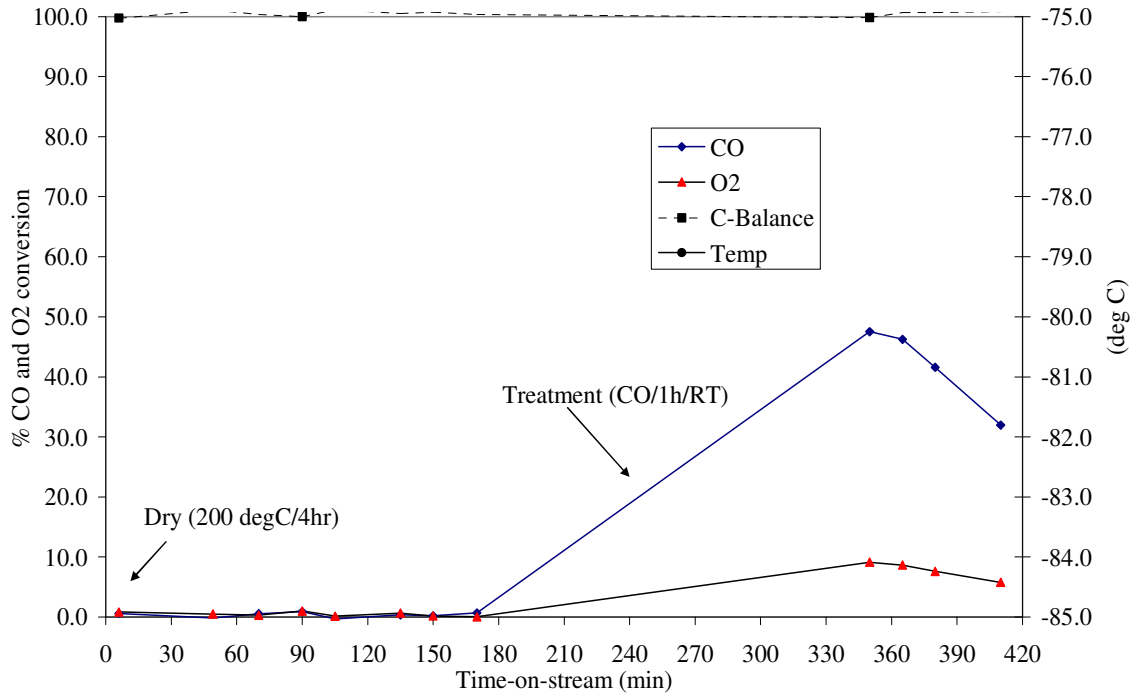

Figure 5.20: Effect of drying on Au/P25 (pH 7) catalyst on CO oxidation at -77 ^{o}C

Figure 5.20 shows that Au/P25 catalyst cannot be activated by drying in helium at 200 ^{o}C for 4h. However, this catalyst can still be activated by treatment with 2% CO/He at room temperature after being subjected to high temperature and achieve over 30% conversion of CO at dry ice temperature which is contrary to the results observed with Au/rutile (figures 5.18 and 5.19). These findings suggest a very sharp difference between the two supports and their effects on gold particles.

5.2.4 H_2 Pulse experiment on Catalysts prepared by method 2

Pulse experiments were conducted on these catalysts where either 100 mg or 200 mg was packed into a quartz u-tube reactor and subjected to a number of H_2 pulses to achieve different degrees of Au reduction. In another set of experiments 5 pulses of

hydrogen were followed by CO oxidation reaction at dry-ice temperature (-78 ^{o}C) in order to assess the change in the catalyst activity with increasing reduction.

The pulses were injected at room temperature, where approximately 2 ml/min of hydrogen was injected into the argon flowing at 50 ml/min into the GC where H_2 consumption was quantified.

The catalyst was then thoroughly purged with 200 ml/min of argon for about 30 min, after which it was cooled to dry-ice temperature for CO oxidation activity test (reaction conditions described in chapter 3). After the reaction, the catalyst was purged again with the same flow rate of argon and the dry-ice dewar was removed leaving the catalyst to warm up to room temperature while purging continued. The next pulse would be injected and the pulse/reaction cycle was repeated until the catalyst could not consume any more hydrogen and a final activity test was conducted in order to assess the activity of the catalyst at this stage.

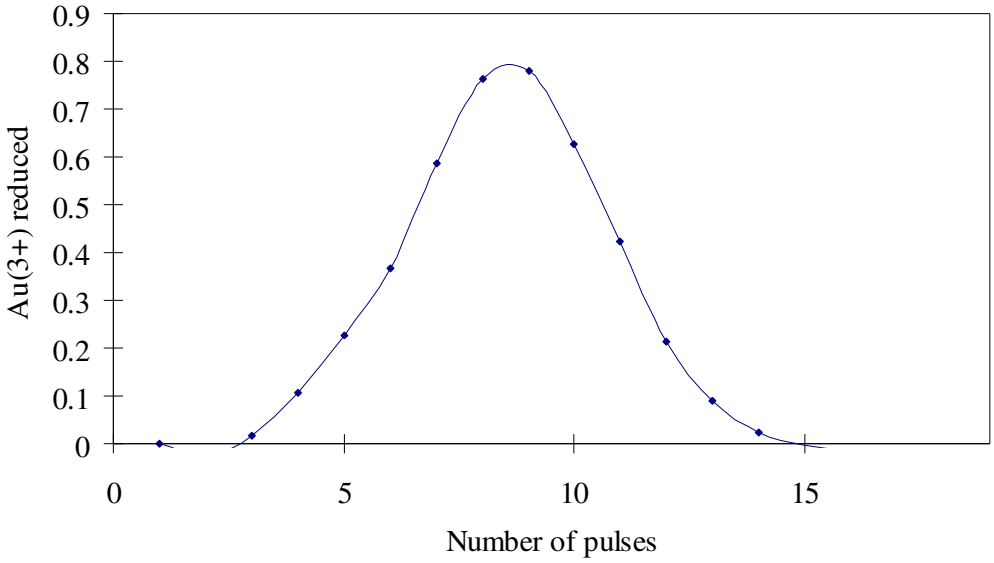

Figure 5.21: Au/rutile (pH 7) catalyst`s reducibility as a function of the number of hydrogen pulses

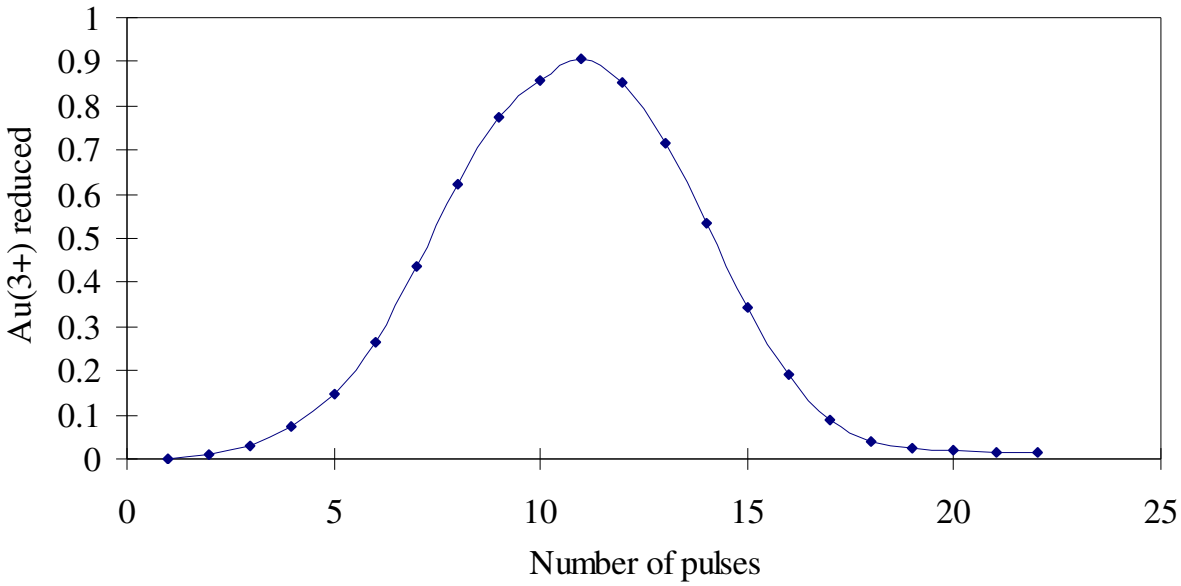

Figure 5.22: Au/rutile (pH 6) catalyst`s reducibility as a function of the number of hydrogen pulses

Comparing figures 5.21 and 5.22 (both Au/rutile), there is no considerable difference in the hydrogen consumption pattern during the first few pulses. However the optimum hydrogen consumption levels are clearly different since that of the catalyst Au/rutile (pH 7) (figure 5.21) is at the 8th pulse whereas that of Au/rutile (pH 6) (figure 5.22) was observed at the 11th pulse. This observation is consistent with the difference in the induction period observed during the CO oxidation reaction at dry ice temperature where Au/rutile (pH 6) (Figure 5.17) showed a longer induction period while a shorter one was observed with Au/rutile (pH 7) (Figure 5.16), suggesting slower agglomeration and reduction process for the Au/rutile (pH 6) catalyst.

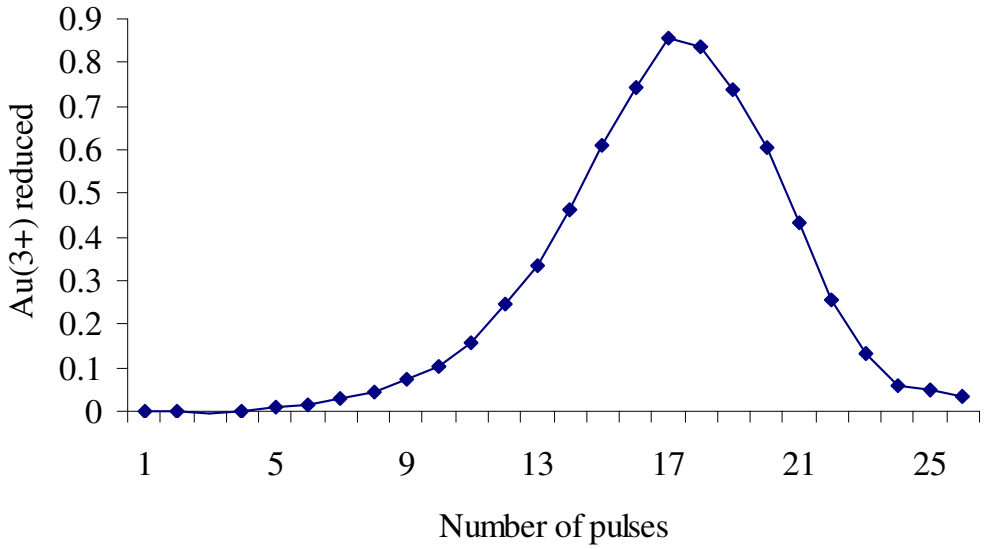

Figure 5.23: Au/P25 (pH 7) catalyst`s reducibility as a function of number of hydrogen pulses

The figures 5.21 and 5.22 above indicate that the rutile-based catalyst is more readily reduced than the P25-based catalyst (figure 5.23). This is evident because the rutile is already completely reduced on the 11th (figure 5.22) and the 8th pulse (figure 5.23) while the P25-based catalyst starts to show its reduction on the 8th pulse and is fully reduced at the 17th pulse (figure 5.23). These results are consistent with the extended induction period of this catalyst during CO oxidation (figure 5.13).

5.2.5 Pulses with CO oxidation interruption

These results confirm the need for the presence of metallic species on the surface of the support for an enhanced CO oxidation activity. We have observed a negligible activity (less than 3% conversion) at dry ice temperature with the catalyst that was not subjected to any H_2 pulse, but the activity increase with increasing amount of pulses which means an increased amount of reduced gold species.

An interesting thing to note is that even though the Au/rutile (figure 5.24) and Au/P25 (figure 5.26) have different induction periods, they achieve equal activities of 45% CO conversion at the stage where they can no longer consume hydrogen. This suggests that the difference between these two catalysts has in the manner in which reduction and/or the rate at which the ionic species are reduced, but once they are fully reduced they have similar structures.

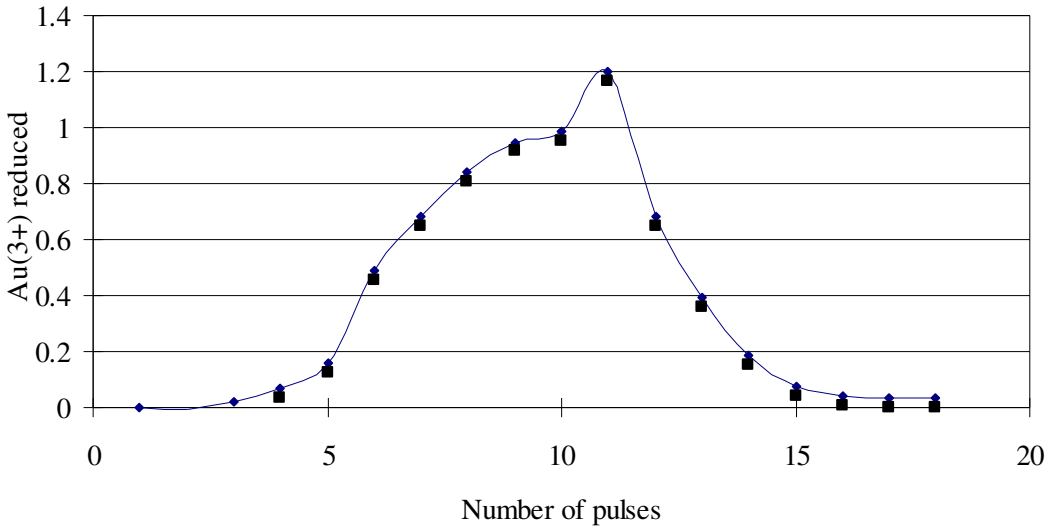

(a)

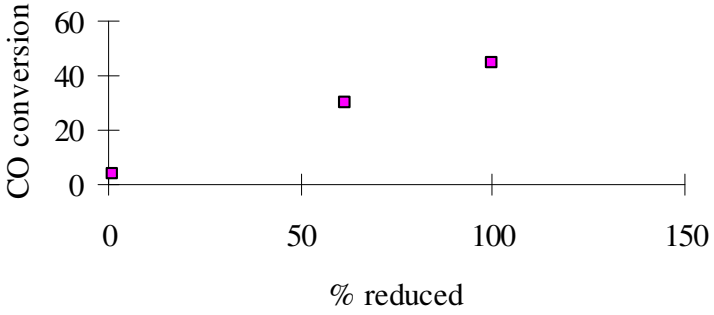

(b)

Figure 5.24: Au/rutile catalyst`s (pH 7) reducibility (a) and activity (b) as a function of number of hydrogen pulses

Figure 5.24 also shows that the gold ions are not immediately reduced by hydrogen but need three to five H_2 pulses to start the reduction process. Figure 5.25 (b) shows an increase in the activity of the catalyst with increasing number of pulses and about

45 % CO conversion was achieved at dry ice temperature with catalyst reaching the point where it does not consume further H_2 and is supposedly highly reduced.

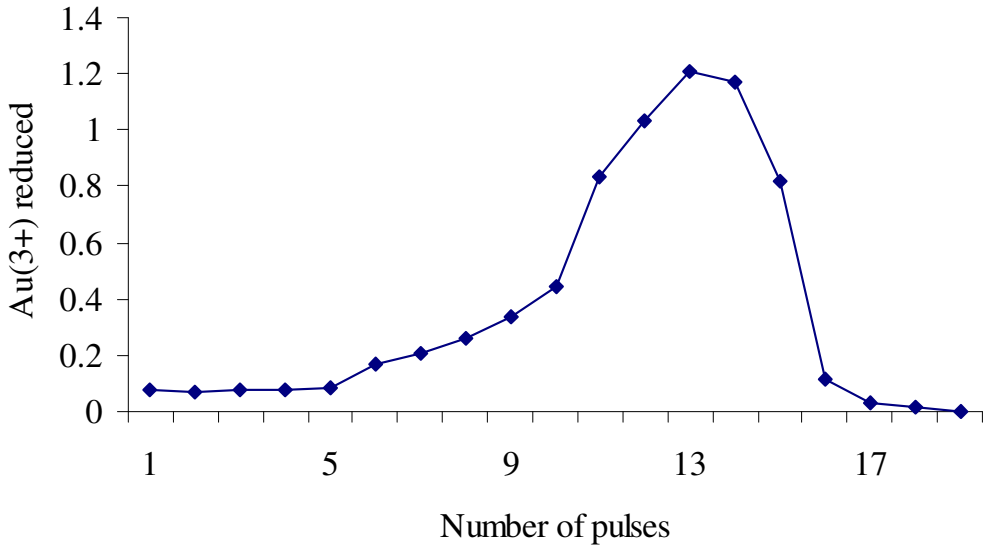

(a)

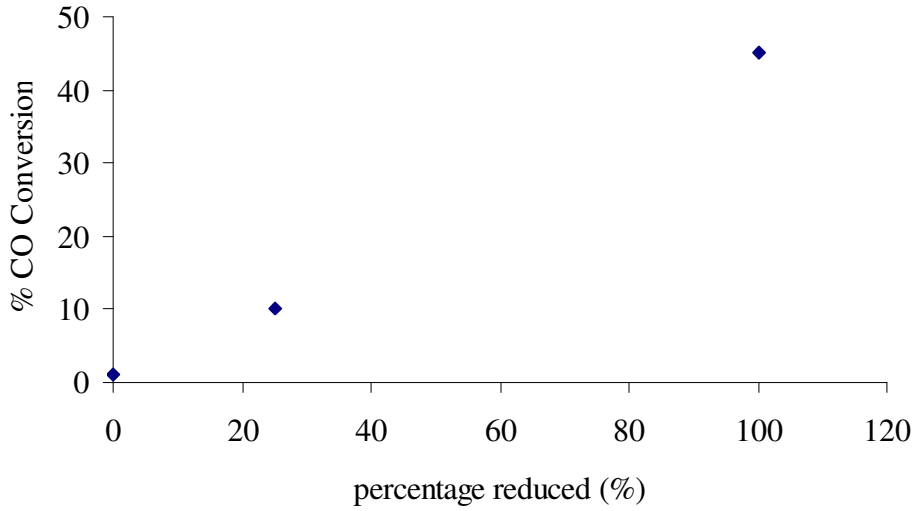

(b)

Figure 5.25: Au/P25 catalyst`s (pH 7) reducibility (a) and activity (b) as a function of number of hydrogen pulses

Figure 5.25 presents similar data obtained for the P25-based catalyst. Before the catalyst is subjected to any pulse, it only showed a negligible activity (<1.5% conversion) at dry ice temperature but increased activity was observed with an increasing number of pulses to about 45% conversion when the catalyst that could no longer consume hydrogen.

5.3 Sample Characterization

5.3.1 TPR

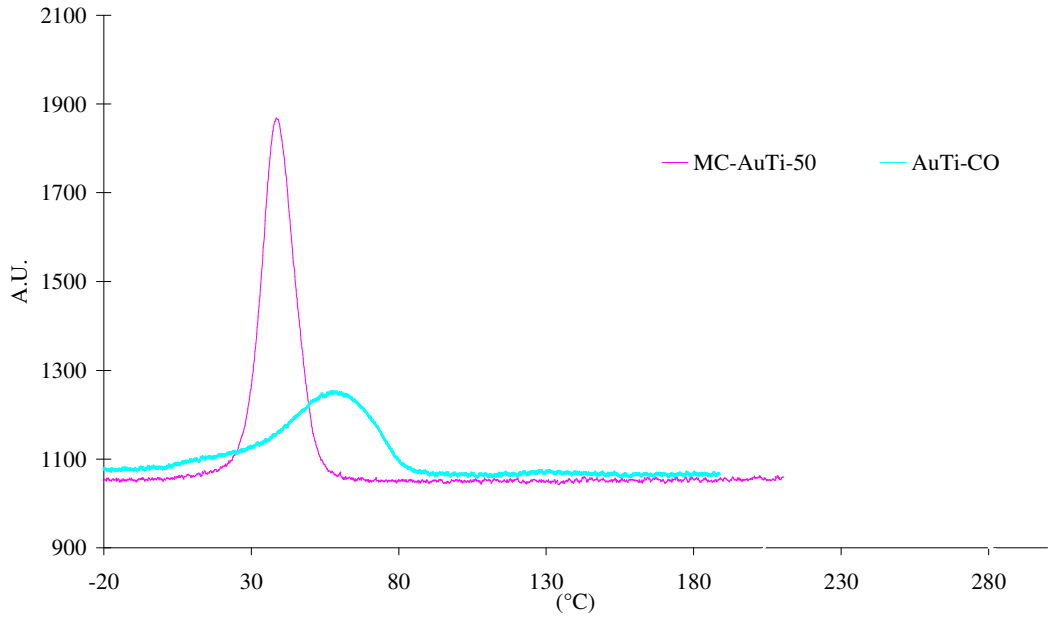

Figure 5.26: Comparison of the TPR spectra of Au/TiO_2 (P25) before (MC-AuTi-50) and after (AuTi-CO) treatment with CO

The TPR spectrum above shows that reduction of gold ions on uncalcined Au/TiO_2 occurs at room temperature. It is also revealed that catalyst treatment with 1% CO/He at room temperature does not totally reduce the catalyst, since such treated catalyst still consumed hydrogen, even though the hydrogen consumption peak is smaller and broader (figure 5.26). These results, therefore confirm that the increased activity of the catalyst treated with CO is due to the presence of both the ionic and metallic gold species.

5.3.2 XANES

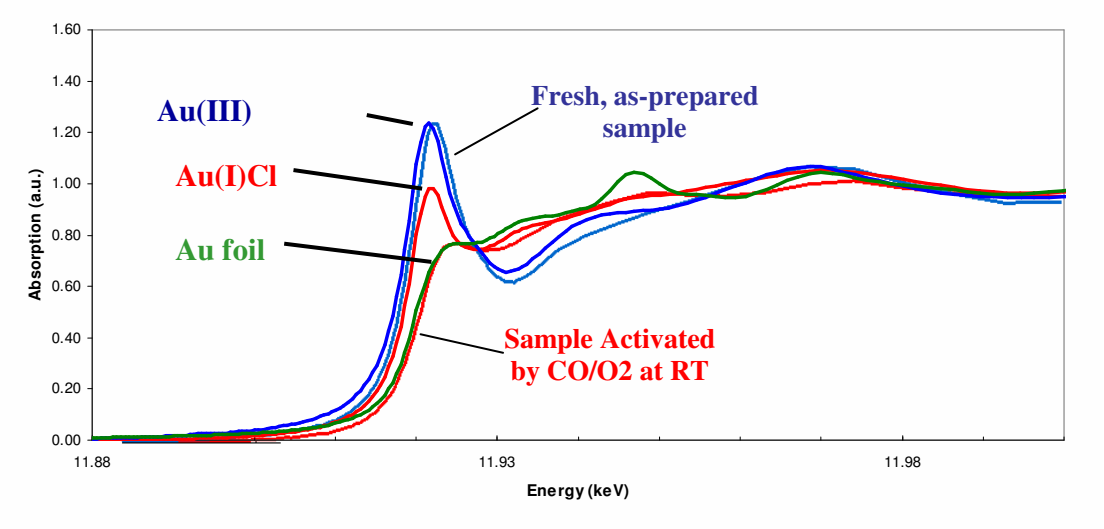

Figure 5.27: XANES spectra of different Au standards compared to as prepared and treated Au catalysts.

Figure 5.27 above shows the XANES spectra of the Au^{III} acetate, $Au^{I}Cl$, and bulk Au^{0} standards. The Au acetate peak is identical to that of the as-prepared Au/TiO_2 catalyst, which evidences that the Au species in our as-prepared catalyst are predominantly Au^{III}. However, exposing such catalyst to CO/O_2 at room temperature results in a rapid reduction of Au^{III} species and the XANES spectrum suggests that reduction largely to Au^{0} has taken place. However, a close examination of these spectra indicates that the catalyst treated with a reacting gas mixture is not completely reduced, and the presence of ionic species is evident.

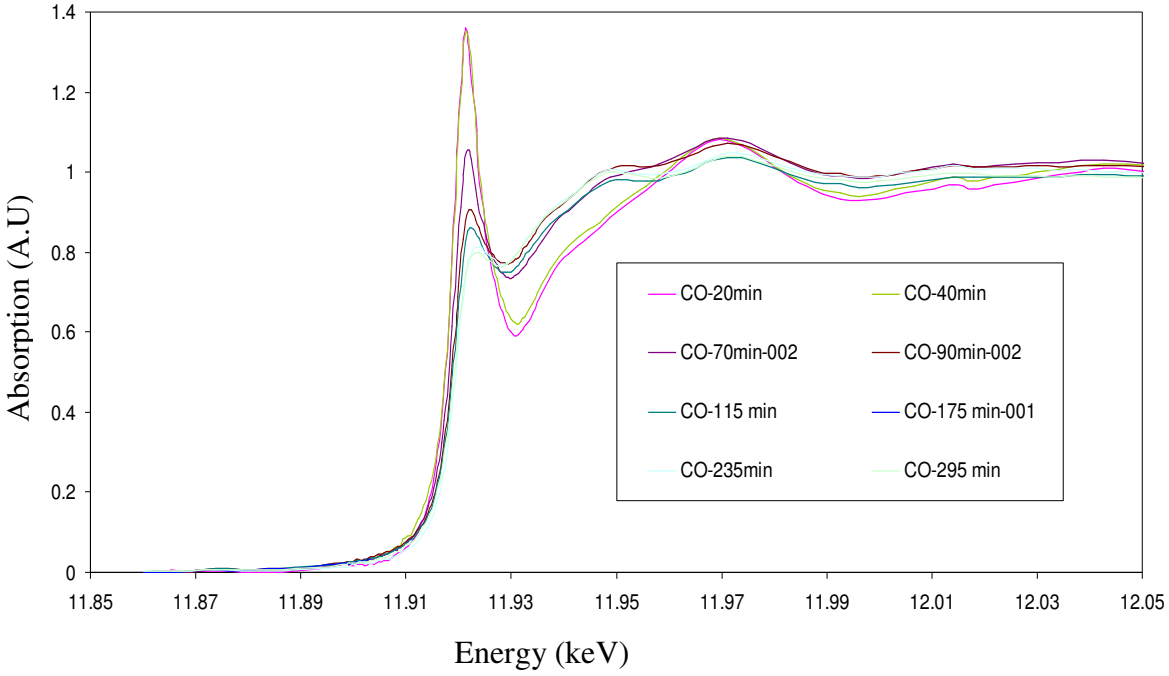

Figure 5.28: XANES spectrum of Au/rutile (pH 7) after different periods of exposure to CO oxidation at -68 ^{o}C.

An intense peak at 11.92 keV reveals that the majority of the gold particles on the catalyst are ionic (Au^{III}). The presence of the reacting gases in the reactor over 40 minutes did not reduce the catalyst (figure 5.29) and no conversion of CO was achieved over this period (figure 5.17). However, over about 70 min the catalyst starts to show some significant reduction (figure 5.29) and CO conversion starts to increase (figure 5.16). From this point we observed an increase in the activity of the catalyst with increasing reduction of ionic Au species until the 235th minute where the activity remained constant and there is no considerable difference in the intensity of this peak at this time and that taken at 295 min. At this stage the catalysts seems to have reached the steady state both with respect to the CO conversion and the extent of reduction. However, there is still evidence for the presence of ionic species on the catalyst, confirming the need both metallic and ionic species to be present for CO oxidation.

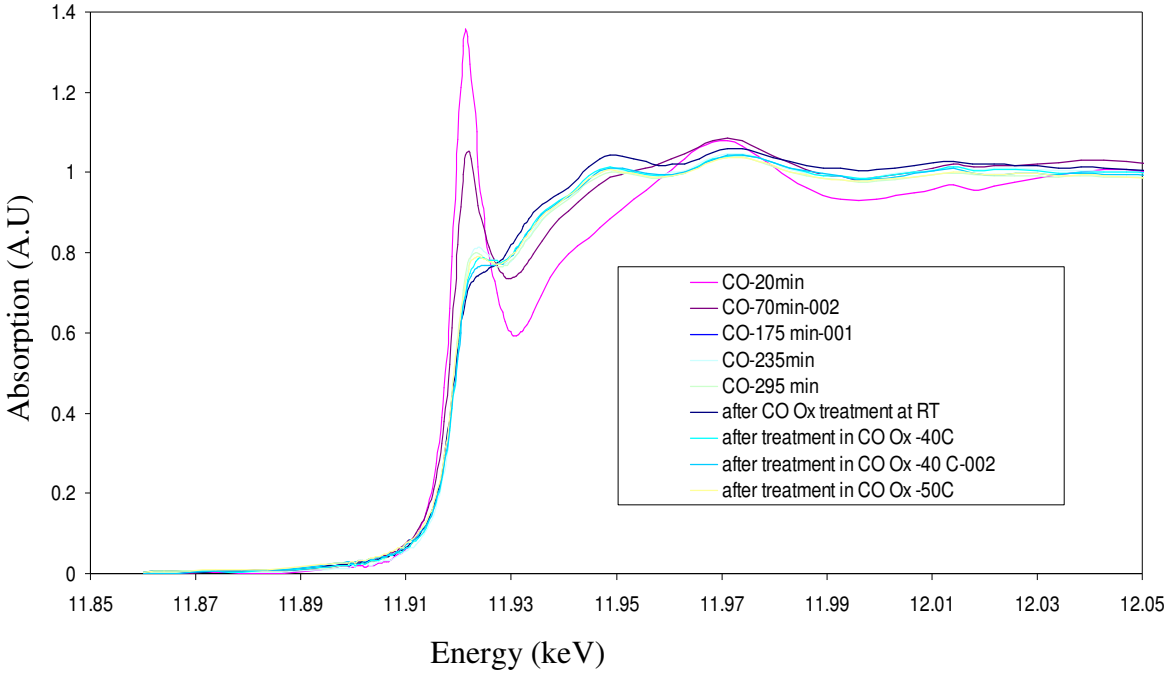

Figure 5.29: XANES spectrum of Au/rutile (pH 7)) after different periods of exposure to CO oxidation with increasing temperature

Figure 5.29 shows data obtained in an experiment in which the activity of the catalyst and its oxidation state were monitored with a gradual increase of temperature. Increasing the temperature from dry ice temperature at the 295th minute of CO oxidation to -50 ^{o}C and subsequently to -40 ^{o}C does not result in a significant change in the oxidation state of the catalyst. But increasing the temperature further to room temperature results in a more reduced catalyst. However it is strongly arguable if such catalyst is totally metallic. The CO oxidation data moreover shows a total conversion at room temperature.

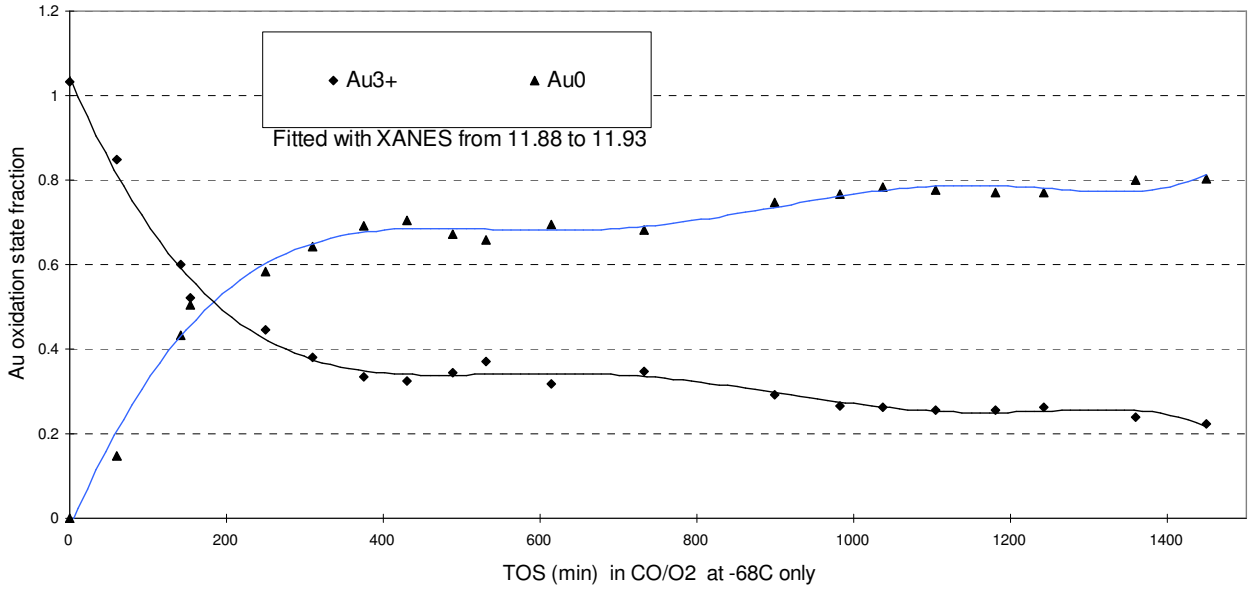

Figure: 5.30: Change in the oxidation state of Au at -68 ^{o}C under reaction mixture

An as-prepared Au/TiO_2 sample before activation contained Au(III) (Figure 5.27, t = 0 min), as indicated by the intense white line absorption at 11.922 keV, a shoulder at around 11.939 eV, and a broad peak at 11.968 keV. These absorption peaks agree well with those for the Au(III) in an Au acetate standard (Figure 5.27). Temperature programmed reduction of such a sample in a micro reactor, starting at -30 ^{o}C (Figure 5.26), showed a H_2 consumption peak at about 25 ^{o}C, and the amount of H_2 consumed was in good agreement with complete reduction of Au(III) to Au(0). Thus, the Au(III) complex, presumably $[Au^{III}(OH)_4]^-$, deposited onto the TiO_2 support is stable in air at room temperature. An identical spectrum was obtained upon repeating the scan in air or He, at room temperature or -68°C, indicating no significant or rapid reduction of the sample by the x-ray beam.

The spectrum changed as a function of time on stream (TOS) in a feed of 1% CO, 2.5% O_2, balance He at –68°C (Figure 5.26). Although the composition of the

reaction mixture was net oxidizing, the catalyst was reduced at an appreciable rate, as indicated by the decrease in the peak intensity at 11.922 keV. Using as standards Au acetate (there was little difference if as-prepared Au/TiO_2 was used) for Au(III), AuCl for Au(I), and Au foil for Au(0), and the LC XANES fit function in the WINXAS program, the 11.88 to 11.95 keV region of the XANES spectra was fitted to obtain the distribution of Au oxidation states. As reduction proceeded, the fraction of Au(I) and Au(0) increased, while that of Au(III) decreased. However, because of the limited number of features, these spectra could be fitted satisfactorily with more than one possible combination of oxidation states. For example, at about 430 min TOS, the spectrum agreed equally well with a distribution of 23% Au(III), 35% Au(I), and 42% Au(0) or 31% Au(III) and 69% Au(0), for an average Au oxidation state of 1.04 or 0.93, respectively. At 1360 min, a distribution of 18% Au(III), 24% Au(I), and 58% Au(0), or 23% Au(III) and 77% Au(0) could fit the data, for an average oxidation state of 0.78 and 0.69, respectively. After the sample had been warmed to room temperature, the spectrum could be fitted better with a distribution of 34% Au(I) and 66% Au(0) than 100% Au(0). Although there was uncertainty in the distribution of oxidation states, there was much less uncertainty in the average oxidation state. The average oxidation states determined by fitting the curves to either Au(III) and Au(0) or to all three oxidation state. It is clear that significant but incomplete reduction of Au occurred over the first 400 min (Figure 5.30), and subsequent reduction was much slower. The sample was not completely reduced even after 24 h. It could be further reduced by warming the sample to room temperature in the reaction mixture.

5.4 Conclusions

Removal of bulk Au by cyanide leaching results in the well distributed small Au particles on the surface of the catalyst. This leads to a high activity of such catalysts. However a severely leached catalyst containing 0.06%Au loading was found to be inactive. This suggests that an optimum particle size is required for high activity of Au catalysts.

The results observed in this study confirmed the need for both the ionic and the metallic gold species for the high activity of the catalysts. This requirement was first reported by Bond *et al.* (2000) followed by other researchers such as Oh *et al.* (2000 and 2001). In this study it was observed that a catalyst which is mostly ionic is inactive for CO oxidation and requires some reduction in order to be active. The difficulty in activating the Au/rutile catalyst after being dried at 200 ^{o}C may suggest that the catalyst with no $Au(OH)_x$ groups is inactive. However, some in-situ XANES or XPS is required to investigate if the drying process removes all hydroxyl groups in the form of water and leave a mostly metallic species. The experiments on the effect of drying have given a hint on the difference between the two supports and the effect they have on the gold species as was observed by Grunwaldt *et al.* (1999). These observations provide a foundation for a thorough investigation on the effect of the support. The need for the induction period at dry ice temperature was observed were a certain proportion of ionic gold species were reduced before the catalyst starts to show its activity. Another question of interest is if agglomeration occurs during reduction, or if it is the requirement for the ionic species to auto reduce. More characterization is required to answer these questions which could lead to a breakthrough on the optimum particle size required for the high activity of these catalysts.

5.5 References

Bailie J.E and Hutchings G.J., *Chem. Comm*., (1999) 2151.

Bond G.C and Thompson D.T, *Gold Bull.,* 33 (2000) 14.

Costello C.K., Kung M.C, Oh S.H., Wang Y., Kung H.H, *Appl. Catal. A*., 232 (2002) 158.

Daté M., Ichihashi Y., Yamashita T., Chiorino A., Boccuzzi F., Haruta M., *Catal. Today,* 72 (2002) 89.

Davis R.J, *Science,* 301 (2003) 926.

Finch R. M., Hodge N.A, Hutchings G.J, Meagher A, Pankhurst Q.A, Rafiq M, Siddiqui H, Wagner F.E, Whyman R, *PCCP,* 1 (1999) 485.

[a]Fu Q., Saltburg H., Flytzani-Stephanopoulus M., *Science*, 301 (2003) 935.

[b]Fu Q., Kudriavtseva S., Saltburg H., Flytzani-Stephanoploulos M., *Chem. Eng. Journal,* 93 (2003) 41.

Gardner S.D, Huflund G.B, Upchurch B.T, Schryer D.R, Kielin E.J, Schryer J., *Catal.*, 129 (1991) 114.

Goosens A., Craje M.W.J, van der Kraan A.M, Zwijnenburg A, Makkee M., Moulijn J.A., de Jongh L.J., *Catal. Today,* 72 (2002) 95.

Grisel R.J.H, Weststrate C., Goosens A., Craje M.W.J, van der Kraan A.M, Nieuwenhys B.E, *Catal. Today.* 72 (2002) 123.

Grunwald J.-D., Keener C., Wogerbauer C., Baiker A., *J. Catal*., 181 (1999) 223.

Grunwaldt J.-D, Teunissen H, *Eur. Patent,* EP1209121 (2002).

Guczi L, Horvath D., Pastel Z., Toth L., Horvath Z.E, Karacs A., *J. Phys. Chem. B*., 104 (2000) 3183.

Guzman J. Gates B., *J. Phys. Chem., B* 106 (2002) 7659.

Haruta M., *Catal., Today*, 36 (1997) 153.

Haruta M, Yamada N, Kobayashi T, *J. Catal*., 144 (1993) 175.

Habashi F., *Bull. Can. Inst. Min. & Metallurgy* 80(905)(1987) 108.

Habashi F., 1993, A *Textbook of Hydrometallurgy*, Metallurgie Extractive Quebec, 800 rue Alain #504, Sainte- Foy, Québec, Canada, GlX 4E7.

Hoflund G.B, Gardner S.D, Schryer D.R, Upchurch B.T, Kielin E.J, *Appl. Catal., B*: 6 (1995) 117.

Jeffrey M.I and Breuer P.L, *Min. Eng.,* 3 (2000) 1092.

Konova P.*,* Naydenov A., Venkov Cv., Mehandjiev D., Andreeva D., Tabakova T., *J. Mol. Catal.* A: 213 (2004) 235.

Kung H.H, Kung M.C, and Costello C.K, *J. Catal.,* 216 (2003) 425.

Lee S., and Gavriilidis A., *J. Catal*., 206 (2002) 305.

[a]Lopez N, Janssens T.V.W, Clausen B.S, Xu Y, Mavrikakis M, Bligaard T, Nørskov J.K, *J. Catal.,* 223 (2004) 232.

[b]Lopez N, Nørskov J.K, Janssens T.V.W, Carlsson A, Puig-Molina A, Clausen B.S, Grunwaldt J.-D, *J. Catal.,* 225 (2004) 86.

Mavrikakis M, Stoltze P, Nørskov J.K, *Catal. Lett.,* 64 (2000) 101.

McArthur J.S., Forrest R.W. and Forrest W., *'Improvements in obtaining gold and silver from ores and other compounds', British Patent,* 14174, 1888.

Minaco S., Scire S.,Crisafulli C, Visco A.M, Galvano S, *Catal. Lett*., 47 (1997) 273.

Minato T, Susaki T, Shiraki S, Kato H.S, Kawai M, Aika K, **in press**, *Surface Science* (2004).

Nechayev Y. A., and Nikolenko N. V., *Geochem. Intl.* 23 (1986) 32.

Oh, H.-S., Costello, C. K., Cheung, C., Kung, H. H., and Kung, M. C., *Stud. Surf. Sci. Catal.* 139 (2001) 229.

Oh S.H, Costello C.K., Cheung C., Kung H.H, Kung M.C, *Proceedings of the papers presented at the Pacific Chem. Conf. Dec.,2000 and at the North American Catalysis Society meeting, June 2001.*

Okumura M, Nakamura S., Tsubota S., *et al*, *Catal. Lett.,* 51 (1998) 53.

Park E.D. and Lee J.S., *J. Catal.,* 186 (1999) 1.

Schumacher B., Denkwitz Y., Plzak V., Kinne M., and Behm R.J., *J. Catal.,* 224 (2004) 449.

Schubert M.M., Hackenberg S, van Veen A.C., Muhler M., Plzak V, Behm R.J, *J. Catal,* 197 (2001) 113.

Soares J.M.C., Morrall P. Crossley A, Harris P, Bowker M, *J. Catal.,* 219 (2003) 17.

Wolf A. and Schuth F. A., *Appl. Catal*., 226 (2002) 1.

Website 1: http://www.rossmining.com.au/Environment1999.html

Yang J.H, Miller J.H, Henao J, Wang Y, Raphulu M.C, Kung M.C, Kung H.H, *"In-situ observation of Genesis of Catalytic Activity of Au/TiO_2"* ***in preparation.***

Zanella R, Giorgio S, Shin C.-H, Henry C.R, Louis C, *J. Catal.,* 222 (2004) 357.

Chapter 6

CO and Methane Oxidation with various Gold Catalysts

6.1 Introduction

Among the different metal oxides used as the support of Au for CO oxidation, cerium oxide has attracted some interest. It is the oxide of the rare-earth metal cerium, which may exist in several compositions, due to the capacity of Ce to switch between two oxidation states of Ce^{3+} and Ce^{4+}. A number of functions have been ascribed to ceria, including promoting water gas shift activity (Barbier and Duprez, 1994, Donka *et al,* 1998), maintaining the dispersion of metals (Diwel *et al,* 1991) and stabilizing the surface area of the support (Ozawa and Kimura, 1993). Extensive research has shown that ceria has a beneficial effect in a number of catalytic reactions. Due to the facile redox reaction cycle, ceria exhibits oxygen storage capacity and improves CO and hydrogen oxidation. Summers and Ausen (1979) claimed that ceria donated oxygen to Pt in their study of the CO oxidation on Pt/CeO_2 catalysts. For CO oxidation, ceria has been found to lower the activation energy, increase the reaction rate and to suppress the usual CO inhibition effect. Ceria promotes the activity of Pt in both lean and rich reactant gases for CO oxidation.

Ceria is presently used as a key component of the three-way-catalyst in automotive exhausts. It is good choice of support for noble metal and base metal catalysts, participating in the redox reaction by supplying oxygen. It is used to maintain noble

metal dispersion and also known to promote water gas shift reaction. Metal-modified cerium oxide has higher oxygen storage than pure ceria (Fu *et al,* 2003; Andreeva *et al,* 2002 and Tabakova *et al,* 2003).

Grisel and Nieuwenhuys (2001) reported that the addition of a metal oxide to Au/Al_2O_3 catalyst improved the catalytic activity in both the low temperature CO oxidation and methane oxidation, though the effect was low for the latter reaction. The measured oxidation activity of methane oxidation over $Au/MOx/Al_2O_3$ decreased in the order: $CuO_x > MnO_x > CrO_x > FeO_x > CoO_x > NiO_x > ZnO_x$. The main aim of this project was to establish if the catalyst which is good for CO oxidation could also be good for methane oxidation. This would shed light on the nature and preparation of a common catalyst for both reactions. For this purpose, the Au/TiO_2, and Au/TiO_2-MO_x (where MO_x is ZrO_2, and CeO_2) were prepared by various methods.

6.2. CO oxidation

6.2.1 Catalyst Characterization

6.2.1.1 BET Surface Area

The table below shows that calcining the Au/CeO_2 catalyst decreases the surface area by about 7 m^2/g while the average pore diameter is increased. A decrease in the surface area could be due to the crystallization of both the gold and the CeO_2 particles. Calcination does not significantly change the surface area and the average pore diameter of the Au/TiO_2-CeO_2 catalysts but that of Au/TiO_2-ZrO_2 is significantly decreased upon calcination. This suggests that the presence of TiO_2 in the catalyst inhibits the sintering of CeO_2 to a greater extent than just the presence of gold as was suggested by Fu *et al.* (2003). The inhibition of CeO_2 crystal growth upon calcination after the addition of the second metal was also observed by Fu *et al.* (2003) for Au/CeO_2-La_2O_3 catalyst. The presence of TiO_2 does not have much effect on the hindering of the growth of ZrO_2 crystallites on the catalyst as can be seen by a decrease in the surface area of the calcined catalyst.

Table 6.1: BET surface area of ceria related catalysts

Catalyst	Surface area (m^2/g)	Single point total pore volume (cm^3/g)	Average pore diameter (nm)
CeO_2	114	0.1786	6.2
Au/CeO_2: uncalcined	53.1	0.0558	4.2
Au/CeO_2: calcined	45.6	0.0680	5.9
Au/TiO_2-CeO_2: uncalcined	52.2	0.0750	5.7
Au/TiO_2-CeO_2: calcined	51.1	0.0740	5.8
TiO_2	49.9	0.0626	5.0
Au/TiO_2: uncalcined	57.9	0.0827	5.7
Au/TiO_2: calcined	51.4	0.0789	6.1
Au/TiO_2-ZrO_2: uncalcined	165	0.1740	4.3
Au/TiO_2-ZrO_2: calcined	120	0.1598	5.4

6.2.1.2 XRD

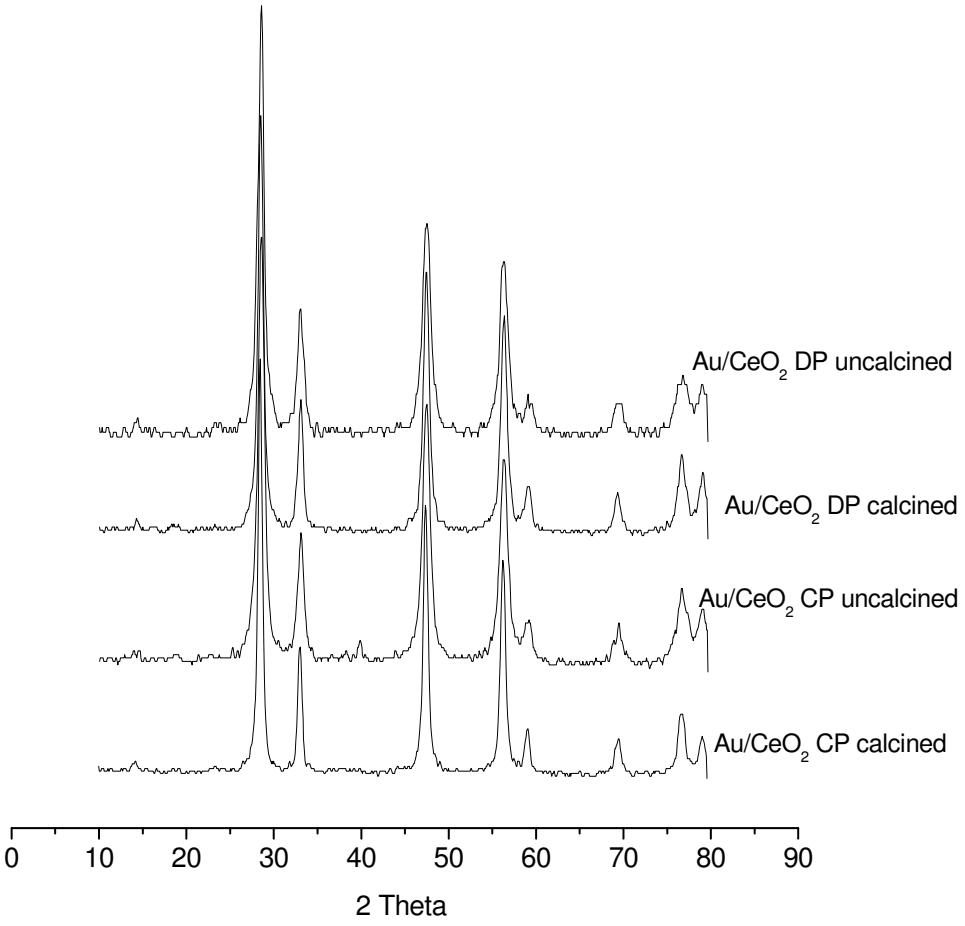

Figure 6.1: XRD spectra of Au/CeO_2 catalysts prepared by co-precipitation and deposition-precipitation.

The figure clearly depicts only the presence of ceria phases with no gold phase observed as was the case with Pd/CeO_2 (Zhu *et al,* 2004), $CuO\text{-}CeO_2$ (Jung *et al,*

2004) and Pt/CeO_2 (Damyanova and Bueno, 2003). The preparation method and catalyst treatment such as calcination does not seem to exert an effect on the crystallinity of gold particles. This effect is shown by Luengnaruemitchai *et al.* (2003), who prepared Au/CeO_2 by co-precipitation and Pt/CeO_2 catalyst by sol-gel and their XRD spectra were identical with neither gold nor platinum phases being observed. The peak size and shapes of CeO_2 do not change either with different method of preparation and calcinations. The absence of gold peaks suggests that they are well dispersed as small particles of the surface on the support (Zhu *et al.* 2004). The absence of gold reflections before and after calcination indicates the strong interaction between the gold and CeO_2 particles on catalyst prepared by both co-precipitation and deposition precipitation (Fu *et al,* 2003). However, Fu *at al.* (2003) observed strong gold reflections with catalysts containing a higher (8 %) amount of gold, prepared by gelation and deposition-precipitation method whereas Centeno *et al,* (2002) observed the appearance of small, peaks due to polycrystalline gold.

.

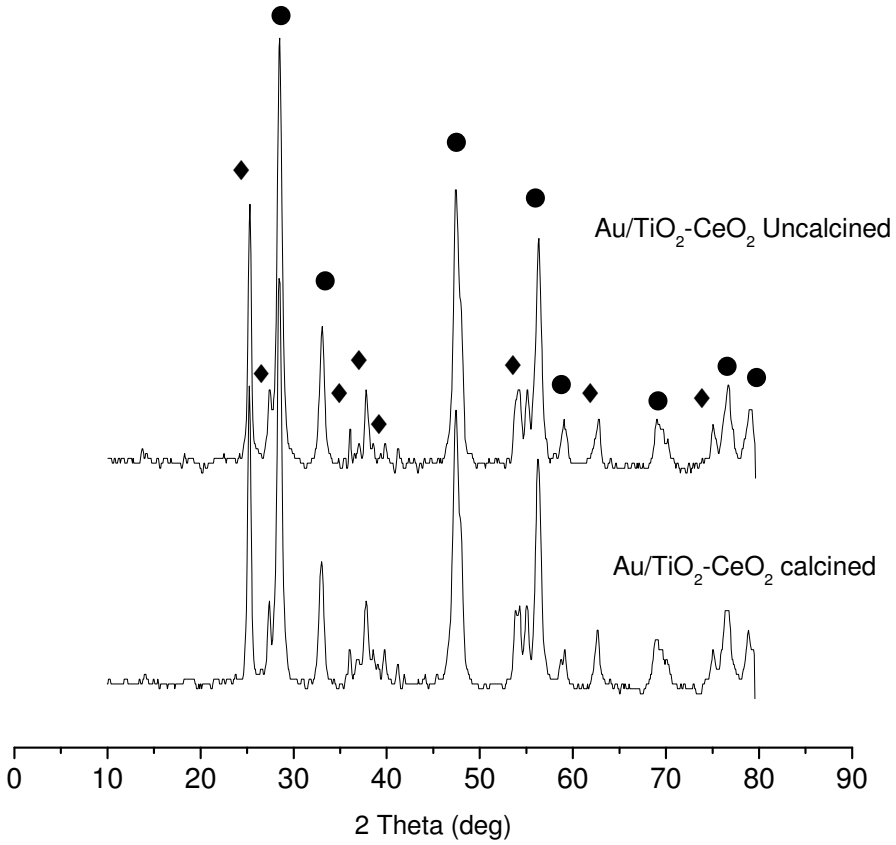

Figure 6.2: XRD spectra of the calcined and uncalcined Au/TiO_2-CeO_2; ♦ = Anatase and rutile TiO_2 crystalline phases and • = Cubic ceria (CeO_2) crystalline phases.

There is no difference in XRD data obtained for the calcined and the uncalcined Au/TiO_2-CeO_2 catalysts. The anatase, rutile and cubic ceria phases are all present in both catalysts. The appearance of distinctive reflections for both TiO_2 and CeO_2 may be an indication that a good solid solution was not formed between the two oxides which is contrary to the results reported by Fu *et al.* (2003); Kundakovic and Flytzani-stephanopoulos (1998) on Au/ (La-doped) CeO_2 catalysts. This may be due to the fact that the amount of both supports were equivalent by mass whereas with the

catalysts reported by the above mentioned authors, the CeO_2 was only doped into small extent. The gold phases are not observed in both the samples, indicating that they are either present as non-crystalline phases or the particles are smaller than 3 nm and finely dispersed on the support (Zhu *et al,* 2004; Jung *et al,* 2004; Fu *et al,* 2003 and Luengnaruemitchai *et al,* 2003) which result is consistent with the high activity of the catalysts.

6.2.2 Catalyst Activity

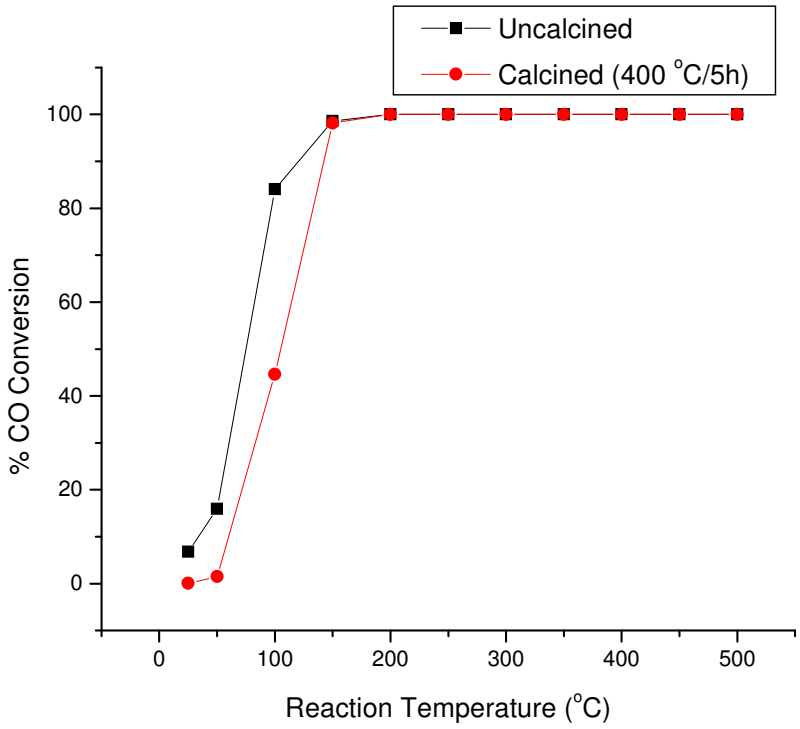

Figure 6.3: The effect of reaction temperature on the calcined and uncalcined Au/CeO_2 synthesized by co-precipitation

The calcined and uncalcined catalysts show low activities below 100 °C, but the uncalcined catalyst has a higher activity than the calcined catalyst. However, both catalysts achieve total conversion at 150 °C. Co-precipitating the noble metal particles on the metal oxide comprising CeO_2 automatically tends to give a high interaction between the two sets of particles. Such a catalyst possesses a geometric and electronic structure which is significantly different from other catalysts. With co-precipitated catalyst, it has been reported that some metal particles are trapped in the support matrix and hence unavailable to the reacting molecules with a reduction in the activity of the catalysts. However, calcining such a catalyst is thought to open the pores into which the metal particles are buried, exposing them to the reacting

molecules (Bond and Thompson, 2000). The calcined catalyst could therefore be expected to give a higher activity than the uncalcined catalyst, which is not the case in the gold-ceria catalyst as is shown in the figure above.

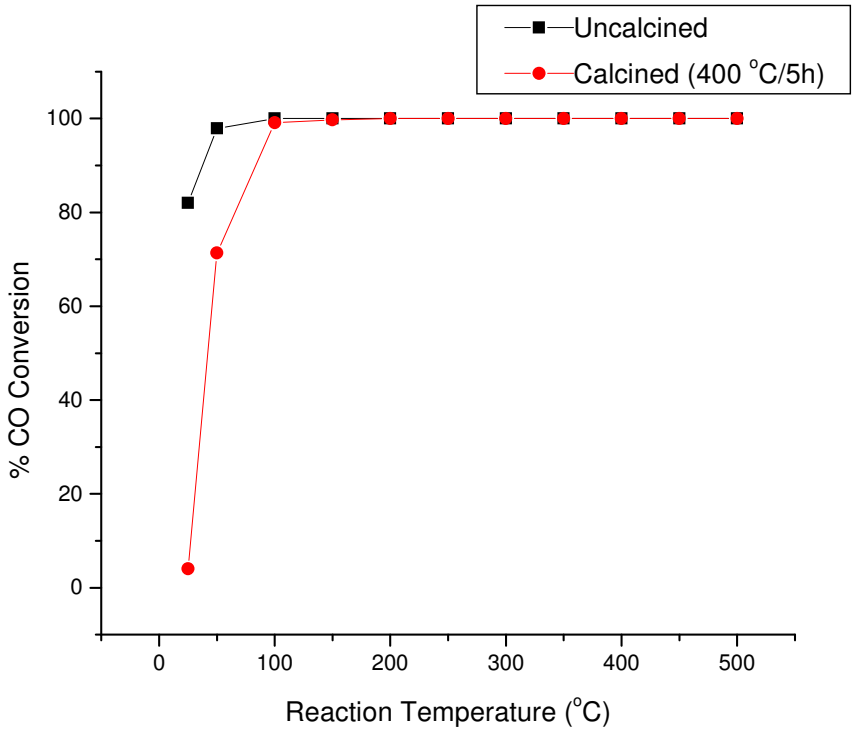

Figure 6.4: The effect of reaction temperature on the calcined and uncalcined Au/CeO_2 synthesized by deposition-precipitation

The figure above shows that calcination also has a detrimental effect on the catalyst synthesized by deposition precipitation. This may be due to the increase in gold particle size with increasing temperature of calcination. This is shown by a very low activity (less than 10% conversion) of the calcined catalyst at 25 °C reaction temperature. The uncalcined catalyst on the other hand exhibits a very high activity

(80% conversion) at the same reaction temperature and total conversion was achieved at 100 ^{o}C. The calcined catalyst achieved total conversion only at 150 ^{o}C.

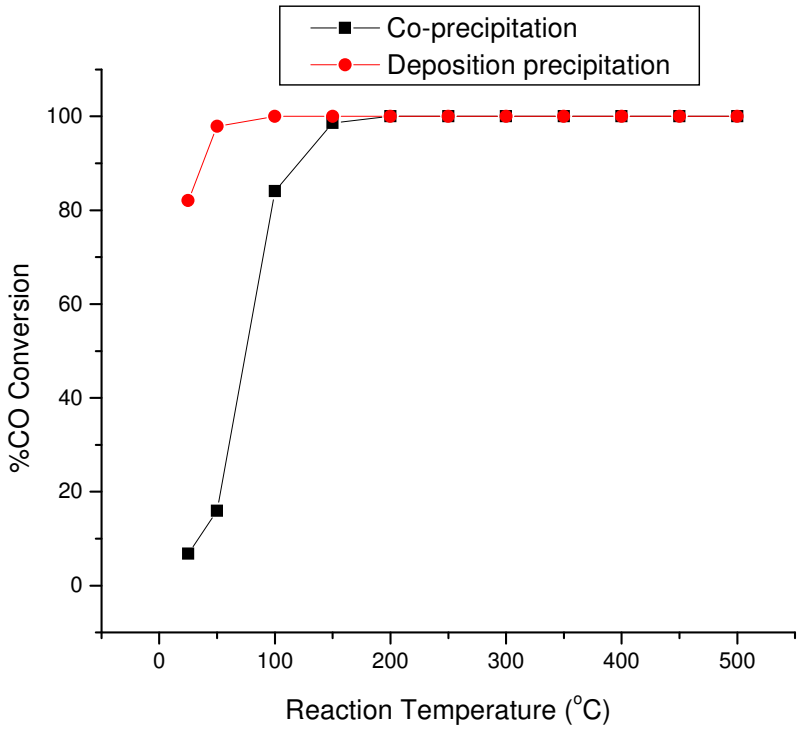

Figure 6.5: The effect of catalyst preparation on uncalcined Au/CeO_2

The figure above reveals that deposition-precipitation produces a more active catalyst system than co-precipitation. This is shown by a high activity of the deposition-precipitation catalyst at room temperature (80% conversion) whereas the co-precipitated catalyst only has a 5% conversion of CO at the same temperature. This catalyst achieves total conversion at 150 ^{o}C whereas the deposition precipitation catalyst achieves its total conversion at 100 ^{o}C. The lower activity of the co-precipitated catalyst might be due to the encapsulation of some of the gold particles by the support resulting in a significant suppression of the carbon monoxide chemisorption.

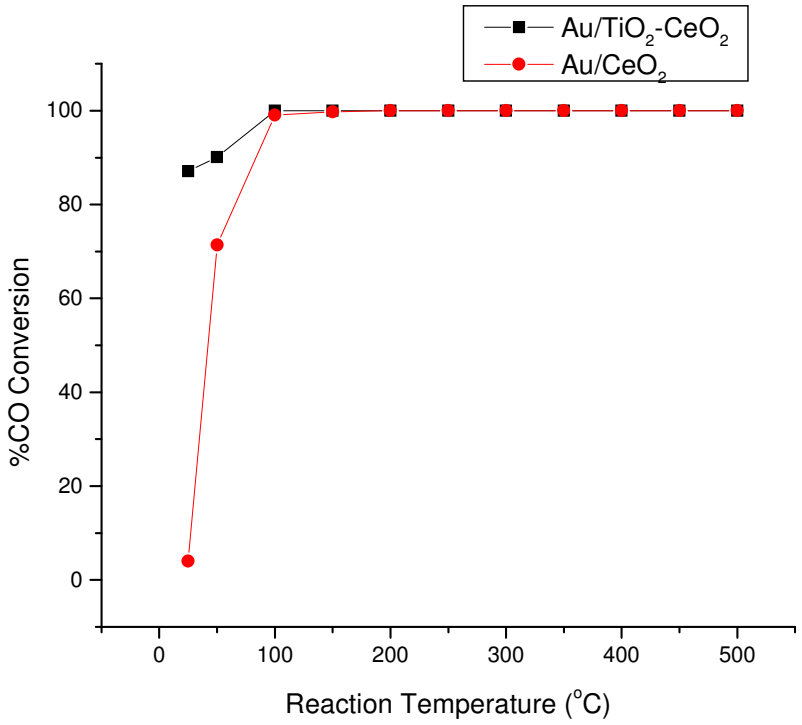

Figure 6.6: The effect of mixed oxides on the catalysts synthesized by deposition precipitation method.

Deposition-precipitation has been a preferred method of catalyst precipitation over co-precipitation (Bond and Thompson, 2000). This is because there is no encapsulation of the metal particles by the support matrix. The above figure compares the use of the single support to the use of mixed oxides as the support for gold. It reveals that the use of mixed oxide supports leads to a higher activity compared to the single support especially at temperatures lower than 100 ^{o}C. The higher activity of gold supported on mixed oxides was also observed with Au/TiO_2-ZrO_2, which exhibited higher activity compared with both Au/TiO_2 and Au/ZrO_2 at similar reaction conditions (Chapter 4). Calcined Au/TiO_2 catalyst was shown in table 6.1 to have a lower surface area compared with that of the uncalcined catalyst and it was

reported that CeO_2 particle size increases upon calcination with resulting lower catalytic activity. Au/TiO_2-CeO_2 on the other hand was shown not to be affected by calcination, suggesting an effect of TiO_2 on the activity and the inhibition of CeO_2 crystal growth hence an improved activity compared with that displayed by Au/CeO_2 catalyst. An improved stability of both the support and the gold particles and the strong interaction between them seems to be the likely cause (Fu *et al,* 2003).

6.3 Methane oxidation

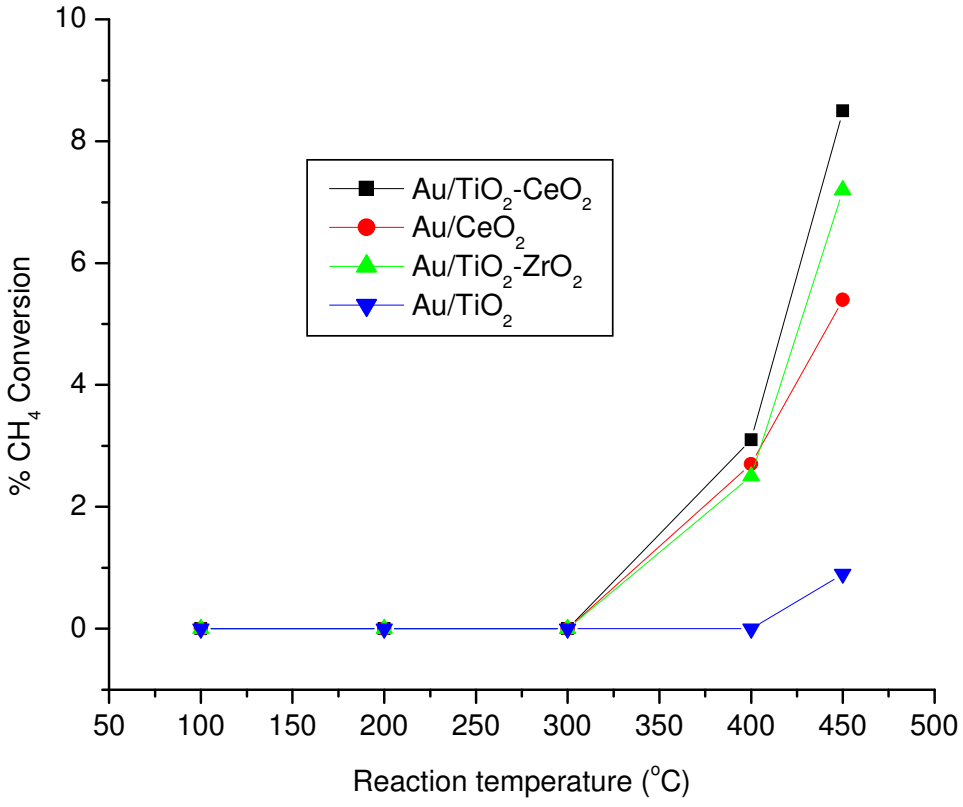

Figure 6.7: Effect of temperature on different catalyst for methane oxidation

The activity of the catalysts for methane oxidation is very low (figure 6.7) compared with that of CO oxidation reaction as shown in the above section and the previous chapters. The trends observed for these catalysts are similar with no methane converted below ca. 300 ^{o}C. This is probably because the adsorption of methane molecules on these catalysts is difficult. The figure above clearly shows the effect of the nature of the support on the methane oxidation reaction. The catalyst supported on CeO_2 is more active than that supported on TiO_2. The fact that CeO_2 is a good oxygen storage support may be playing a role here. Furthermore, CeO_2 has been reported to improve the metal dispersion (Andeeva *et al,* 2002). In chapter 4 of this document, XPS has shown that the dispersion of gold particles decreased upon calcination. It is therefore speculated that a good dispersion is one of the requirements for the methane oxidation reaction as it is for CO oxidation.

These are calcined catalysts and according to Mössbauer effect spectroscopy, (Chapter 4) Au/TiO_2-ZrO_2 contains mainly metallic gold, even though some ionic species have been detected. This therefore shows that the metallic surfaces of gold do not adsorb methane molecules hence low activity of the catalysts. The use of mixed oxides as support is beneficial for the methane oxidation reaction. The presence of CeO_2 and ZrO_2 on the catalyst improves the oxygen storage capacity of the catalyst as well as the dispersion of the supported metal. XPS data in chapter 4 has shown that the catalyst containing ZrO_2 containing more surface gold species than Au/TiO_2 catalyst for identical gold loading.

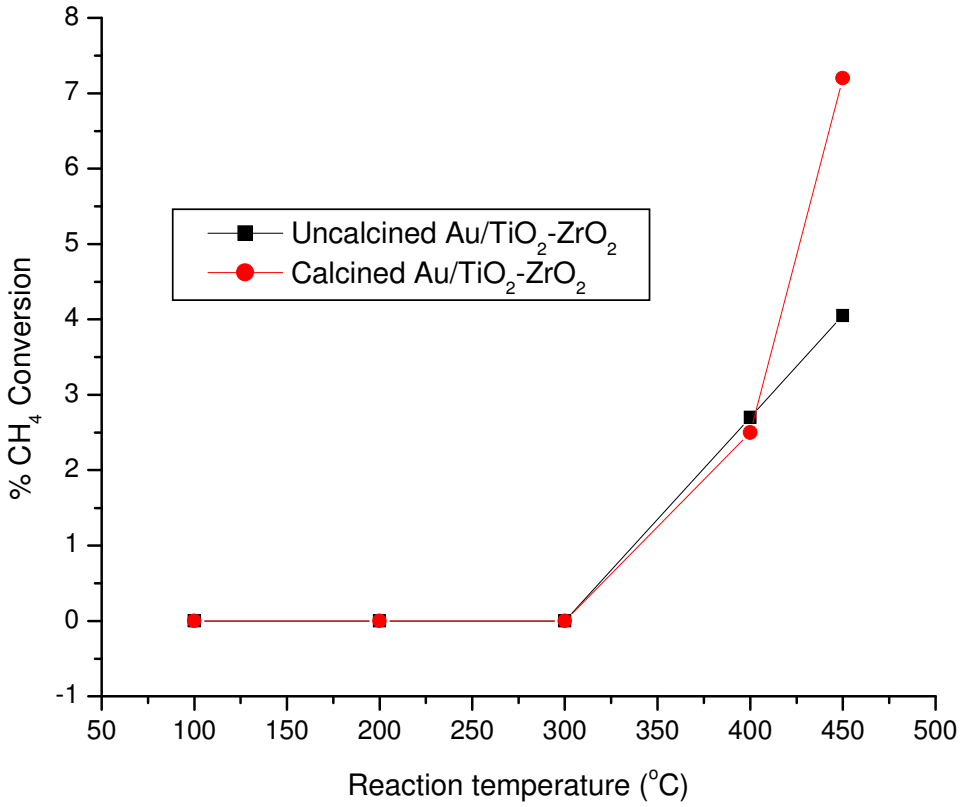

Figure 6.8: Effect of catalyst calcination on methane oxidation

In chapter 4, the uncalcined catalyst was found to contain mostly ionic gold species and the lack of methane conversion at low temperatures (100 ^{o}C) suggests that ionic species are not the active site for this reaction. Some low activity is observed at the temperature at which the catalyst was calcined (400 ^{o}C) and beyond this temperature, the pre-calcined catalyst shows a higher conversion of methane than the uncalcined catalyst.

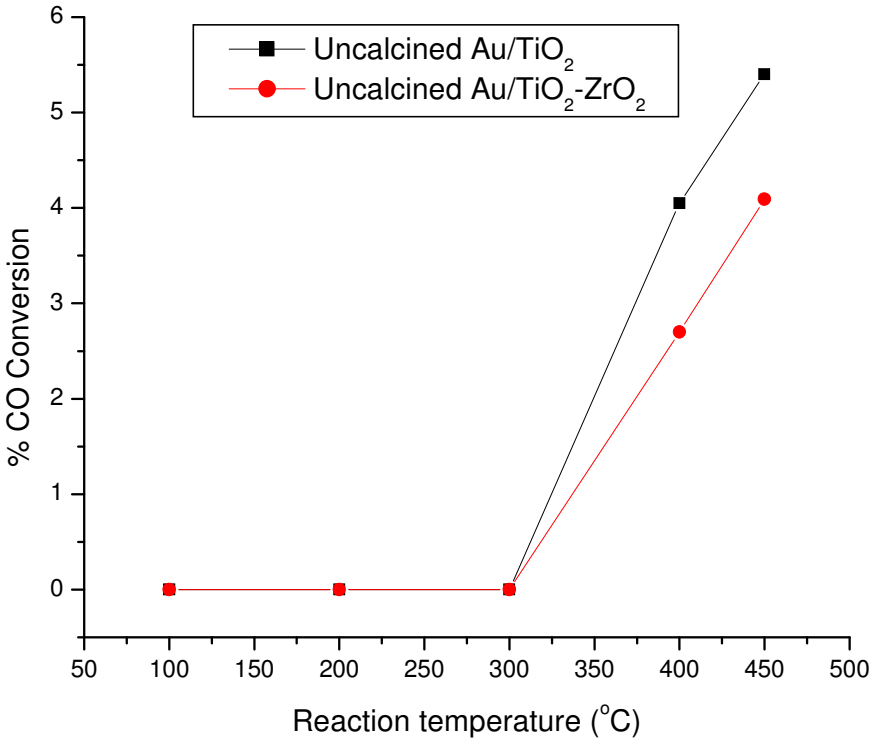

Fig 6.9: The effect of temperature on uncalcined catalysts for methane reaction

The uncalcined Au/TiO_2 was found to be more active than the uncalcined composite catalyst. This behaviour is not understood since with other catalysts, calcination was found to be beneficial for methane oxidation. It is noted however that the Au/TiO_2 catalyst is not active for this reaction, distinguishable from the other catalysts by virtue of its much lower activity (Figure 6.7).

6.4 Conclusion

Ceria-related catalysts were found to be active for CO oxidation. However, preparation method was found to play an important role in producing a good catalyst. Though the catalysts prepared by co-precipitation were active, they were not as active as those prepared by deposition-precipitation. The use of mixed oxides support was also found to be beneficial both in CO oxidation and methane oxidation whereas single support catalyst showed lower activities for both reactions. Methane oxidation was difficult and did not easily proceed at temperatures below ca. 400 ^{o}C, which contrasts with CO oxidation reaction which proceed readily, even at room temperature.

6.5 References

Andreeva D., Tabakova T., Idakiev V., Ilieva L., Falaras P., *Appl. Catal., A*: 72 (2002) 51.

Andreeva D., Tabakova T., Idakiev V., Christov P., and Giovanoli R., *Appl., Catal., A*: 169 (1998) 9.

Barbier Jr J, Duprez D., *Appl. Catal. B*: 4 (199) 105.

Bond G.C, Thompson D.T., *Gold Bull.,* 33 (2000) 41.

Centeno M.A., Paulis M., Montes M., Odriozola J.A., *Appl. Catal.,* 234 (2002) 65.

Damyanova S., Bueno J.M.C*., Appl. Catal. A:* 253 (2003) 135.

Diwell A, RajaramR, Shaw H, Truex T, *Stud Surf Sci. Catal.,* 71 (1991) 139.

Fu Q, Kudriavtseva S, Saltsburg H, Flytzani-Stephanopoulos M., *Chem Eng J*., 93 (2003) 41.

Grisel R.J.H and Nieuwenhuys B.E., *J. Catal*., 199 (2001) 48.

Jung C.R, Han J., Nam S.W., Lim T.-H, Hong S.-A., Lee H.-I., *Catal. Today*, 93-95 (2004) 183.

Kundakovic Lj, Flytzani-Stephanopoulos M, *Appl. Catal., A:* 171 (1998) 13.

Luengnaruemitchai A., Asuwan S., Gulari E., *Catal. Comm.,* 4 (2003) 215.

Ozawa O, Kimura M. E, *J Mater. Sci. Lett*., 9 (1990) 291.

Summers J.C, Ausen S.A., *J. Catal*., 58 (1979) 131.

Luengnaruemitchai A, Osuwan S, Gulari E, *Intl. J. Hydro. Energy*, 29 (2004) 429.

Tabakova T, Boccuzzi F, Manzoli M, Andreeva D, *Appl. Catal. A:* 252 (2003) 385.

Zhu H, Shen M, Kong Y, Hong J, Hu Y, Liu T, Dong L, Chen Y, Jian C, Liu Z, *J. Mol. Catal A:* 219 (2004) 155.

Chapter 7
General Conclusions

From the literature review, it was conclusive that gold catalysts have high activity for the oxidation of carbon monoxide at low temperature ranging from below 25 to 100 ^{o}C. However, certain aspects, such as the particle size, oxidation state of an active catalyst, and catalyst support were still being discussed with uncertainties and disputes among different research groups. The purpose of this study was to contribute to the research leading to the general consensus regarding these and other disputed issues concerning gold catalysis. Another aspect of great importance to us was to establish if the catalyst active for CO oxidation at certain reaction conditions would also be active for methane oxidation, leading to the simultaneous removal of these pollutants from the indoor air conditioning systems at the same temperature and we have succeeded in answering some of these questions.

In this study, it has been established that certain conditions are to be met during the synthesis and pretreatment of gold catalysts. It is concluded that preparation conditions such as synthesis temperature, period of ageing, pH and thermal treatment all exert strong influences on the structure and properties as well as the catalytic activity of the catalyst. Catalyst calcination and feed flow rate were also found to have a significant influence. Higher conversions of CO with catalysts produced by deposition-precipitation method were observed compared to those observed by catalysts prepared by co-precipitation.

The effect of the amount of gold on the catalyst was also found to be very important for CO oxidation. The removal of bulk Au by cyanide leaching result in well distributed small Au particles on the surface of the catalyst. This led to a high activity of the catalysts. However, a severely leached catalyst containing 0.06% Au loading was found to be inactive. This suggests a requirement for the optimum particle size of Au catalysts. It was not established if catalyst leaching was successful in removing all the metallic gold leaving only the ionic species. Even if this was the case, some metallic species could have been formed during subsequent catalyst treatment at 100 ^{o}C for 1 h, in 20 % O_2/He.

The results observed in this study confirmed the need for both the ionic and the metallic gold species for the high activity of the catalysts. Mössbauer Effect spectroscopy revealed that an Au/TiO_2-ZrO_2 catalyst which had higher activity contained a higher proportion of Au^{I} species (chapter 4) and that the activity was proportional to the amount of these species on the catalyst. XANES revealed that the as-prepared Au/TiO_2 catalyst which mainly contains Au^{III} species is inactive for CO oxidation and required some reduction for the development of activity (Chapter 5). It was also observed that an induction period at dry-ice temperature is required where a certain proportion of ionic gold species were reduced before the catalyst starts to show any activity. Another question of interest is if agglomeration occurs during reduction, or if it is the requirement for the ionic species to auto reduce. More thorough characterization is required in order to answer these questions which could lead to a breakthrough on the question of the gold particle size required for the high activity of these catalysts.

It was also concluded that ZrO_2 stabilizes the Au ions against total reduction during the CO oxidation reaction as is shown in figure 4.4. When calcination has a detrimental effect on the catalysts, the presence of zirconia was found to decrease this

effect. It is evident in figure 4.18 that even the catalyst that is calcined at 600 ^{o}C still has a considerable conversion of about 40%. Though the spectroscopic analysis on this particular catalyst has not been performed, it is speculated that small amount of Au^{I} ions are still present in such catalyst, and may be influencing the catalyst performance by stabilizing gold species by maintaining a strong interaction between the metallic gold and the support.

Mössbauer effect spectroscopy revealed that zirconia-containing catalysts still contain Au^{I} species even after calcination at high temperature (400 ^{o}C) whereas those that do not contain zirconia were found to be have no ionic species present after calcination. It is speculated that the presence of zirconia increases the number of OH groups on the surface of the catalyst and stabilize ionic gold species on the surface of the support. XPS revealed that the most active catalysts such as the uncalcined Au/TiO_2-ZrO_2 contained more than one gold species, which was indicated by higher peak widths and contributions from higher binding energies. It is therefore safe to conclude that the presence of both ionic and metallic gold species on the catalysts is a desired aspect in the oxidation of carbon monoxide.

In this study, a decrease in the activity of the catalyst with an increasing calcination temperature was observed. This was accompanied by sintering of the Au particles verified by HRTEM (Chapter 4) and a decrease in the surface area of the catalysts. XPS data also showed that the calcined catalysts contained smaller amount of gold on the surface of the support, which is consistent with agglomeration process.

The nature of pretreatment gas also has an effect on the Au/TiO_2-ZrO_2 catalyst activity, where reductive pretreatment conditions were found to be more beneficial than oxidizing conditions. The pH at which the catalyst is precipitated is also crucial.

An increase in the pH at which the catalyst was precipitated increases the dispersion of gold particle on the surface of the support according to XRD data that showed a decrease in the intensity of gold peak with increasing pH. Poor activity was achieved with those catalysts precipitated at pH lower than 9. It is also important to age the precipitates for a longer period such as 12h to allow the maximum amount of gold species to be well dispersed on the support. Shorter ageing periods (< 12 h) were found to result in catalysts with poor activities. For Au/TiO_2 catalyst, more conversion was observed with the catalyst precipitated at pH 7. This shows that the presence of ZrO_2 increases the point of zero charge of the support and more base is require for the total or appreciable hydrolysis of $HAuCl_4.xH_2O$ complex.

It has been observed that sol-gel method is not an ideal preparation method for Au catalysts. The TGA results show the presence of organic molecules which are removed during calcinations but the activity is not as good as that of the catalysts prepared by deposition precipitation. Even though calcination removes the organic species from the surface of the catalyst, it results in the agglomeration of Au particles hence low activity.

Ceria-related catalysts were found to be active for CO oxidation. The activities of these catalysts were found to be higher than those of Au/TiO_2 and Au/TiO_2-ZrO_2 catalysts. However, preparation method was found to play an important role in producing a good catalyst. Catalysts prepared by co-precipitation were not as active as those prepared by deposition-precipitation.

The methane oxidation reaction proceeded with difficulty at temperatures below ca. 400 ^oC, which suggests that the activation of the catalyst for such a reaction occurs at high temperatures as compared to CO oxidation which proceed even at room

temperature. Since CO oxidation proceeds at lower temperature regions, where oxidation of methane does not occur with all the catalyst tested for both reactions, it can be concluded that our catalysts can not oxidize both molecules in the same stream at low temperatures. In contrast, for CO oxidation, where calcination was found to be detrimental to the catalyst, higher conversions for methane were achieved with the calcined catalyst than with the uncalcined. This suggests differences in the nature of the suitable catalyst and active sites for these two reactions.